

UNCLASSIFIED

AD NUMBER

AD850447

LIMITATION CHANGES

TO:

Approved for public release; distribution is unlimited.

FROM:

Distribution authorized to DoD only;  
Administrative/Operational Use; JAN 1969. Other requests shall be referred to Army Electronics Command, Attn: AMSEL-KL-TQ, Fort Monmouth, NJ 07703.

AUTHORITY

USAEC ltr dtd 26 Oct 1970

THIS PAGE IS UNCLASSIFIED

4

*Handwritten initials/signature*

AD



Research and Development Technical Report  
ECOM-02289-F

*Handwritten circled number 20*

# HIGH CURRENT DENSITY CATHODES

AD 850 447

FINAL REPORT

DDC  
RECEIVED  
APR 21 1969  
REGULATED

By

*Handwritten signature* B

R. J. BONDLEY — W. T. BOYD — R. G. LOCK  
T. J. NALL — M. J. SLIVKA

JANUARY 1969

AD NO. FILE COPY

DISTRIBUTION STATEMENT

Each transmittal of this document outside the Department of Defense must have prior approval of CG, U. S. Army Electronics Command, Fort Monmouth, N. J. 07703 Attn: AMSEL-KL-TQ

# ECOM

UNITED STATES ARMY ELECTRONICS COMMAND - FORT MONMOUTH, N. J., 07703  
CONTRACT DA 28-043 AMC-02289-F  
GENERAL ELECTRIC COMPANY  
Schenectady, N. Y.

ACCESSION FOR	
DEFENSE	WHITE SECTION <input type="checkbox"/>
LOG	BUFF SECTION <input checked="" type="checkbox"/>
ANNOUNCED	<input type="checkbox"/>
CLASSIFICATION	
BY	
DISTRIBUTION/AVAILABILITY CODES	
DIST.	AVAIL. and/or SPECIAL
A	

## NOTICES

### Disclaimers

The findings in this report are not to be construed as an official Department of the Army position, unless so designated by other authorized documents.

The citation of trade names and names of manufacturers in this report is not to be construed as official Government indorsement or approval of commercial products or services referenced herein.

### Disposition

Destroy this report when it is no longer needed. Do not return it to the originator.

1773

Reports Control Symbol

OSD-1366

⑩ JANUARY 1969

⑫ 207.

Research and Development Technical Report

ECOM 02289.F

⑮

⑰

① HIGH CURRENT DENSITY CATHODES.

② Rept. no. 7 (FINAL) REPORT,  
1 JUNE 1966 - 31 AUGUST 1968,

Report No. 7

⑬ CONTRACT NO. DA-28-043-AMC-02289(E)

DA Project No. ⑭ DA-222001-A-055/01 Task-01

Prepared by

⑯ R. J./BONDLEY, - W. T./BOYD, - R. G./LOCK,  
T. J./NALL - M. J./SLIVKA

GENERAL ELECTRIC COMPANY  
SCHENECTADY, NEW YORK

For

US ARMY ELECTRONICS COMMAND, FORT MONMOUTH, N. J. 07703

DISTRIBUTION STATEMENT

Each transmittal of this document outside the Department of Defense must have prior approval of CG, U. S. Army Electronics Command, Fort Monmouth, N. J. 07703 Attn: AMSEL-KL-TQ

11/14/1100

## ABSTRACT

This is the last of a series of reports describing an experimental study of the critical factors and mechanisms involved in achieving high-emission-density cathodes capable of long life and reliable operation in electron tubes. Detailed results of the work of the last reporting period of this investigation are included herein, along with a review of the more significant developments of the entire two-year program. All of the objectives of the program have essentially been met, and in some cases exceeded, resulting in a tungstate cathode which represents an advance in the state of the art for high current density emitters. Reliability and reproducibility were demonstrated by consecutively fabricating and life testing eighteen cathodes. No rejects or deviations were encountered, and initial characteristics were uniform for the entire group.

The tungstate cathode is unique in that it can supply higher continuous emission currents over longer periods of time than any other known cathode system. Such performance was substantiated by extensive life testing in diode tubes during the program. This investigation also has led to the development of generally optimum composition and processing procedures (see Appendix A). The tungstate cathode upon which the bulk of the work was placed is a metal-matrix unit containing porous tungsten as the matrix. Distributed uniformly throughout the matrix in specific proportions are a barium-strontium-tungstate compound corresponding to the formula  $\text{Ba}_5\text{Sr}(\text{WO}_6)_2$ , and zirconium. After processing, a surface film of barium zirconate was identified.

In addition to life testing of the standard-composition cathode, as defined in Appendix A, studies were made of other compositions including those containing greater zirconium content. During the last reporting period, eighteen new cathodes, all containing extra zirconium, were started on life test under widely differing emission densities and temperatures. The increased zirconium appears to have stabilized the very low temperature operation, and six cathodes are now beyond the 2,000-hour point with no downward deviations in emission levels.

An analysis of two tungstate cathodes, one of which had completed life test, and the other a new and unactivated cathode, was made of electron diffraction, electron microprobe, electron microscopy, and x-ray diffraction to gain an insight into the emission mechanisms of the barium-strontium-tungstate cathodes. Structural and chemical changes that occur with life were identified.

A review of the resistance to poisoning by various gases and metal vapor deposits on tungstate cathodes was completed.

Sublimation rates for tungstate cathodes were reviewed and compared to the rates of other cathode systems.

Noise properties of the tungstate cathode were determined. The noise properties of a standard barium oxide-on-nickel emitter, and a commercially available barium-aluminate cathode, were evaluated on the same equipment for purposes of comparison.

The emitting characteristics of tungstate cathodes were studied with an emission microscope. The existence of local areas of high emission density dispersed through other areas of low activity was verified at typical operating levels in a diode containing a dissecting anode aperture and an auxiliary current probe.

## FOREWORD

This research and development program was directed toward an experimental study of high current density cathodes for long life and reliable operation in electron tubes. Sponsored by the U.S. Army Electronics Command under Contract DA 28-043 AMC-02289(E), the work was conducted under the technical guidance of the USAECOM Electron Tubes Division, Techniques Branch, and followed Technical Guidelines TT-29A dated 19 November 1965.

TABLE OF CONTENTS

	Page
REPORT . . . . .	1
INTRODUCTION . . . . .	1
LIFE TESTING . . . . .	2
ANALYSIS AND CHARACTERIZATION OF EMITTING SURFACE OF OPTIMUM CATHODES . . . . .	75
POISONING OF TUNGSTATE CATHODES BY GASES AND METAL VAPORS . . . . .	79
Cathode Poisoning by Gases . . . . .	81
Cathode Poisoning by Metal Vapor . . . . .	94
SUBLIMATION FROM BARIUM-STRONTIUM- TUNGSTATE CATHODES . . . . .	96
CATHODE NOISE . . . . .	100
EMISSION MICROSCOPE STUDIES . . . . .	138
CONCLUSIONS AND RECOMMENDATIONS . . . . .	149
REFERENCES . . . . .	153
APPENDIX A - Preparation of Barium-Strontium- Tungstate Cathodes . . . . .	157
APPENDIX B - Surface Characterization of Tungsten Cathodes . . . . .	159
APPENDIX C - Preparation and Processing of Barium- Strontium Tungstate Cathodes Containing Extra Amounts of Zirconium Hydride . . . . .	185

LIST OF ILLUSTRATIONS

Figure		Page
1	Life Test Diode Assembly . . . . .	3
2	Overall Summary of Life versus Temperature for Standard Tungstate Cathodes Measured in Close-Spaced Diodes . . . . .	5
3	Life Test Record of HCD-3 Cathode . . . . .	12
4	Retest of HCD-4 Cathode (800°C) . . . . .	13
5	Life Test Record of HCD-9 Cathode . . . . .	14
6	Life Test Record of HCD-17 Cathode . . . . .	15
7	Life Test Record of HCD-25 Cathode . . . . .	16
8	Life Test Record of HCD-26 Cathode . . . . .	17
9	Life Test Record of HCD-32 Cathode . . . . .	18
10	Life Test Record of HCD-37 Cathode . . . . .	19
11	Life Test Record of HCD-40 Cathode . . . . .	20
12	Life Test Record of HCD-47 Cathode . . . . .	21
13	Life Test Record of HCD-49 Cathode . . . . .	22
14	Life Test Record of HCD-50 Cathode . . . . .	23
15	Initial Emission Characteristics of HCD-50 Cathode at 850°C, 900°C, 950°C and 975°C . . . . .	24
16	Life Test Record of HCD-51 Cathode . . . . .	25
17	Initial Emission Characteristics of HCD-51 Cathode at 600°C and 650°C . . . . .	26
18	Initial Emission Characteristics of HCD-51 Cathode at 850°C, 900°C and 950°C . . . . .	27
19	Life Test Record of HCD-52 Cathode . . . . .	28
20	Initial Emission Characteristics of HCD-52 Cathode at 850°C, 900°C and 950°C . . . . .	29

Figure		Page
21	Life Test Record of HCD-53 Cathode . . . . .	30
22	Initial Emission Characteristics of HCD-53 Cathode at 850 <sup>o</sup> C, 900 <sup>o</sup> C, 950 <sup>o</sup> C and 975 <sup>o</sup> C . . . . .	31
23	Life Test Record of HCD-54 Cathode . . . . .	32
24	Initial Emission Characteristics of HCD-54 Cathode at 850 <sup>o</sup> C, 900 <sup>o</sup> C, 950 <sup>o</sup> C and 975 <sup>o</sup> C . . . . .	33
25	Life Test Record of HCD-55 Cathode . . . . .	34
26	Initial Emission Characteristic of HCD-55 Cathode at 650 <sup>o</sup> C . . . . .	35
27	Initial Emission Characteristics of HCD-55 Cathode at 850 <sup>o</sup> C, 900 <sup>o</sup> C, 950 <sup>o</sup> C and 975 <sup>o</sup> C . . . . .	36
28	Life Test Record of HCD-56 Cathode . . . . .	37
29	Initial Emission Characteristic of HCD-56 Cathode at 650 <sup>o</sup> C . . . . .	38
30	Initial Emission Characteristics of HCD-56 Cathode at 850 <sup>o</sup> C, 900 <sup>o</sup> C and 950 <sup>o</sup> C . . . . .	39
31	Retest of HCD-56 Cathode (1100 <sup>o</sup> C). . . . .	40
32	Life Test Record of HCD-57 Cathode . . . . .	41
33	Initial Emission Characteristics of HCD-57 Cathode at 650 <sup>o</sup> C . . . . .	42
34	Initial Emission Characteristics of HCD-57 Cathode at 850 <sup>o</sup> C, 900 <sup>o</sup> C and 950 <sup>o</sup> C . . . . .	43
35	Retest of HCD-57 Cathode (1100 <sup>o</sup> C). . . . .	44
36	Retest of HCD-57 Cathode (650 <sup>o</sup> C) . . . . .	45
37	Life Test Record of HCD-58 Cathode . . . . .	46
38	Initial Emission Characteristics of HCD-58 Cathode at 650 <sup>o</sup> C . . . . .	47
39	Initial Emission Characteristics of HCD-58 Cathode at 850 <sup>o</sup> C, 900 <sup>o</sup> C and 950 <sup>o</sup> C . . . . .	48
40	Life Test Record of HCD-59 Cathode . . . . .	49
41	Initial Emission Characteristic of HCD-59 Cathode at 650 <sup>o</sup> C . . . . .	50

Figure		Page
42	Initial Emission Characteristics of HCD-59 Cathode at 850 <sup>o</sup> C, 900 <sup>o</sup> C and 950 <sup>o</sup> C . . . . .	51
43	Life Test Record of HCD-60 Cathode . . . . .	52
44	Initial Emission Characteristics of HCD-60 Cathode at 850 <sup>o</sup> C, 900 <sup>o</sup> C and 950 <sup>o</sup> C . . . . .	53
45	Initial Emission Characteristics of HCD-60 Cathode at 1100 <sup>o</sup> C . . . . .	54
46	Life Test Record of HCD-61 Cathode . . . . .	55
47	Initial Emission Characteristic of HCD-61 Cathode at 650 <sup>o</sup> C . . . . .	56
48	Initial Emission Characteristic of HCD-61 Cathode at 900 <sup>o</sup> C . . . . .	57
49	Life Test Record of HCD-62 Cathode . . . . .	58
50	Initial Emission Characteristics of HCD-62 Cathode at 850 <sup>o</sup> C, 900 <sup>o</sup> C and 950 <sup>o</sup> C . . . . .	59
51	Life Test Record of HCD-63 Cathode . . . . .	60
52	Initial Emission Characteristics of HCD-63 Cathode at 850 <sup>o</sup> C, 900 <sup>o</sup> C and 950 <sup>o</sup> C . . . . .	61
53	Life Test Record of HCD-64 Cathode . . . . .	62
54	Initial Emission Characteristics of HCD-64 Cathode at 850 <sup>o</sup> C, 900 <sup>o</sup> C, 950 <sup>o</sup> C and 975 <sup>o</sup> C . . . . .	63
55	Life Test Record of HCD-65 Cathode . . . . .	64
56	Initial Emission Characteristics of HCD-65 Cathode at 850 <sup>o</sup> C, 900 <sup>o</sup> C and 950 <sup>o</sup> C . . . . .	65
57	Life Test Record of HCD-66 Cathode . . . . .	66
58	Initial Emission Characteristic of HCD-66 Cathode at 650 <sup>o</sup> C . . . . .	67
59	Initial Emission Characteristics of HCD-66 Cathode at 850 <sup>o</sup> C, 900 <sup>o</sup> C and 950 <sup>o</sup> C . . . . .	68
60	Life Test Record of HCD-67 Cathode . . . . .	69
61	Initial Emission Characteristic of HCD-67 Cathode at 650 <sup>o</sup> C . . . . .	70

Figure		Page
62	Initial Emission Characteristic of HCD-67 Cathode at 950 <sup>o</sup> C . . . . .	71
63	Vacuum System Used for Cathode Poisoning Studies . . . . .	80
64	Emission Poisoning by Oxygen . . . . .	82
65	Emission Poisoning by Carbon Monoxide . . . . .	83
66	Emission Poisoning by Carbon Dioxide . . . . .	84
67	Emission Enhancement by Methane and Hydrogen . . . . .	85
68	Emission Poisoning by Oxygen . . . . .	86
69	Emission Poisoning by Carbon Monoxide . . . . .	87
70	Emission Poisoning by Carbon Dioxide . . . . .	88
71	Emission Poisoning by Oxygen over Longer Period of Time . . . . .	89
72	Emission Poisoning by Carbon Dioxide over Longer Period of Time . . . . .	90
73	Comparison of Emission Poisoning by Oxygen of a UHR-CRT Cathode with a Conventional-Size Tungstate Cathode and a Barium Orthosilicate Cathode . . . . .	91
74	Survey of Sublimation Rates of Various Cathode Systems . . . . .	98
75	Sublimation Rates of Various Cathode Systems Measured by Deposit Thickness Monitor . . . . .	99
76	Current Density versus Evaporation Rate . . . . .	101
77	Simplified Circuit Diagram of Diode and RF Circuitry Used in Noise Measurement . . . . .	102
78	Block Diagram of Noise Measuring Equipment . . . . .	103
79	Diode Characteristic Measured by Williams . . . . .	105
80	Noise Measured by Williams . . . . .	106
81	Noise for High Anode Potentials Measured by Williams . . . . .	107

Figure		Page
82	Noise Normalized to Temperature-Limited Value (Tube No. 112) . . . . .	108
83	Noise Normalized to Space-Charge Limited Value (Tube No. 112) . . . . .	109
84	Current Analysis for Tube No. 112 at 550 <sup>o</sup> C . . . . .	111
85	Current Analysis for Tube No. 112 at 600 <sup>o</sup> C . . . . .	112
86	Current Analysis for Tube No. 112 at 725 <sup>o</sup> C . . . . .	113
87	Current Analysis for Tube No. 112 at 850 <sup>o</sup> C . . . . .	114
88	Measured Noise Normalized to the Temperature-Limited Value for Tube No. HCD-67 . . . . .	115
89	Measured Noise Normalized to the Space-Charge Limited Value for Tube No. HCD-67 . . . . .	116
90	Current Analysis for Tube No. HCD-67 at 550 and 600 <sup>o</sup> C . . . . .	117
91	Current Analysis for Tube No. HCD-67 at 650 <sup>o</sup> C . . . . .	118
92	Current Analysis for Tube No. HCD-67 at 725 <sup>o</sup> C (first run) . . . . .	119
93	Current Analysis for Tube No. HCD-67 at 725 <sup>o</sup> C (second run) . . . . .	120
94	Current Analysis for Tube No. HCD-67 at 800 <sup>o</sup> C . . . . .	121
95	Current Analysis for Tube No. HCD-67 at 850 <sup>o</sup> C . . . . .	122
96	Measured Noise Normalized to Temperature-Limited Value for Tube No. HCD-9 . . . . .	123
97	Measured Noise Normalized to Space-Charge Limited Value for Tube No. HCD-9 . . . . .	124
98	Current Analysis for Tube No. HCD-9 at 850 <sup>o</sup> C . . . . .	125
99	Current Analysis for Tube No. HCD-9 at 900 <sup>o</sup> C . . . . .	126
100	Measured Noise Normalized to Temperature-Limited Value for Tube No. 116 . . . . .	128
101	Measured Noise Normalized to Space-Charge Limited Value for Tube No. 116 . . . . .	129

Figure		Page
102	Current Analysis for Tube No. 116 at 1000 <sup>o</sup> C . . .	130
103	Current Analysis for Tube No. 116 at 1100 <sup>o</sup> C . . .	131
104	Measured Noise Normalized to Temperature- Limited Value for Tube No. HCD-44 . . . . .	132
105	Measured Noise Normalized to Space-Charge Limited Value for Tube No. HCD-44 . . . . .	133
106	Current Analysis for Tube No. HCD-44 at 1000 <sup>o</sup> C . . . . .	134
107	Current Analysis for Tube No. HCD-44 at 1050 <sup>o</sup> C . . . . .	135
108	Current Analysis for Tube No. HCD-44 at 1100 <sup>o</sup> C . . . . .	136
109	Emission Properties of Various Cathodes Measured for a Constant Noise Performance . . .	137
110	Electron Gun Schematic . . . . .	139
111	Electron Gun Used in Emission Microscope Study .	140
112	Emission Microscope Assembly . . . . .	141
113	Representative Emission Patterns . . . . .	142
114	Photomicrograph of a Machined Tungstate Cathode .	144
115	Details of Diode Used for Analyzing Emissive Surface . . . . .	145
116	Emission Profile Across a 0.110-Inch Diameter Tungstate Cathode . . . . .	146

## REPORT

### INTRODUCTION

This final report includes a review of the salient results of the entire program, in addition to the more detailed results of the work performed since the publication of Tri-annual Report No. 2, dated May 1968.

The technical guidelines for this program cover the requirements for an experimental study of high emission density cathodes for long life and reliable operation in electron tubes. The major objective of this research and development program was a study of the critical factors and mechanisms involved in achieving reproducible high emission density cathodes for the following specific applications:

- (a) Cathodes with very long life (tens of thousands of hours), low sublimation rates at temperatures below  $600^{\circ}\text{C}$ , with the objectives of  $500^{\circ}\text{C}$  at a current density of  $50 \text{ MA}/\text{cm}^2$ .
- (b) Long life cathodes (thousands of hours) for reliable operation in the  $3\text{-}10 \text{ A}/\text{cm}^2$  current density range, with low sublimation rates at the lowest possible temperature.
- (c) Cathodes capable of delivering  $30 \text{ A}/\text{cm}^2$  with reproducible life (hundreds of hours), reasonable sublimation rates and high reliability.

In addition to the studies concerning cathode composition, preparation and processing, other tasks include:

- (a) Measurement of current density as a function of temperature and plate voltage, and a derivation of work function.
- (b) Measurement of sublimation rate and products.
- (c) Measurement of poisoning by gases and metal vapors.
- (d) Measurement of noise.

- (e) Electron-beam microscope analyses of the cathode surface.
- (f) X-ray emission spectroscopy analysis of optimum cathodes.
- (g) Surface characterization in an attempt to determine the emission mechanisms.
- (h) Evaluation of cathode reliability and reproducibility.

## LIFE TESTING

The initial characteristics of a cathode can be determined rapidly after activation and preliminary aging. However, the relationships between cathode life and its composition, preparation, and processing can only be derived with assurance by actual life testing. In order to evaluate the cathode alone, ie., in an environment free from variables introduced by the test vehicle, it was necessary to first design a life test diode capable of dissipating high emission currents, and also possessing a high degree of reproducibility.

Such a diode was developed and subsequently used in all the cathode life tests, proving to be a very reliable and satisfactory vehicle for the purpose. Its general construction is shown in Figure 1. Pertinent features include an all metal-ceramic vacuum enclosure to impart dimensional stability; a water-cooled copper anode to allow high energy concentration; and a sapphire viewing window for optically monitoring cathode temperature, as a cross-check on the temperature determined by means of a platinum, platinum-rhodium thermocouple attached to the cathode sleeve. A small ion pump served the dual purpose of maintaining the integrity of the vacuum and monitoring the gas evolution patterns throughout the test.

Previous studies<sup>1,2</sup> established the potential of the barium-strontium-tungstate activated matrix cathode for high emission densities and long life. In the present program, additional studies were conducted on modifications of the basic tungstate matrix cathode, including the composition and processing of the cathode materials and life testing in a standardized diode under various temperatures and current densities. The effects of evaporated metallic coatings over the cathode emitting surfaces were evaluated, and various analytical techniques, such as x-ray and emission microscope, electron diffraction, electron microscope and microprobe analysis were conducted to characterize the emitting surface and to gain an understanding of the mechanisms of the cathode.

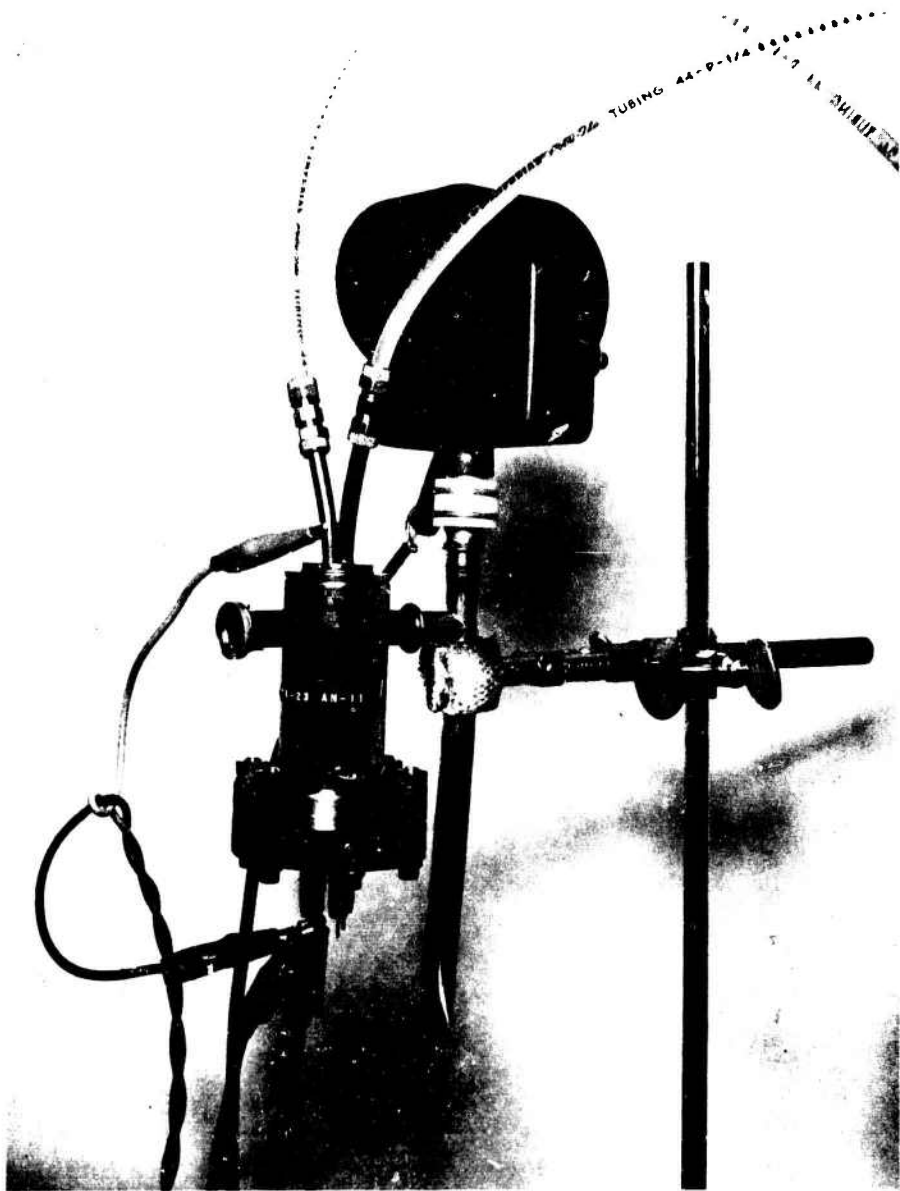


Figure 1 - Life Test Diode Assembly

From the many cathodes studied, 66 cathodes were chosen as being worthy of extended life test evaluations. From this number, only 56 cathodes had accumulated hours on test, with the other ten being lost during diode assembly, processing, or from vacuum leaks in the diode bodies. Life characteristics were taken over a wide range of temperatures and current densities, ranging from 600°C to 1100°C, and from 50 milliamperes to 30 amperes per square centimeter, respectively.

Figure 2 is a summary of life versus temperature for standard tungstate cathodes as measured in close-spaced diodes during the program. These data were selected from those cathodes that have reached end of life (a point arbitrarily chosen as the value where cathode emission has fallen 10 percent or more from its initial value) due to natural wearout. No included are the failures induced by other unrelated causes. The solid line on this curve represents an average of actual accumulated data, while the dotted portion is an extrapolation for predicting cathode life at the lower temperature conditions. These results are typical of those encountered in low-voltage diodes, and should be indicative of life in favorable tube environments. In less favorable tube environments, however, life predictions may be significantly altered by conditions such as excessive ion bombardment resulting from the presence of residual gases in high-voltage tubes, or the presence of evaporated metallic coatings caused by electron collection on various tube components. To achieve the maximum life of any thermionic cathode system -- the tungstate cathode is no exception -- a non-hostile environment must be provided.

At the close of this final reporting period, a total of 56 cathodes had been started on life test. Eighteen of these -- numbers HCD-50 through HCD-67 -- were new cathodes not previously reported. Nine cathodes -- numbers HCD-3, -25, -37, -49, -58, -59, -60, -63, and -65 -- were removed from test, leaving a total of twenty cathodes still operating.

The final eighteen cathodes placed on test, a group having identical composition and uniform processing, contained double the amount of zirconium employed in the standard mix defined in Appendix A. The intention for this group, in addition to determining the effects of the extra zirconium, was to gain an insight into the spread of emission characteristics and variations in life that can be expected from repetitive construction of tungstate cathodes.

In preparing this group of cathodes containing double the amount of zirconium, a different compaction pressure and sintering schedule were found to be necessary. Details for this composition are given in Appendix C. Once this new schedule was established, all eighteen cathodes -- HCD-50 through HCD-67 -- were assembled in sequence with no rejects or defects occurring during processing or testing. The initial characteristics of this group of

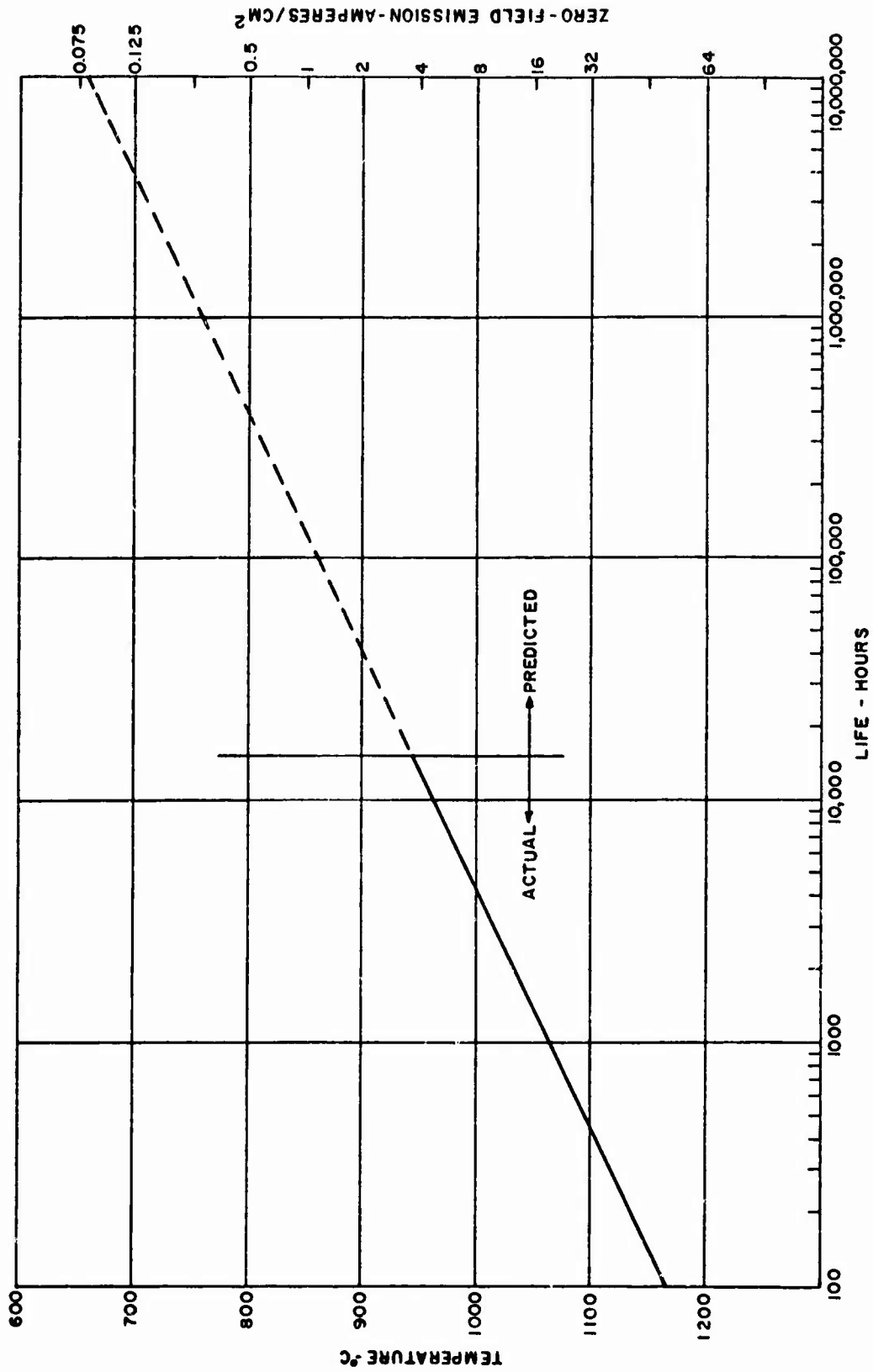


Figure 2 - Overall Summary of Life versus Temperature for Standard Tungstate Cathodes Measured in Close-Spaced Diodes

cathodes, as shown by the corresponding emission/temperature data curves taken from life test diodes, were remarkably uniform.

A summary of the results of all the cathodes that were on life test at the start of the last reporting period, and of the new cathodes placed on life during this interval, follows. Associated curves for the final-period cathodes are also included as Figures 3 through 62. These curves are tabulated on the next page opposite their corresponding tube designations to facilitate reference. A comprehensive summary of all life test results up to the close of the final period is given in Tables I and II. Cathodes having completed test are presented in Table I on pages 72 and 73, with cathodes currently on test given in Table II on page 74.

<u>Fig. No.</u>	<u>Tube No.</u>	<u>Fig. No.</u>	<u>Tube No.</u>
3	HCD-3 (Life Test)	33	HCD-57 (Emission)
4	HCD-4 (Retest)	34	HCD-57 (Emission)
5	HCD-9 (Life Test)	35	HCD-57 (Retest)
6	HCD-17 (Life Test)	36	HCD-57 (Retest)
7	HCD-25 (Life Test)	37	HCD-58 (Life Test)
8	HCD-26 (Life Test)	38	HCD-58 (Emission)
9	HCD-32 (Life Test)	39	HCD-58 (Emission)
10	HCD-37 (Life Test)	40	HCD-59 (Life Test)
11	HCD-40 (Life Test)	41	HCD-59 (Emission)
12	HCD-47 (Life Test)	42	HCD-59 (Emission)
13	HCD-49 (Life Test)	43	HCD-60 (Life Test)
14	HCD-50 (Life Test)	44	HCD-60 (Emission)
15	HCD-50 (Emission)	45	HCD-60 (Emission)
16	HCD-51 (Life Test)	46	HCD-61 (Life Test)
17	HCD-51 (Emission)	47	HCD-61 (Emission)
18	HCD-51 (Emission)	48	HCD-61 (Emission)
19	HCD-52 (Life Test)	49	HCD-62 (Life Test)
20	HCD-52 (Emission)	50	HCD-62 (Emission)
21	HCD-53 (Life Test)	51	HCD-63 (Life Test)
22	HCD-53 (Emission)	52	HCD-63 (Emission)
23	HCD-54 (Life Test)	53	HCD-64 (Life Test)
24	HCD-54 (Emission)	54	HCD-64 (Emission)
25	HCD-55 (Life Test)	55	HCD-65 (Life Test)
26	HCD-55 (Emission)	56	HCD-65 (Emission)
27	HCD-55 (Emission)	57	HCD-66 (Life Test)
28	HCD-56 (Life Test)	58	HCD-66 (Emission)
29	HCD-56 (Emission)	59	HCD-66 (Emission)
30	HCD-56 (Emission)	60	HCD-67 (Life Test)
31	HCD-56 (Retest)	61	HCD-67 (Emission)
32	HCD-57 (Life Test)	62	HCD-67 (Emission)

HCD-3 Cathode (Figure 3): This cathode operated at a temperature of 950°C and a current level of 6.5 A/cm<sup>2</sup> out to 6700 hours. Although a minor decline in emission was noted after a cooling-water stoppage occurred at this point, the cathode was still operating at 5.75 A/cm<sup>2</sup> at the 11,700-hour mark. After 14,000 hours of operation, emission declined rapidly to approximately 2 A/cm<sup>2</sup> at 14,300 hours, at which point testing was terminated.

HCD-4 Cathode (Figure 4): The HCD-4 cathode has accumulated 16,500 hours of operation at 800°C, with a constant current density of approximately 0.40 A/cm<sup>2</sup>. Life testing continues.

HCD-9 Cathode (Figure 5): At 10,450 hours, this cathode was operating at a current level of 5.15 A/cm<sup>2</sup> at a temperature of 900°C. Emission has steadily declined thereafter to approximately 3 A/cm<sup>2</sup> at 16,000 hours. Life testing continues.

HCD-17 Cathode (Figure 6): This cathode differs from the standard composition in that the tungstates were fired three times while they were being prepared, instead of the two firings usually employed. After operating steadily at 900°C at an emission of 1.65 A/cm<sup>2</sup> out to 10,000 hours, the emission increased to 2.16 A/cm<sup>2</sup> at the 13,000-hour point. At 15,000 hours, emission still continues stably at the 2.16 A/cm<sup>2</sup> level. Life testing continues.

HCD-25 Cathode (Figure 7): The processing of this cathode deviated from standard, in that the preactivation step (a 10 minute flash at 1200°C) was not used. Operating at 950°C, the HCD-25 cathode emitted stably out to 8500 hours, at which point the test was terminated. Over this interval, the initial current density of 4 A/cm<sup>2</sup> declined only slightly to approximately 3.5 A/cm<sup>2</sup> at end of test, despite a cooling-water deficiency which occurred at the 3500-hour point.

HCD-26 Cathode (Figure 8): Originally operating at 950°C and 5 A/cm<sup>2</sup>, this cathode continues to exhibit increasing emission, reaching 5.5 A/cm<sup>2</sup> at 9,000 hours and 6 A/cm<sup>2</sup> at 13,000 hours. Life testing continues.

HCD-32 Cathode (Figure 9): The HCD-32 cathode was placed on operation at 750°C and a current density of 0.15 A/cm<sup>2</sup>. This emission has increased with time, as shown in Figure 9, and is currently at 0.24 A/cm<sup>2</sup> after logging 12,000 hours. Life testing continues.

HCD-37 Cathode (Figure 10): This test was one of a series conducted to determine the lowest stable operating temperature of the standard-mix cathode. The HCD-37 cathode was placed on life test at 700°C on a emission density of 0.05 A/cm<sup>2</sup>. After an initial drop, emission remained stable at 0.045 A/cm<sup>2</sup> up to 5200 hours, at which point it was removed from test.

HCD-40 Cathode (Figure 11): The HCD-40 cathode, which contains a higher zirconium content (0.734 w/o) than the standard mix, began operation at 650°C and 0.075 A/cm<sup>2</sup>. Generally stable emission has been maintained at this level out to the 1,000-hour point. Life testing continues.

HCD-47 Cathode (Figure 12): This cathode constituted a special test involving twice the normal zirconium content, a compaction pressure of 78 TSI and 2.5 minutes of sintering. Starting on test at a temperature of 650°C and an emission density of 0.12 A/cm<sup>2</sup>, this cathode has exhibited stable emission with time and has currently logged 8000 hours of operation. A definite improvement in the low-temperature operation of tungstate cathodes is in evidence here, through the use of additional zirconium. Life testing continues.

HCD-49 Cathode (Figure 13): The HCD-49 cathode was identical to HCD-47 in composition and processing, with the exception that a compacting pressure of 95 TSI was applied in this case. The higher pressure was used because it has been observed that the denser compacts improve the machining properties of the cathode. Through evaluations of life versus various compaction pressures, the optimum cathode density can be ascertained. Operating at 1050°C, this cathode remained within the range of 13 to 14.75 A/cm<sup>2</sup> through 2500 hours, followed by a gradual decline to approximately 9 A/cm<sup>2</sup> at 3000 hours, at which point the test was terminated.

HCD-50 through HCD-67 Cathodes (Figure 14-62): This group comprises the final eighteen cathodes placed on life test during the program. All of these cathodes contained double the zirconium content (Appendix C) employed in the standard mix (Appendix A). Special emphasis was placed on making them uniform in terms of composition and processing. Six cathodes of this group were started on life at 650°C at a current density of approximately 0.050 A/cm<sup>2</sup>; six were started at 975°C and 8 A/cm<sup>2</sup>; and six were started at 1100°C and 30 A/cm<sup>2</sup>.

It was the initial intent of this portion of the life test program to operate the second group of six cathodes at 950°C and at a current density of 8 A/cm<sup>2</sup>. The first diodes constructed for life test indicated that this emission level was borderline with the particular batch of emission material prepared for this test. With the concurrence of the sponsoring agency, the cathode

temperature was increased to 975°C for the 8 A/cm<sup>2</sup> condition. At the same time, a new batch of emission material was processed, and all eighteen life test cathodes were made from this new batch.

An examination of the characteristic curves (Figures 14 through 62) reveals the excellent uniformity existing throughout this group. The initial emission appeared to be comparable to that obtained from the majority of the standard composition cathodes. However, in the high-temperature and high-emission tests (Conditions "b" and "c"), the cathode emission declined uniformly with time. Figures 14, 19, 21, 23, 62, and 64 illustrate this for Condition "b" (8 A/cm<sup>2</sup>). Such a decline in emission might be caused by operating the cathode too close to the knee of the volt/ampere curve (the point where the emission changes from space-charge-limited current to temperature-limited conditions).

This decline in emission with time did not occur in most of the standard composition cathodes life tested under similar conditions. For example, in reviewing the performance of standard composition cathodes, cathode number BTA-6, which was operated at a lower temperature of 950°C and 8 A/cm<sup>2</sup>, exhibited a rising emission during the first 800 hours on life, and in spite of equipment difficulties, remained quite constant over a 2200-hour period. Similarly, cathode HCD-2, operating at 8 A/cm<sup>2</sup>, but at the higher temperature of 1000°C, showed constant emission characteristics over the first 1800 hours on life. Cathode HCD-3, operating at 950°C, but at a current density of 6.5 A/cm<sup>2</sup>, had a flat emission characteristic to well past 10,000 hours. Cathode HCD-14, operating at 1000°C exhibited a rising emission current from 7.5 A/cm<sup>2</sup> to 8.5 A/cm<sup>2</sup> over the first 300 hours on life. Other life test cathodes -- numbers HCD-15, HCD-25, HCD-26, HCD-27, HCD-31, and HCD-33 -- all operating at 950°C, but at lower emission levels, exhibited either a flat or rising current during the early stages of life testing.

The decline in emission experienced with the double zirconium cathodes life tested at 1100°C, 30 A/cm<sup>2</sup> (Condition "c") can be seen in the data for cathodes HCD-58, HCD-60, HCD-63, and HCD-65 (Figures 37, 43, 51 and 55, respectively). Three other cathodes of this group -- HCD-56, HCD-57, and HCD-59 -- received special aging in an attempt to stabilize emission at this high current level. Of these three, cathode HCD-59 alone exhibited superior performance and maintained a flat emission characteristic to 800 hours.

By comparison, standard composition cathodes operated under Condition "c" -- HCD-5, HCD-6, HCD-7, HCD-8, HCD-12, and HCD-21 --

generally exhibited the flat or rising emission patterns during the early stages on life test. There was a wider spread in characteristics in this group, but this spread could be attributed to minor variations in processing which were being studied with these cathodes.

This pattern was reversed at very low temperature (Condition "a"), however, where the emission of the double zirconium cathodes remained constant or increased with time, thus providing a high degree of probability that the extremely long life objective of this program has been met. Although the 500°C target was not attained, the 600°C objective has been demonstrated in life test diode HCD-51. The remaining seven cathodes are on life test at 650°C. Several of these -- namely, HCD-47, HCD-57, HCD-61, and HCD-66 -- all have a 0.050 A/cm<sup>2</sup> emission capability at 600°C, although they are on test at 650°C and at higher current densities. Two cathodes, HCD-40 and HCD-47, are well beyond 10,000 hours on life test with no indication of emission deterioration. Cathodes HCD-51 and HCD-55 are beyond the 5,000 hour mark with similar stable characteristics.

Further, in preparing the final eighteen life-test cathodes, some evidence was encountered that prolonged operation at a low temperature and low current density contributed to more stable operation at the 30 A/cm<sup>2</sup> levels (as shown by the excellent performance of cathode HCD-59, where a preliminary aging of 600 hours at 650°C preceded the high-temperature tests). Accordingly, cathode HCD-57, which had operated for 1600 hours at 0.117 A/cm<sup>2</sup> at 650°C, was rescheduled to 30 A/cm<sup>2</sup> (Condition "c"). However, a power failure of the DC lines to the building at the 100-hour point allowed the cathode to overheat due to the loss of electron cooling at this high emission level. A declining emission up to the 250-hour point (as possibly caused by the overtemperature) made this test inconclusive and the cathode was again rescheduled to its original condition ("a"). Although the emission remained fairly constant during the next 1600 hours, it is only half that of the original level of 0.117 A/cm<sup>2</sup>, indicating that the activity was impaired during the high current or overtemperature exposure during operation at 1100°C.

Two exceptions to the otherwise consistent pattern of the double zirconium cathodes were noted in HCD-48 and HCD-59. HCD-48 was the first of the double zirconium cathodes operated for any length of time at 30 A/cm<sup>2</sup>. This test was made to evaluate the effects of the shorter sintering schedule used with this composition. HCD-48 had outstanding emission properties. During the first 250 hours, emission rose from 37 A/cm<sup>2</sup> to over 46 A/cm<sup>2</sup>, and remained at that level to the 500 hour point, where equipment failure

caused permanent damage to the cathode. In subsequent tests, using the same materials and processing procedures, the superior emission properties could not be duplicated.

In summarizing the overall life test results, and in particular the cathodes containing double zirconium it appears that the extra zirconium increases the low temperature activity and makes possible the achievement of goals for Condition "a", i.e., very low temperature, long life, low current density operation. Although the initial activity of this group of cathodes is high, as discussed above, most of these cathodes exhibit a slow but steady drop in emission versus time under Conditions "b" and "c". This behavior is typical of barium oxide on nickel cathodes, where the nickel substrate contains large amounts of active reducing elements; initial activity is high, but emission tends to fall more rapidly with time than in cathodes made with less active nickel.

In spite of the added complications encountered with the cathodes containing the extra zirconium, all eighteen cathodes were processed in sequence, and all exhibited uniform emission characteristics in test diodes. None of the cathodes were rejected at any stage of manufacture or processing. This degree of consistency on a small quantity of eighteen suggests that reproducibility should be no problem on a large manufacturing scale.

It was observed that cathodes containing the higher zirconium content were more susceptible to deterioration by atmospheric moisture after the sintering. Also, in machining these cathodes it was more difficult to obtain a smooth and flawless surface. These observations suggest that it might be profitable to individually adjust cathode composition for every specific current density, or other environmental condition, to obtain maximum life. Many additional life tests are necessary to bracket and document these parameters.

If the factors that contribute to the extremely high activity of cathode HCD-48 can be identified and duplicated, the usefulness of the tungstate matrix cathode could be upgraded by at least another 50 percent. In spite of intensive efforts, the reasons for the appearance of the occasional super cathode have not been isolated. The existence of such cathodes offers unrefuted evidence that a potential for additional upgrading of the tungstate cathode still exists. As a result of the studies conducted during the past two years, cathodes can now be reliably manufactured to consistently deliver 30 A/cm<sup>2</sup> emission. Even further progress in cathode performance can be expected with continued research.

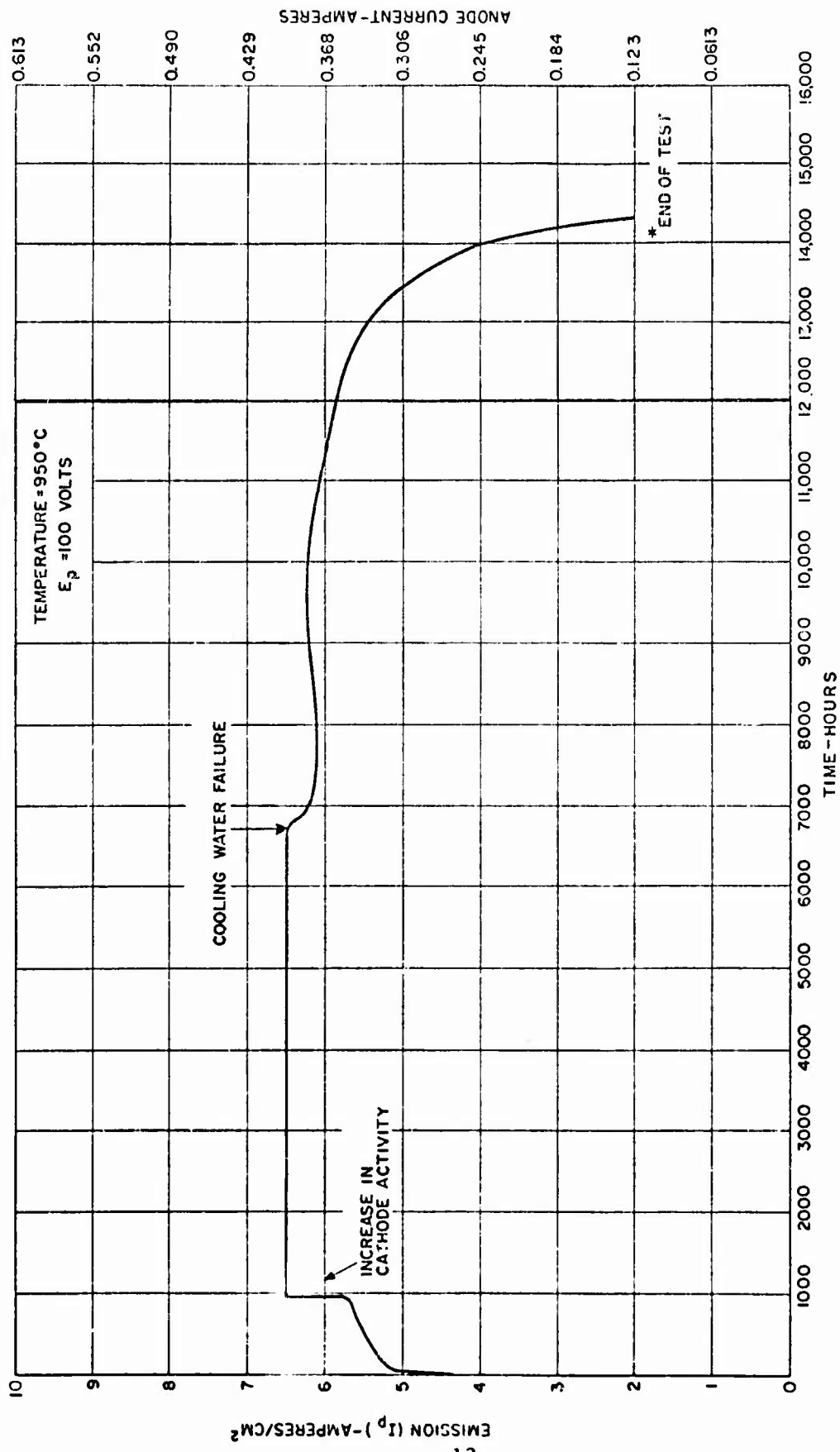


Figure 3 - Life Test Record of HCD-3 Cathode

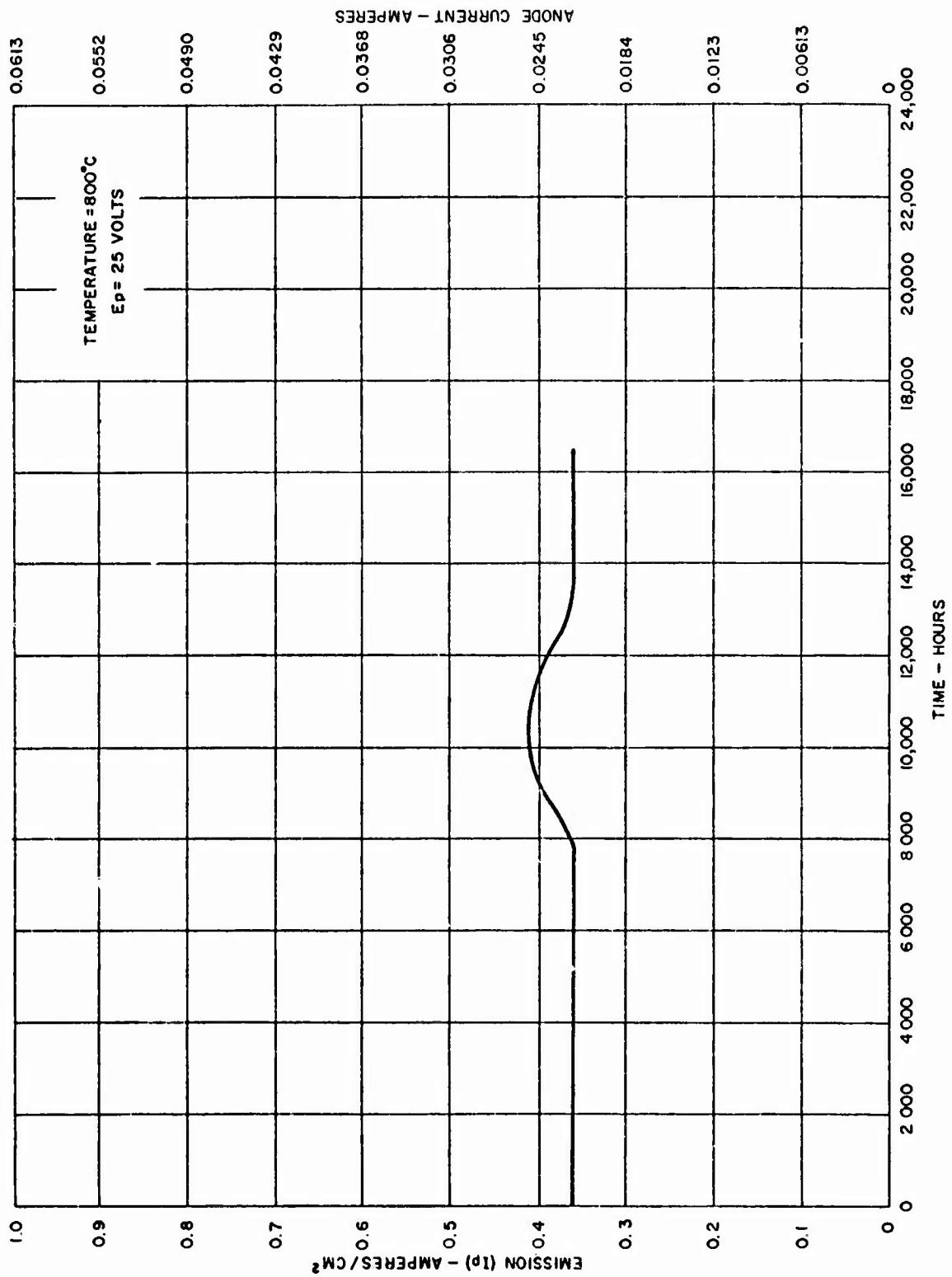


Figure 4 - Retest of HCD-4 Cathode (800°C)

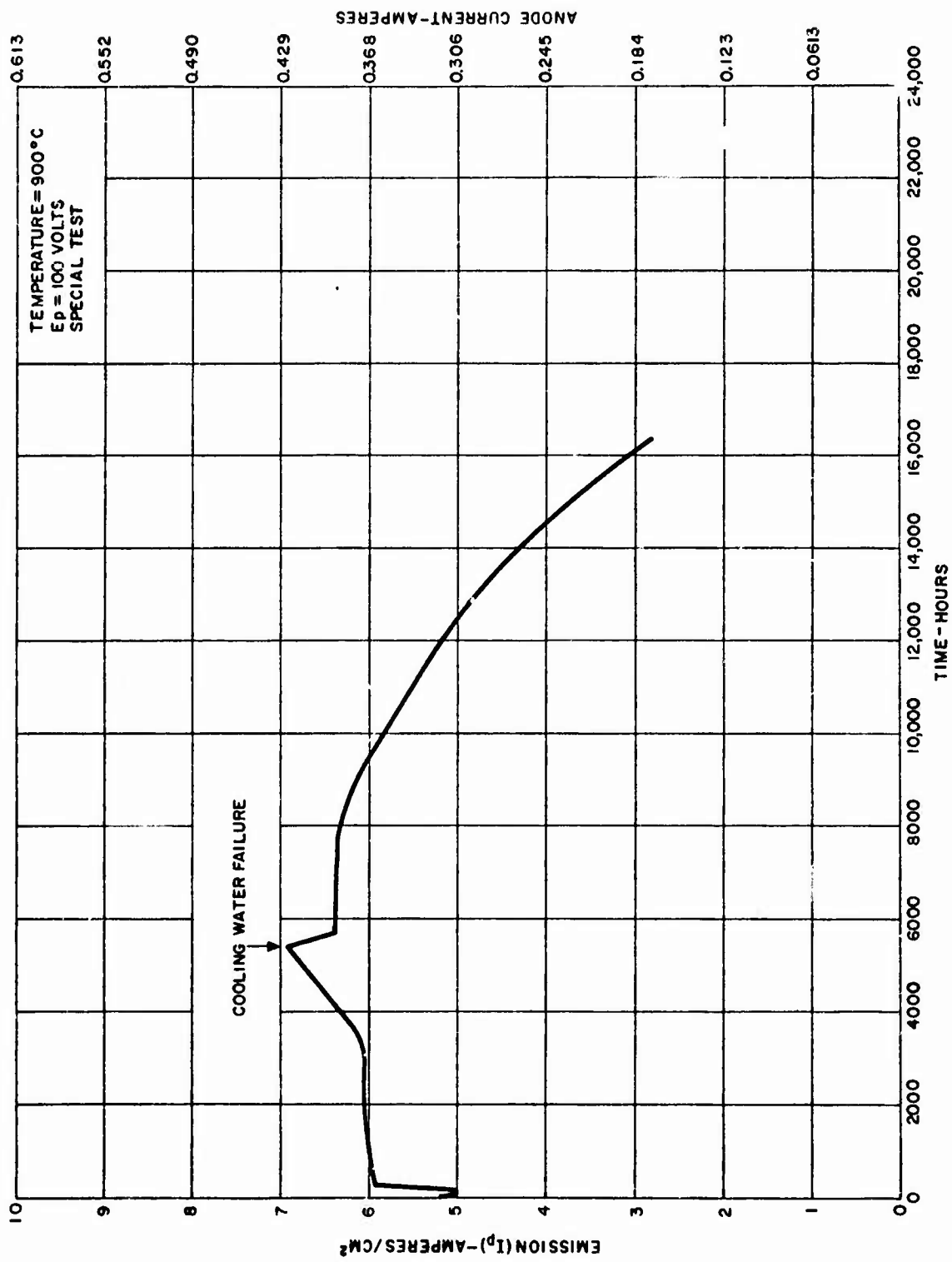


Figure 5 - Life Test Record of HCD-9 Cathode

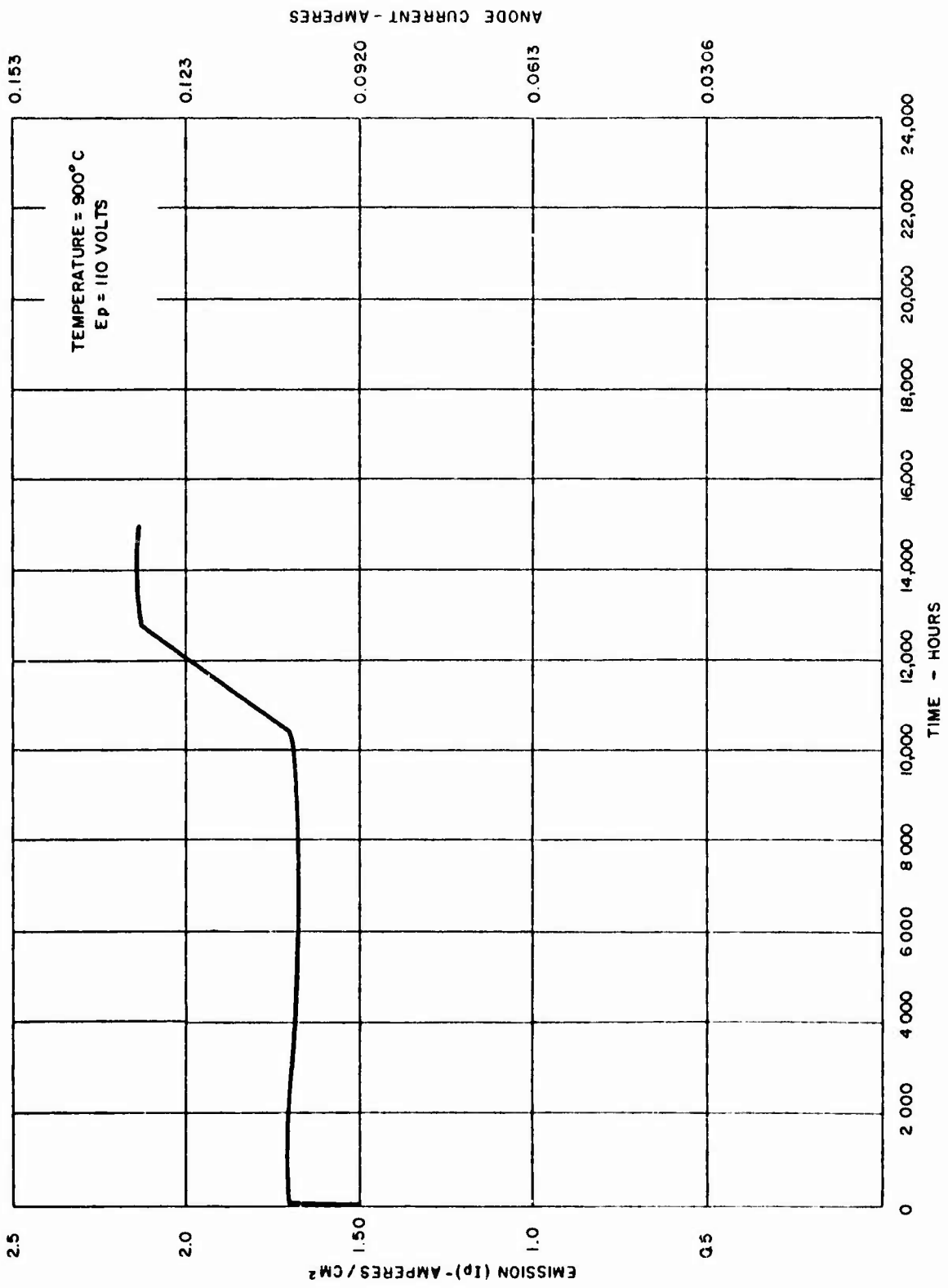


Figure 6 - Life Test Record of HCD-17 Cathode

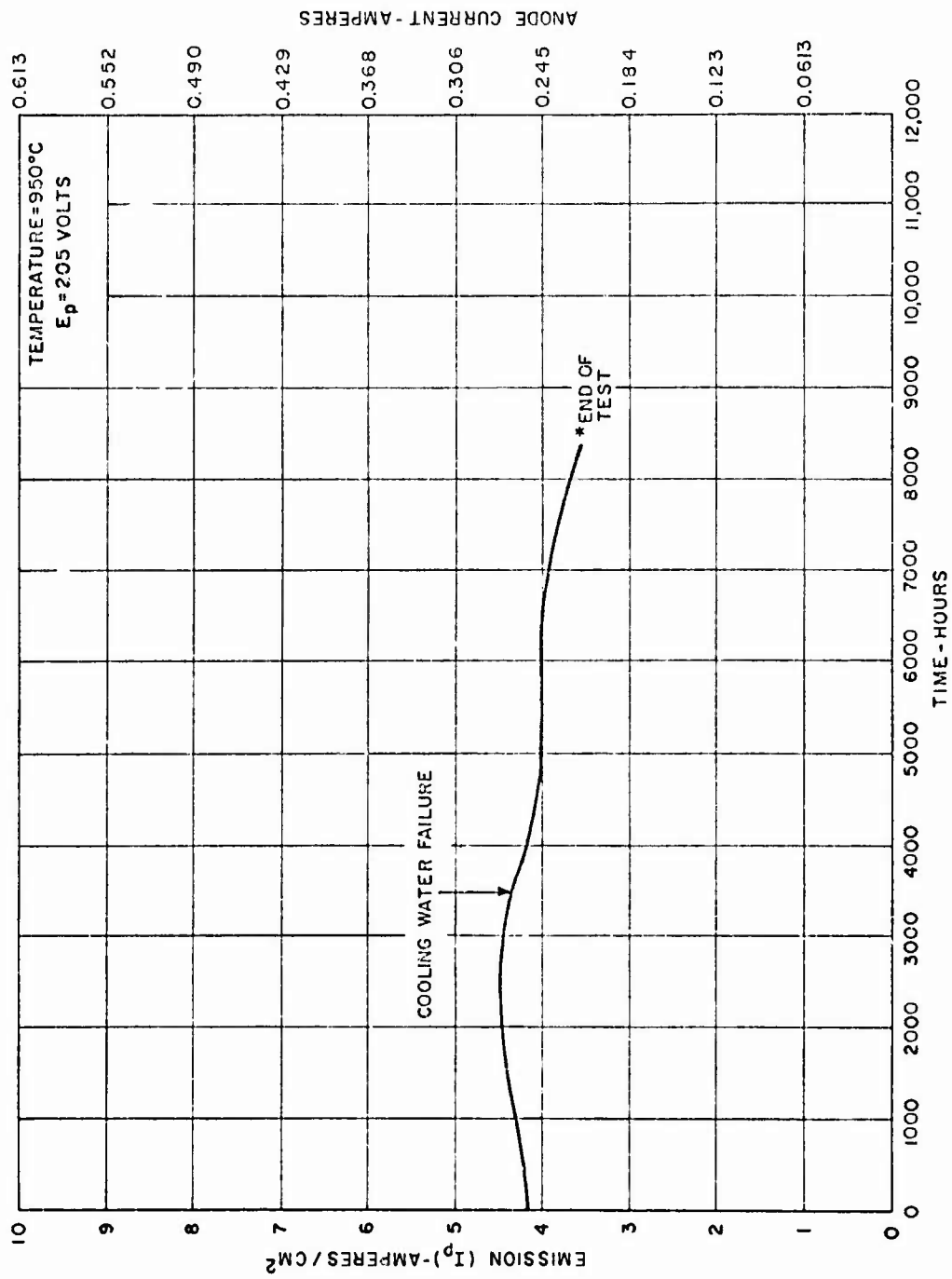


Figure 7 - Life Test Record of HCD-25 Cathode

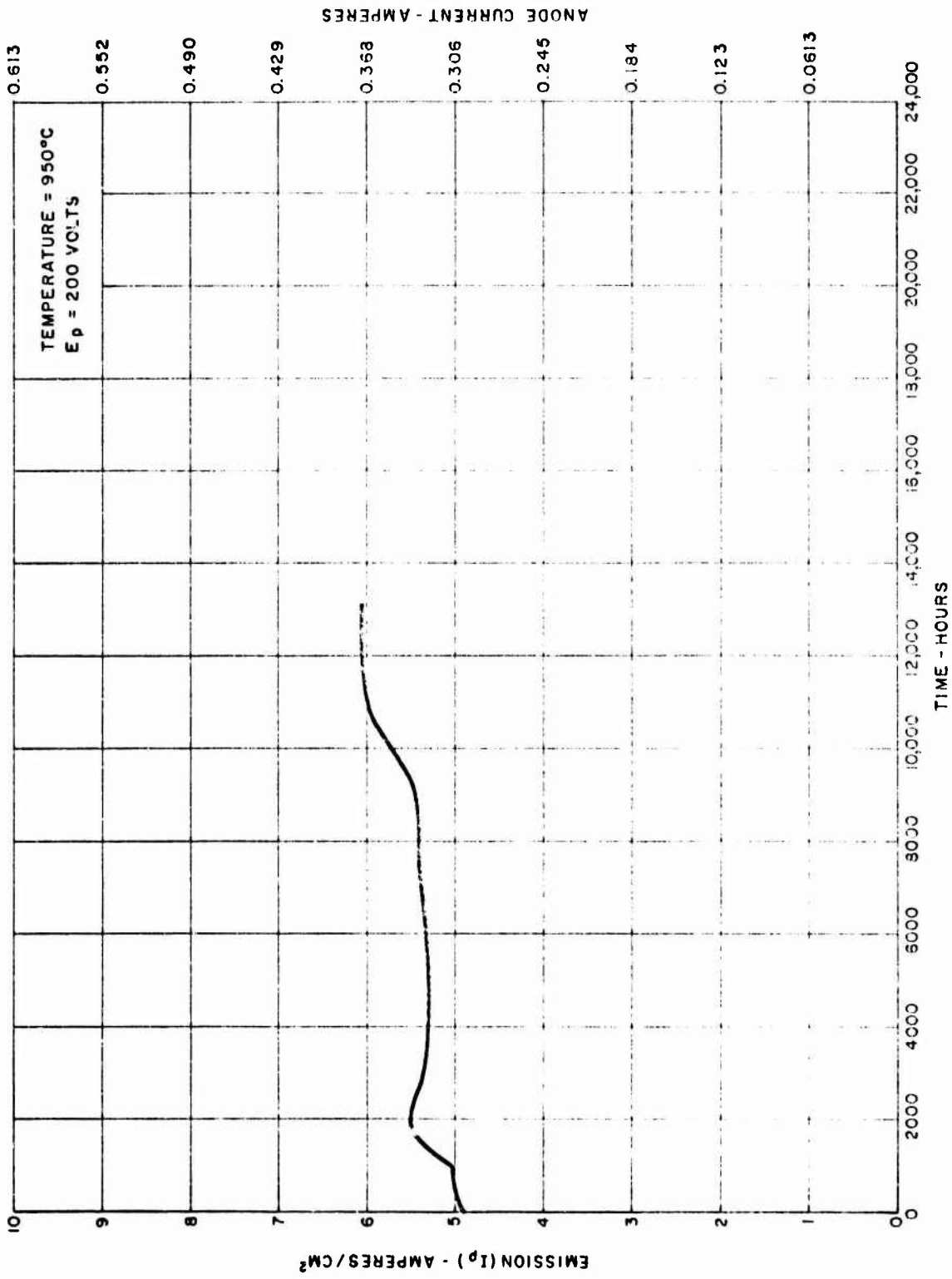


Figure 8 - Life Test Record of HCD-26 Cathode

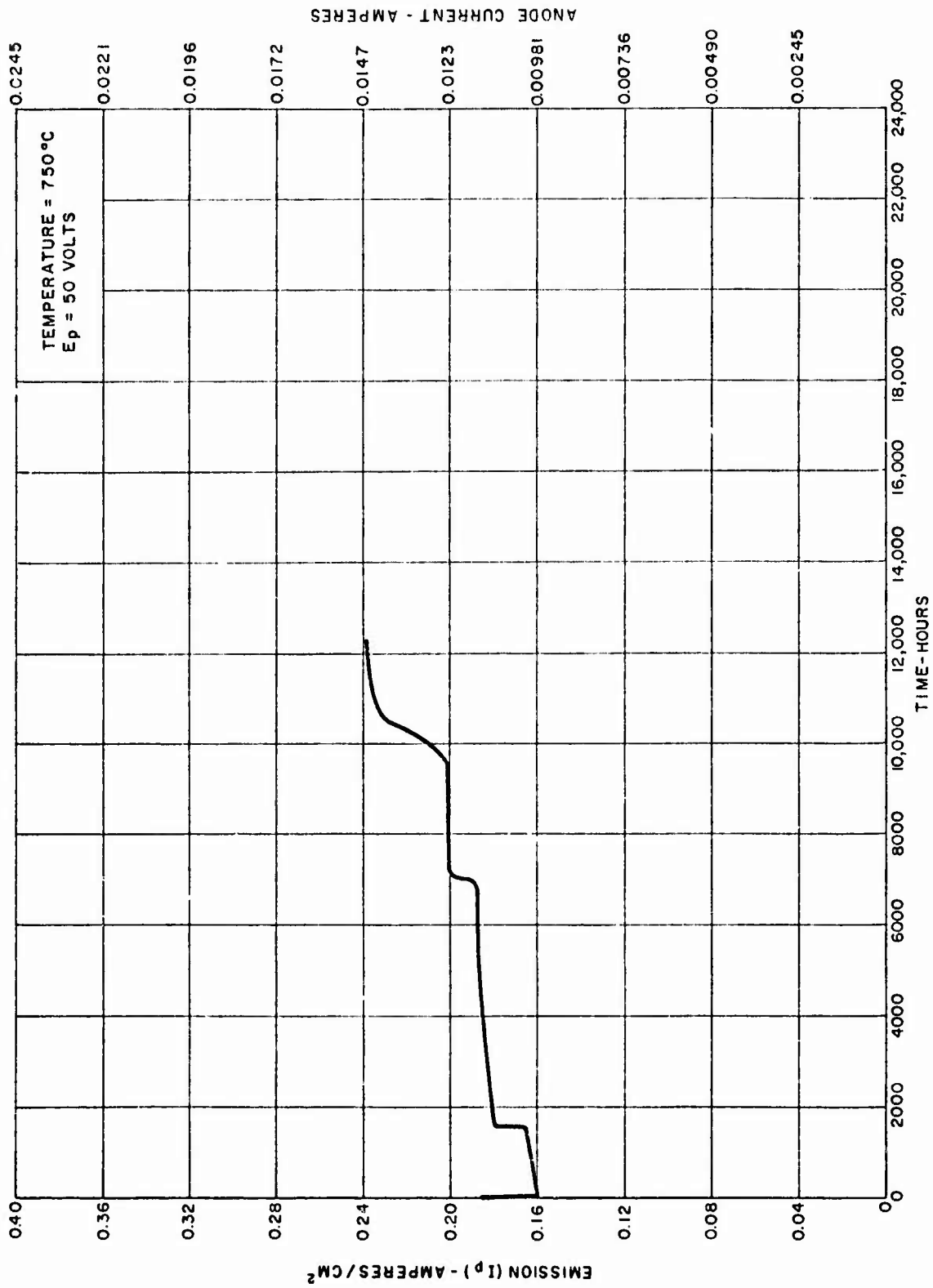


Figure 9 - Life Test Record of HCD-32 Cathode

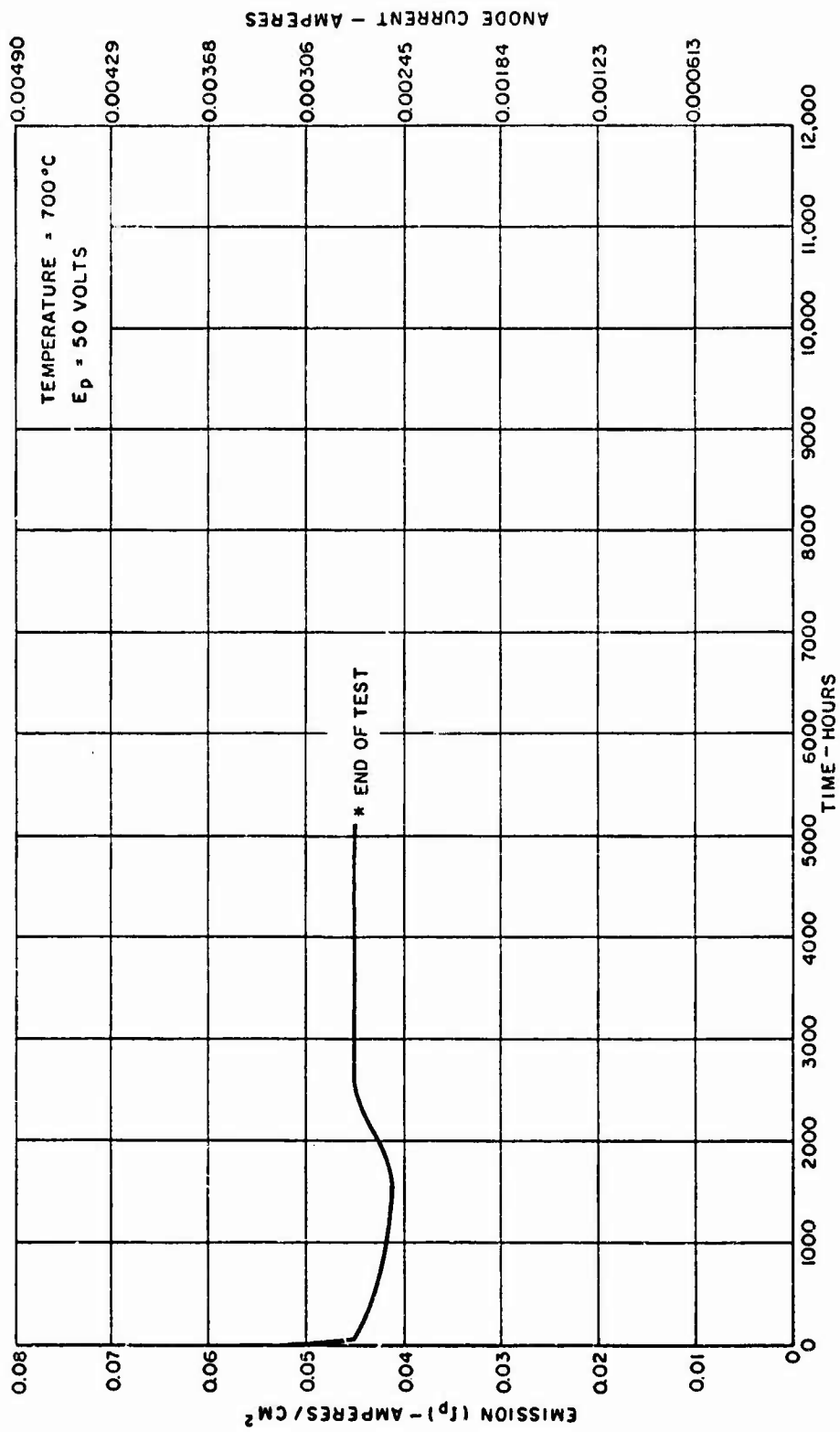


Figure 10 - Life Test Record of HCD-37 Cathode

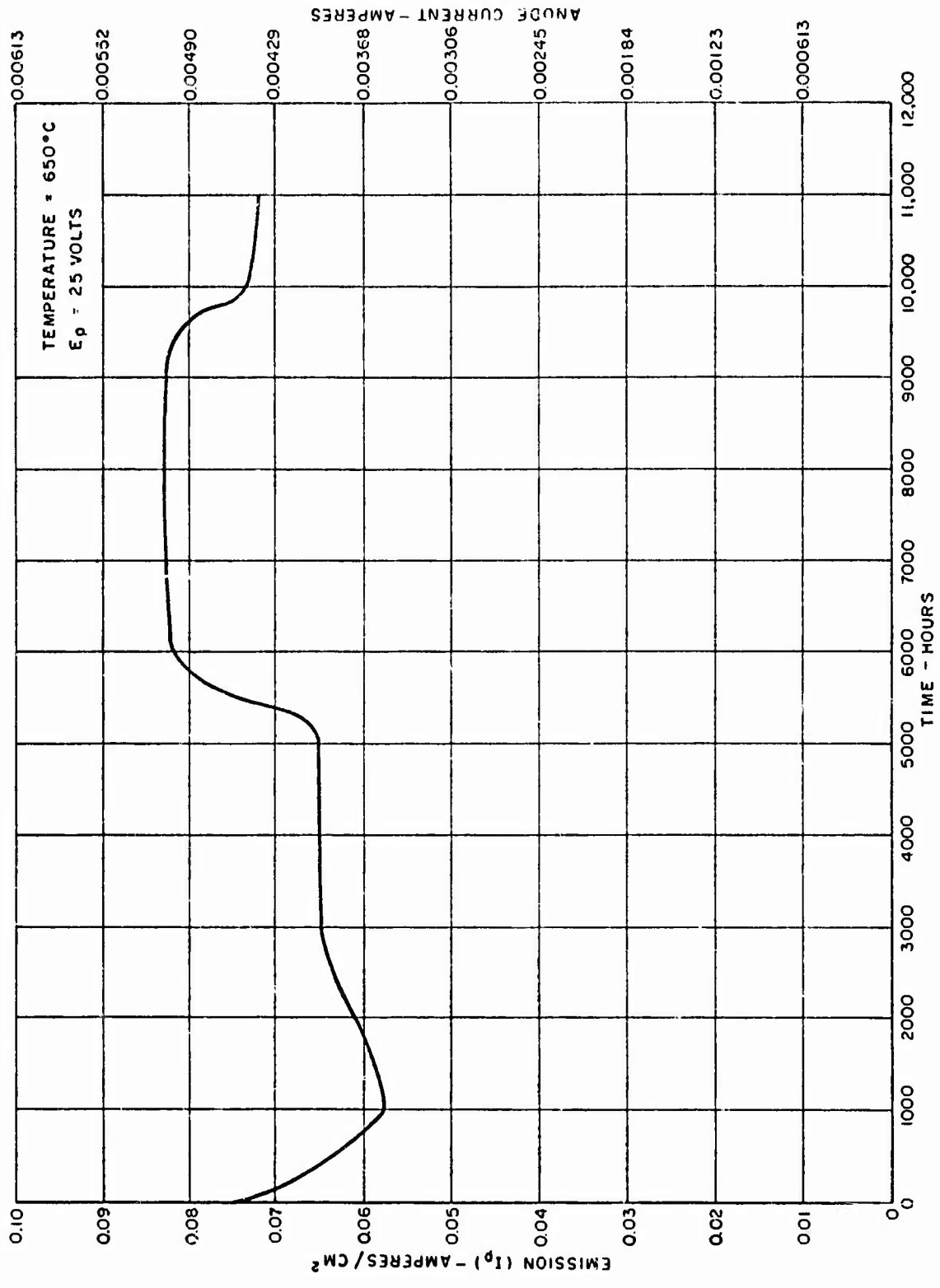


Figure 11 - Life Test Record of HCD-40 Cathode

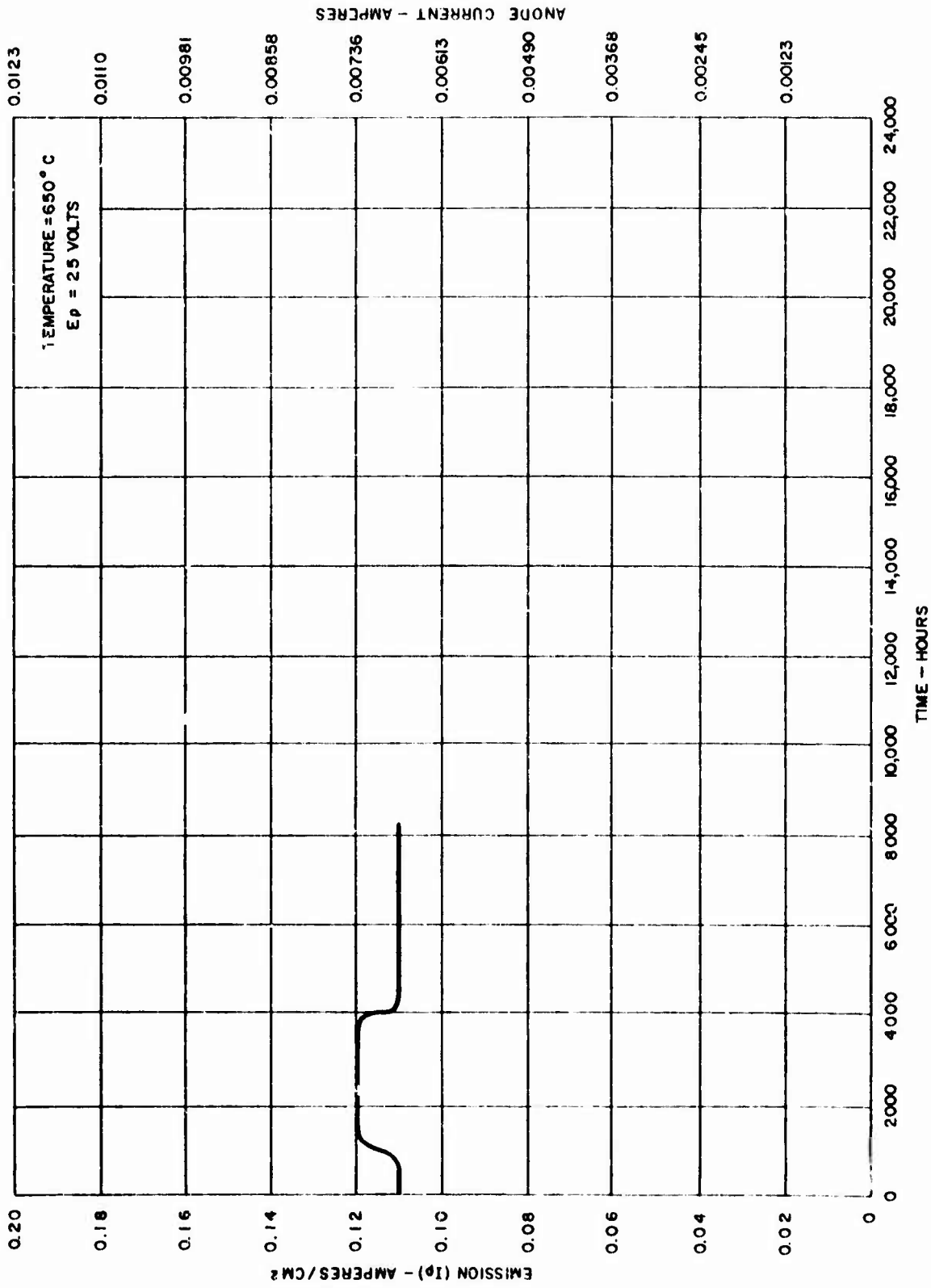


Figure 12 - Life Test Record of HCD-47 Cathode

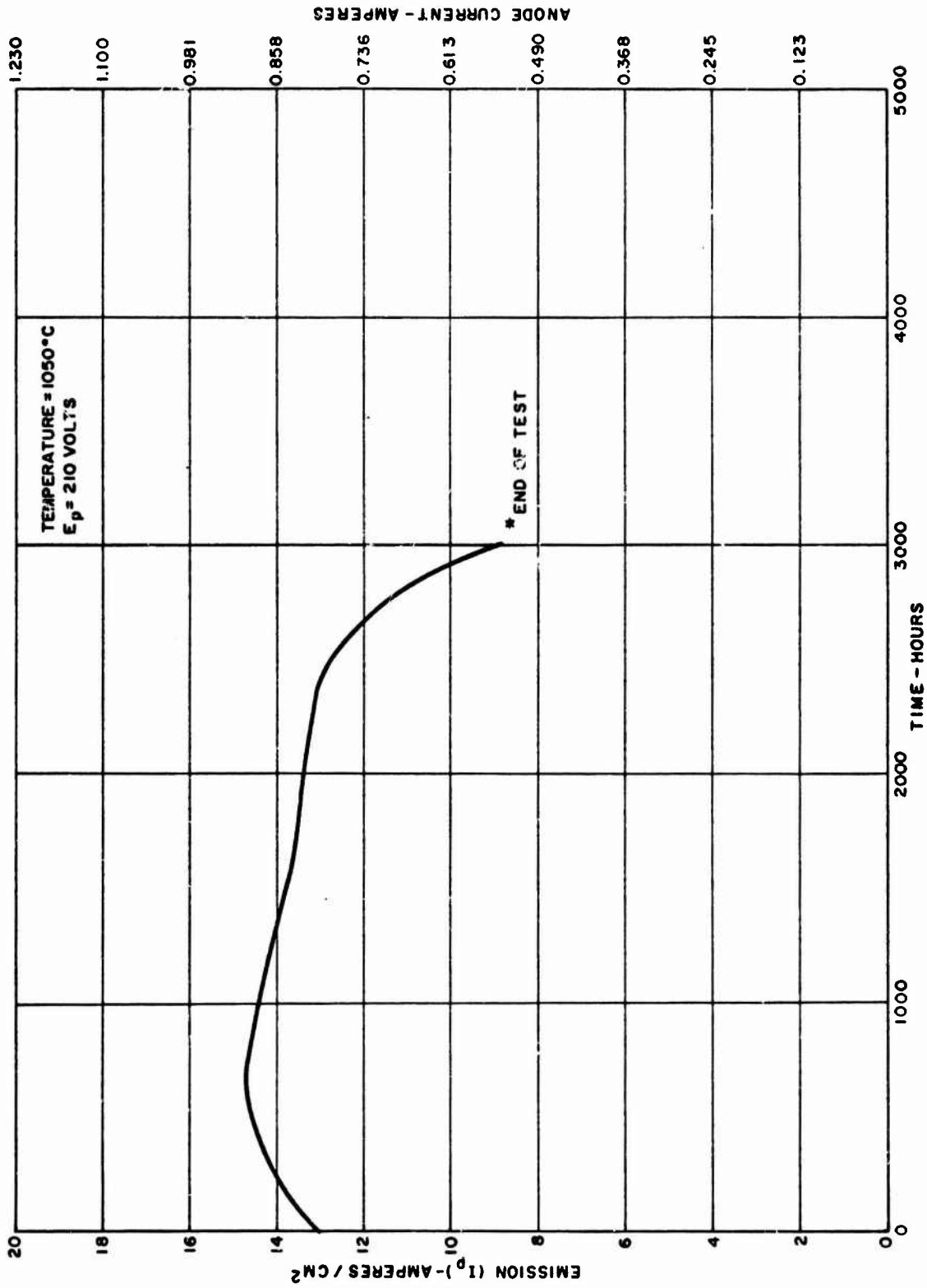


Figure 13 - Life Test Record of HCD-49 Cathode

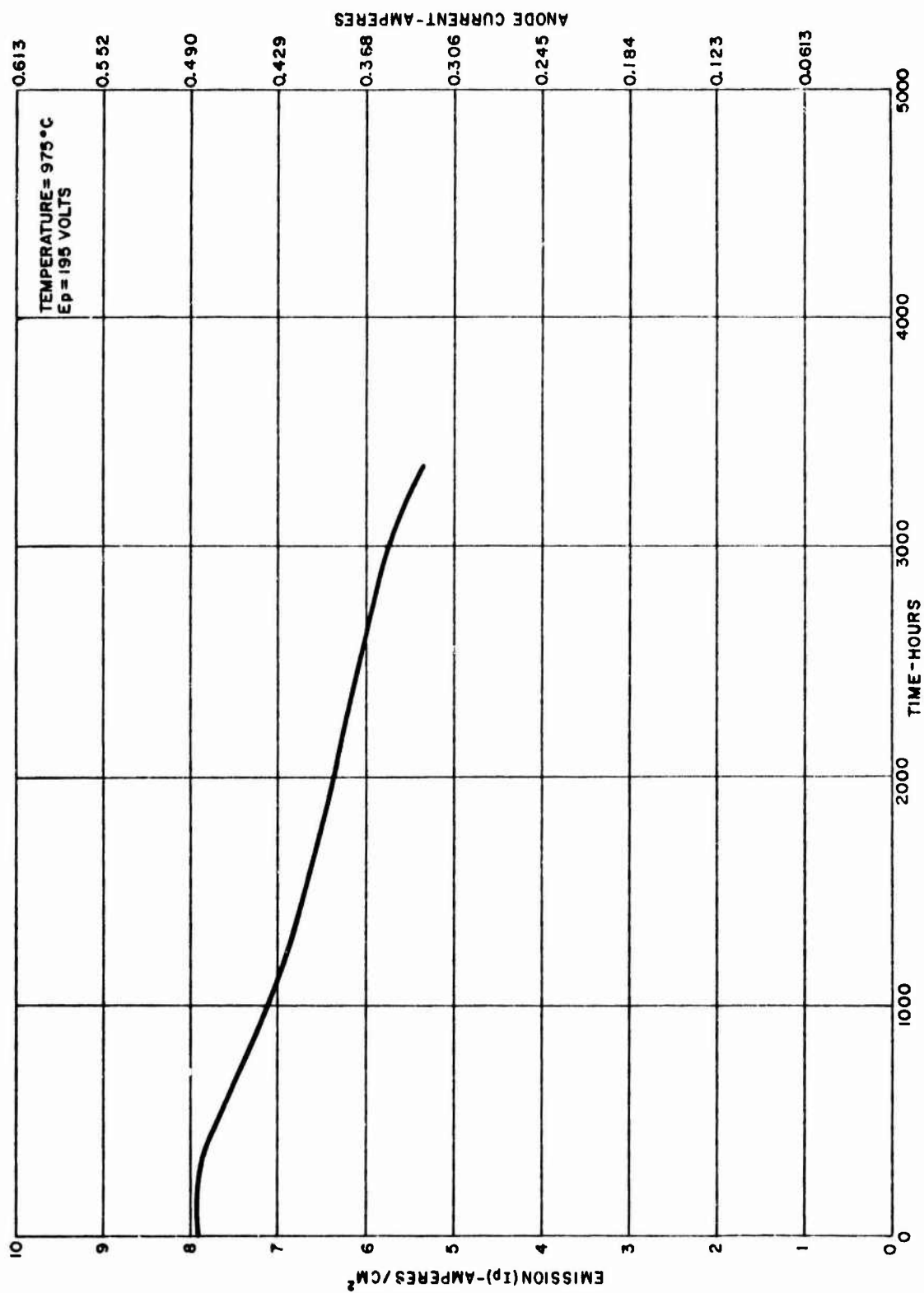


Figure 14 - Life Test Record of HCD-50 Cathode

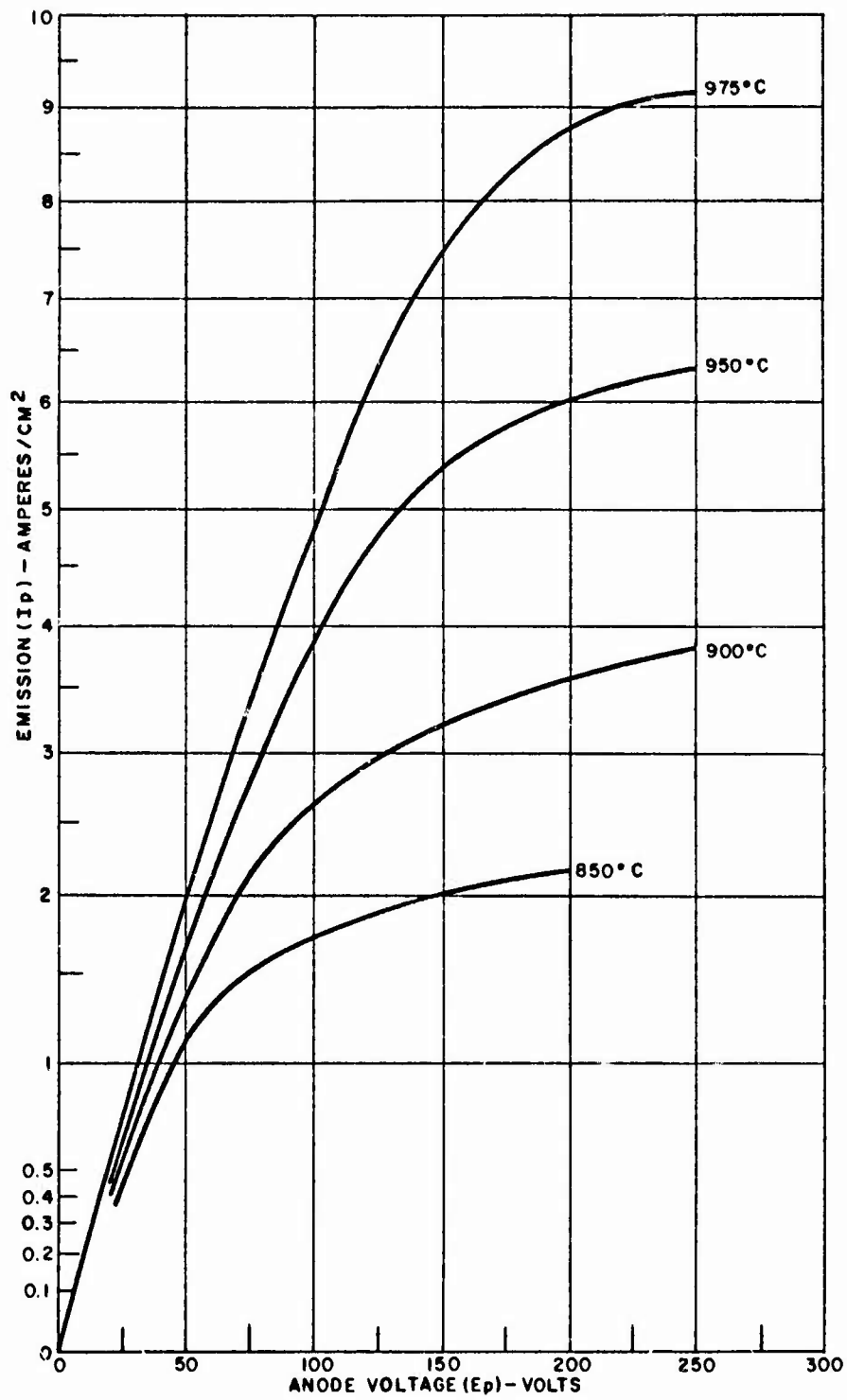


Figure 15 - Initial Emission Characteristics of HCD-50 Cathode at 850°C, 900°C, 950°C and 975°C

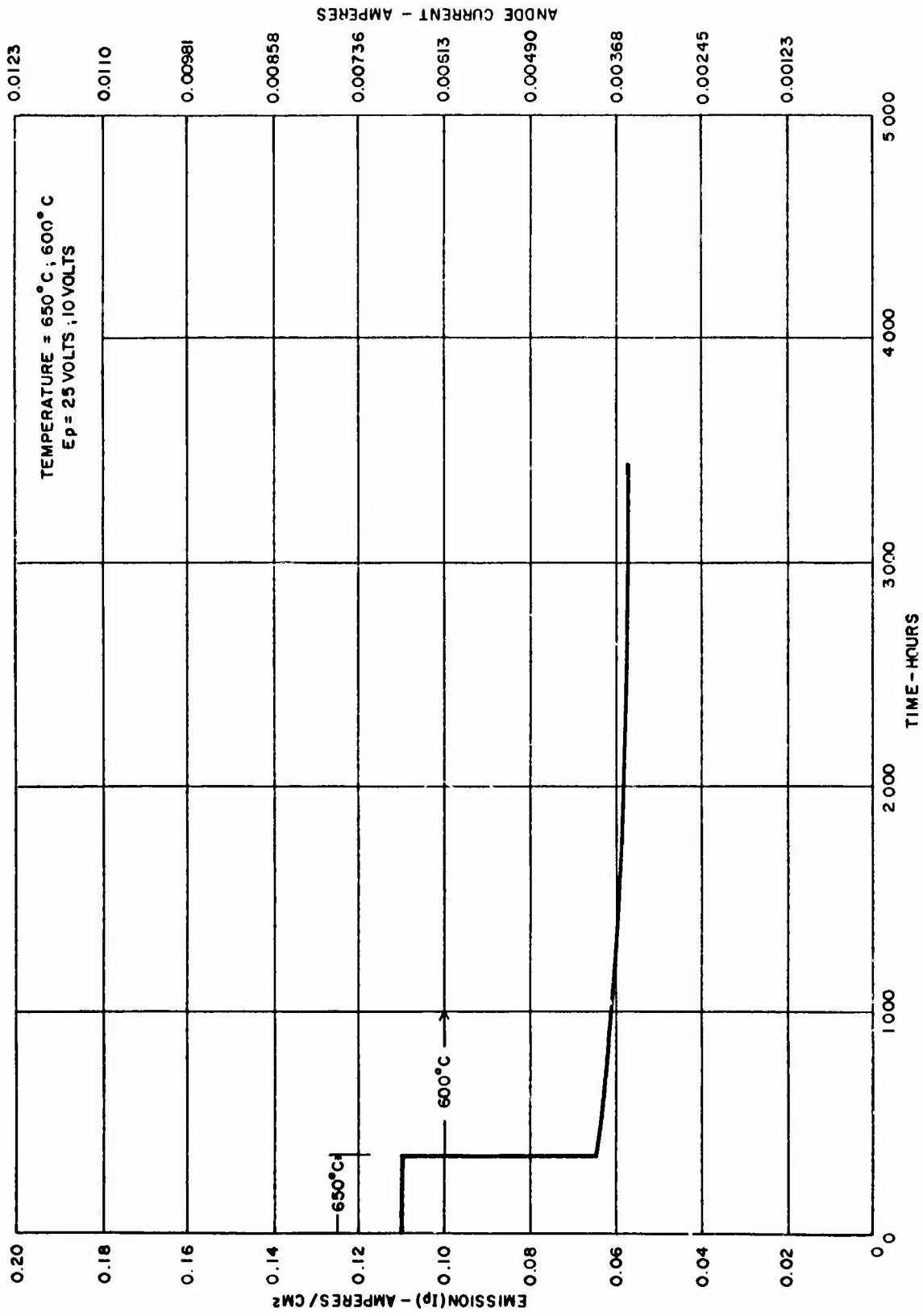


Figure 16 - Life Test Record of HCD-51 Cathode

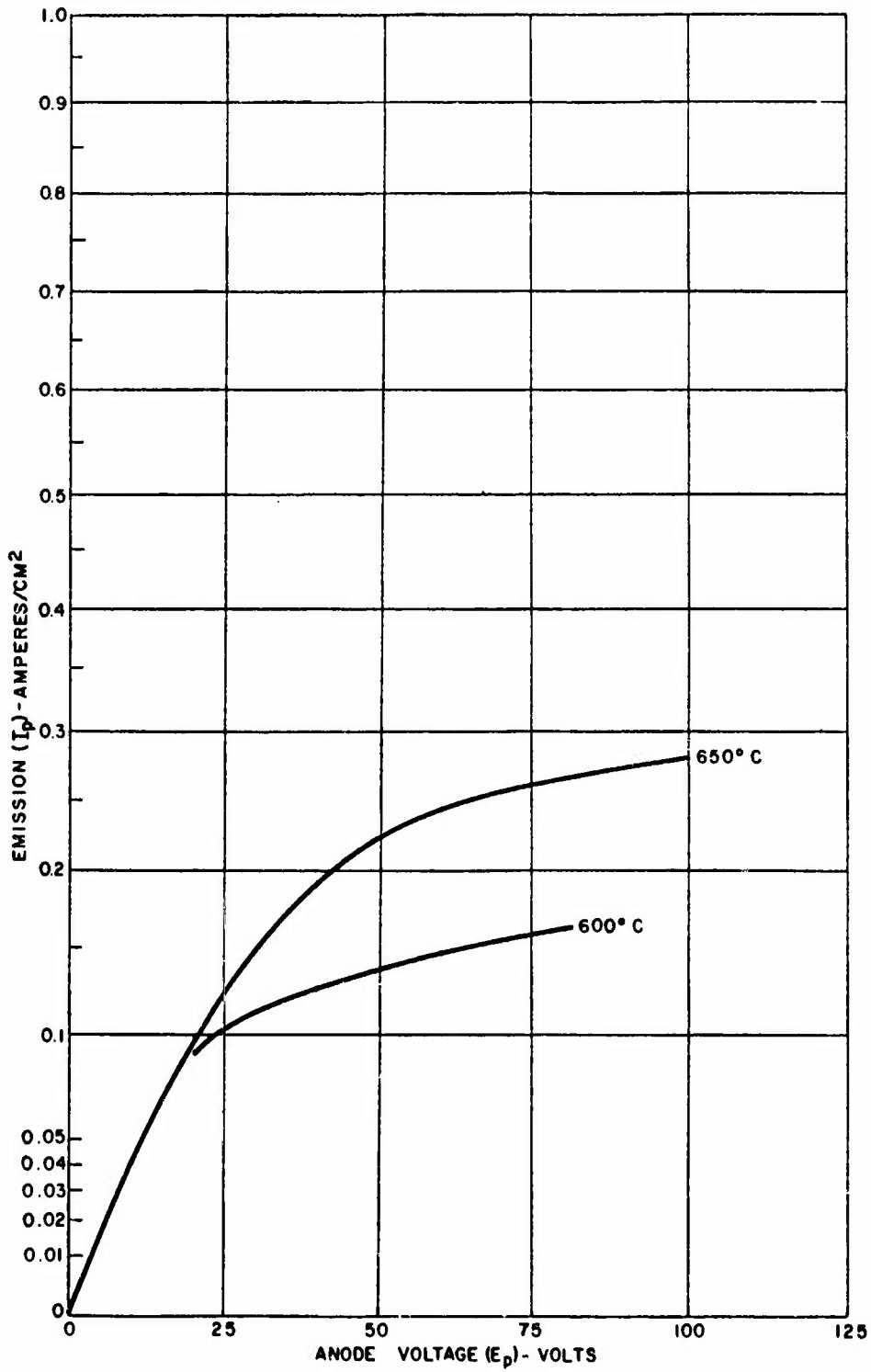


Figure 17 - Initial Emission Characteristics of HCD-51 Cathode at 600°C and 650°C

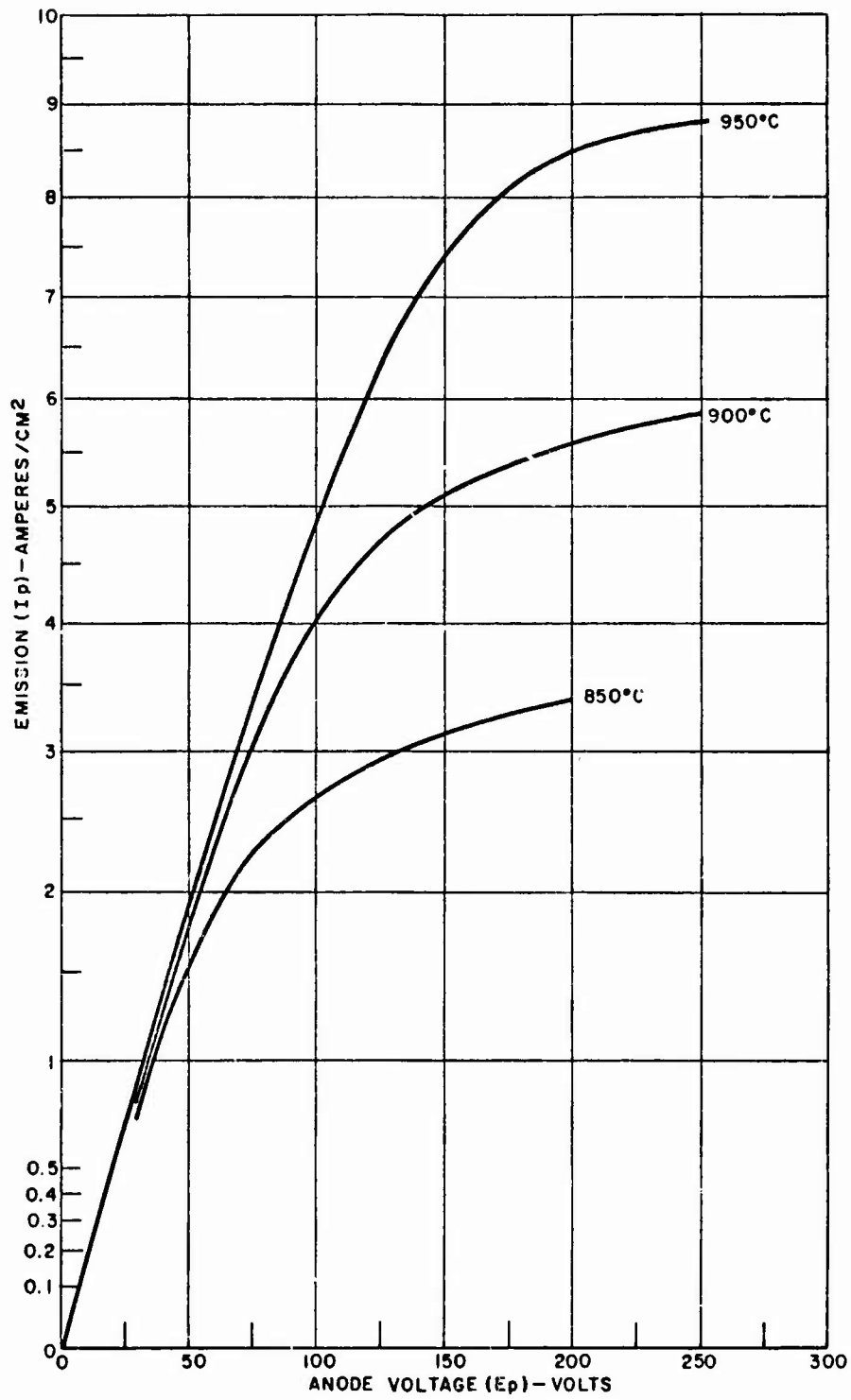


Figure 18 - Initial Emission Characteristics of HCD-51 Cathode at 850°C, 900°C, and 950°C

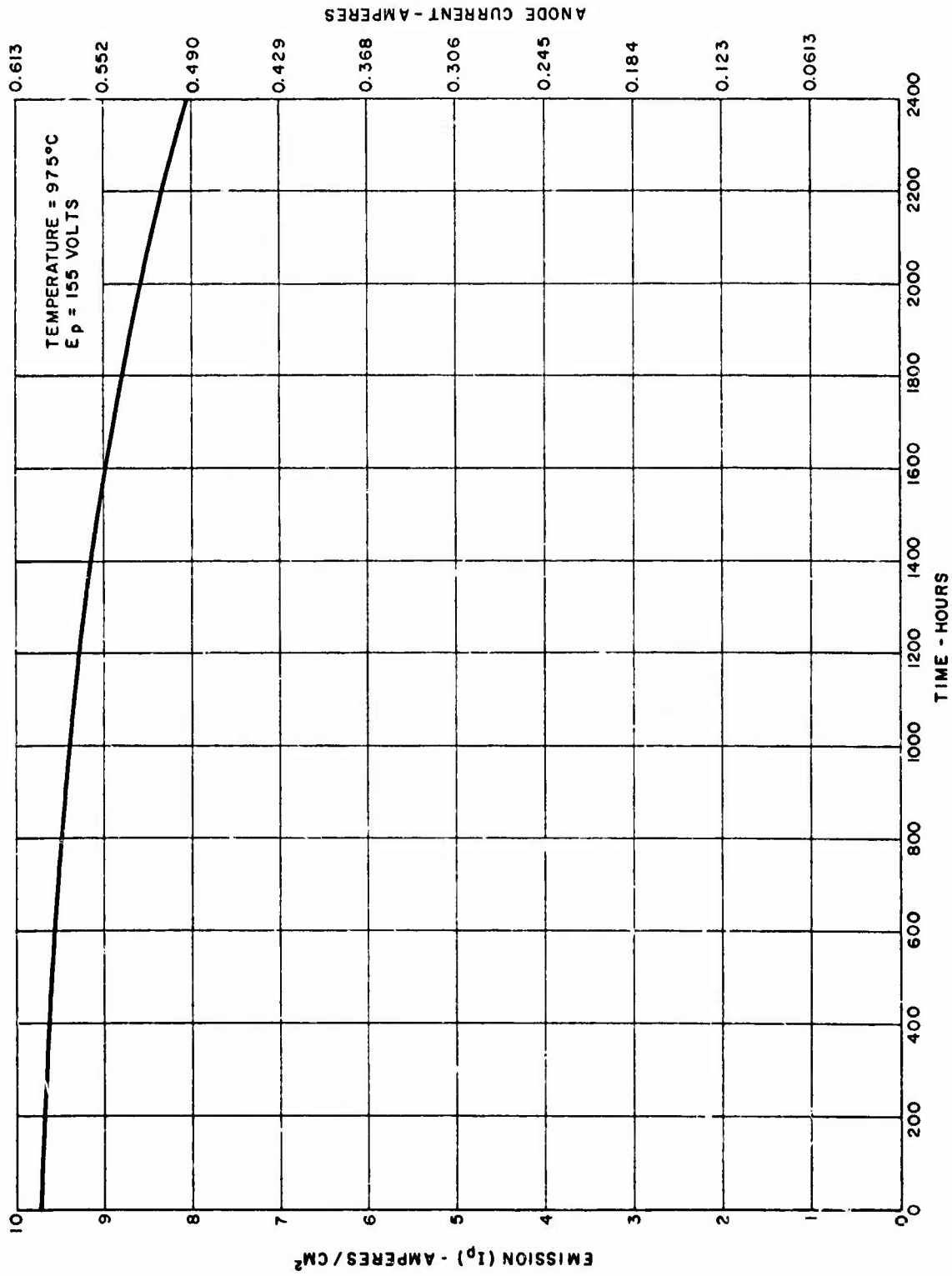


Figure 19 - Life Test Record of HCD-52 Cathode

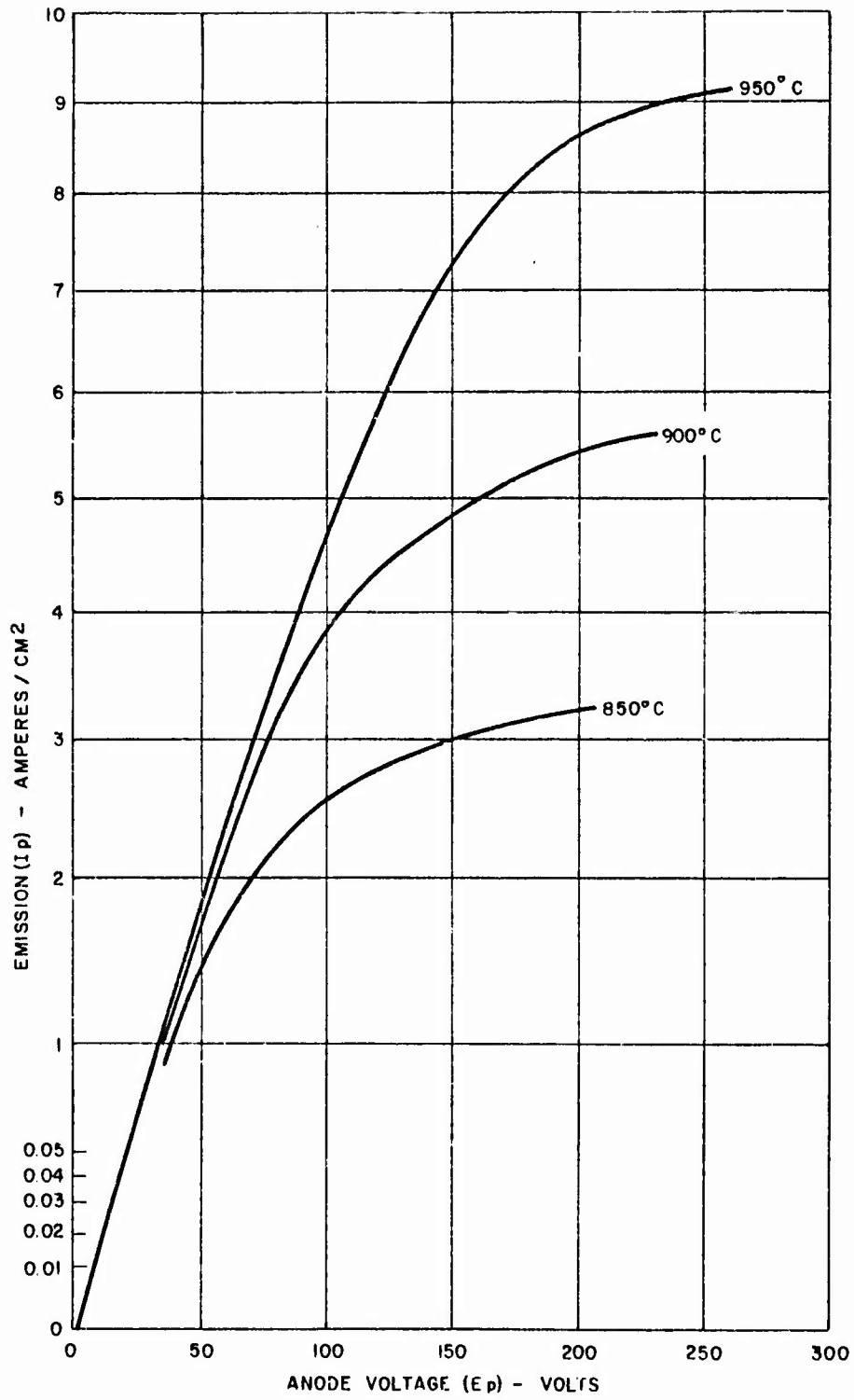


Figure 20 - Initial Emission Characteristics of HCD-52 Cathode at 850°C, 900°C, and 950°C

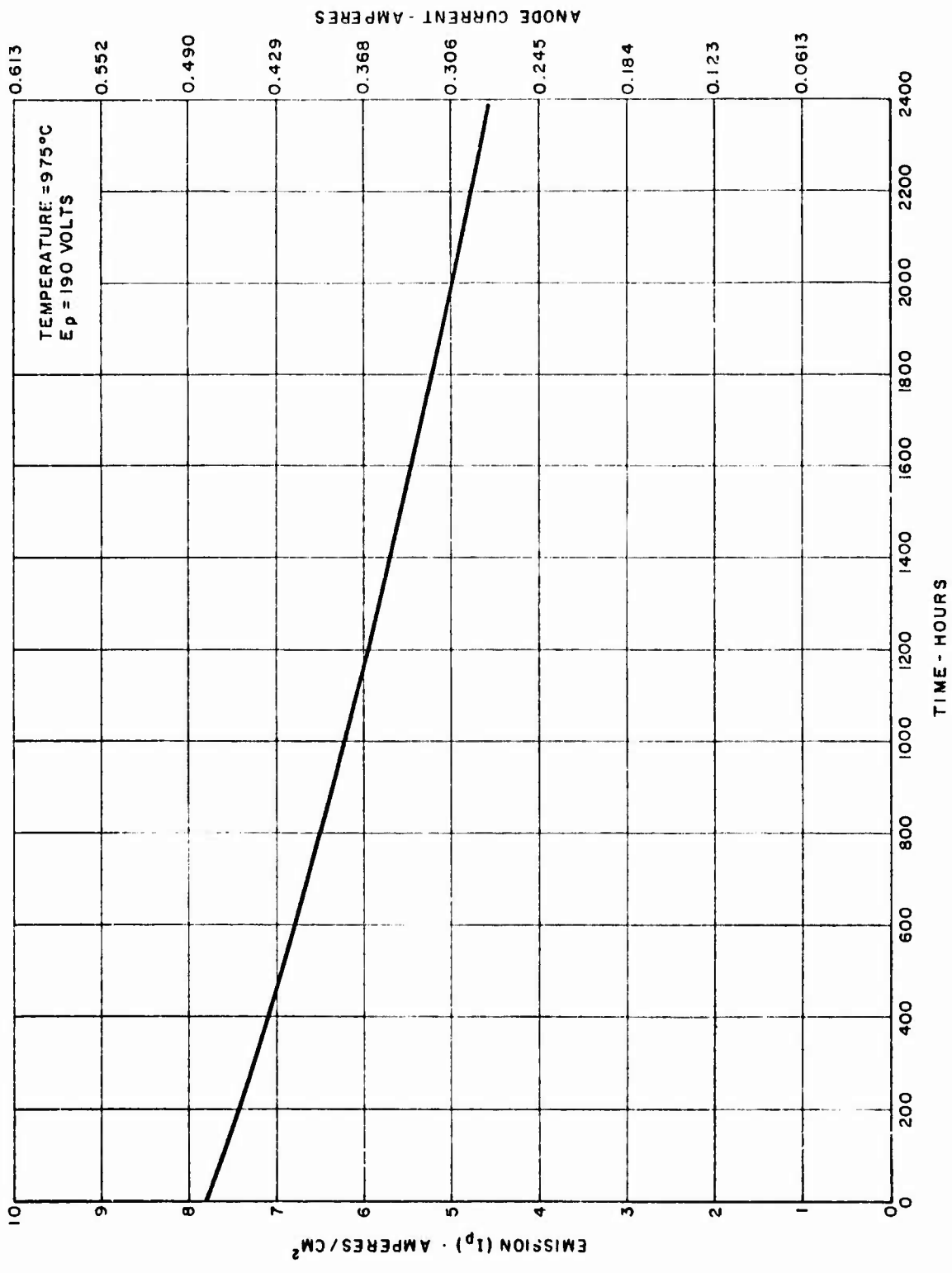


Figure 21 - Life Test Record of HCD-53 Cathode

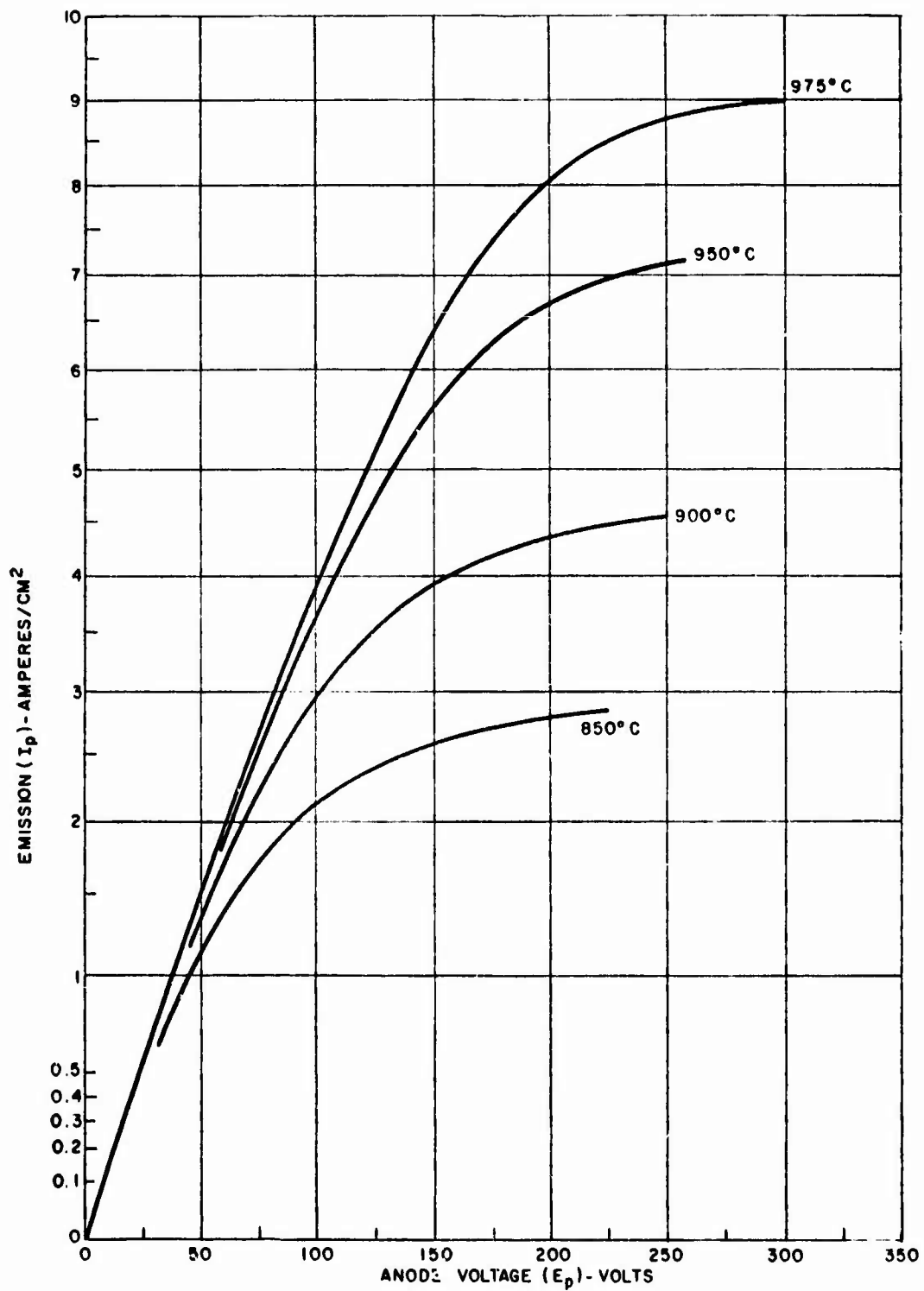


Figure 22 - Initial Emission Characteristics of HCD-53 Cathode at 850°C, 900°C, 950°C, and 975°C

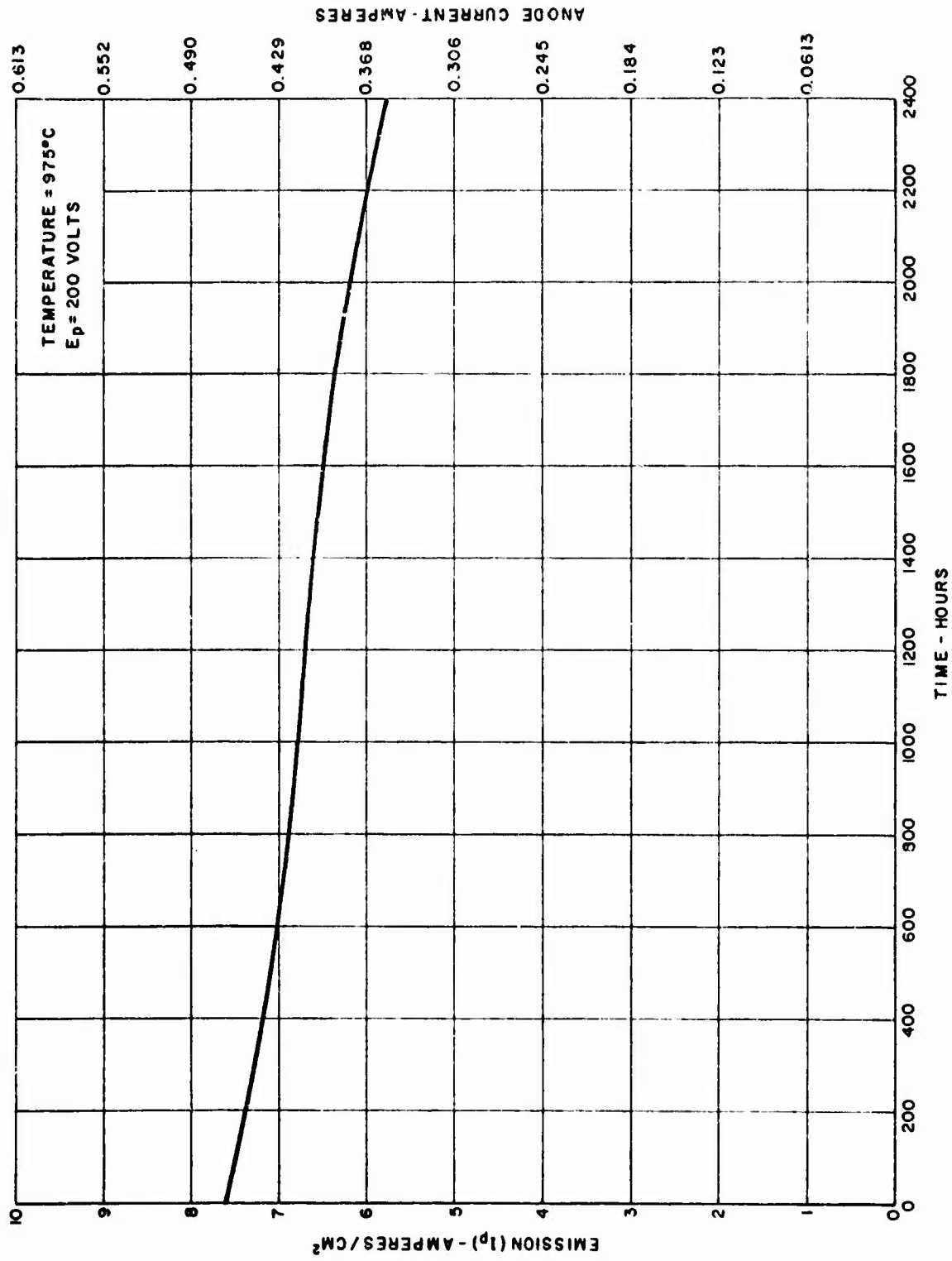


Figure 23 - Life Test Record of HCD-54 Cathode

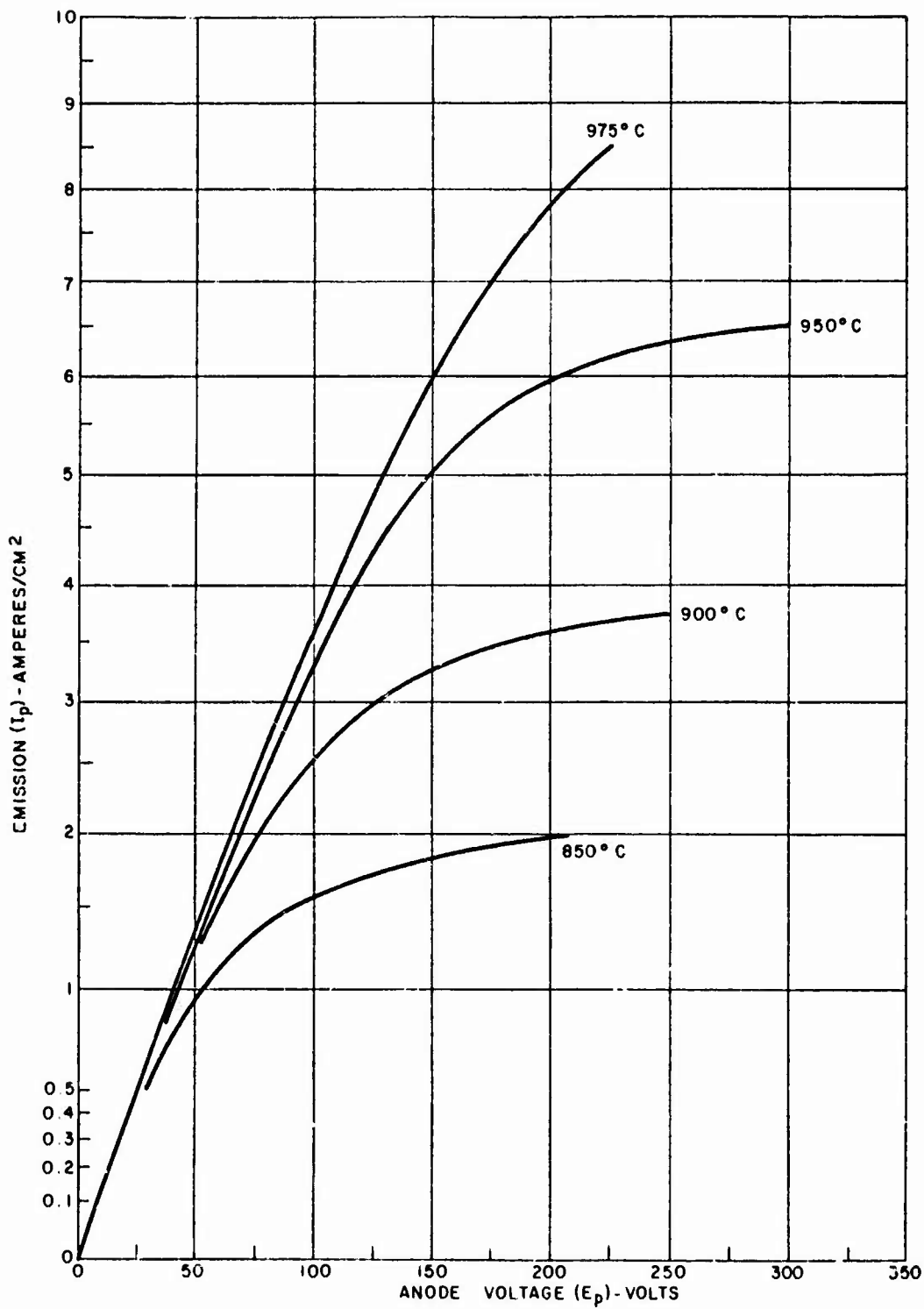


Figure 24 - Initial Emission Characteristics of HCD-54 Cathode at 850°C, 900°C, 950°C and 975°C

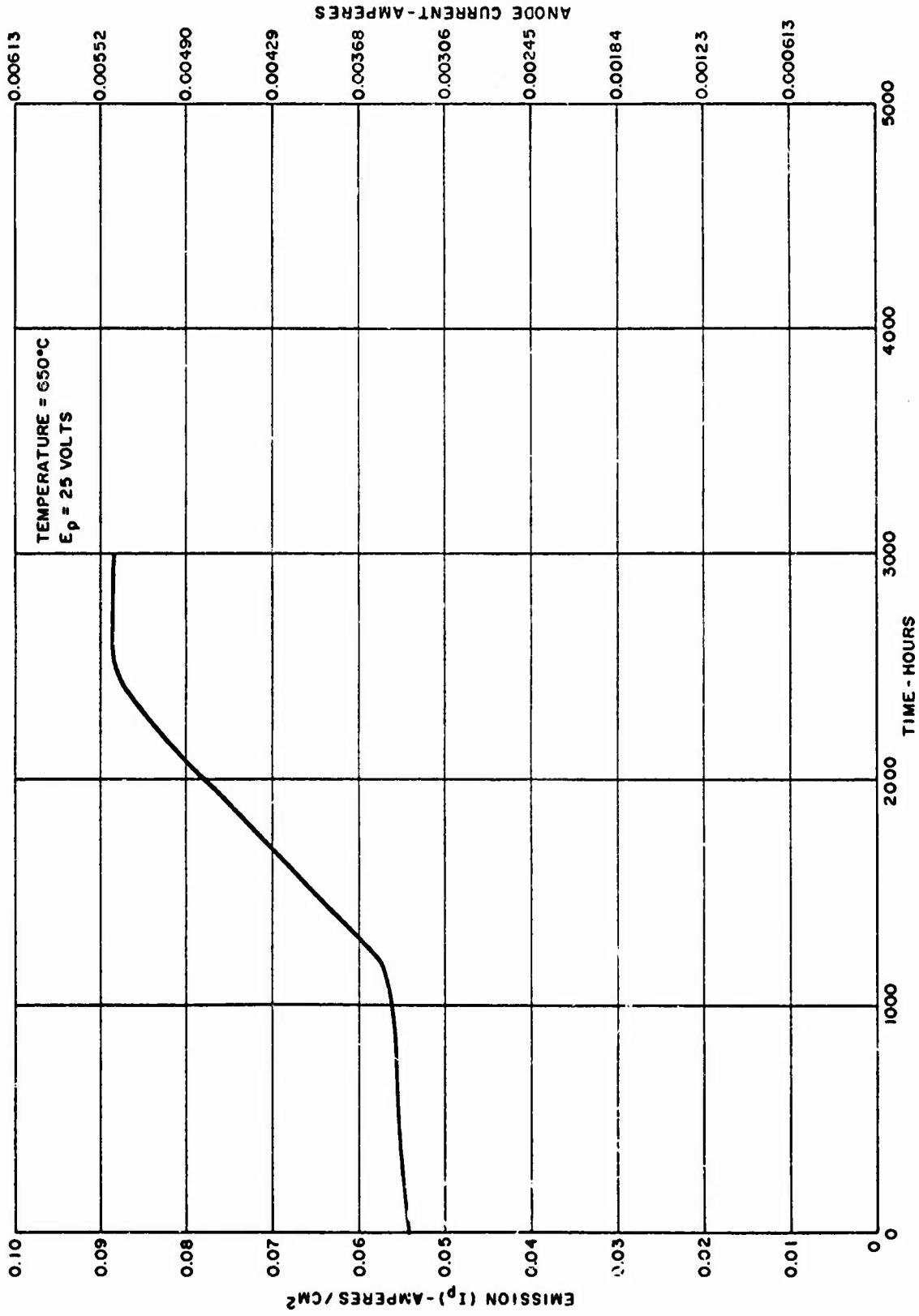


Figure 25 - Life Test Record of HCD-55 Cathode

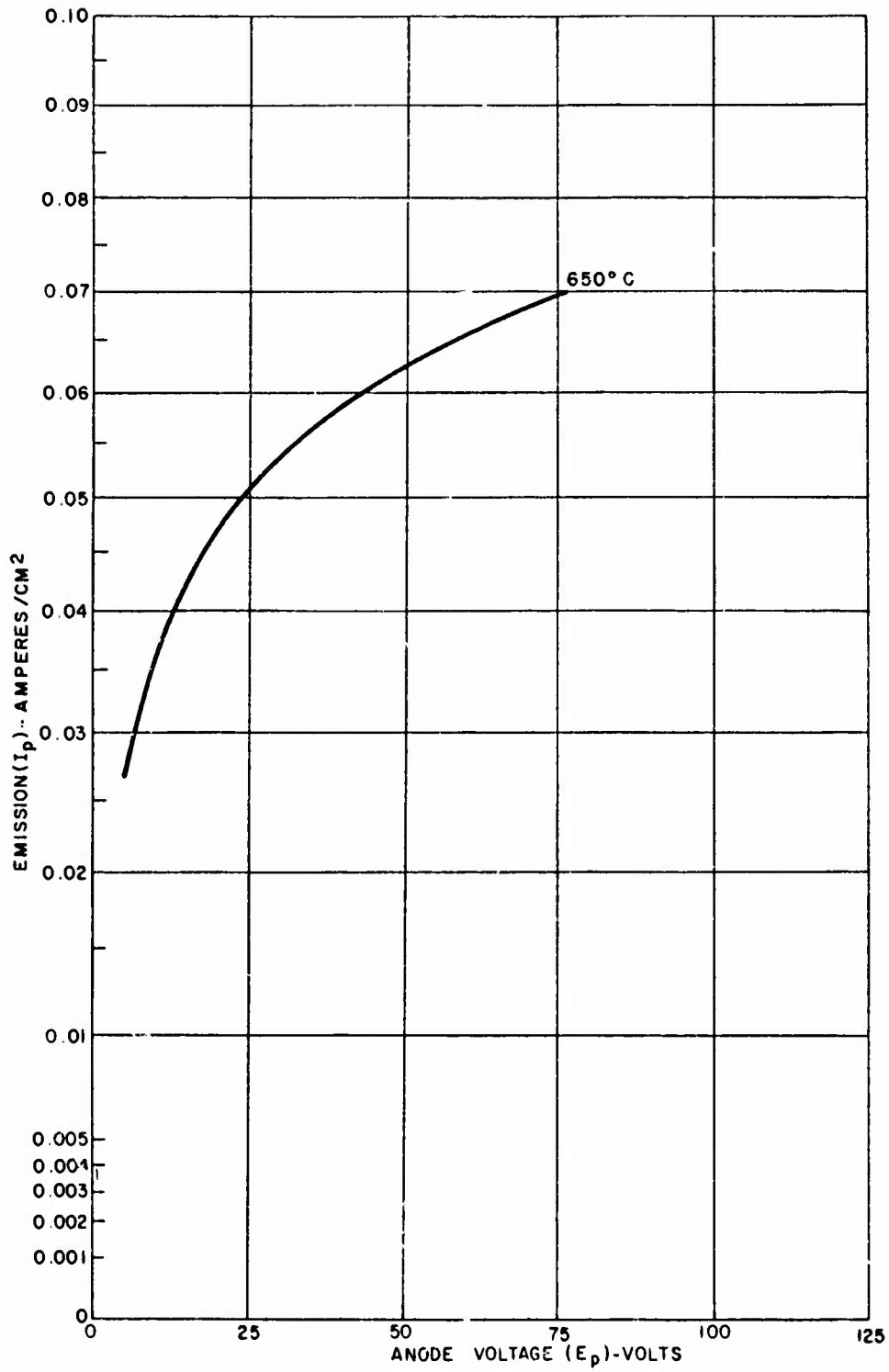


Figure 26 - Initial Emission Characteristic of HCD-55 Cathode at 650°C

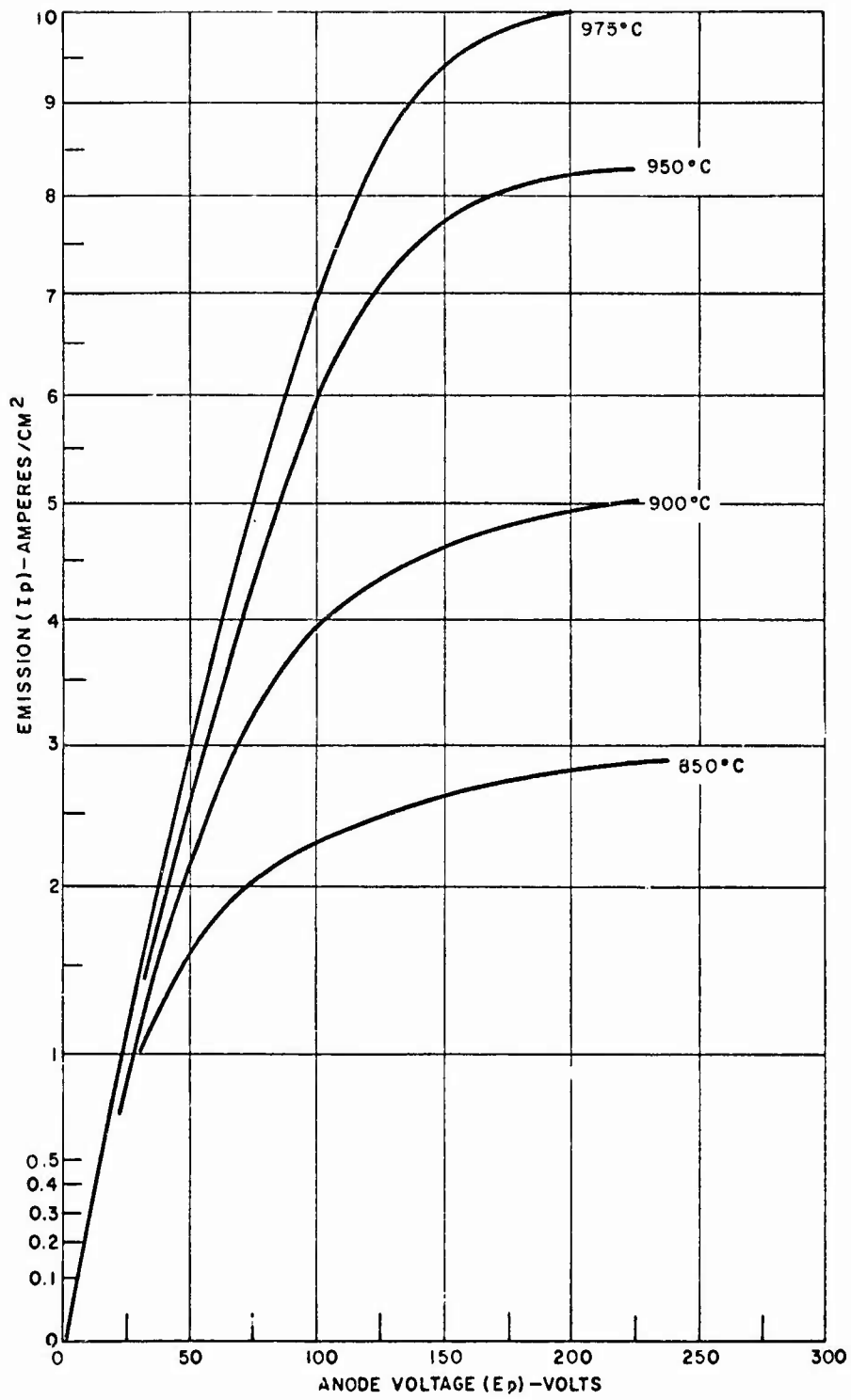


Figure 27 - Initial Emission Characteristics of HCD-55 Cathode at 850°C, 900°C, 950°C, and 975°C

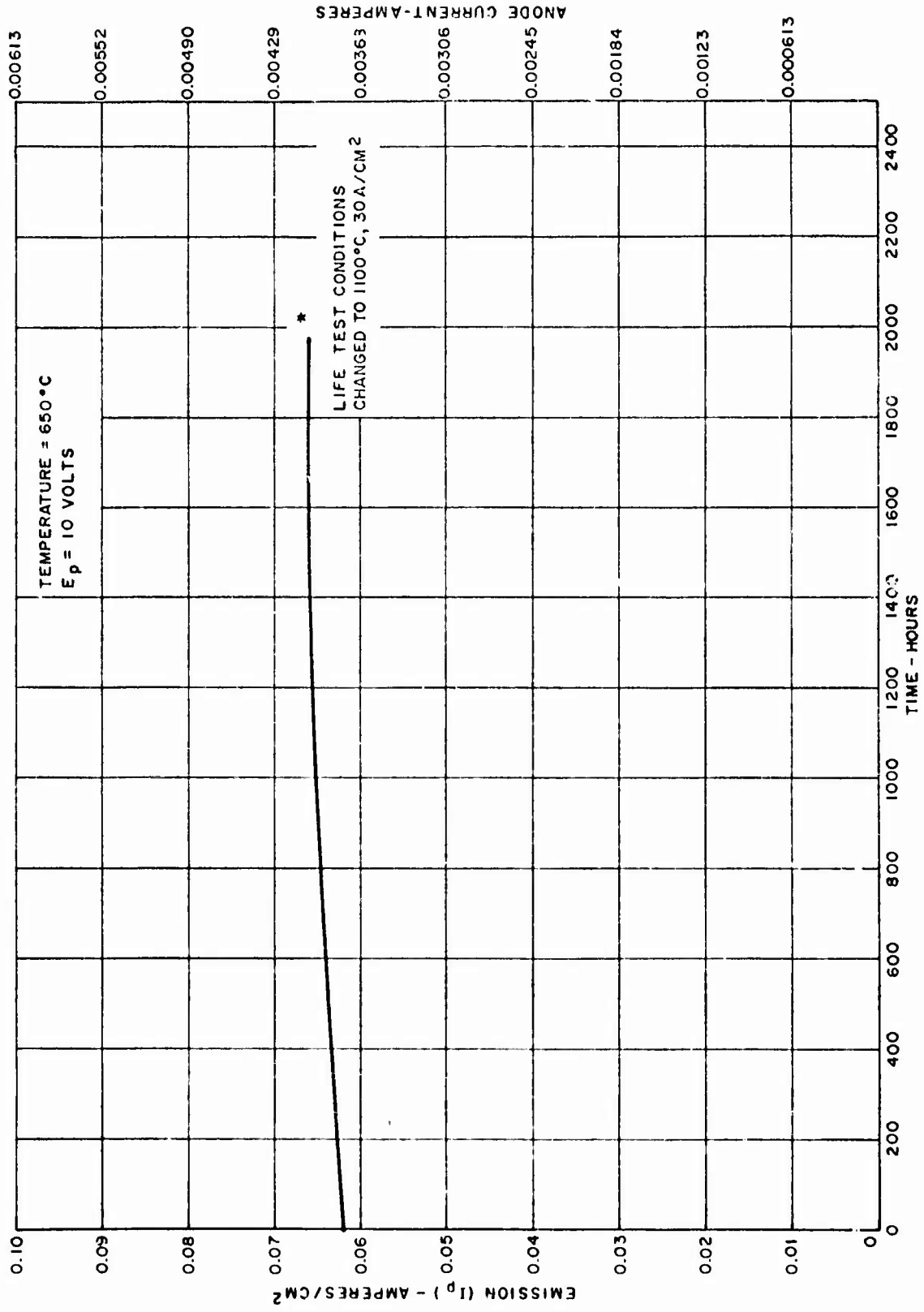


Figure 28 - Life Test Record of HCD-56 Cathode

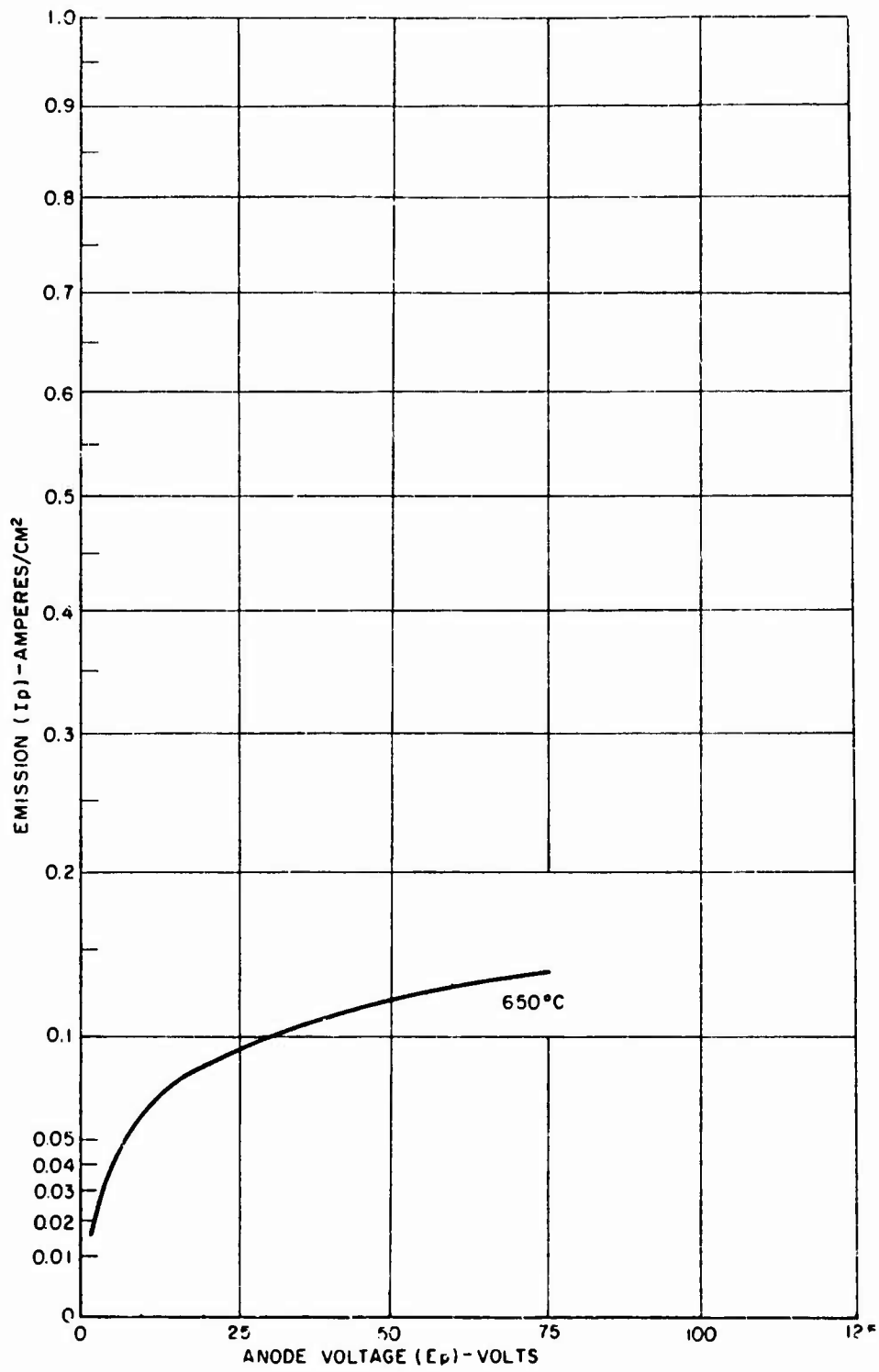


Figure 29 - Initial Emission Characteristic of HCD-56 Cathode at 650°C

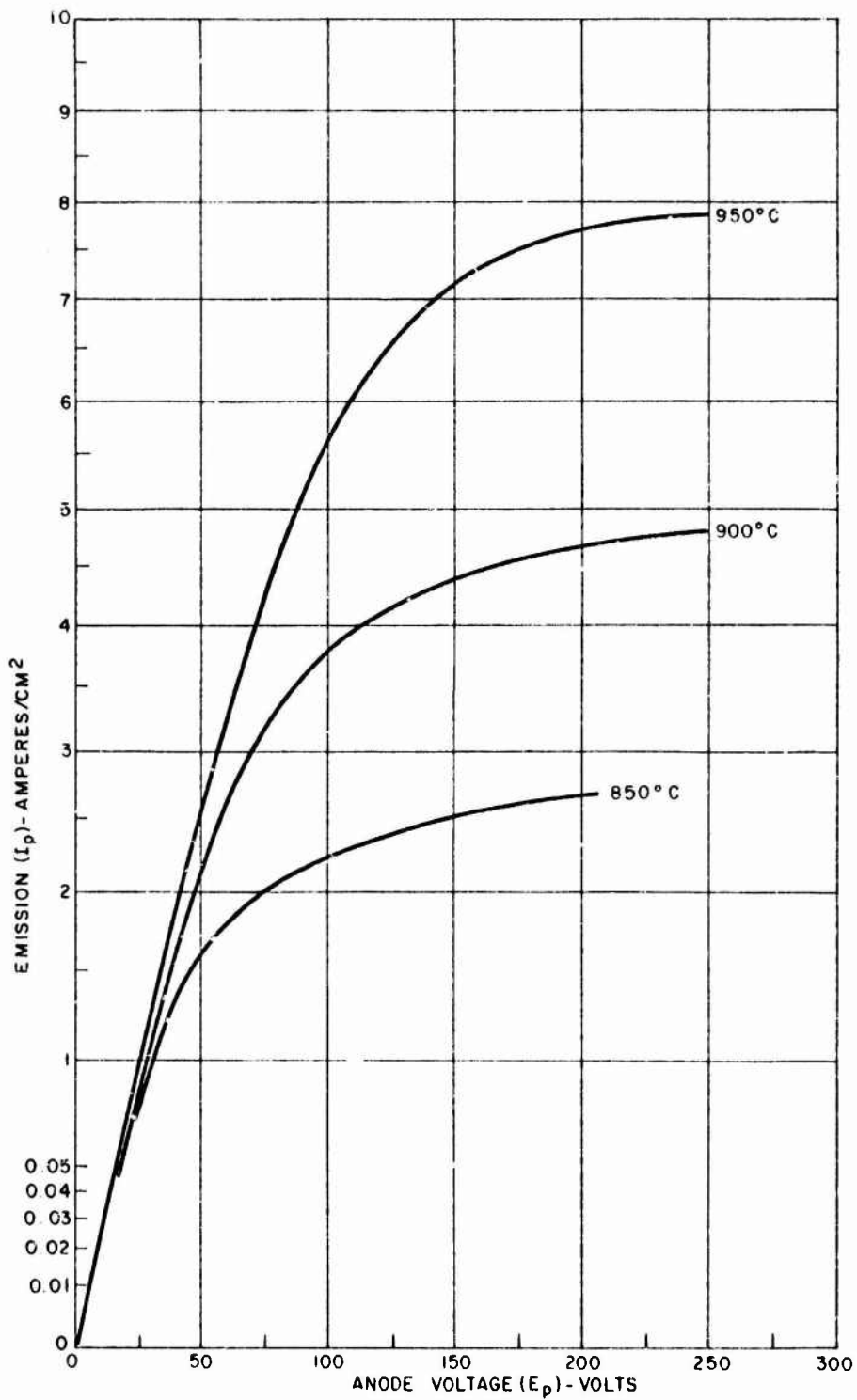


Figure 30 - Initial Emission Characteristics of HCD-56 Cathode at 850°C, 900°C, and 950°C

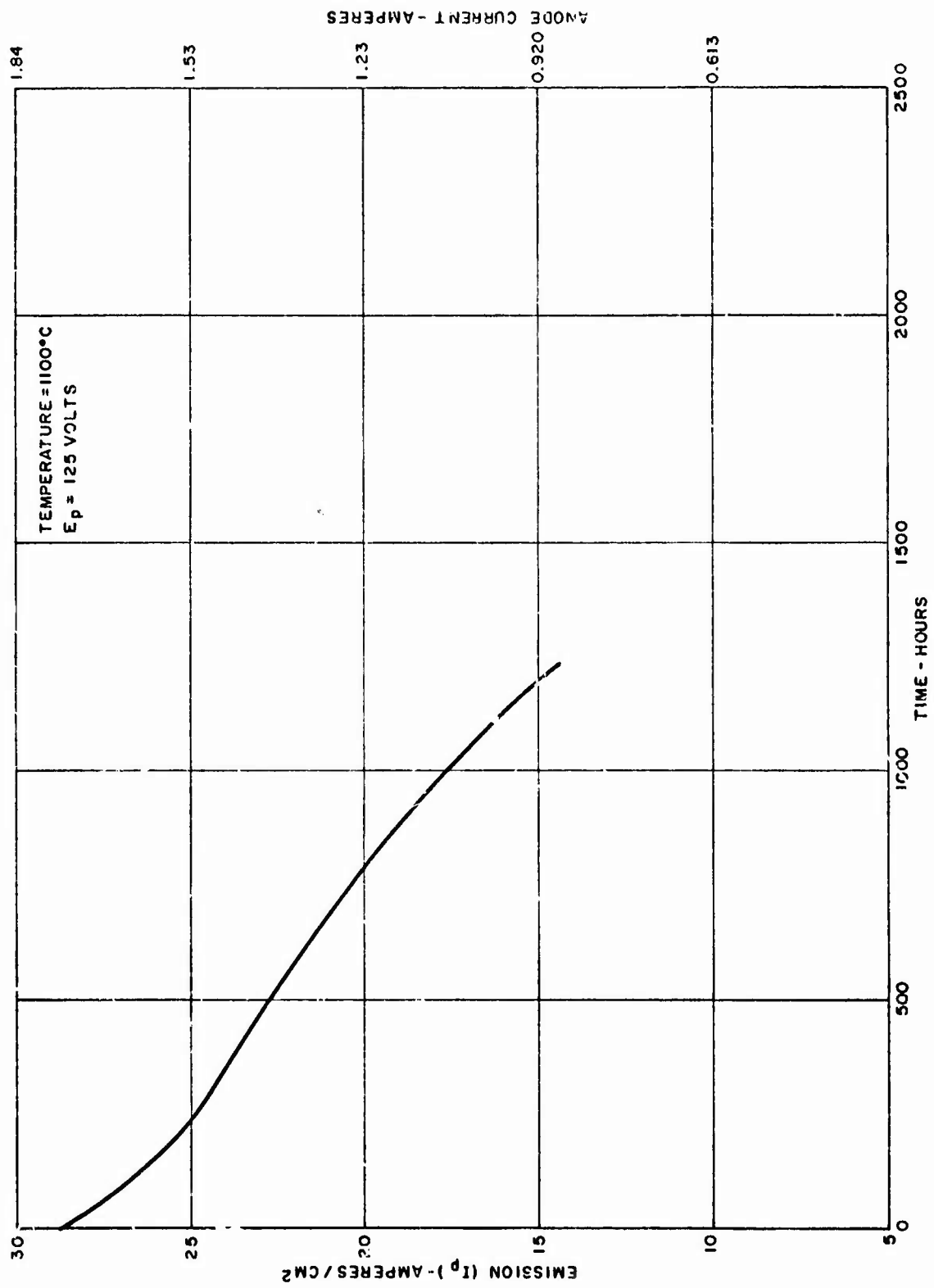


Figure 31 - Retest of HCD-56 Cathode (1100°C)

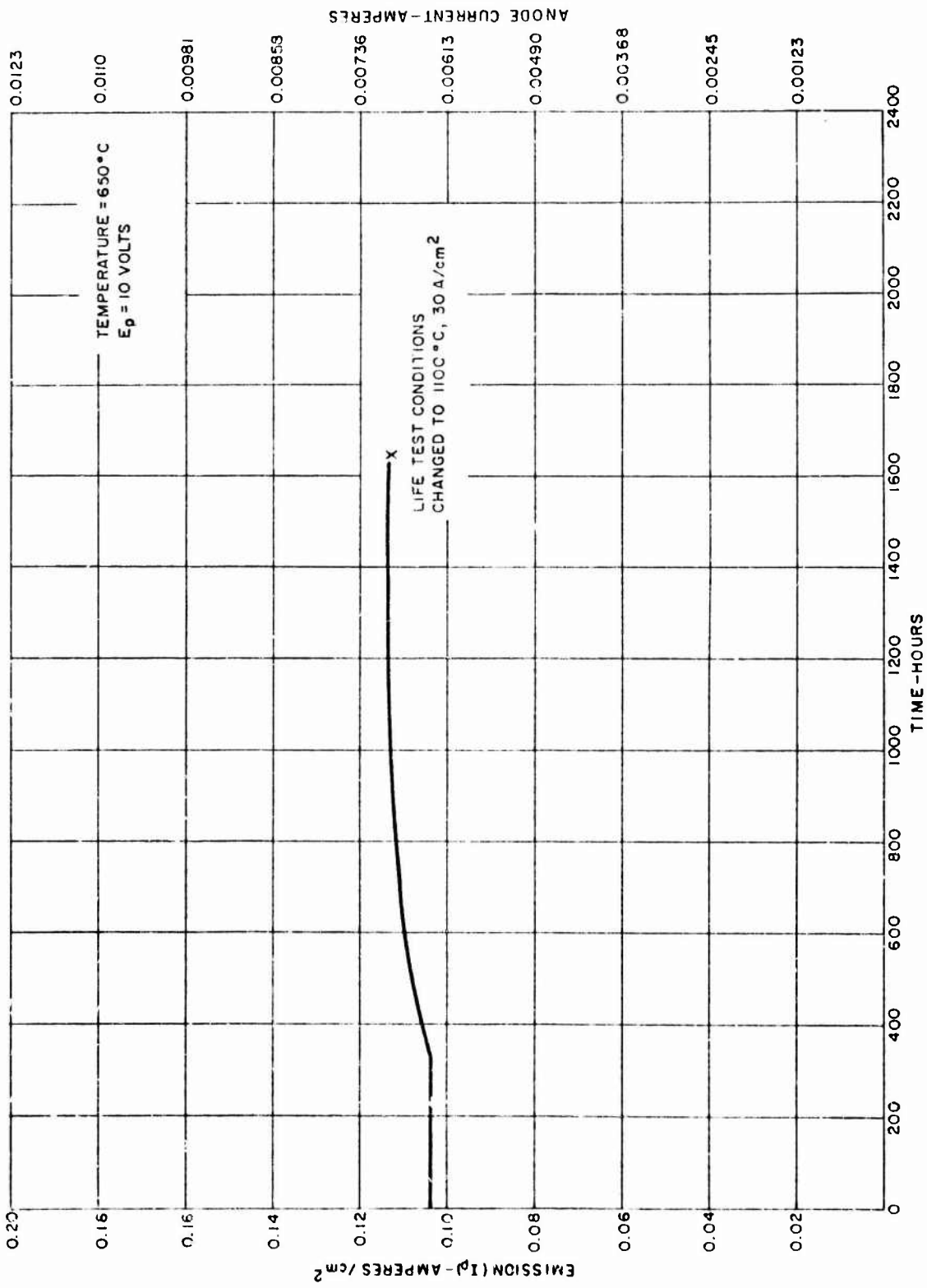


Figure 32 - Life Test Record of HCD-57 Cathode

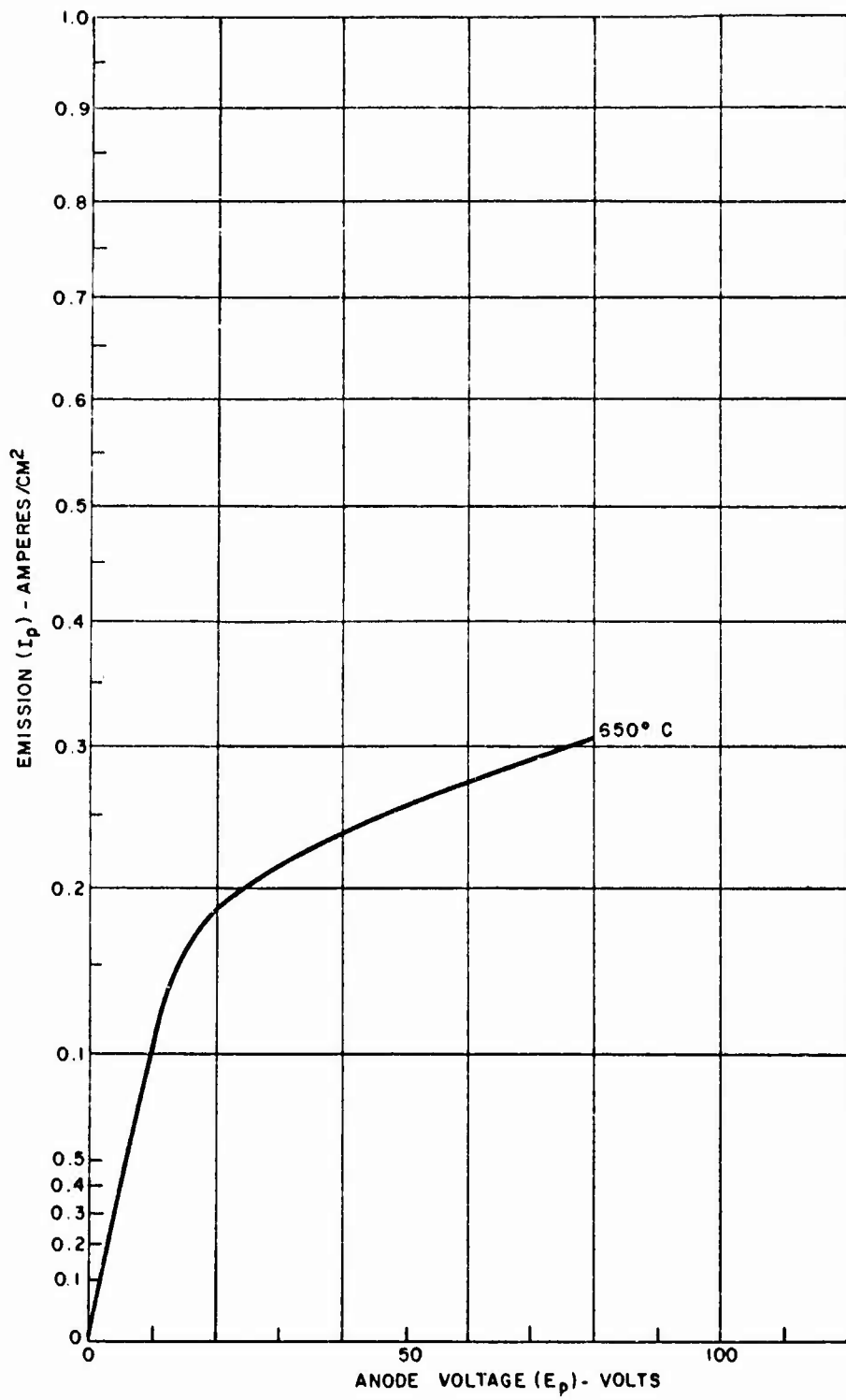


Figure 33 - Initial Emission Characteristics of HCD-57 Cathode at 650°C

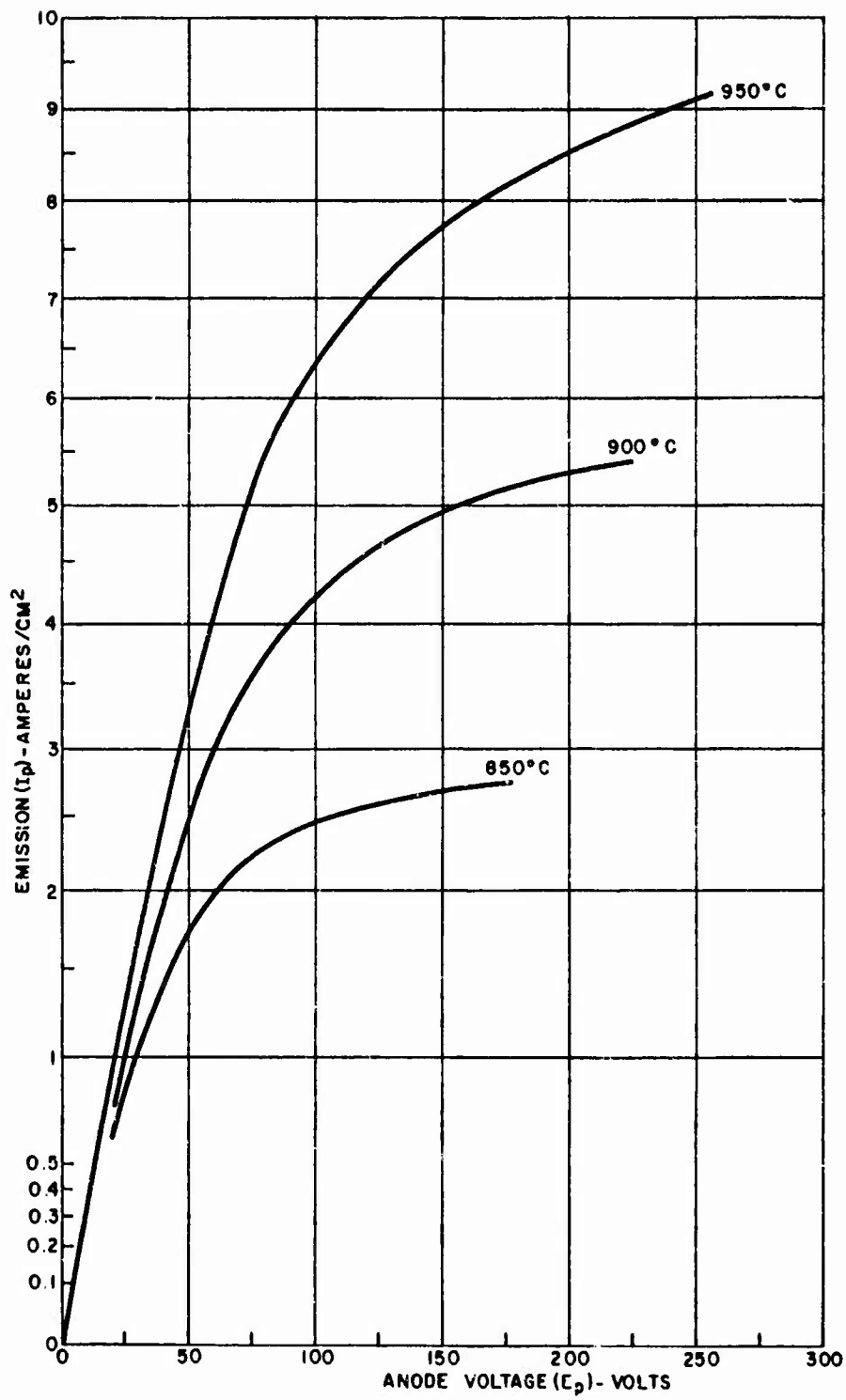


Figure 34 - Initial Emission Characteristic of HCD-57 Cathode at 850°C, 900°C, and 950°C

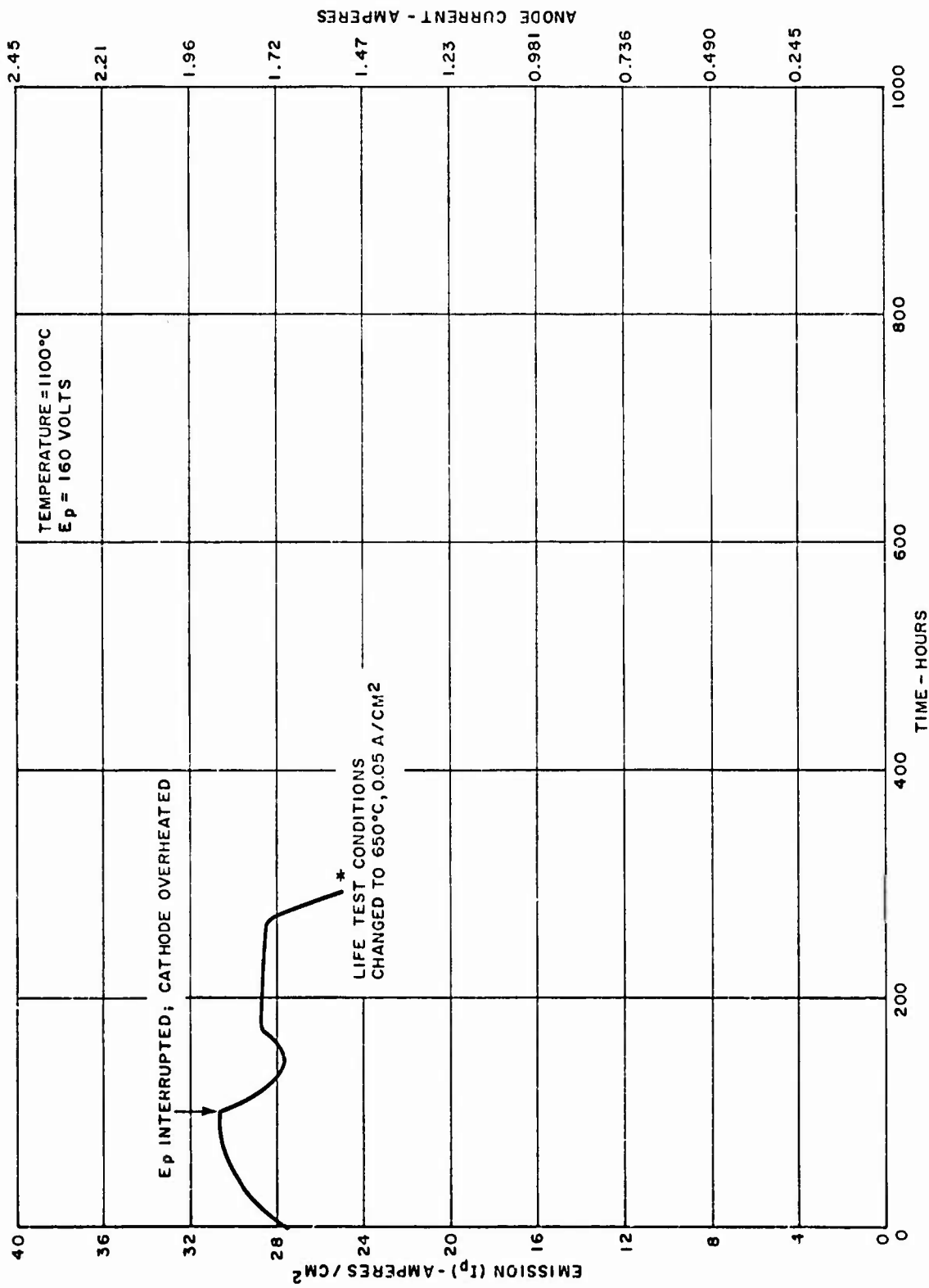


Figure 35 - Retest of HCD-57 Cathode (1100°C)

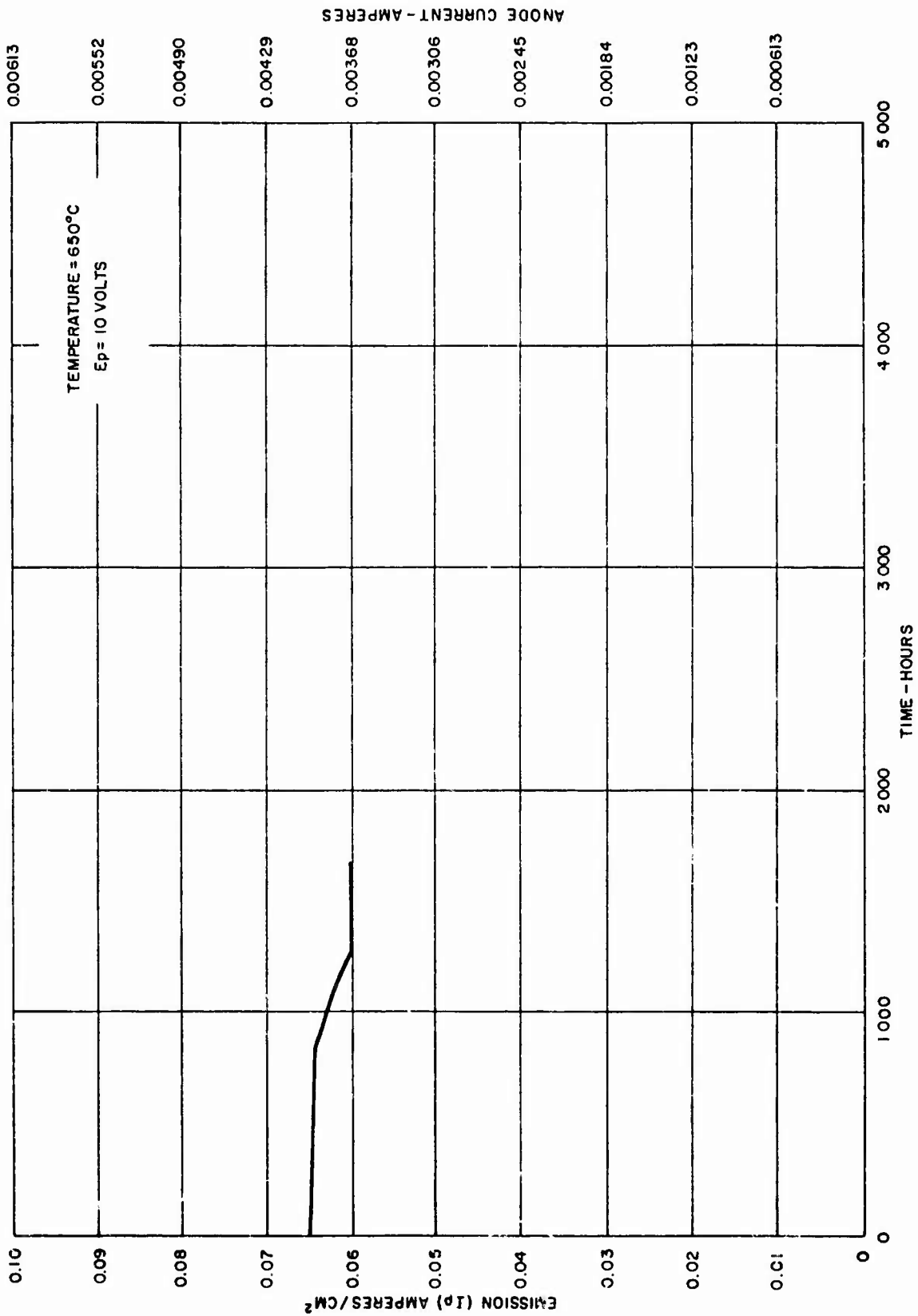


Figure 36 - Retest of HCD-57 Cathode (650°C)

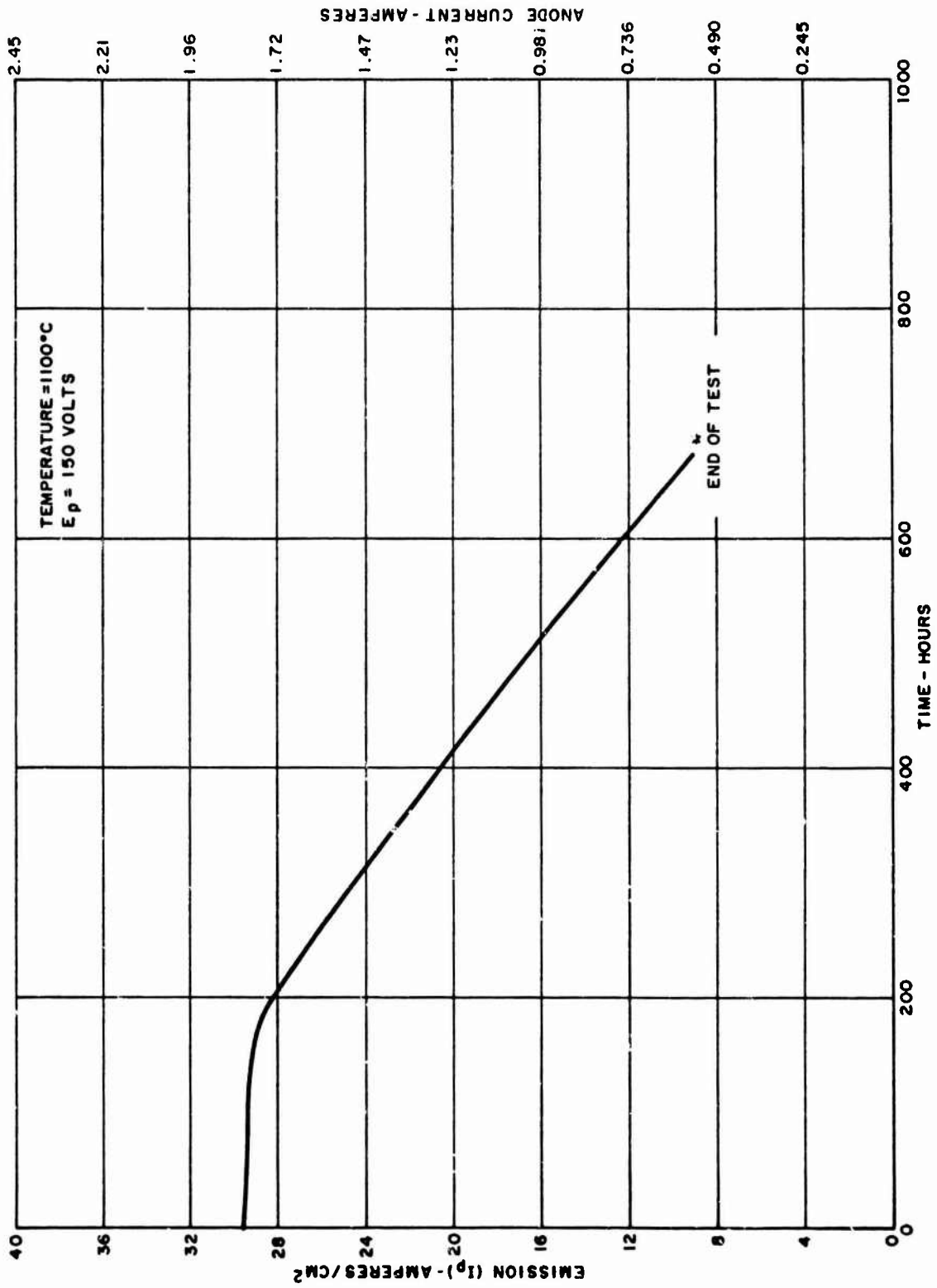


Figure 37 - Life Test Record of HCD-58 Cathode

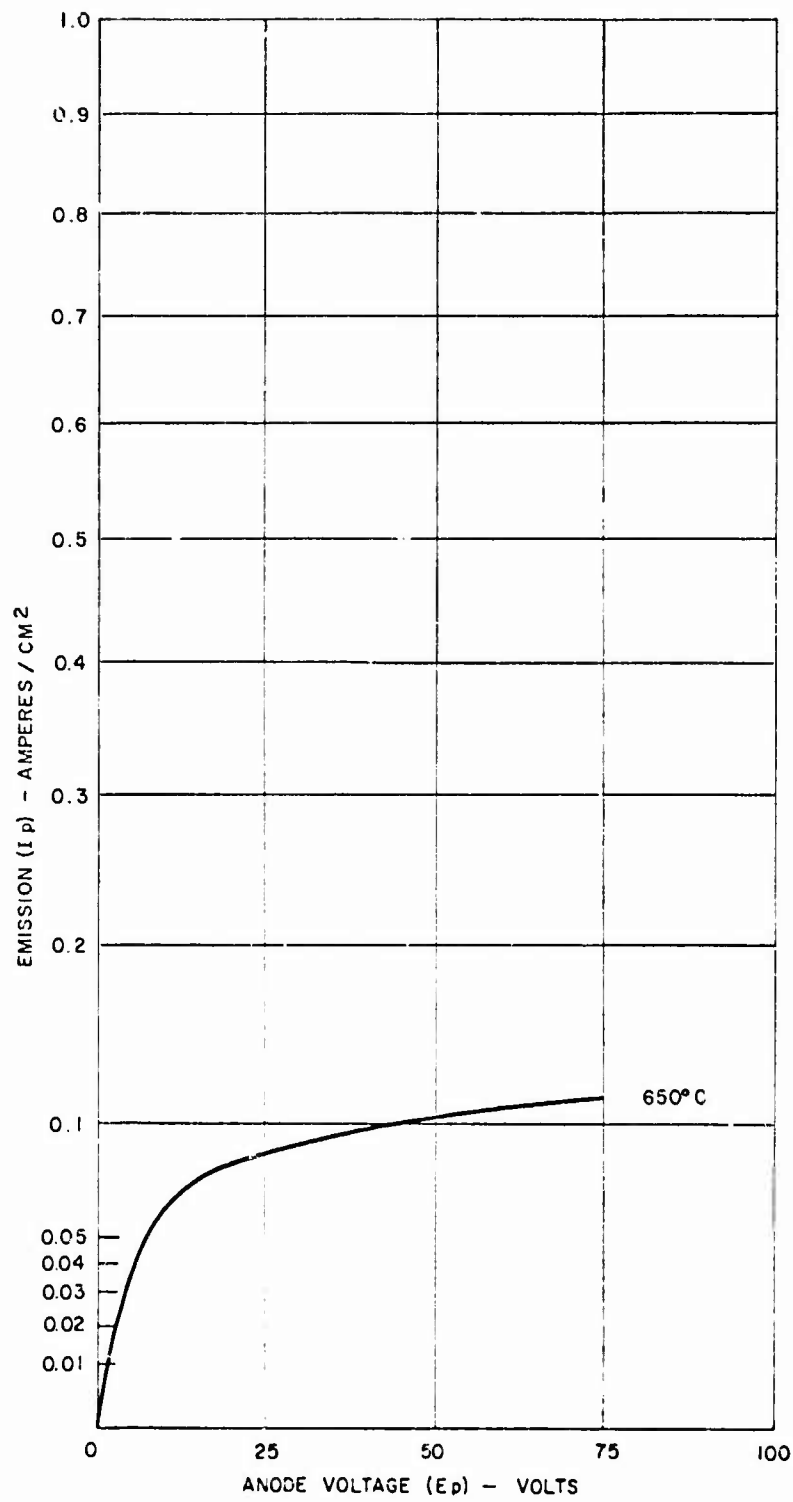


Figure 38 - Initial Emission Characteristics of HCD-58 Cathode at 650°C

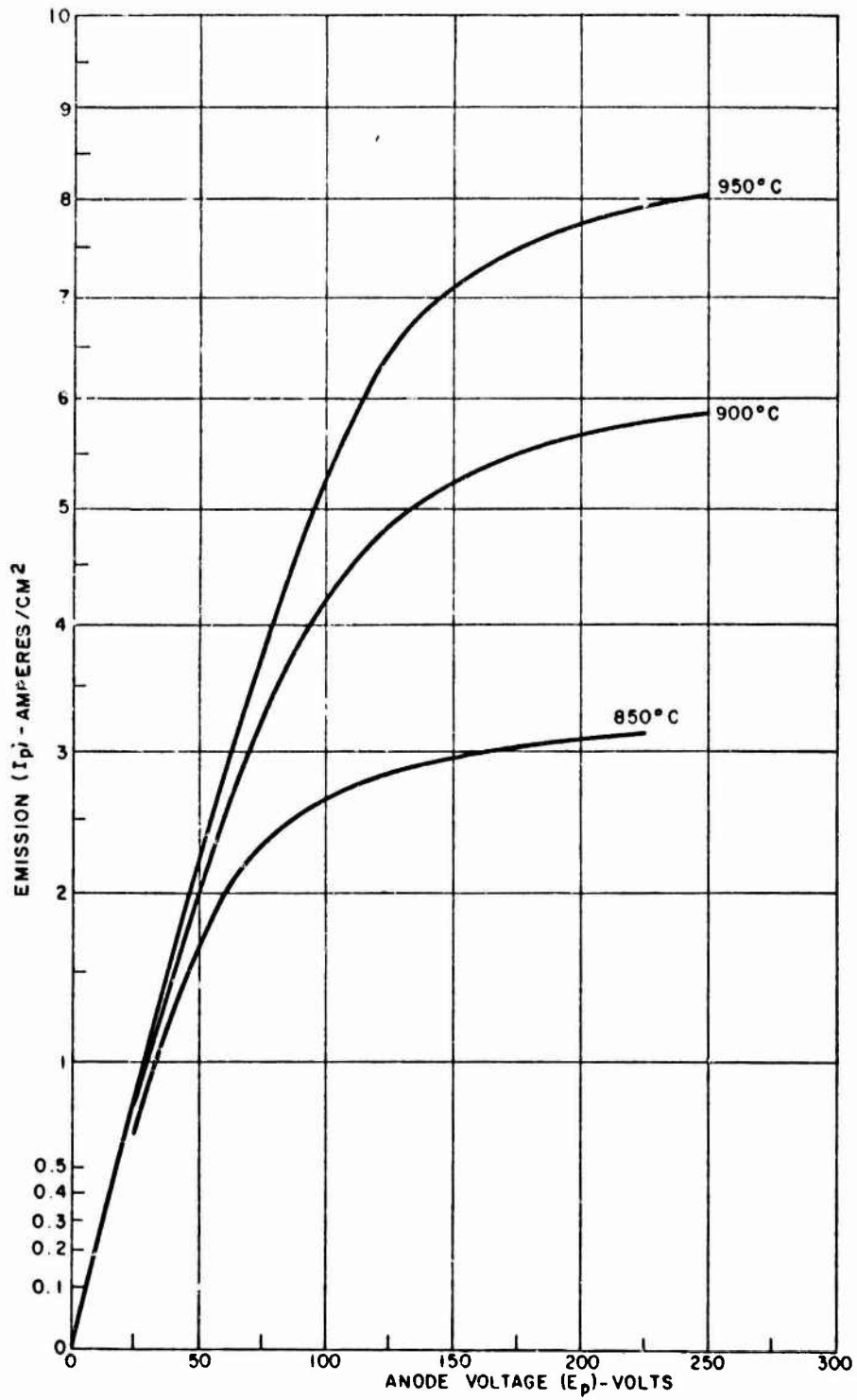


Figure 39 - Initial Emission Characteristics of HCD-58 Cathode at 850°C, 900°C, and 950°C

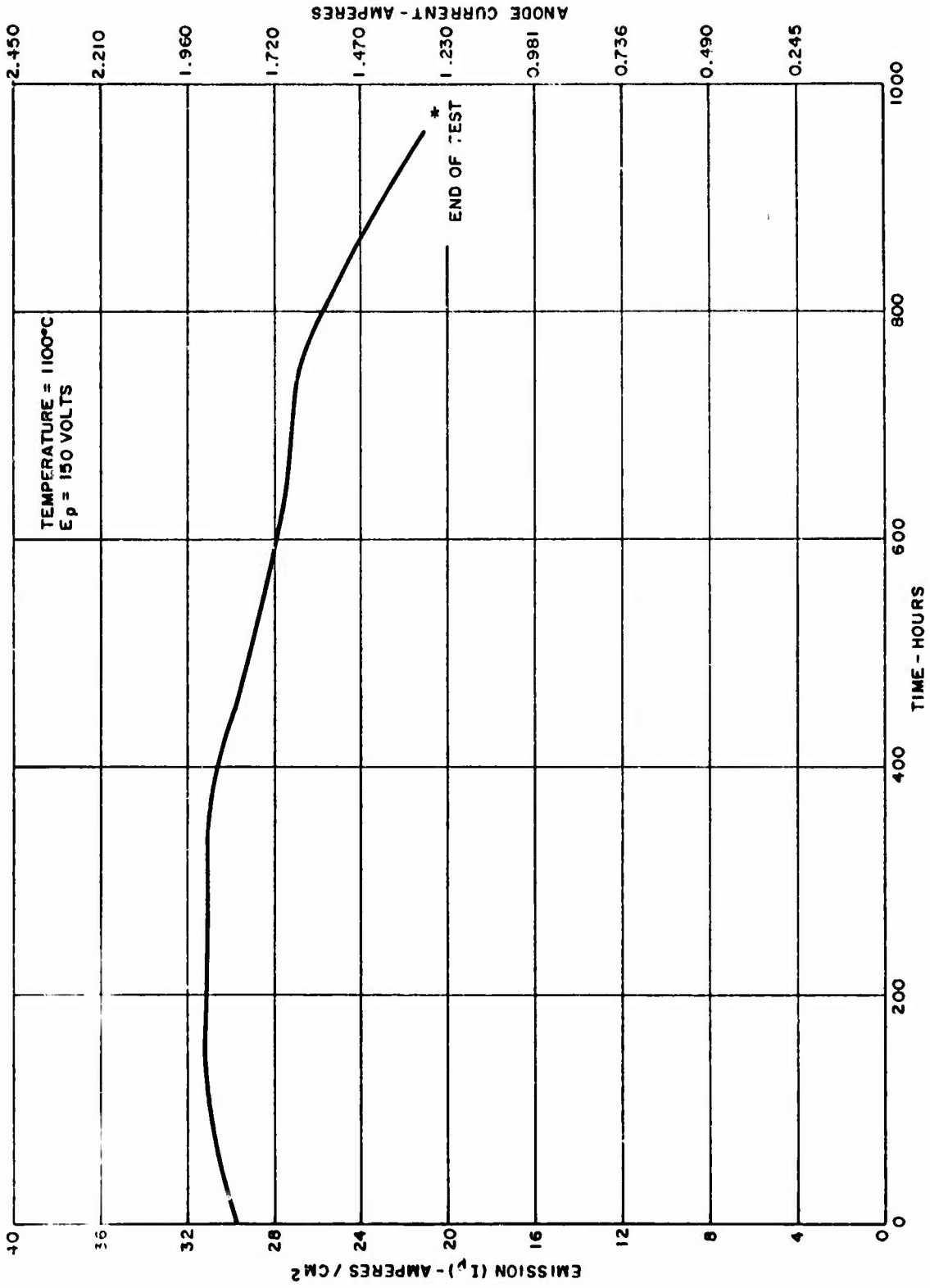


Figure 40 - Life Test Record of HCD-59 Cathode

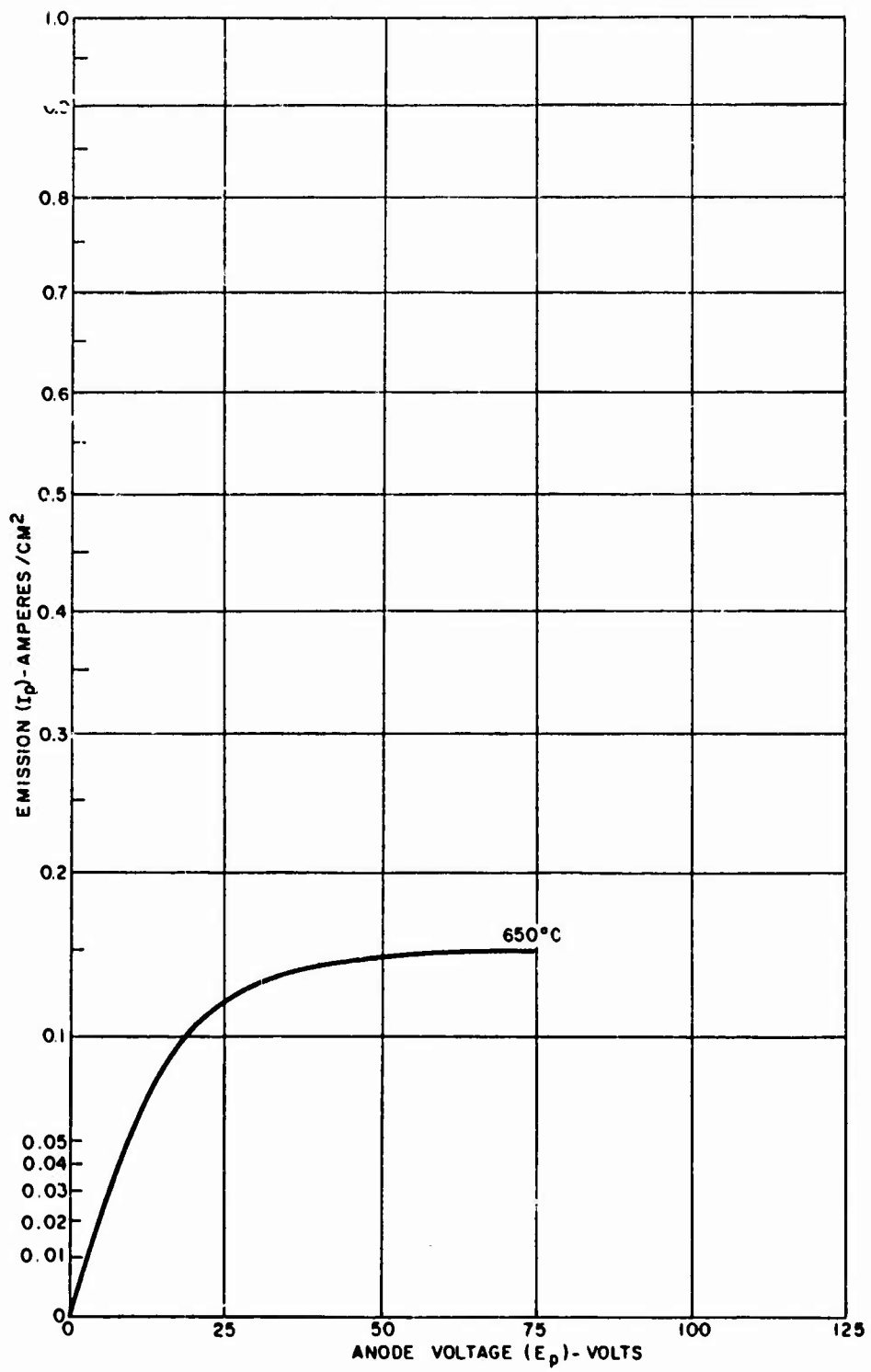


Figure 41 - Initial Emission Characteristic of HCD-59 Cathode at 650°C

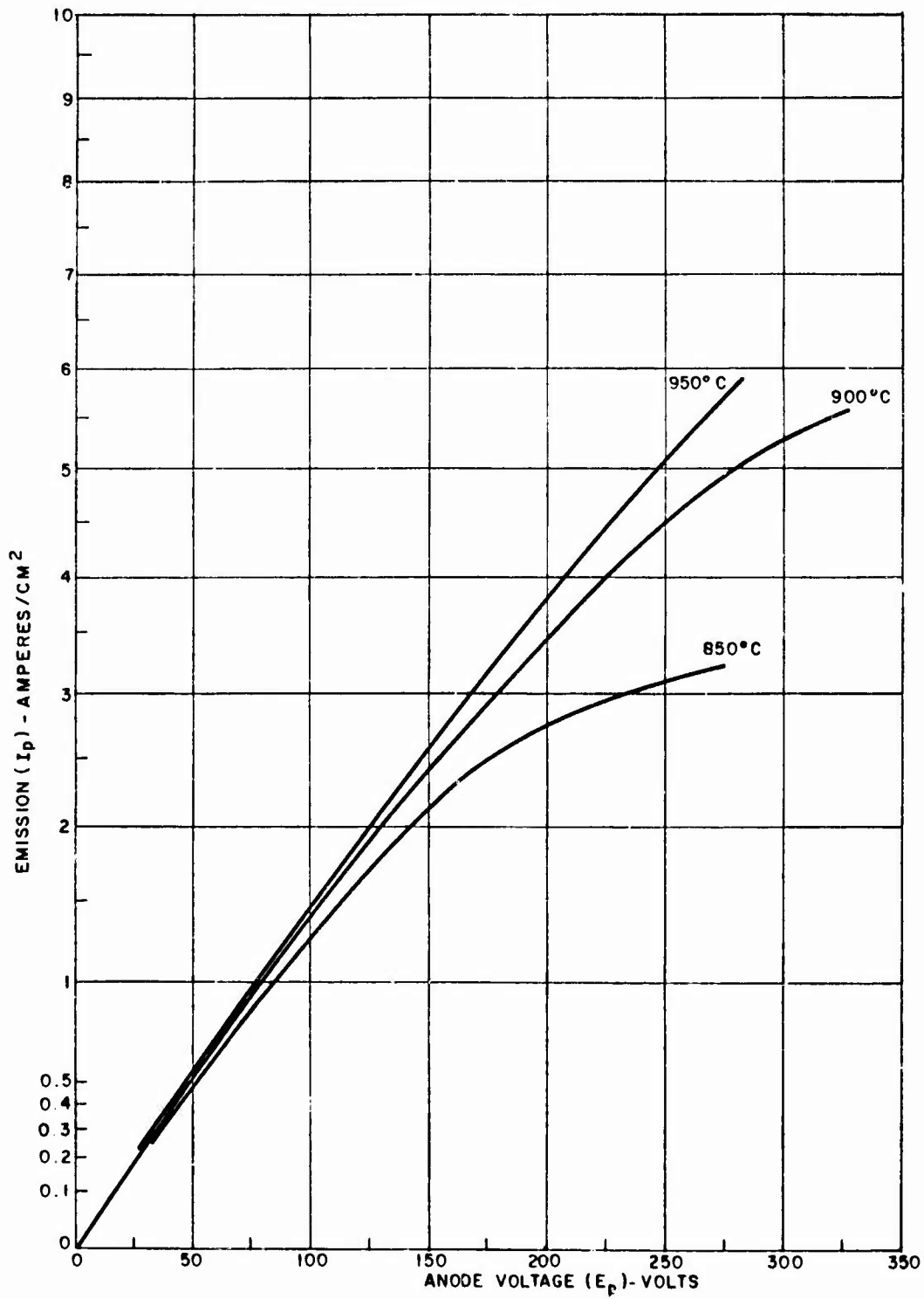


Figure 42 - Initial Emission Characteristics of HCD-59 Cathode at 850°C, 900°C, and 950°C

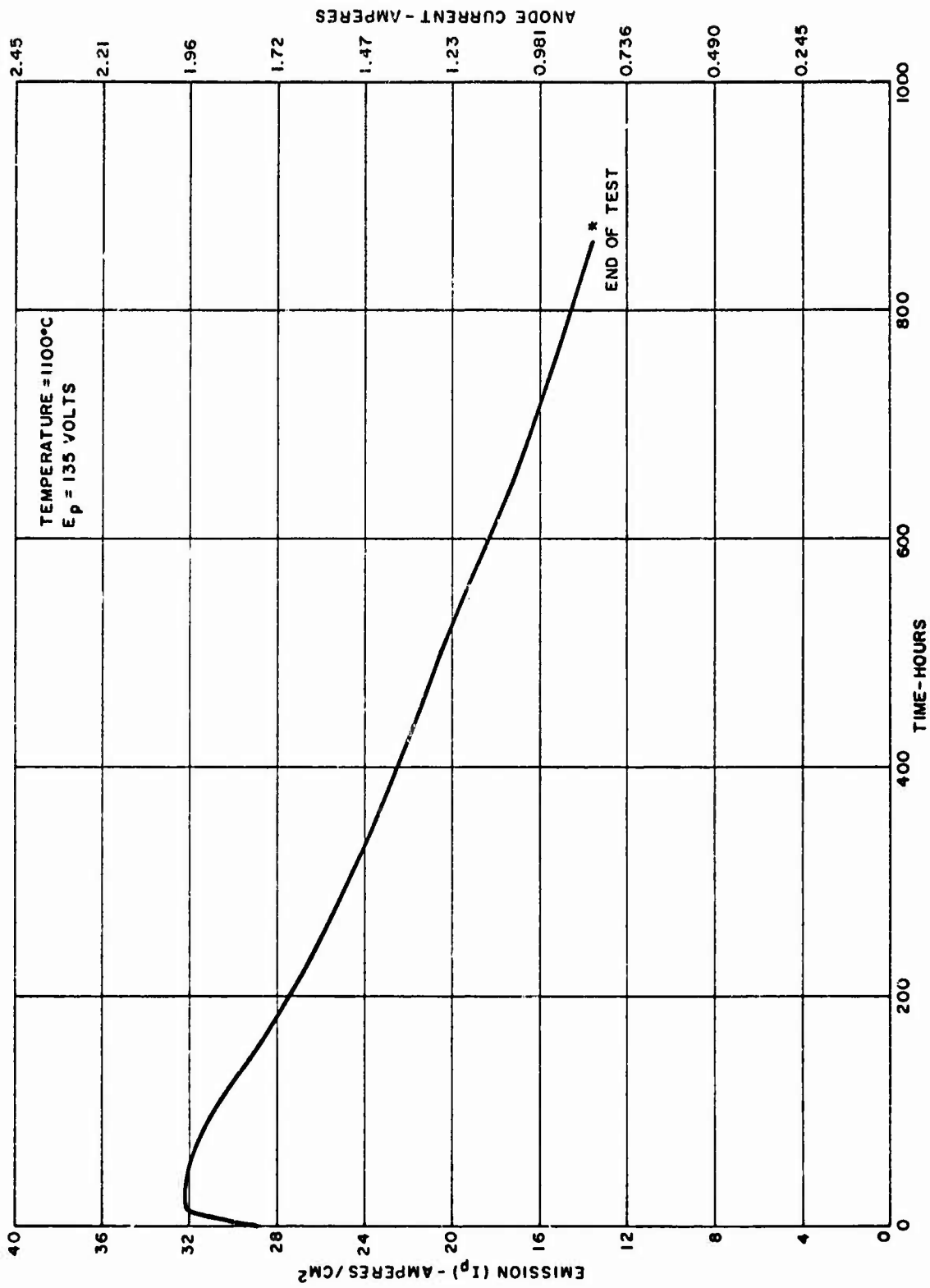


Figure 43 - Life Test Record of HCD-30 Cathode

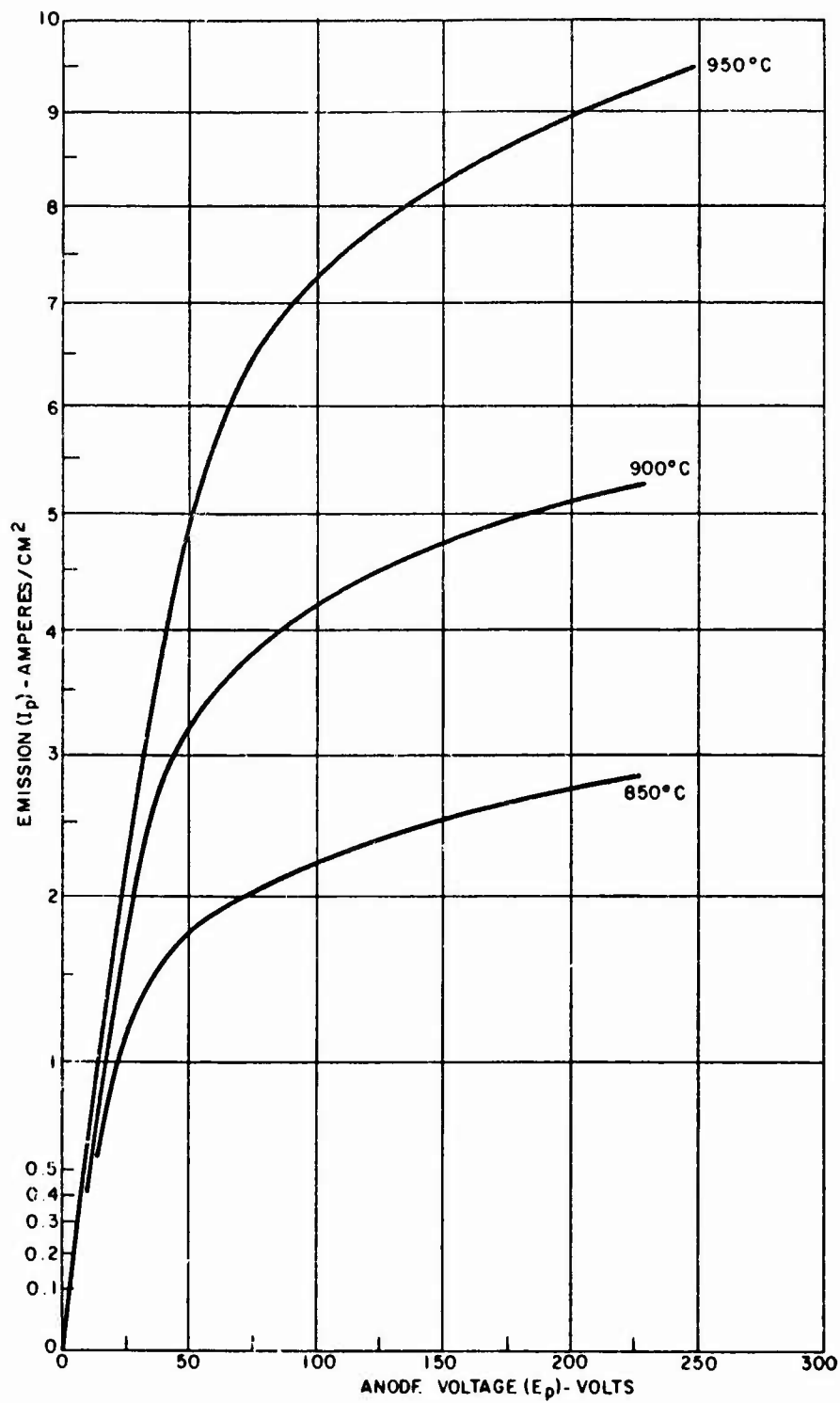


Figure 44 - Initial Emission Characteristics of HCD-60 Cathode at 850°C, 900°C, and 950°C

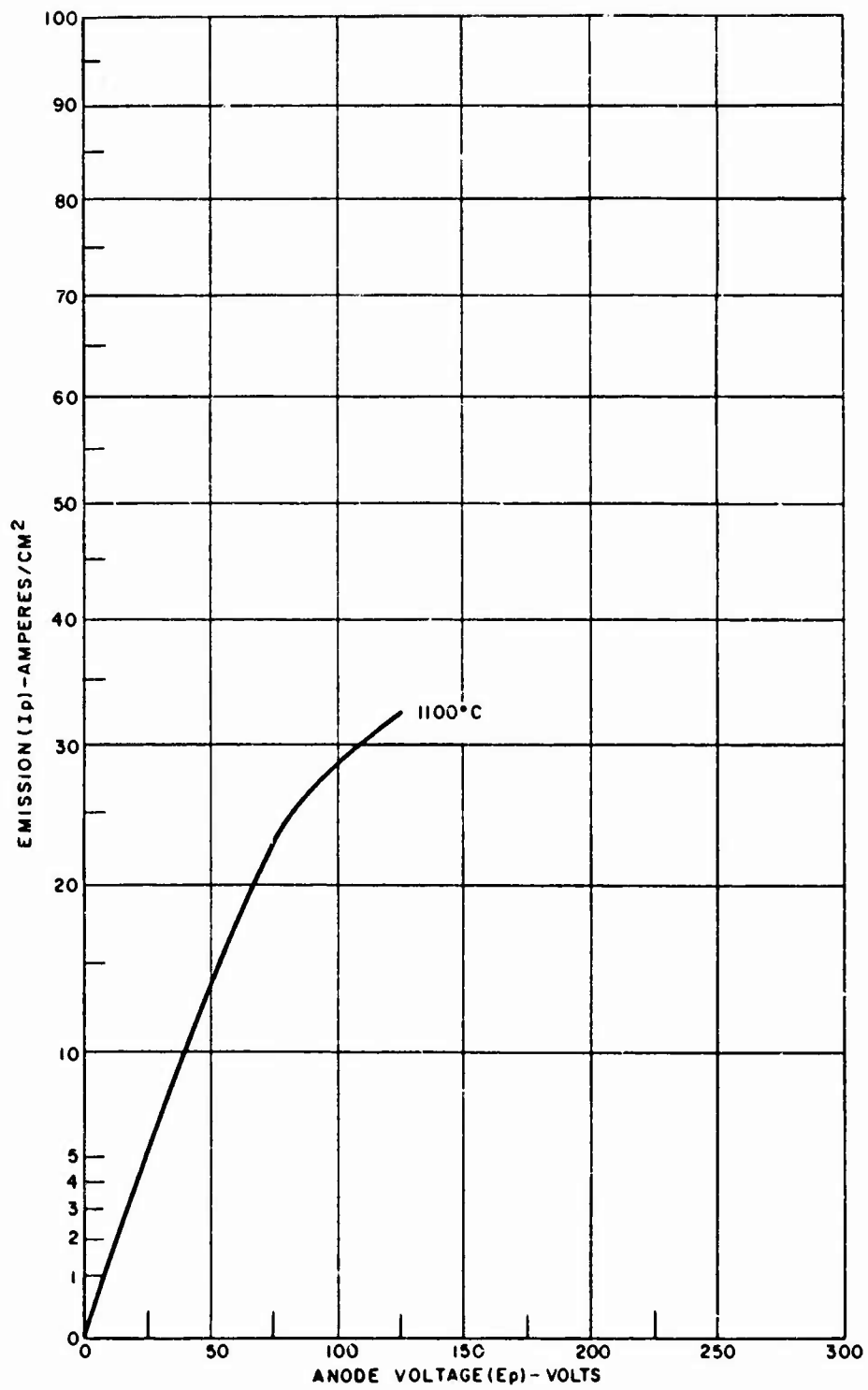


Figure 45 - Initial Emission Characteristics of HCD-60 Cathode at 1100°C

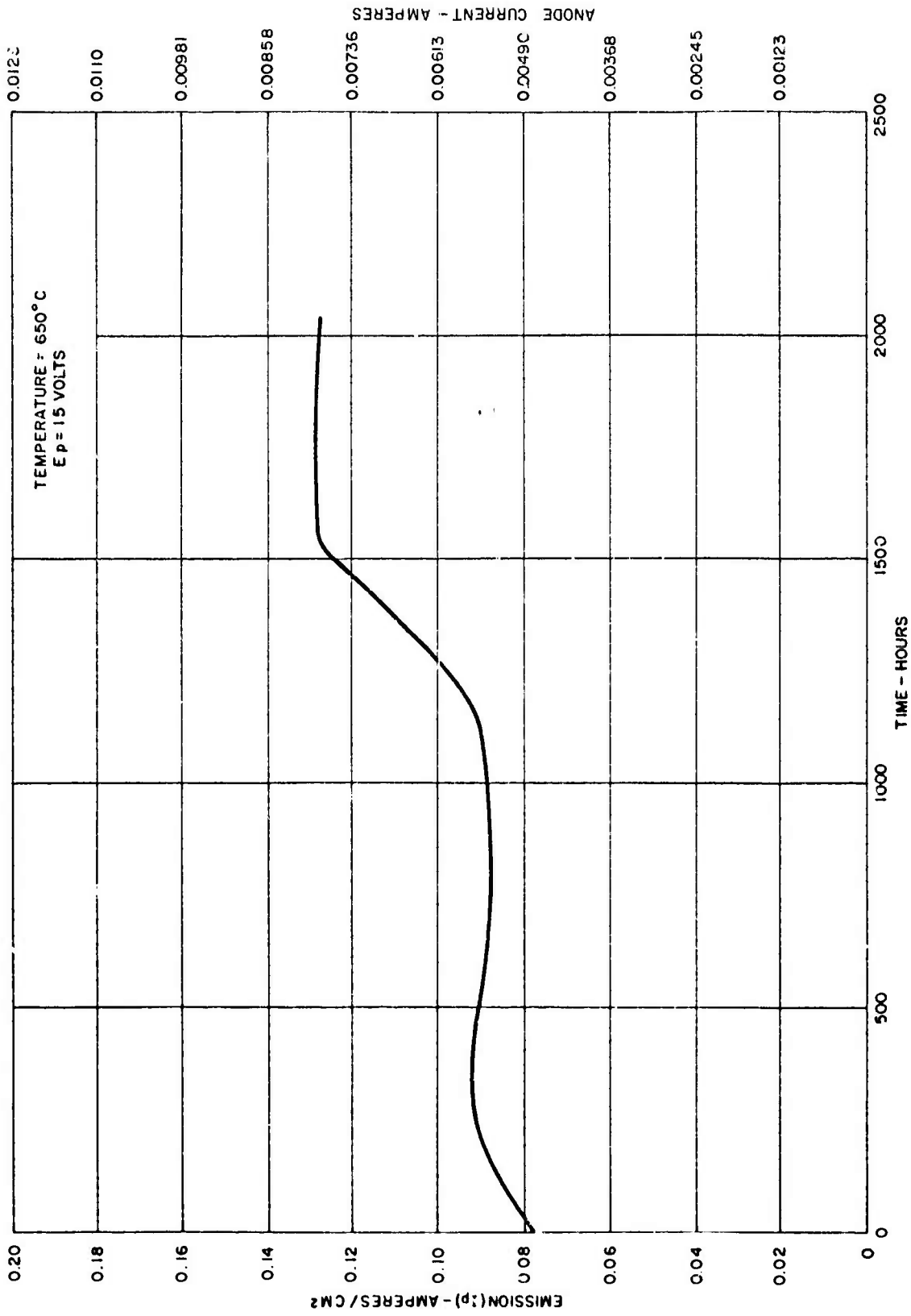


Figure 46 - Life Test Record of HCD-61 Cathode

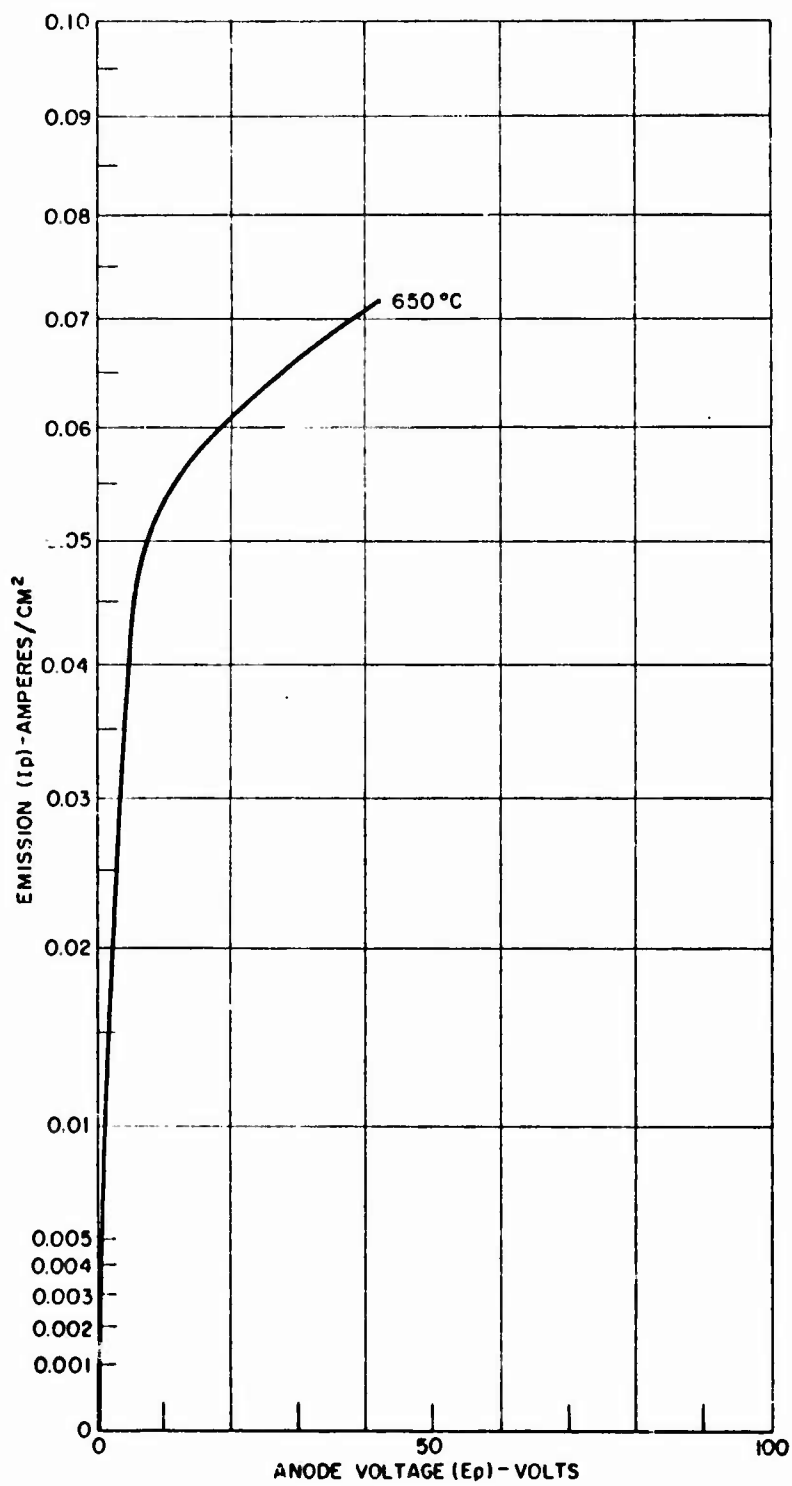


Figure 47 - Initial Emission Characteristic of HCD-61 Cathode at 650°C

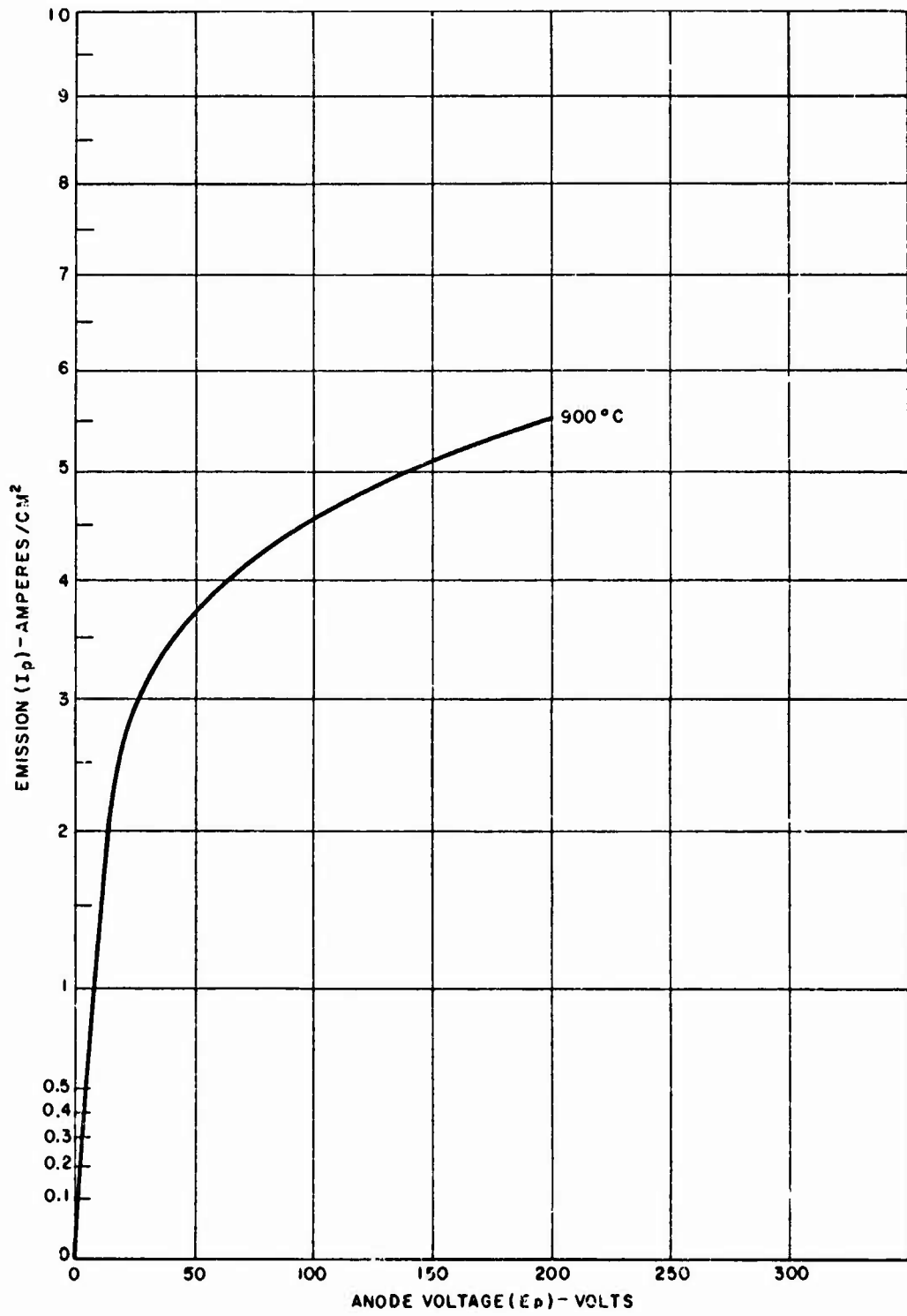


Figure 48 - Initial Emission Characteristic of HCD-61 Cathode at 900°C

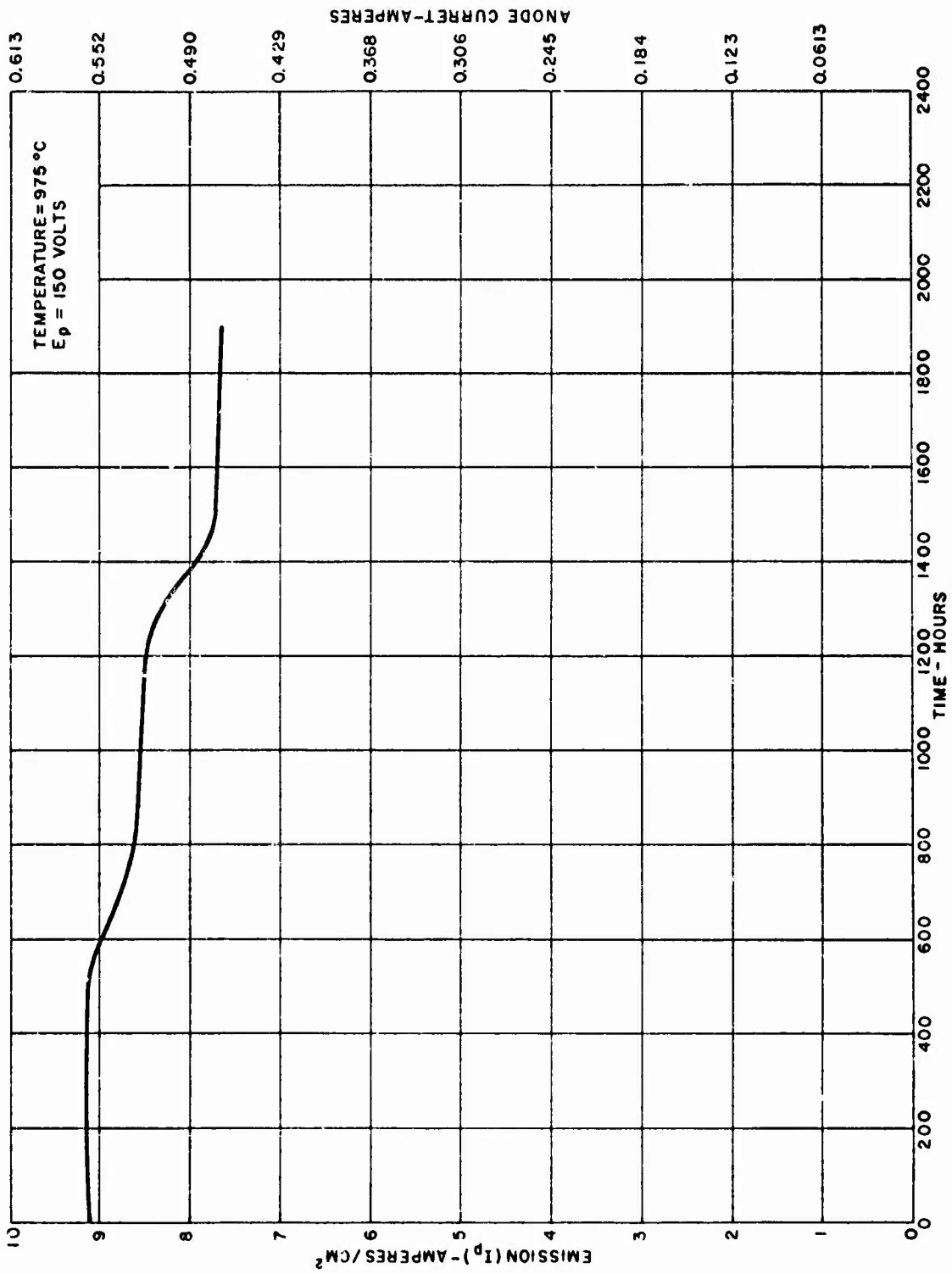


Figure 49 - Life Test Record of HCD-62 Cathode

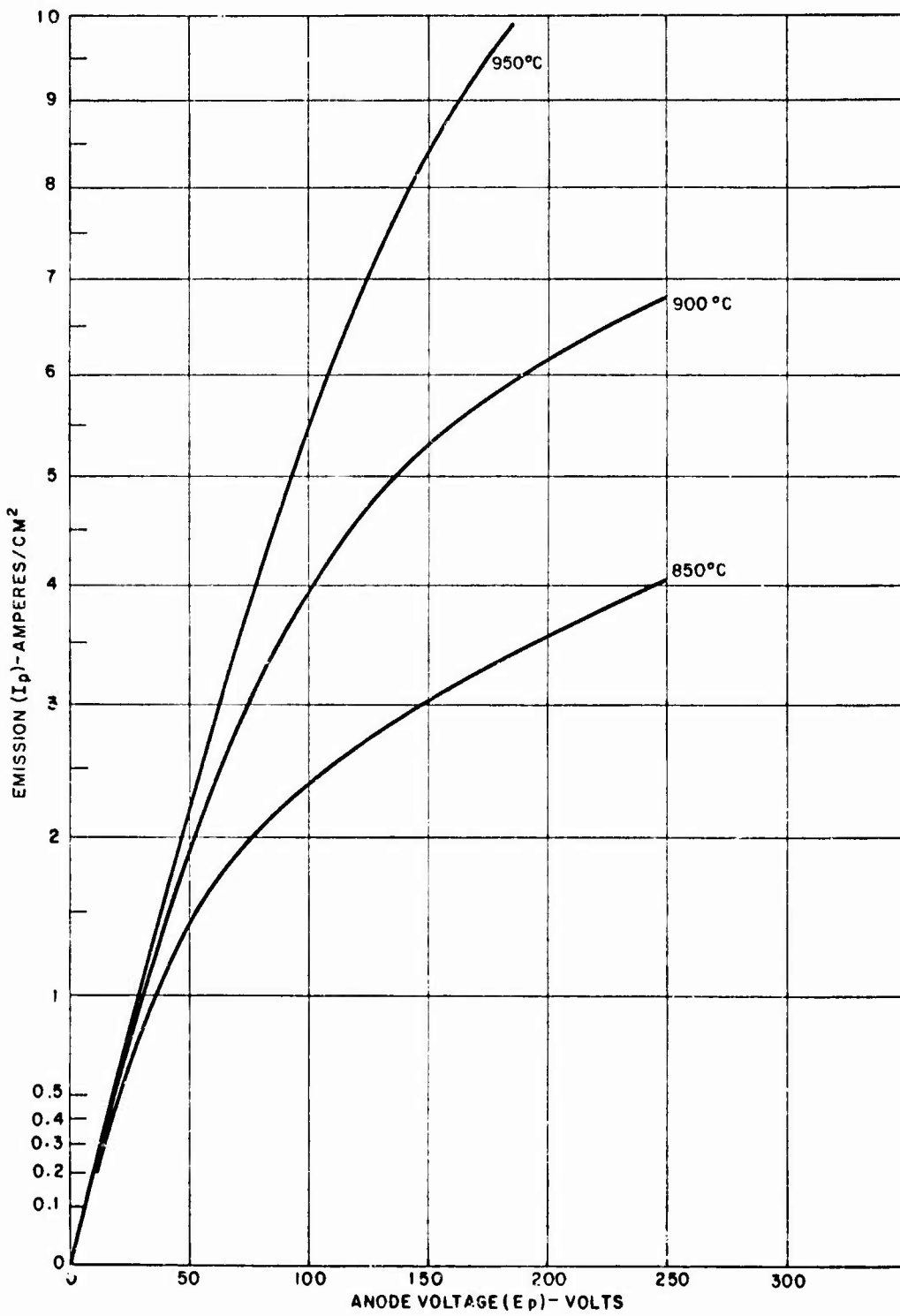


Figure 50 - Initial Emission Characteristics of HCD-62 Cathode at 850°C, 900°C, and 950°C

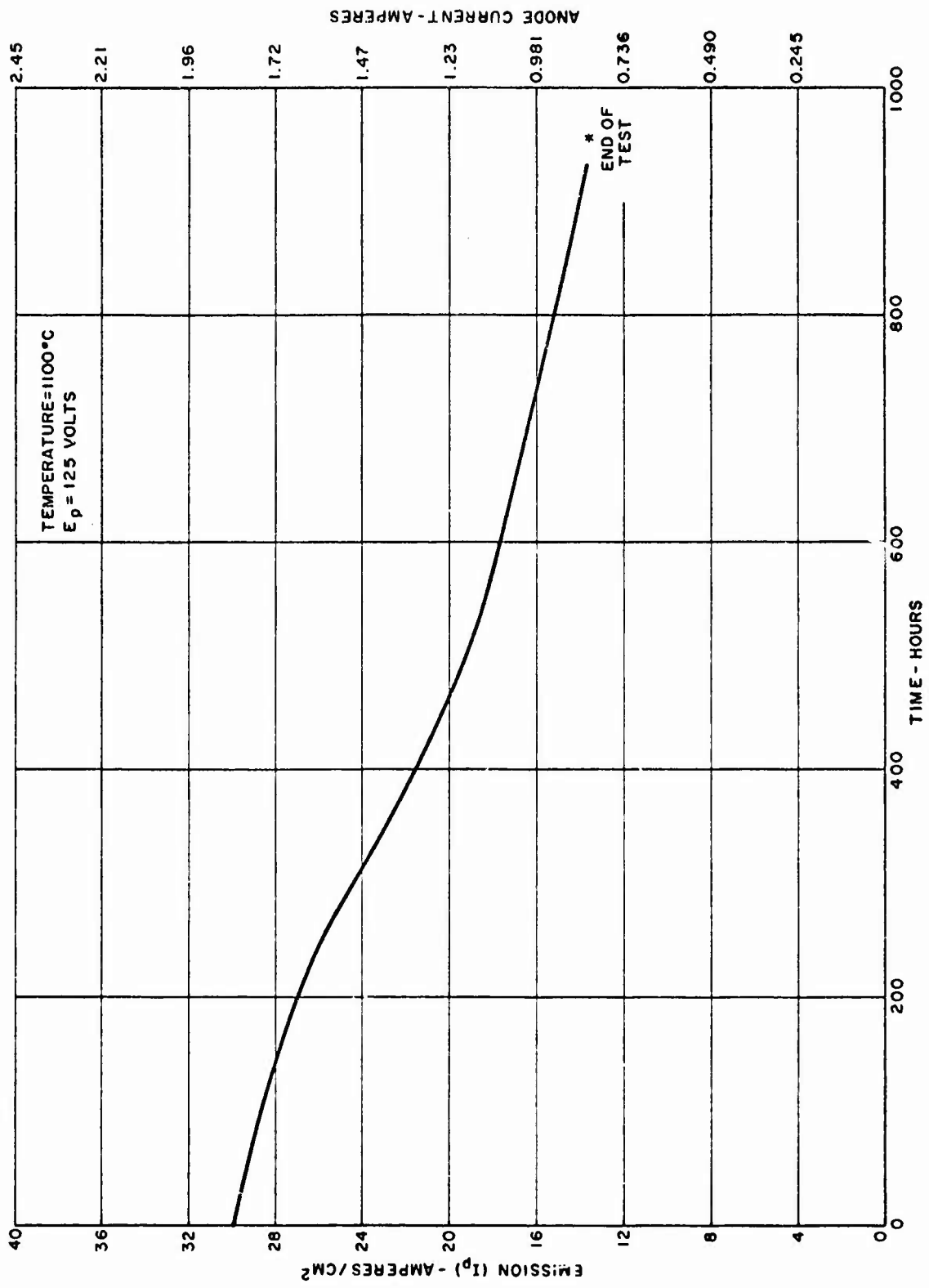


Figure 51 - Life Test Record of HCD-63 Cathode

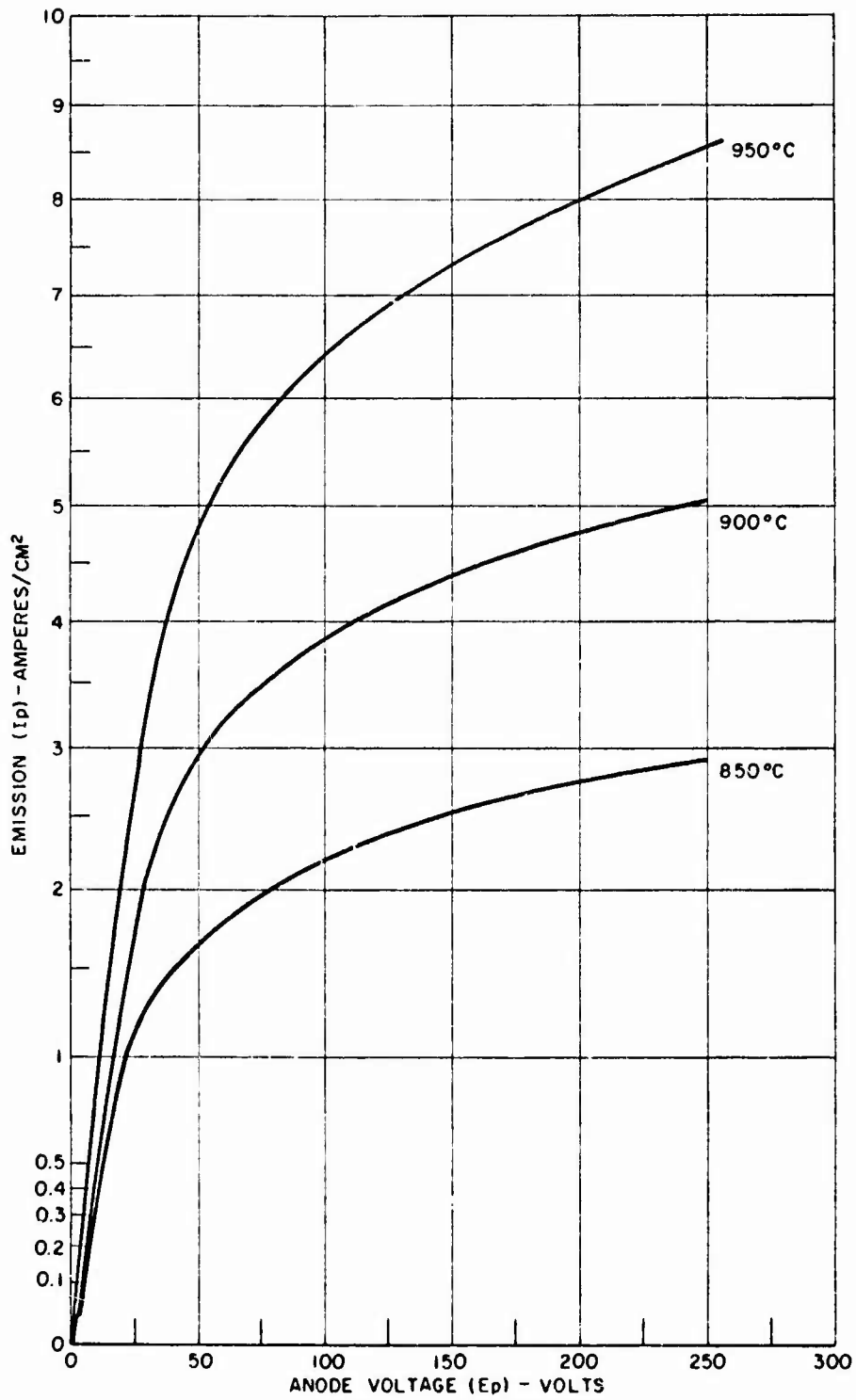


Figure 52 - Initial Emission Characteristics of HCD-63 Cathode at 850°C, 900°C, and 950°C

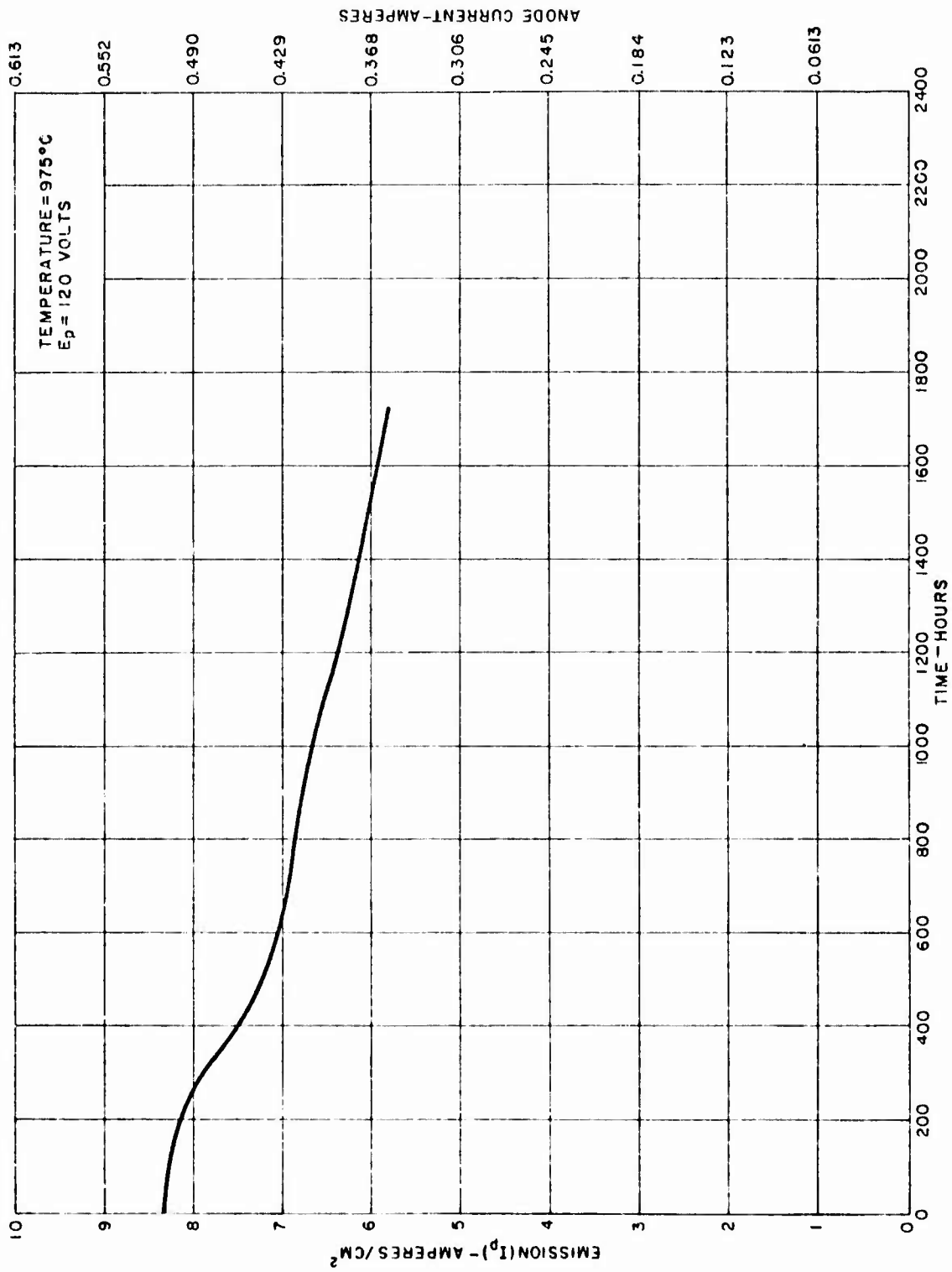


Figure 53 - Life Test Record of HCD-64 Cathode

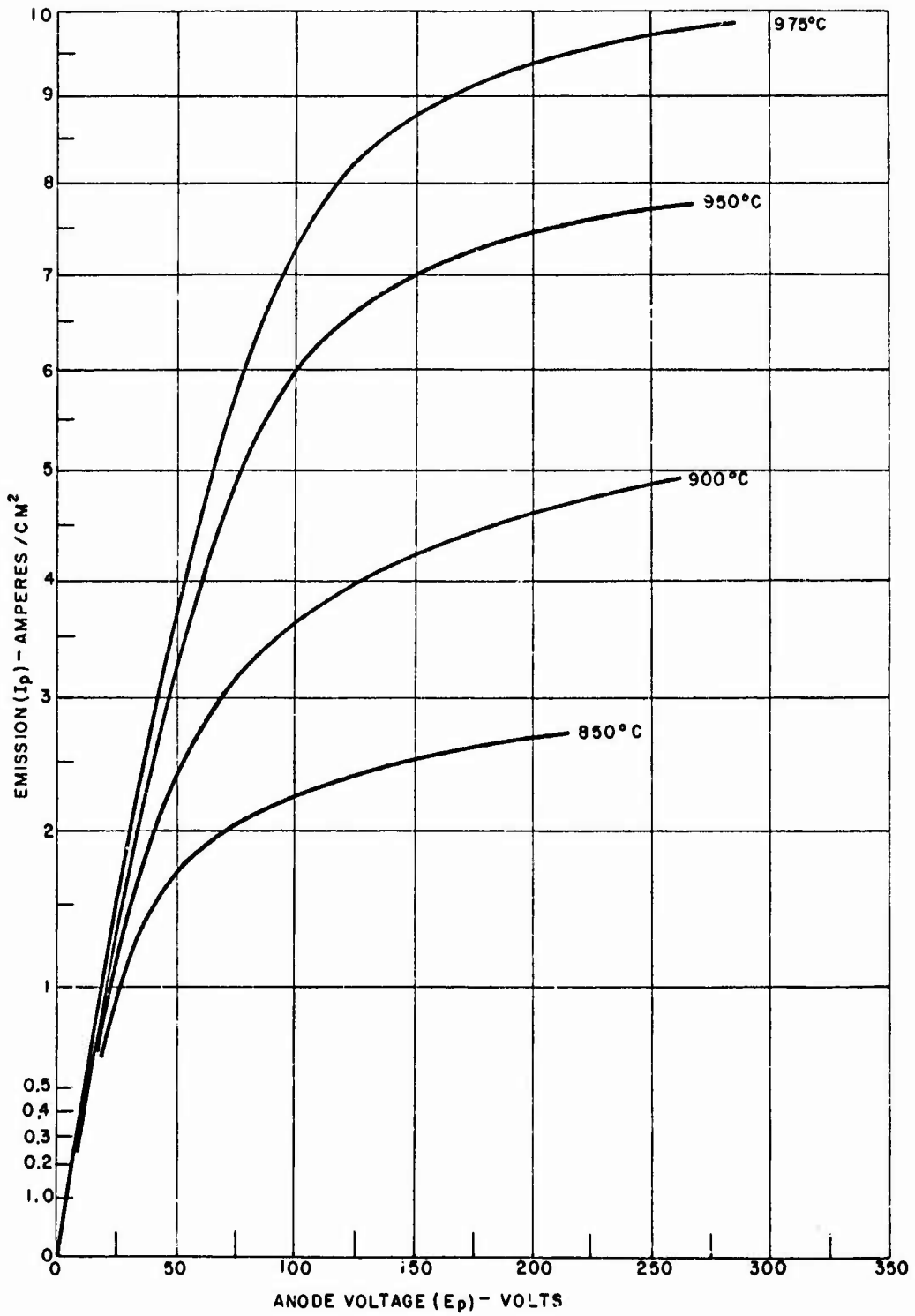


Figure 54 - Initial Emission Characteristics of HCD-64 Cathode at 850°C, 900°C, 950°C, and 975°C

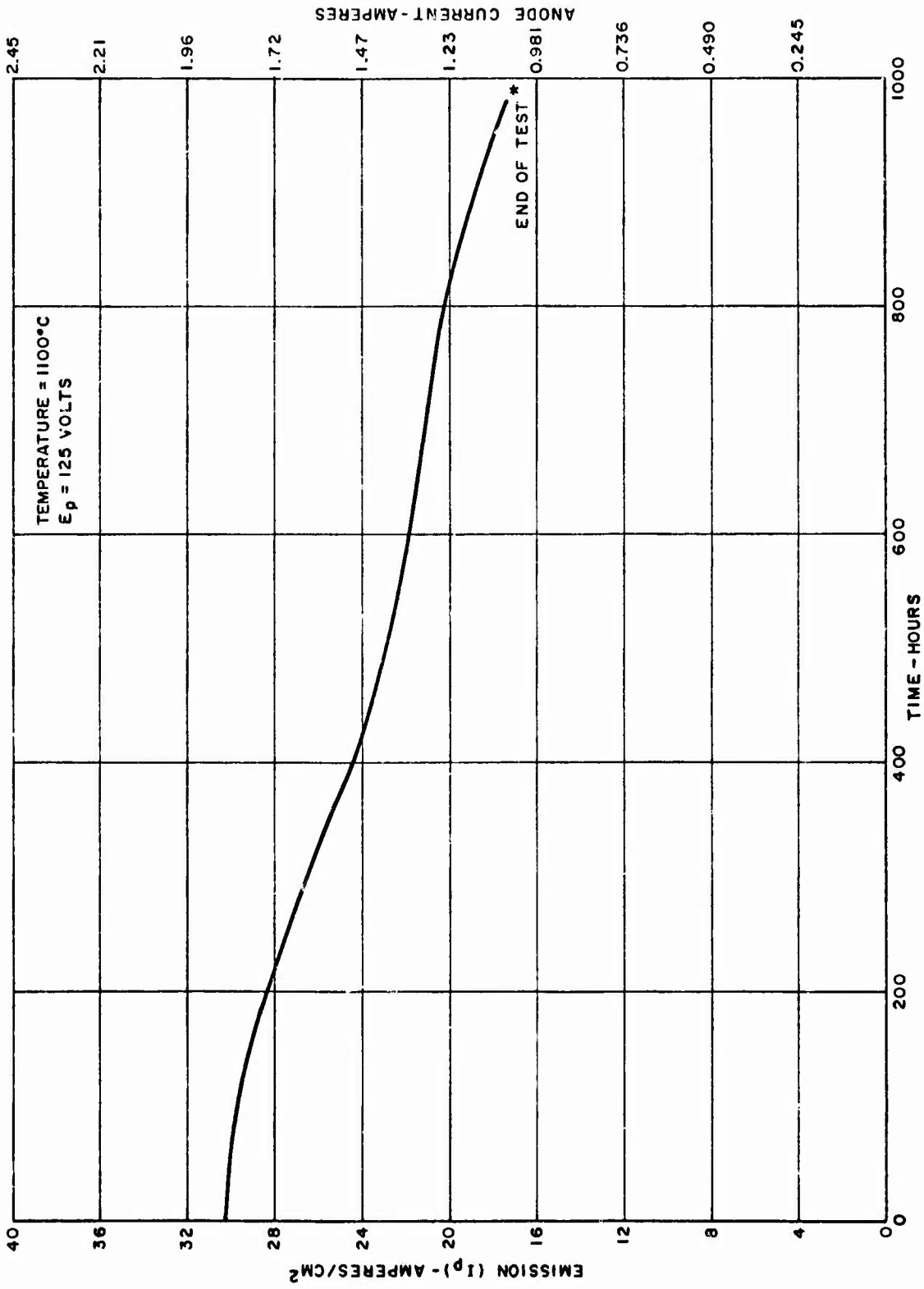


Figure 55 - Life Test Record of HCD-65 Cathode

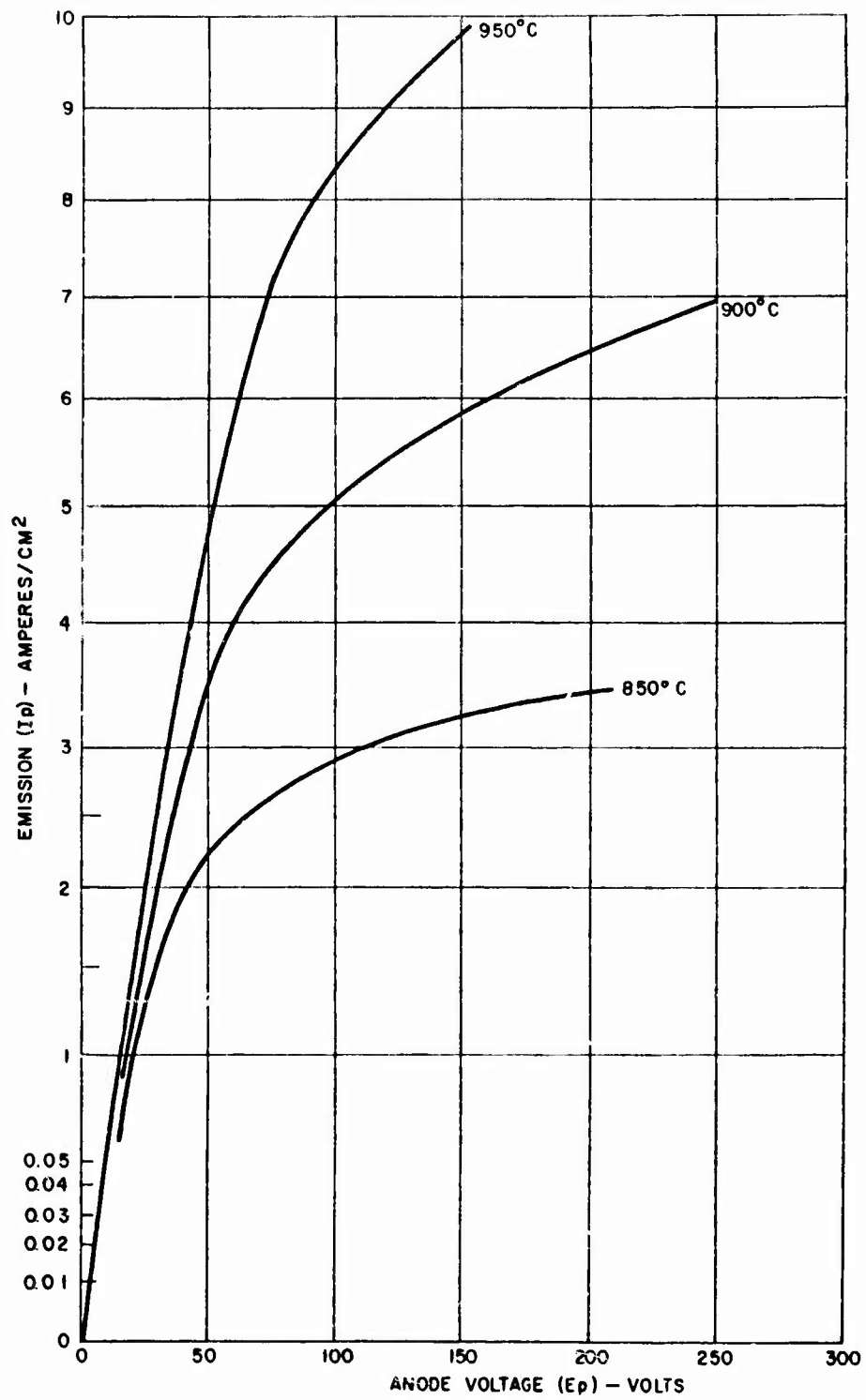


Figure 56 - Initial Emission Characteristics of HCD-65 Cathode at 850°C, 900°C, and 950°C

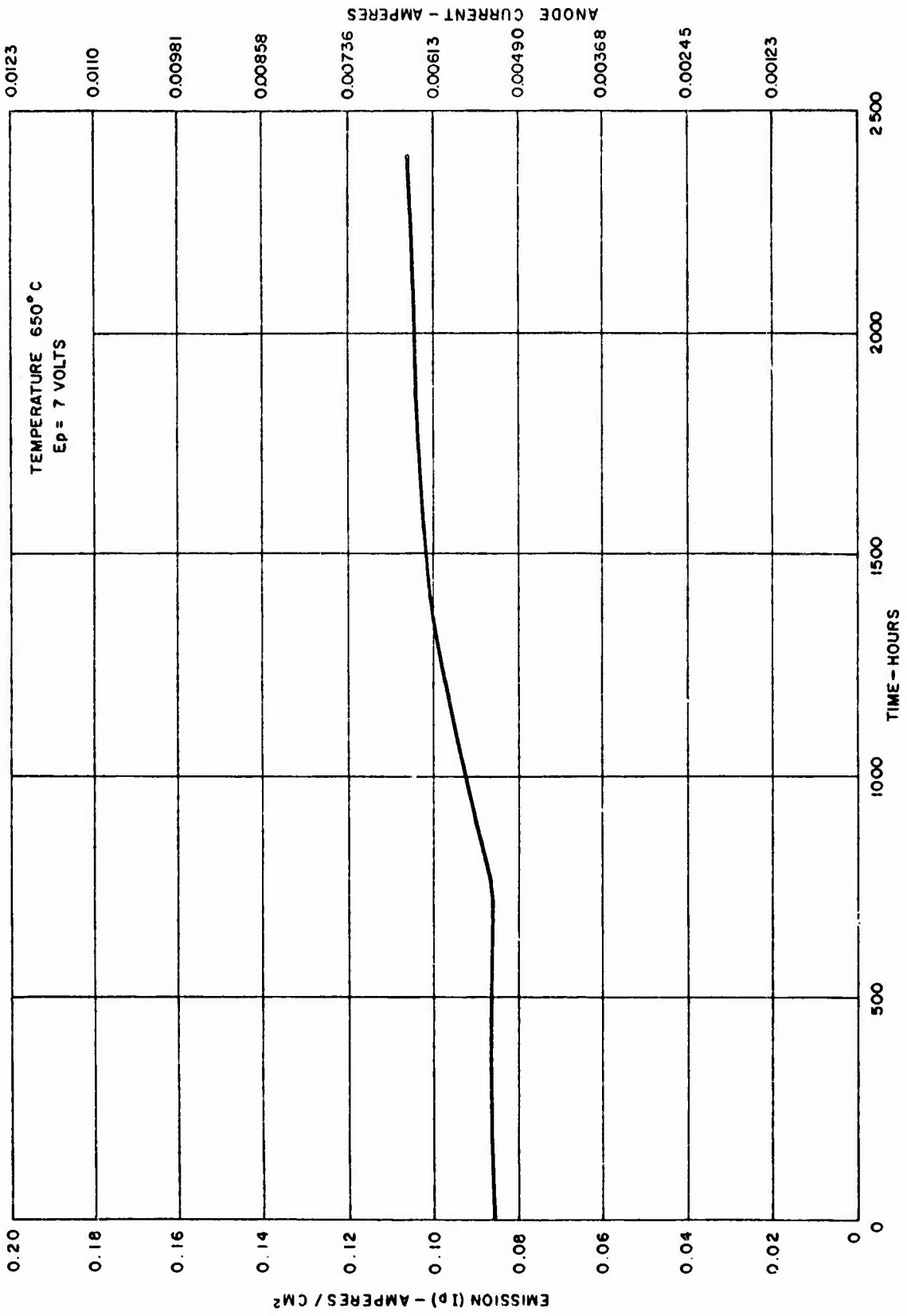


Figure 57 - Life Test Record of HCD-66 Cathode

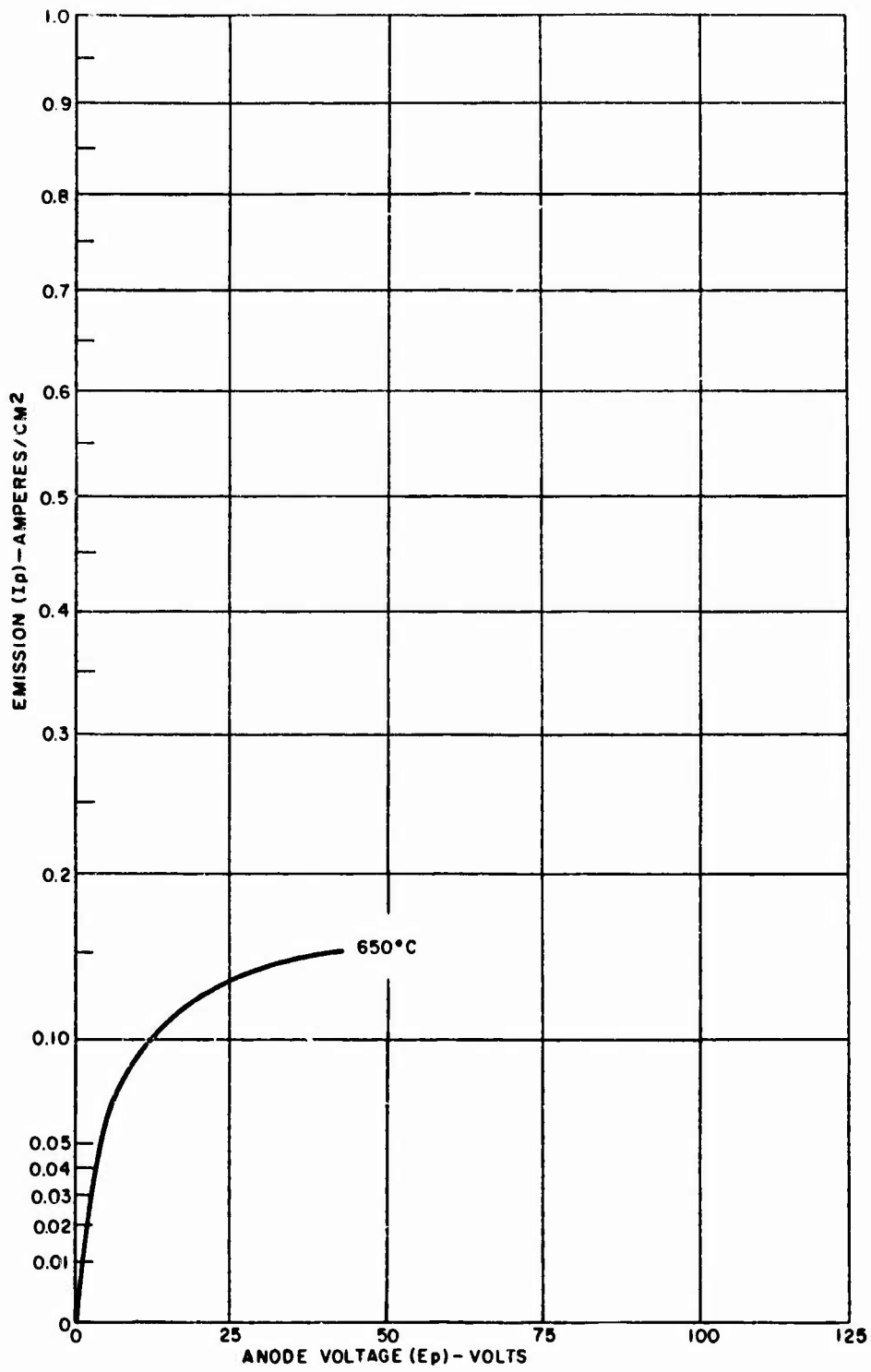


Figure 58 - Initial Emission Characteristic of HCD-66 Cathode at 650°C

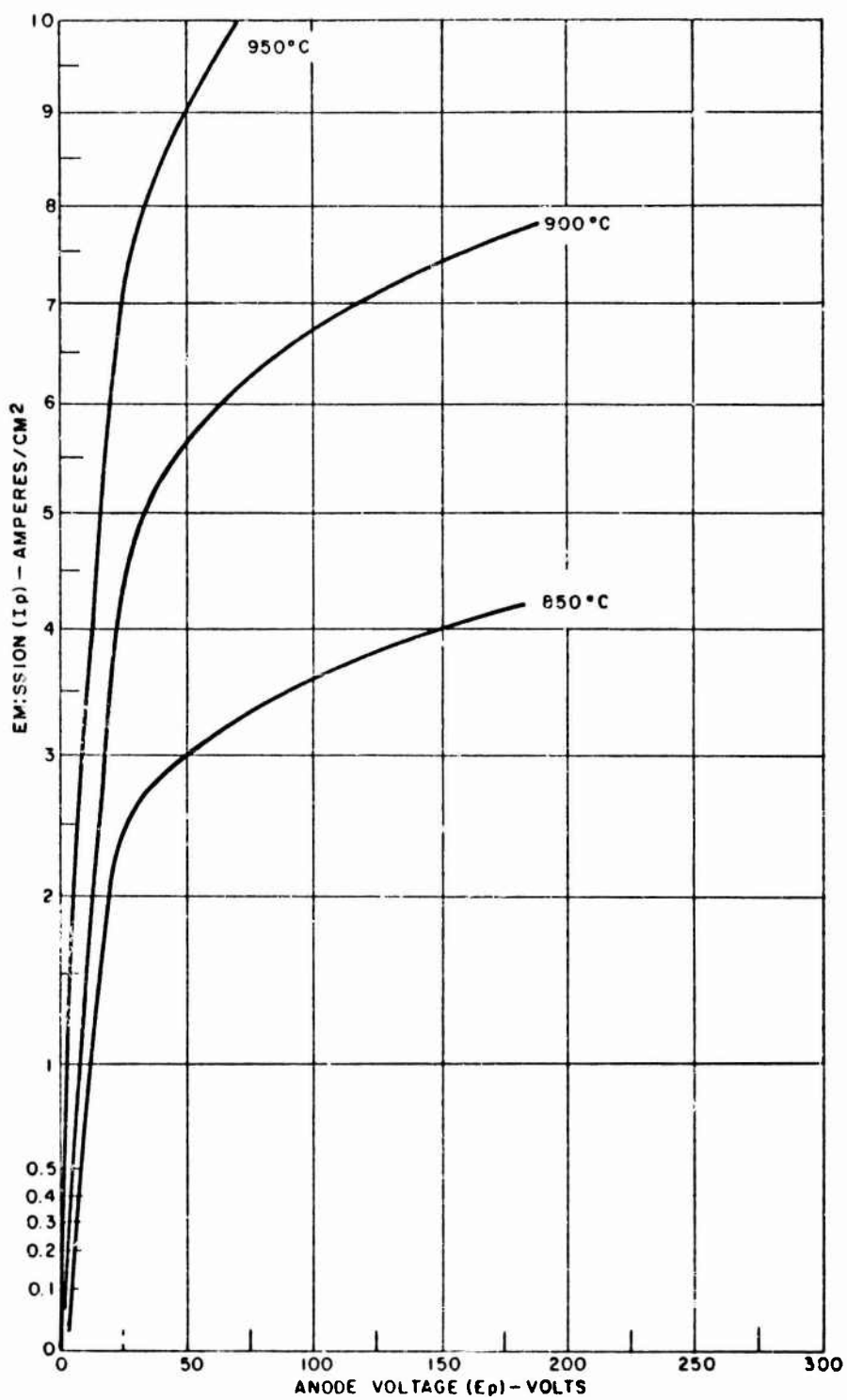


Figure 59 Initial Emission Characteristics of HCD-66 Cathode  
 a. 850°C, 900°C, and 950°C

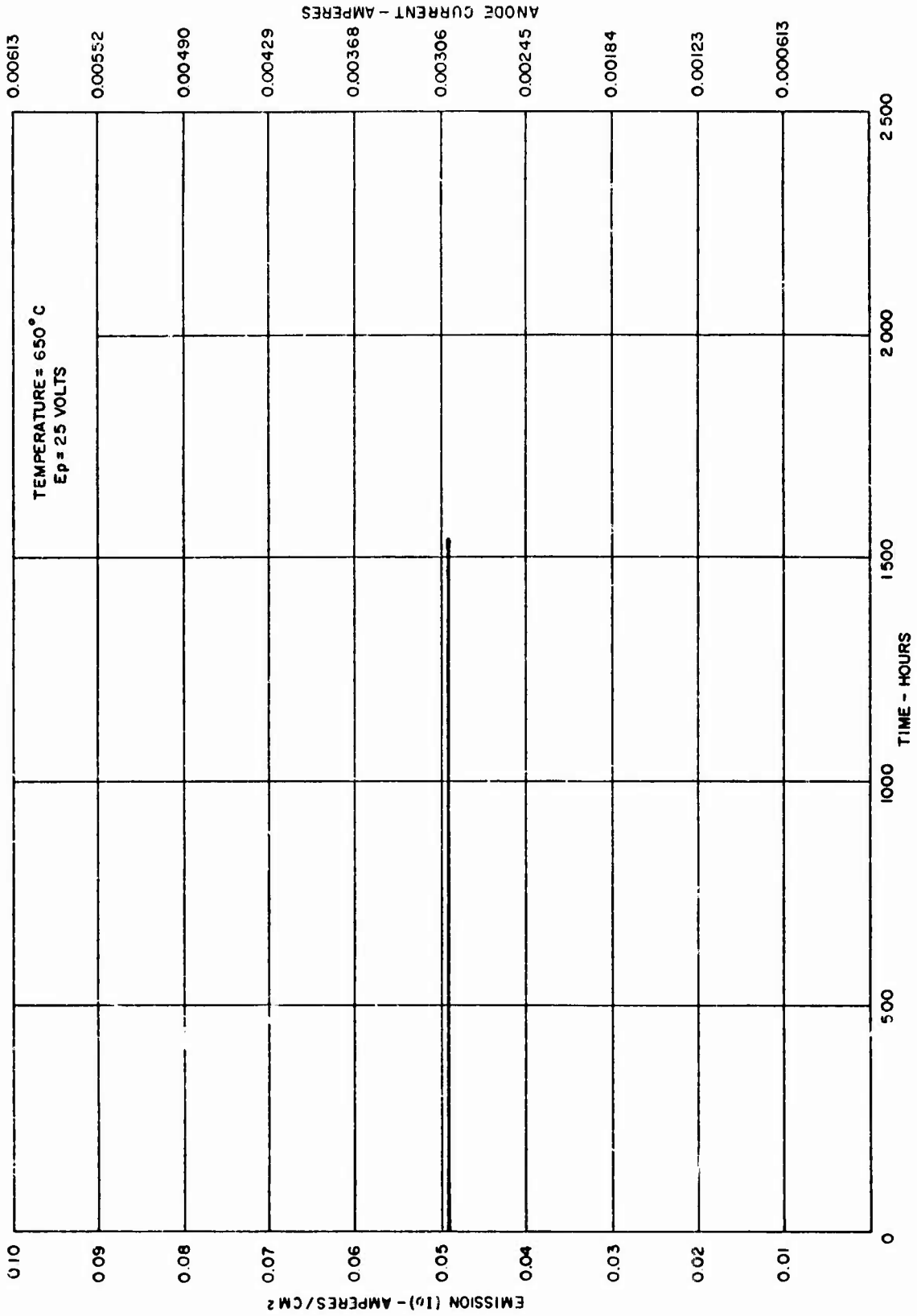


Figure 60 - Life Test Record of HCD-67 Cathode

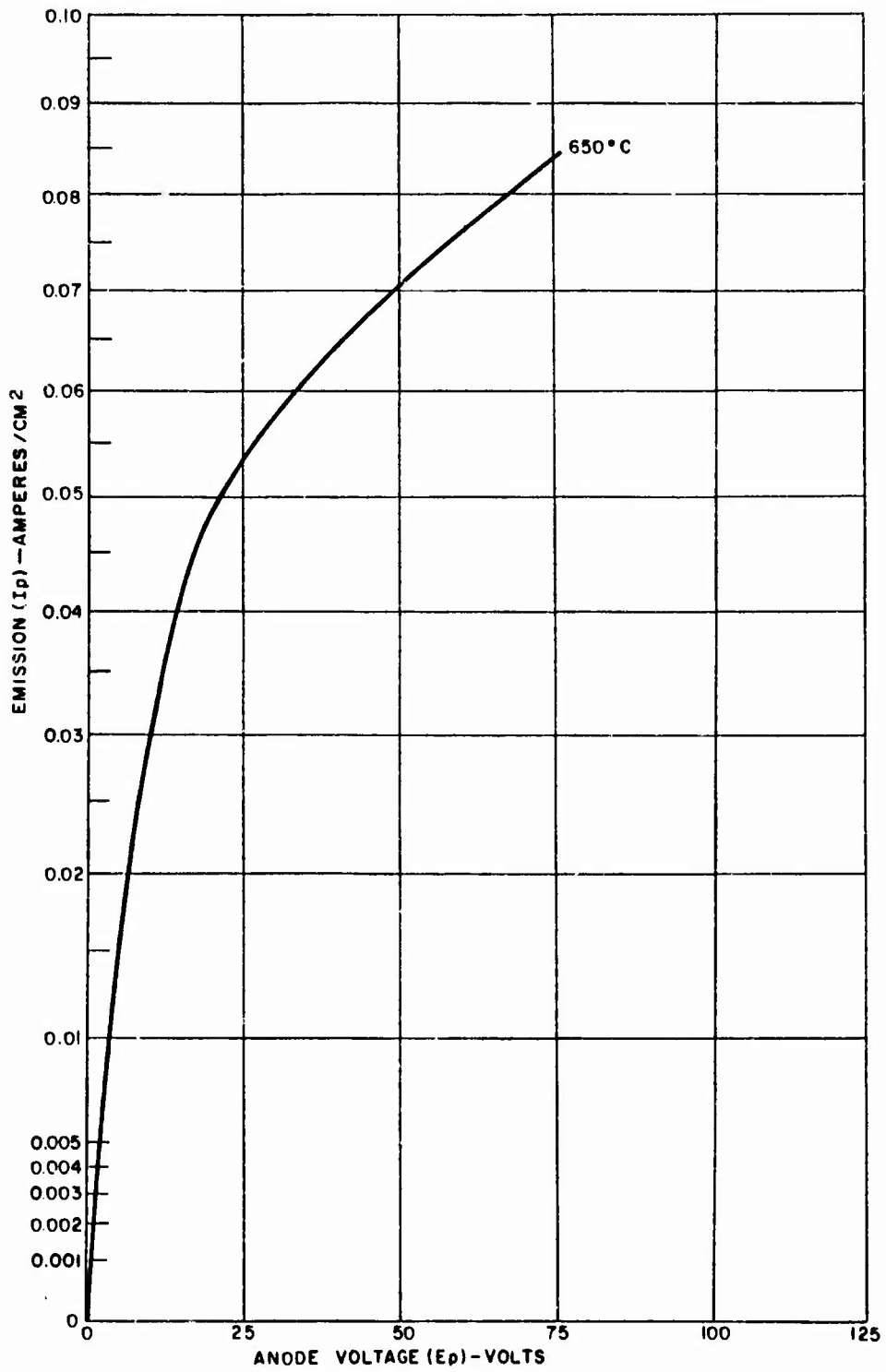


Figure 61 - Initial Emission Characteristic of HCD-67 Cathode at 650°C

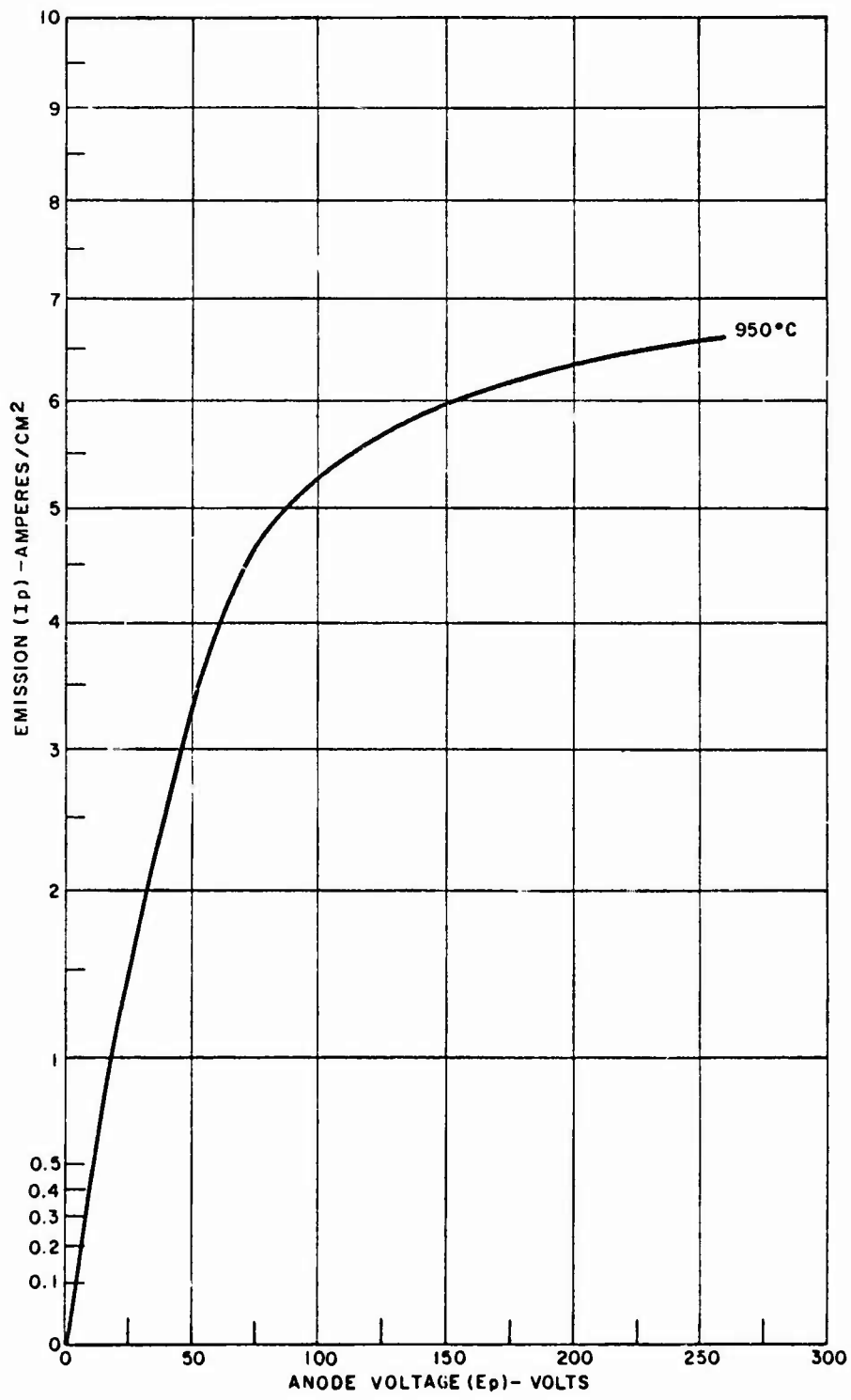


Figure 62 - Initial Emission Characteristic of HCD-67 Cathode at 950°C

Table I - Summary of Life Test Results Completed to Date

Diode** (Cath. No.)	Cathode Temp. (°C)	Life* Test Cond.	Initial Current (A/cm <sup>2</sup> )	Hours on Life	Remarks
BTA-6	950-974	b	8	2500	Rescheduled at 750 hours
HCD-1	650 850	a a	0.655 1.5	1200 8800	Rescheduled at 850°C at end of 1200 hours; stable emission, followed by gradual decline; at 4700 hours cooling-water failed, resulting in decline in emission to 0.65 A/cm <sup>2</sup> at 5000 hours, recovering to 0.775 A/cm <sup>2</sup> at 7200 hours.
HCD-2	1000	b	8.4	5300	Stable to 1600 hours; decreasing emission to 5300 hours
HCD-3	950	b	5	14300	Useful life approx. 14,000 hours; water failure at 7000-hour point may have contributed to early failure
HCD-5	1050	c	13-15.8	750	Stable over first 500 hours; decreased to 8.5 A/cm <sup>2</sup> at 750 hours
HCD-6	1100	c	18-24	800	Stable over first 500 hours; decreased to 4 A/cm <sup>2</sup> at 800 hours
HCD-7	1075	c	31+	410	Stable to 300 hours; decreased to 26 A/cm <sup>2</sup> at 410 hours
HCD-8	1050	c	15.5	1100	Generally stable to 1000 hours; decreased to 10.5 A/cm <sup>2</sup> at 1100 hours
HCD-11	1100	b	8	550	Rapid drop in emission with time; anode cooling-water failure
HCD-12	1100	c	30	890	Good emission after 80 hours (see Second Quarterly); generally stable to 300 hours followed by decreasing emission
HCD-13	1100	b	8	1250	Stable for first 550 hours, followed by decreasing emission
HCD-14	1000	b	7.5	1909	Emission passed through maximum of 8.5 A/cm <sup>2</sup> at 250 hours, followed by decreasing emission after 900 hours
HCD-15	950	b	4.75	4000	Generally stable through 930 hours, decreasing thereafter
HCD-16	1100	c	10-12	325	Special cathode, triple fired tungstate (see text); rise in emission from 10 to 12 A/cm <sup>2</sup> in first 20 hours, then rapid drop in emission; cooling-water failure
HCD-18	1100	b	7.5	210	Special cathode, double zirconium concentration, (see Third Quarterly); erratic emission; cathode expanded
HCD-20	1100	b	4.25	750	Lower compaction pressure, stable emission for 400 hours, followed by decreasing emission
HCD-21	1100	c	19	736	Lower compaction pressure, emission stabilized at 22 A/cm <sup>2</sup> in first 120 hours; rose suddenly to 29 A/cm <sup>2</sup> ; stable at 29 A/cm <sup>2</sup> to 340 hours followed by decreasing emission
HCD-25	950	b	4	8500	Special test. Stable emission over this time span
HCD-27	950	b	5-11	6020	Special test - mixed Ba <sub>5</sub> Sr(WO <sub>6</sub> ) <sub>2</sub> ; emission improved with life to time of cooling-water incident, declining thereafter to present value of 6.5 A/cm <sup>2</sup>
HCD-28	1000	b	5	4300	Special test - HfH <sub>2</sub> substituted for ZrH <sub>2</sub> , decreasing after 800 hours
HCD-31	950	b	5	4400	Special test on machining, emission constant at 1200 hours, followed by decreasing emission after cooling-water failure

Table I - (Cont)

Diode ** (Cath. No.)	Cathode Temp. (°C)	Life * Test Cond.	Initial Current (A/cm <sup>2</sup> )	Hours on Life	Remarks
HCD-33	950	b	3.75	2500	Special test on sintering; emission stable through 920 hours, falling off thereafter to 2.17 A/cm <sup>2</sup>
HCD-35	1030	b	5	1880	Special test on copper coatings; emission constant out to 1000 hours, declining gradually thereafter to 1.9 A/cm <sup>2</sup> at end of test; rate of decline became more rapid after cooling-water failure
HCD-37	700	a	0.050	5200	Stable emission up to time of removal from test
HCD-38	1000	b	4.7	2660	Special cathode containing nickel layer; stable emission for 800 hours, followed by progressive decline to 2.5 A/cm <sup>2</sup>
HCD-42	1050	b	9	1240	Special test using evaporated nickel layer on cathode (see test); after preliminary test at 700°C, re-scheduled at 1050°C, 9 A/cm <sup>2</sup> ; emission stable to 400 hours, declining progressively to 3 A/cm <sup>2</sup> at 1240 hours
HCD-43	1050	c	13.6	2710	Special cathode containing double the standard amount of zirconium and prepared with reduced compacting pressure (60 TSI); emission stable at 13.4 A/cm <sup>2</sup>
HCD-44	---	-	--	----	Philips cathode for noise measurement only
HCD-45	---	-	--	----	Not tested. Discarded due to short circuit anode-cathode
HCD-46	1050	c	13.5	2960	Same composition as HCD-43, except that compaction pressure of 78 TSI was used
HCD-48	1100	c	37-46.5	500	Double zirconium; 78 TSI compaction pressure
HCD-49	1050	c	13	3000	Double zirconium. Special test of higher compaction pressure at 95 TSI
HCD-58	1100	c	29	720	Double zirconium mix. Emission declining after 200 hours
HCD-59	1100	c	30	960	Double zirconium mix. Excellent life for this current. Cathode preaged for 600 hours at 0.100 A/cm <sup>2</sup> and 650°C
HCD-60	1100	c	30	850	Double zirconium mix. Emission shows steady decline after initial 40 hours
HCD-63	1100	c	30	925	Double zirconium mix. Steady declining emission throughout life
HCD-65	1100	c	30	990	Double zirconium. Steady decline to 17 A/cm <sup>2</sup> at 900 hours

\* Life-Test Conditions:  
a - 0.050 A/cm<sup>2</sup>  
b - 3 to 10 A/cm<sup>2</sup>  
c - 30 A/cm<sup>2</sup>

\*\* Cathodes numbered HCD-10, -19, -22, -23, -24, -29, -30, -34 and -36 were not placed on life test because of various mechanical or electrical defects, such as open heaters, leakers, cathode-to-anode shorts, excessive gas, etc., which occurred during assembly or processing, thus making them unsuitable for life test purposes.

Table II - Summary of Life Test Results of Tubes  
Operating at End of Program

Diode (Cath. No.)	Cathode Temp. (°C)	Life* Test Cond.	Initial Current (A/cm <sup>2</sup> )	Life Hours to Date	Remarks
HCD-4	800	a	0.400	16,500	Stable emission at 0.370 A/cm <sup>2</sup>
HCD-9	900	b	6	16,000	Stable emission to 10,000 hours. Declining emission to 1/2 initial at 16,000-hour point
HCD-17	900	b	1.7	15,000	Emission increased at 10,000-hour point. Stable emission at 2.16 A/cm <sup>2</sup> after 13,000-hour point
HCD-26	950	b	5	13,000	Emission increasing with time, stabilizing at 6 A/cm <sup>2</sup> after 11,000 hours
HCD-32	750	a	0.160	12,200	Emission increasing with time; now at 0.240 A/cm <sup>2</sup>
HCD-40	650	a	0.075	11,000	Special test. Higher zirconium content. Generally stable emission
HCD-47	650	a	0.120	8,000	Special test; double zirconium, 78 TSI compaction pressure. Stable emission with time
HCD-50	975	b	8	3,400	Double zirconium; emission decreas- ing with time
HCD-51	600	a	0.060	3,400	Double zirconium. Stable emission
HCD-52	975	b	9.75	2,400	Double zirconium 18% decline in emission during this interval
HCD-53	975	b	8	2,400	Double zirconium. Steady decline in emission to 4.5 A/cm <sup>2</sup>
HCD-54	975	b	7.5	2,400	Double zirconium. Steady decline in 5.75 A/cm <sup>2</sup>
HCD-55	650	a	0.055	3,000	Double zirconium. Rising emission to 0.088 A/cm <sup>2</sup>
HCD-56	650	a	0.065	2,000	Double zirconium. Steady emission to 2000 hours
HCD-56	1100	c	29	1,200	Rescheduled to 1100° and condition c. Emission fell to 1/2 initial during this 1200-hour period
HCD-57	650	a	0.105	1,600	Double zirconium. Steady emission to 1600-hours. Changed to 1100°
HCD-57	1100	c	30	250	30 A/cm <sup>2</sup> . Steady at this level for 250 hours. Changed back to original conditions. Emission steady at approx. 1/2 of original value
HCD-57	650	a	0.065	1,700	
HCD-61	650	a	0.080	2,100	Double zirconium. Emission rising to 0.130 A/cm <sup>2</sup> with time
HCD-62	975	b	9.2	1,900	Double zirconium. Emission steady to 600 hours. Slow decline to 7.7 A/cm <sup>2</sup>
HCD-64	975	b	8	1,775	Double zirconium. Steady decline to 5.75 A/cm <sup>2</sup> at 1775 hours
HCD-66	650	a	0.085	2,400	Double zirconium. Rising emission trend to 0.126 A/cm <sup>2</sup> at 2400 hours
HCD-67	650	a	0.042	1,650	Double zirconium. Steady emission

## ANALYSIS AND CHARACTERIZATION OF EMITTING SURFACE OF OPTIMUM CATHODES

Amendment No. 1 dated 17 October 1966, to Technical Guidelines TT29-A, outlines the task, "Where feasible, x-ray emission spectroscopy analysis of optimum cathodes will be performed".

Exhaustive investigation of composition and processing, as verified by life testing, has established that the performance of the barium-strontium-tungstate matrix cathode as defined in Appendix A is near optimum. Further, as discussed previously, more recent modifications utilizing extra zirconium give promise of extending the temperature range and useful life of the tungstate cathode. Thus one cathode of each composition was fabricated and delivered to Ernest F. Fullam, Inc., Scientific Consultants, for analysis. Before delivery, these cathodes were pre-tested, to ensure that emission characteristics were of acceptable quality, and encapsulated in evacuated glass tubes.

These cathodes were examined by reflection electron diffraction, electron microprobe analysis, and replicated for electron microscopy. Although no significant differences could be detected between them, some totally unexpected findings did come out of this investigation, as will be discussed below.

To complement and broaden the scope of the analysis, two more cathodes were delivered to Fullam, Inc. for additional tests. One cathode was newly fabricated, but not activated or operated in vacuum. The second cathode was removed from a life test diode. Before removal from the life test, the cathode was purposely operated at a high rating to accelerate the depletion of emission.

The report of this second series of investigations is reproduced in total in Appendix B. In summarizing the findings of the investigations, several valuable concepts and some totally unexpected results are noted. Perhaps the most novel was the discovery of the formation of barium zirconate ( $\text{BaZrO}_3$ ) compound, and the change in its distribution during the life of the cathode. From evidence obtained in this study, it is concluded that during the useful portion of the life of the cathode,  $\text{BaZrO}_3$  is present in concentrated form in the immediate vicinity of pores in the surface. As a cathode approaches end of life, the quantity of  $\text{BaZrO}_3$  is diminished, and the distribution of this compound over the surface becomes diffuse. In the final stages, the barium is greatly diminished and the zirconium appears predominately as  $\text{ZrO}_2$ .

The function of strontium in the cathode is, for the present, obscure. It has been demonstrated that it must be present in the tungstate activator to achieve high emission. On unactivated cathodes, it can be detected at the surface, but once the cathode is activated by current, the strontium disappears from the emitting surface, as was disclosed by microprobe analysis. However, it is still present within the body of the cathode, as shown by x-ray diffraction.

During the course of extended operation of the cathode, several physical and chemical changes occurred. A replicated surface of a freshly machined but unactivated cathode (under a magnification of 10,000X) reveals the smooth and sheared grains of the matrix. A scanning electron micrograph of this surface reveals the concentration of active emitting material in the pores and grain boundaries.

As the cathode ages, the tungsten particles begin to recrystallize, and definite crystal faces become evident. Coalescence occurs within the tungsten grains with resultant enlargement of the pore areas. Electron micrographs of replicated surfaces reveal the presence of dark particles, identified as  $\text{BaZrO}_3$ . After extended life, to the point of substantially reduced emission, an overall depletion of barium occurs, although the zirconium level remains unchanged.

The phenomena governing the changes described -- namely, chemical reduction, evaporation, and self diffusion in the tungsten grains -- are time-temperature dependent. It is concluded that the life of the tungstate cathode should be predominately dependent upon its operating temperature. This has been verified in life tests conducted at  $1100^\circ\text{C}$  under widely differing current densities (4 to  $46 \text{ A/cm}^2$ ). These tests have resulted in essentially equivalent cathode life relatively independent of the current density.

It was requested by the sponsoring agency that an effort be made to determine the emission mechanism of the tungstate cathode. While the above investigation gives valuable insight into the physical and chemical properties of the tungstate cathode, and the manner in which these properties change with time, a great amount of work may be required to develop a valid theory of how it emits.

In metals, electrons can move freely within the metal. However, to remove the electrons from the metal into a vacuum space requires energy, since the negatively charged electrons are strongly attracted by the positive

charges within the metallic atoms. Heat is one such source of energy which may move electrons up to higher levels where they can escape from the metal surface. The highest energy possessed by any electron at 0° Kelvin is less than that required to overcome the potential at the surface to make escape from the metal possible. The difference between this highest energy and the energy that an electron must have to overcome the electrostatic binding forces is usually expressed in energy per unit charge, or electron volts, and is called the work function.

Most common metals have work functions falling in the range of 3 to 5 electron volts. However, if these metals are coated with another metal, usually of the alkaline earth series, or more particularly, with the oxides of these metals, the work functions fall dramatically. For example, tungsten has a work function of 4.5 electron volts. If a layer of barium metal is sputtered on tungsten, the work function is reduced to the range of 2.11 to 2.29 electron volts.<sup>3</sup> Barium oxide on tungsten results in an effective work function of  $1.4 + 7 \times 10^{-4} T$ , when T is the temperature in degrees Kelvin.

An intensive amount of investigation has been conducted over many years on the barium oxide cathode, and its emission mechanisms. Authorities are still not in agreement on the many concepts proposed or expounded by various investigators.

In the late 1920's, it was concluded that an excess of barium is adsorbed on the oxide particles as a monoatomic layer, and the dipole layer due to the adsorbed layer is responsible for the low work function.<sup>4, 5</sup> This concept was undisputed for many years, and in the mid 1940's, the emission decay of oxide cathodes under high pulse conditions was explained by means of the adsorbed barium hypothesis.<sup>6</sup>

Additional investigations cast doubt on the adsorption hypothesis.<sup>7</sup> With the advent of semiconductor theory,<sup>8</sup> it was shown that several properties of oxide cathodes could be explained by semiconductor theories. Other investigators<sup>9, 10, 11, 12, 13</sup> experienced difficulty, however, in seeking a semiconductor model for the oxide cathode which would explain its electron emission properties.

New concepts were introduced by the dispenser and matrix types of cathode, and theories pertaining to the operation of this class of emitters have been generated. For example, it has been observed,<sup>14</sup> by comparing the emission density of different poly-crystalline metal substrates, that the metal with the highest work function when uncoated, shows the lowest work function when coated with alkaline earth compounds.

In an investigation of the adsorption of barium on individual crystal planes of tungsten, <sup>15</sup> the work function of the (110) face was 6.0 eV before coating, and was the lowest after coating with a thermally equilibrated layer of barium. The clean, atomically rougher planes all have work functions lower than the ionization energy of barium, and no simple correlation was found between the work function of the bare faces and the sequence of the minimum work function after coating.

In an extensive review and analysis <sup>16</sup> of thermionic cathodes, the conclusion was reached that, "There is no fundamental difference between thin-film-on-metal cathodes and oxide-coated cathodes. In both cases a monolayer (or less) of adsorbed atoms on a substrate determines the emission properties. For a thin film cathode, it is desirable to use a substrate whose work function is as high as possible in order that the adsorption of electro-positive atoms becomes a maximum."

In reviewing the properties of tungstate cathode and, in particular, how its particular characteristics fall within the various theories, certain facets stand out: (1) It is necessary to machine the surface of the tungstate cathode after sintering in such a manner that the individual grains of tungsten are cleaved or sheared. Such a procedure may expose preferential crystal faces on the tungsten. (2) The average work function of the tungstate cathode ( $\phi_{\text{eff}} = 1.15 + 5.5 \times 10^{-4} T$ ) is lower than that obtained by barium metal films on tungsten, thus eliminating this emission mechanism. (3) Microprobe analysis reveals a film of barium zirconate,  $\text{BaZrO}_3$ , on the emitting surfaces, and a heavy concentration of the compound in the grain boundaries of the cathode. (4) Emission microscope displays of the emission pattern reveal a very patchy emitting surface, with the emission concentrated predominately from spots on the surface. This patchy emission behavior is also evident from an analysis of the noise properties of the cathode.

It would appear that if some means for increasing the number of emitting patches on the cathode could be found, the emission capability would be correspondingly improved. This may explain the occasional cathode that exhibits greater emission than that obtained from the average tungstate composition. In these instances, by some undiscovered quirk in the processing, the number or size of active emitting sites is unusually high.

## POISONING OF TUNGSTATE CATHODES BY GASES AND METAL VAPORS

Most thermionic cathodes are used in sealed vacuum devices. During processing and outgassing of the internal surfaces of the device, the cathode may be subjected to deleterious gases or high vapor-pressure metals. After pinch-off, in the absence of continuous pumping, the low pressure existing in the device may be altered by an increasing partial pressure of evolved gases. Energetic electron beams impinging on metallic surfaces may also evaporate metal which, in turn, may coat the surface of the cathode and alter its emission properties. Thus, a study of the effects of residual gases or evaporated metal coatings on the high emission tungstate cathode was undertaken during this program.

Gas pressure and gas composition are the major factors influencing cathode poisoning at a specified cathode temperature. Also, in selecting a method for conducting poisoning tests, other factors such as electrode spacing and anode voltage must be considered in comparing poisoning data. One method -- based on the theory that cathodes are normally used in sealed devices -- is to fill the device with a known partial pressure of contaminant and observe the emission with time. This method leads to several difficulties, however. Any pressure monitoring device attached to the tube may introduce its own pumping action, or it may evolve gas in the absence of external pumping. The gettering action of the cathode itself will alter, or may even remove, the original contaminant gas. At best, the gas pressure will vary continuously until it is finally adsorbed by the gettering action usually observed in sealed-off electron devices.

A second method, dynamic in nature, involves the maintenance of a specific flow of gas through the diode under test, providing a non-varying environment for determining emission susceptibility to gas environment. Gas flow through the diode system is controlled at a specified system pressure by balancing the input flow against the pumping rate of the vacuum pump. Pressure readings are made with an ionization gage corrected for gas sensitivities.<sup>17</sup> Such a system (Figure 63) was employed in this program, and in the previous studies of cathode poisoning reviewed below. A demountable diode structure was utilized, and variable anode-to-cathode spacing was provided by a water-cooled copper anode attached to a bellows movement actuated by a 40-thread-per-inch drive screw. The cathodes were processed under established optimized conditions.

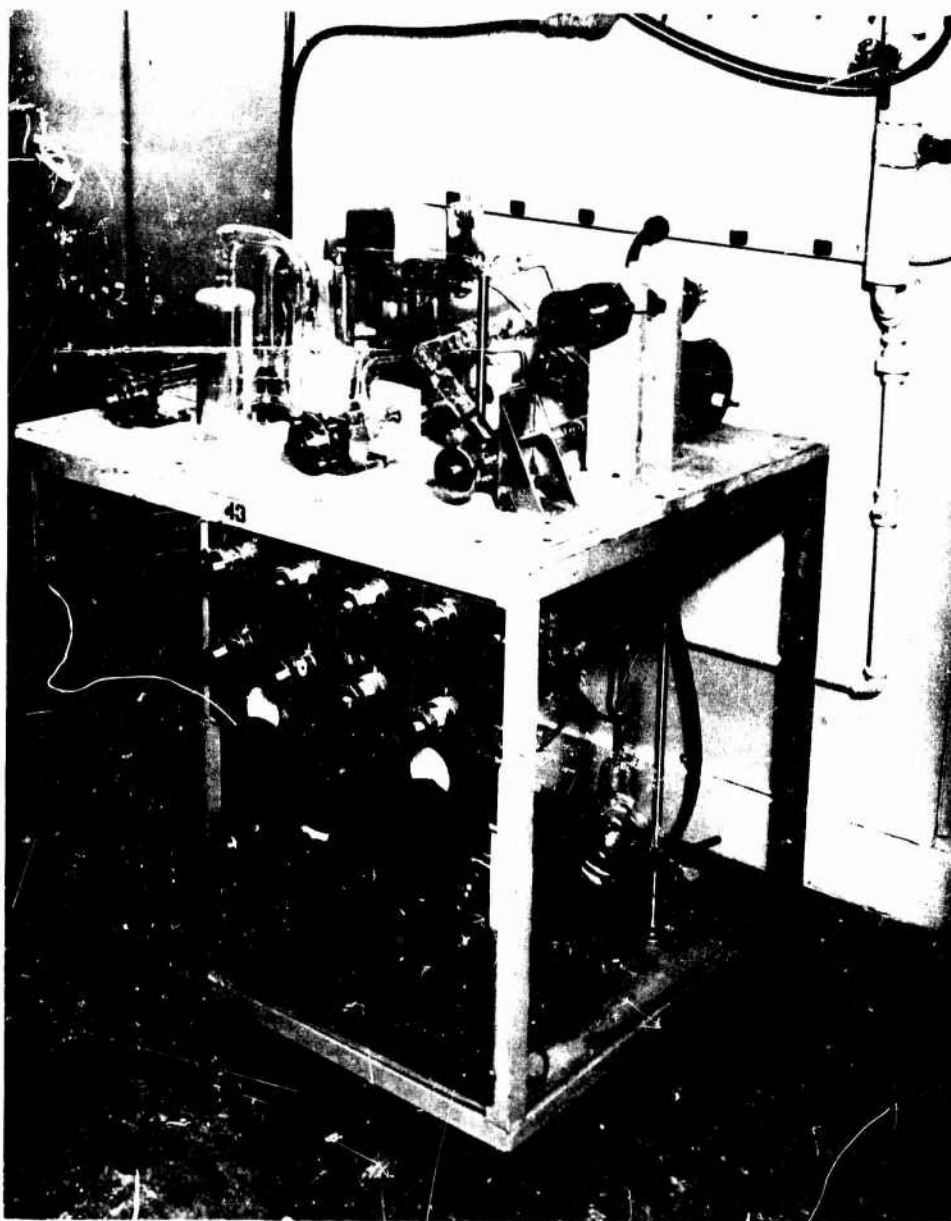


Figure 63 - Vacuum System Used for Cathode Poisoning Studies

## Cathode Poisoning by Gases

Five gases --  $O_2$ ,  $CH_4$ ,  $CO_2$ ,  $CO$ , and  $H_2$  -- have been evaluated in previous studies.<sup>1,2</sup> These constitute the residual gases normally found in vacuum systems containing thermionic emitters. Water vapor, a contaminant usually found in unbaked vacuum systems, was not recorded. Although water vapor is believed to be the major cause of deterioration of tungstate cathodes exposed to the atmosphere, measuring the background pressure of water vapor at the vacuum levels necessary to operate thermionic cathodes proved to be an elusive problem.

In one series of tests,<sup>1</sup> standard composition (Appendix A) cathodes were operated at  $950^\circ C$  with current densities of about  $3 A/cm^2$ , and with 100 volts on the anode. The poisoning effects of  $O_2$ ,  $CO$ , and  $CO_2$  were studied. Data taken in terms of degree of poisoning plotted versus time are shown in Figures 64, 65 and 66.

Oxygen, at a pressure of  $5 \times 10^{-6}$  torr, dropped emission by only 0.5 percent during a 30-minute exposure. Increasing the oxygen pressure to  $2 \times 10^{-5}$  torr dropped the emission by 6 percent. A 25-minute exposure to a pressure of  $6 \times 10^{-5}$  torr caused a 50-percent drop in emission. Strangely, this cathode, sealed overnight in oxygen at a pressure of  $2 \times 10^{-5}$  torr, exhibited a 4-percent recovery in emission.

Carbon monoxide at a pressure of  $8 \times 10^{-5}$  torr caused a 10-percent reduction in emission during a 50-minute exposure. A rapid decrease of 30 percent occurred during an 8-minute exposure to  $CO$  at a pressure of  $4 \times 10^{-4}$  torr.

Carbon dioxide caused a reduction in emission of less than 1 percent during a 70-minute exposure at a pressure of  $5 \times 10^{-5}$  torr. A much higher pressure,  $1.2 \times 10^{-4}$  torr, caused a 40-percent drop during a 6-minute exposure. Emission continued to drop, however, when pressure was reduced to the original  $5 \times 10^{-5}$  torr. When the  $CO_2$  gas was removed from the system, emission recovered completely.

In another series of gas poisoning studies made on standard composition tungstate cathodes,<sup>2</sup> the rate of poisoning and the subsequent recovery rate observed when the contaminating gas was removed are plotted in Figures 67 through 73. The cathodes were of the type used in ultra-high resolution (UHR) cathode-ray tubes, in which the emitting diameter was 0.010 inch. The cathodes were activated at a base pressure of  $2 \times 10^{-9}$  torr. The emission conditions used in all of these tests were:

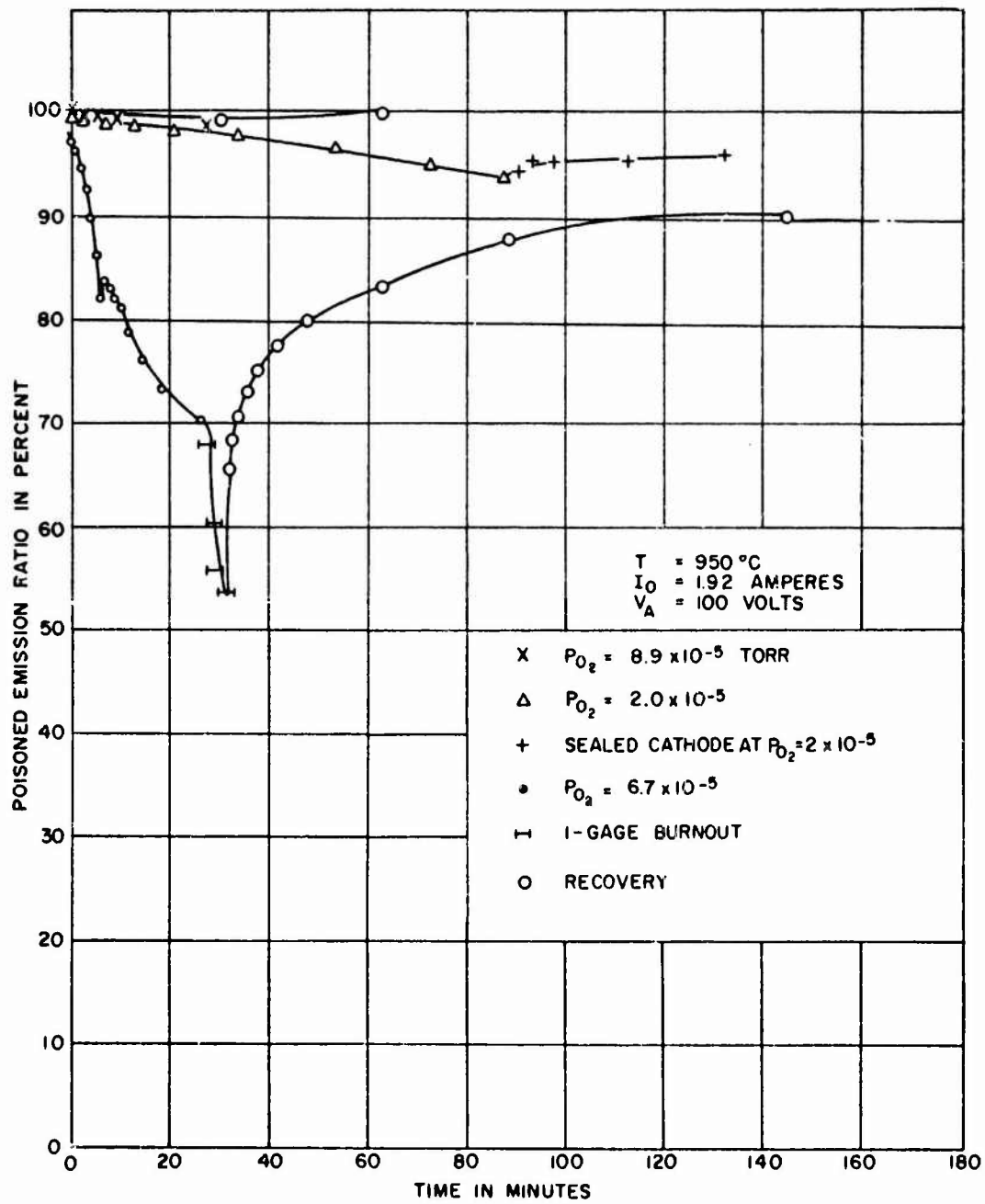


Figure 64 - Emission Poisoning by Oxygen

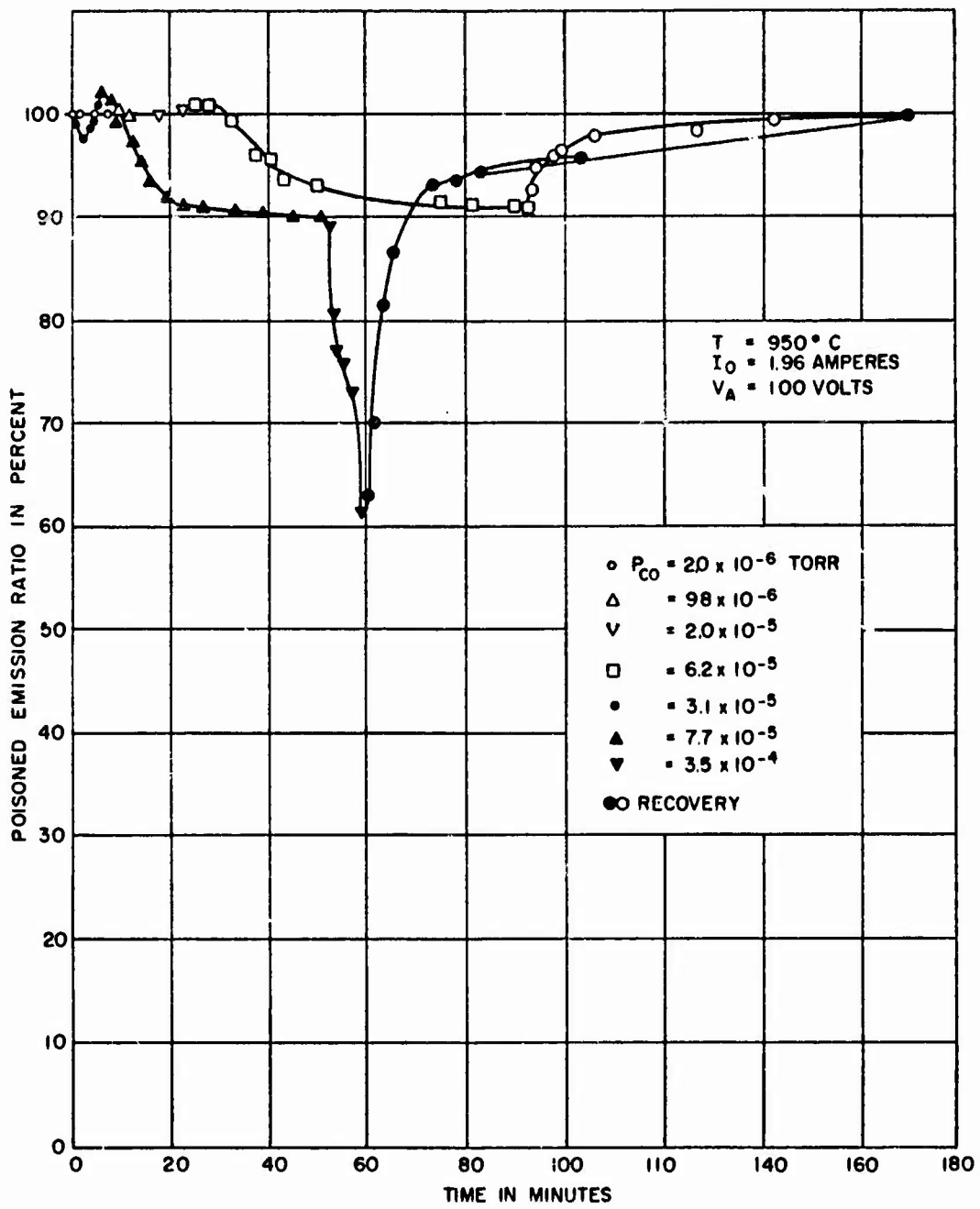


Figure 65 - Emission Poisoning by Carbon Monoxide

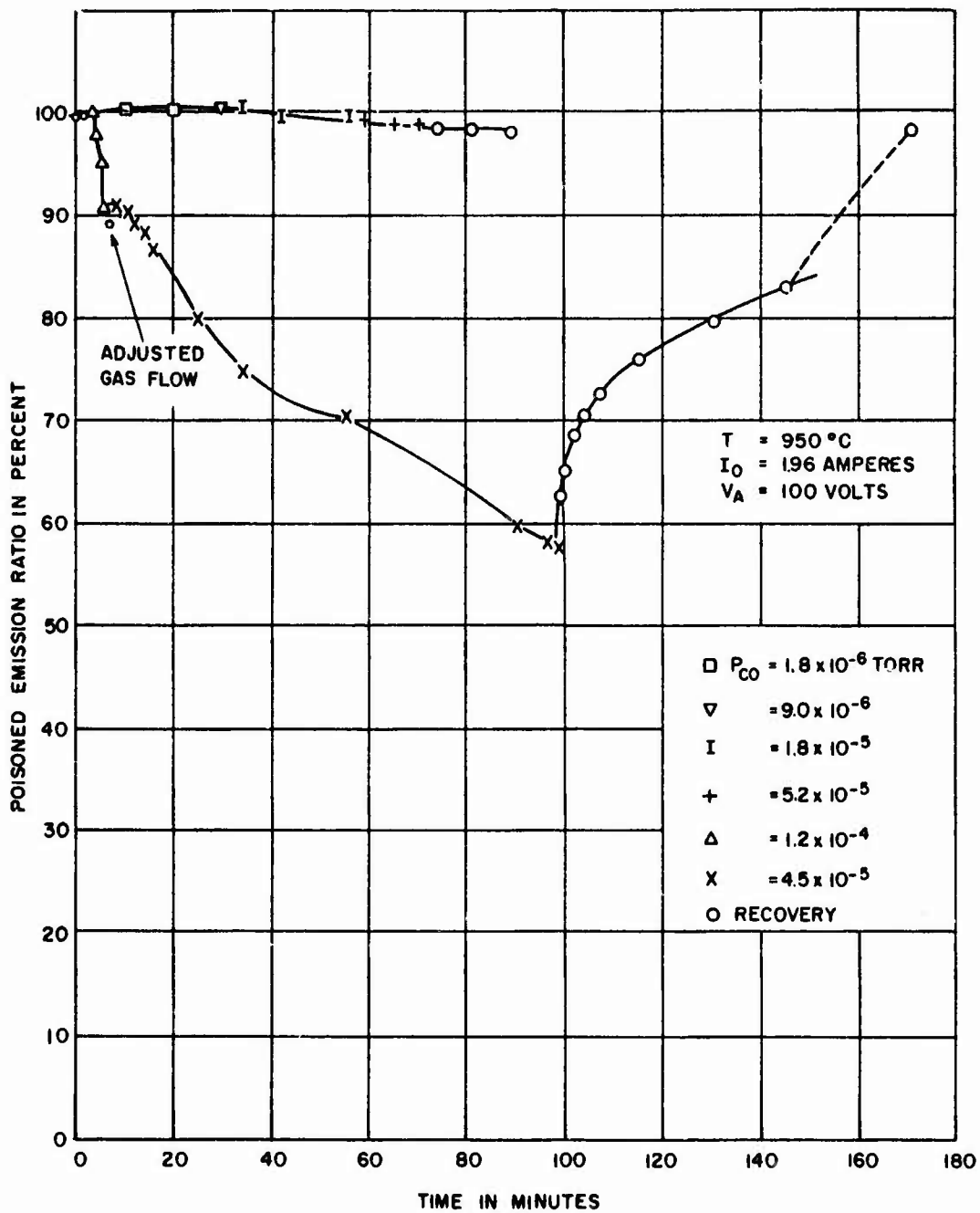


Figure 66 - Emission Poisoning by Carbon Dioxide

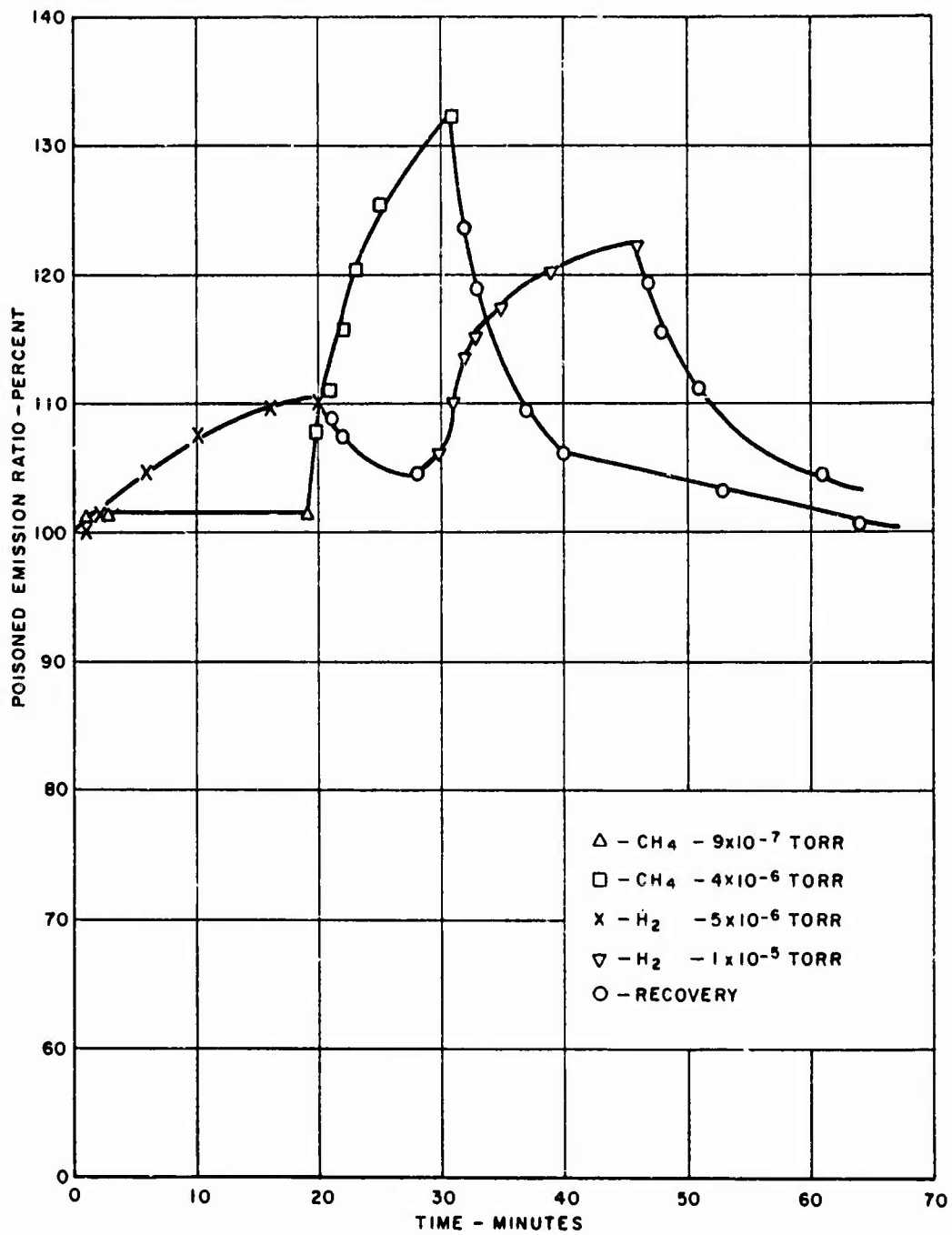


Figure 67 - Emission Enhancement by Methane and Hydrogen

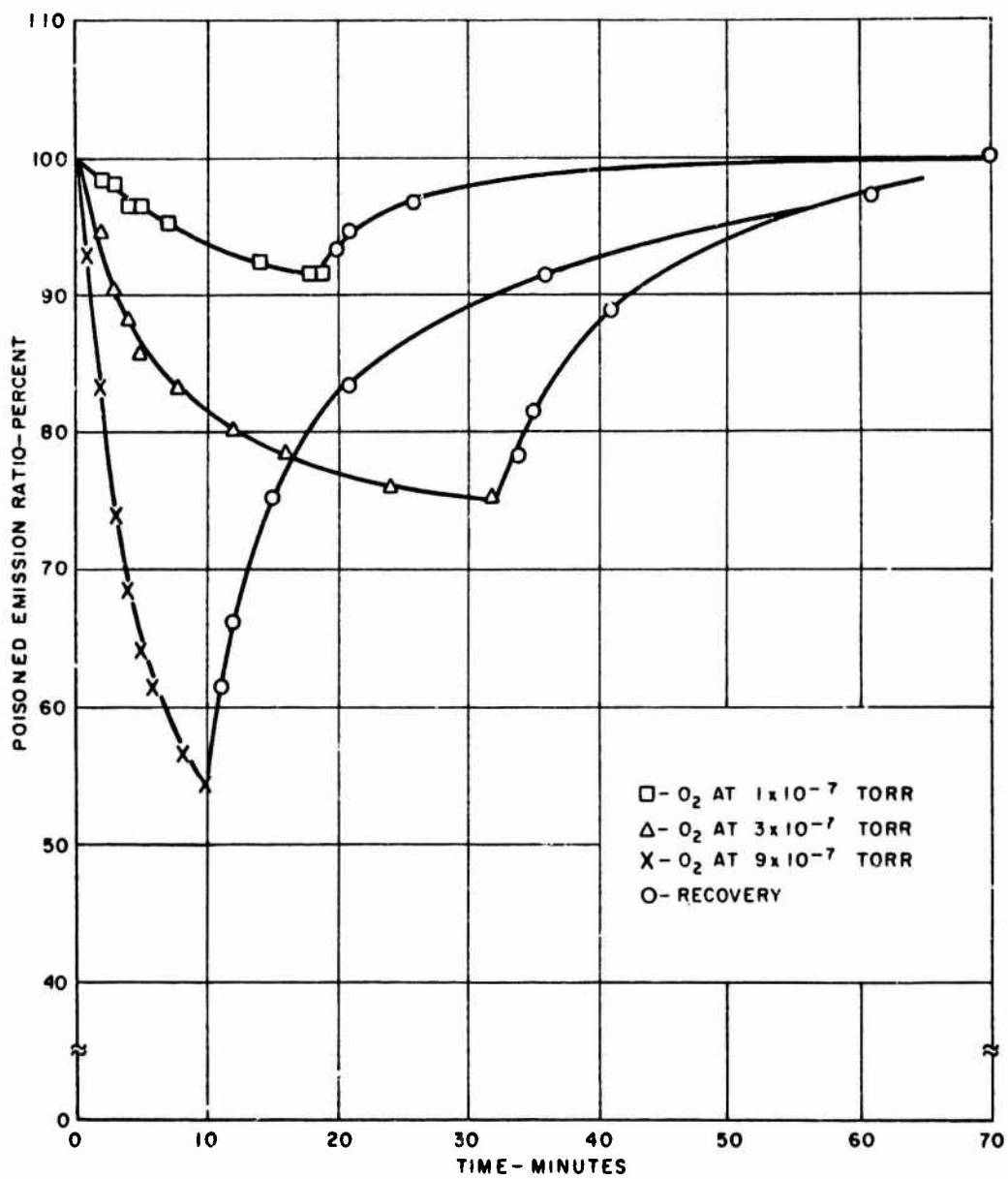


Figure 68 - Emission Poisoning by Oxygen

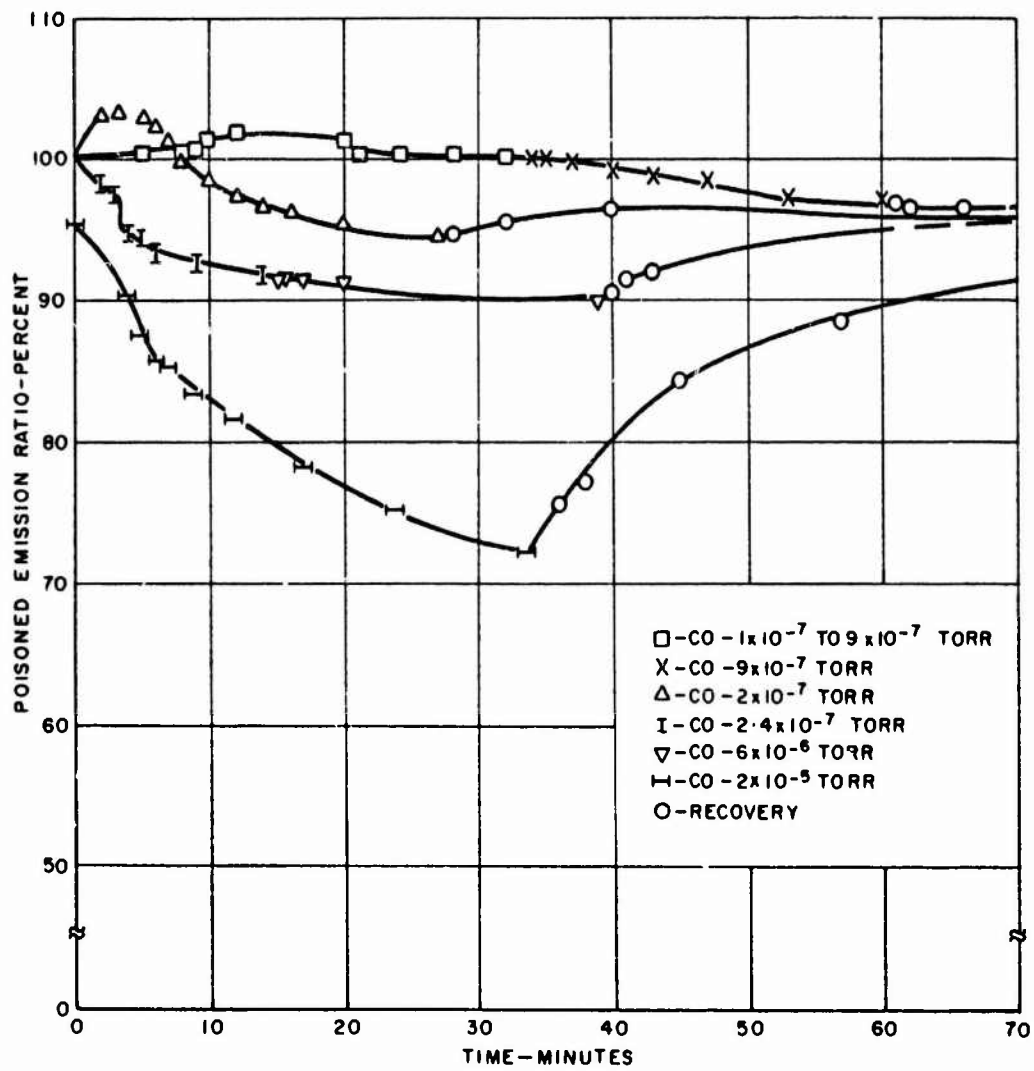


Figure 69 - Emission Poisoning by Carbon Monoxide

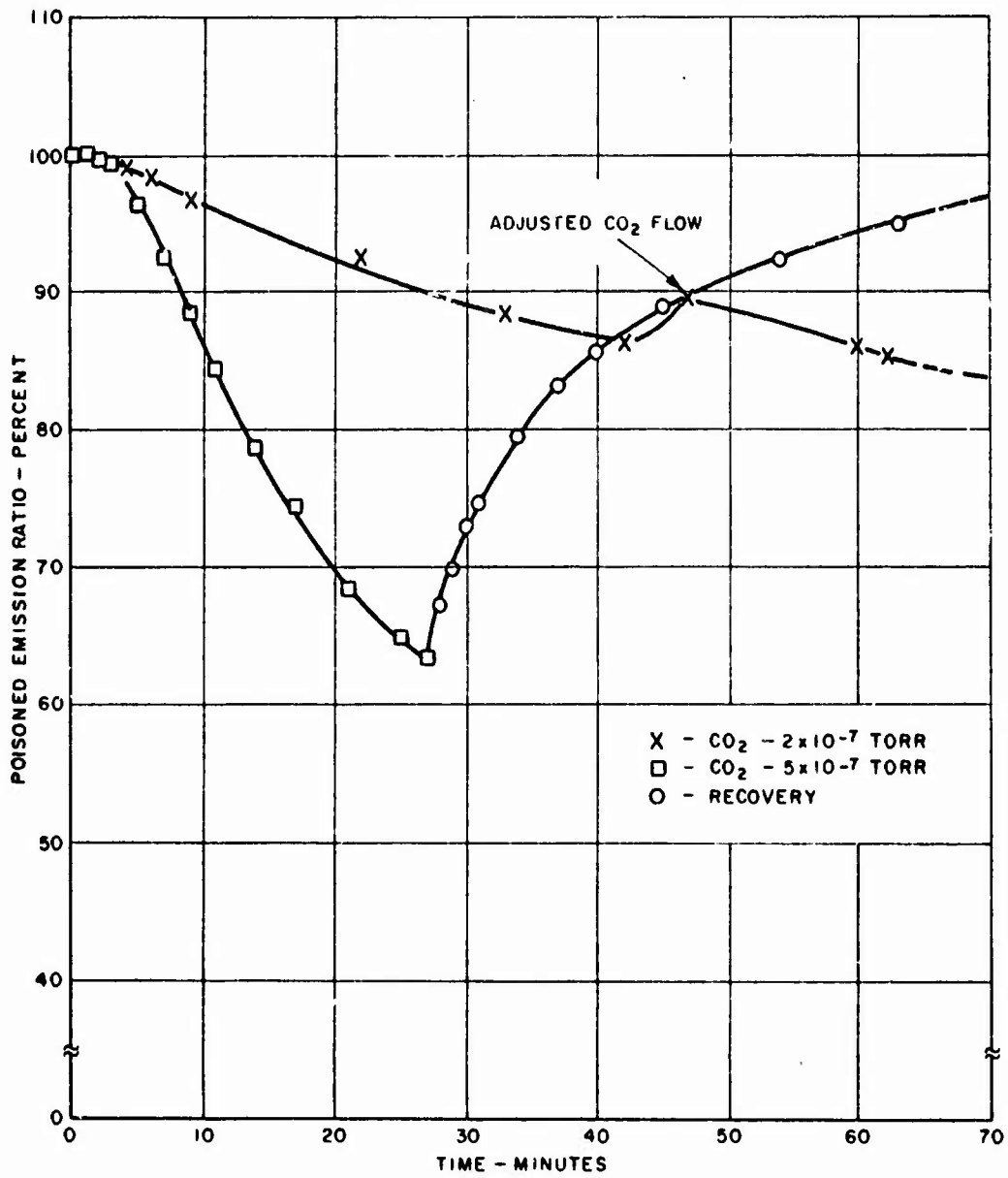


Figure 70 - Emission Poisoning by Carbon Dioxide

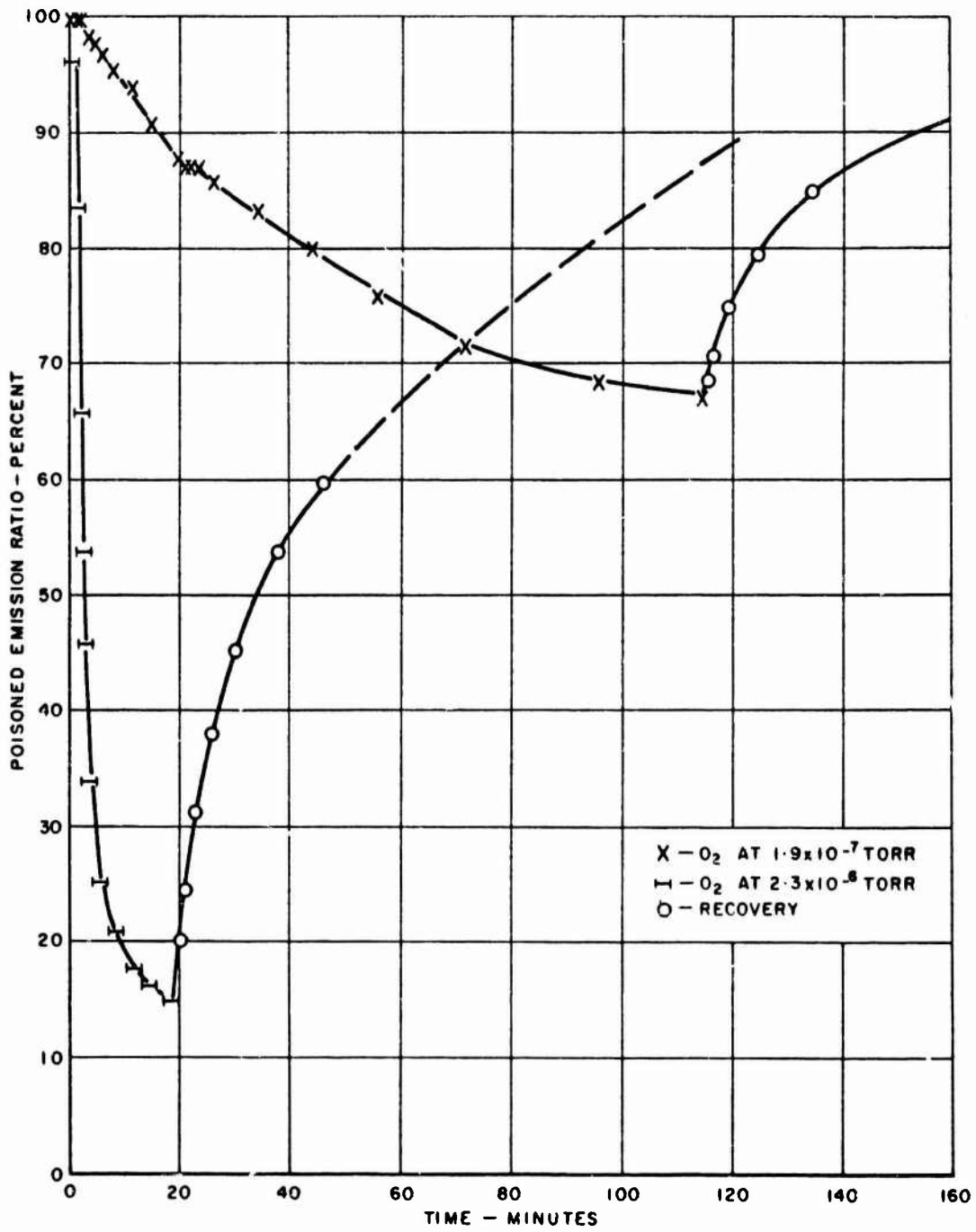


Figure 71 - Emission Poisoning by Oxygen over Longer Period of Time

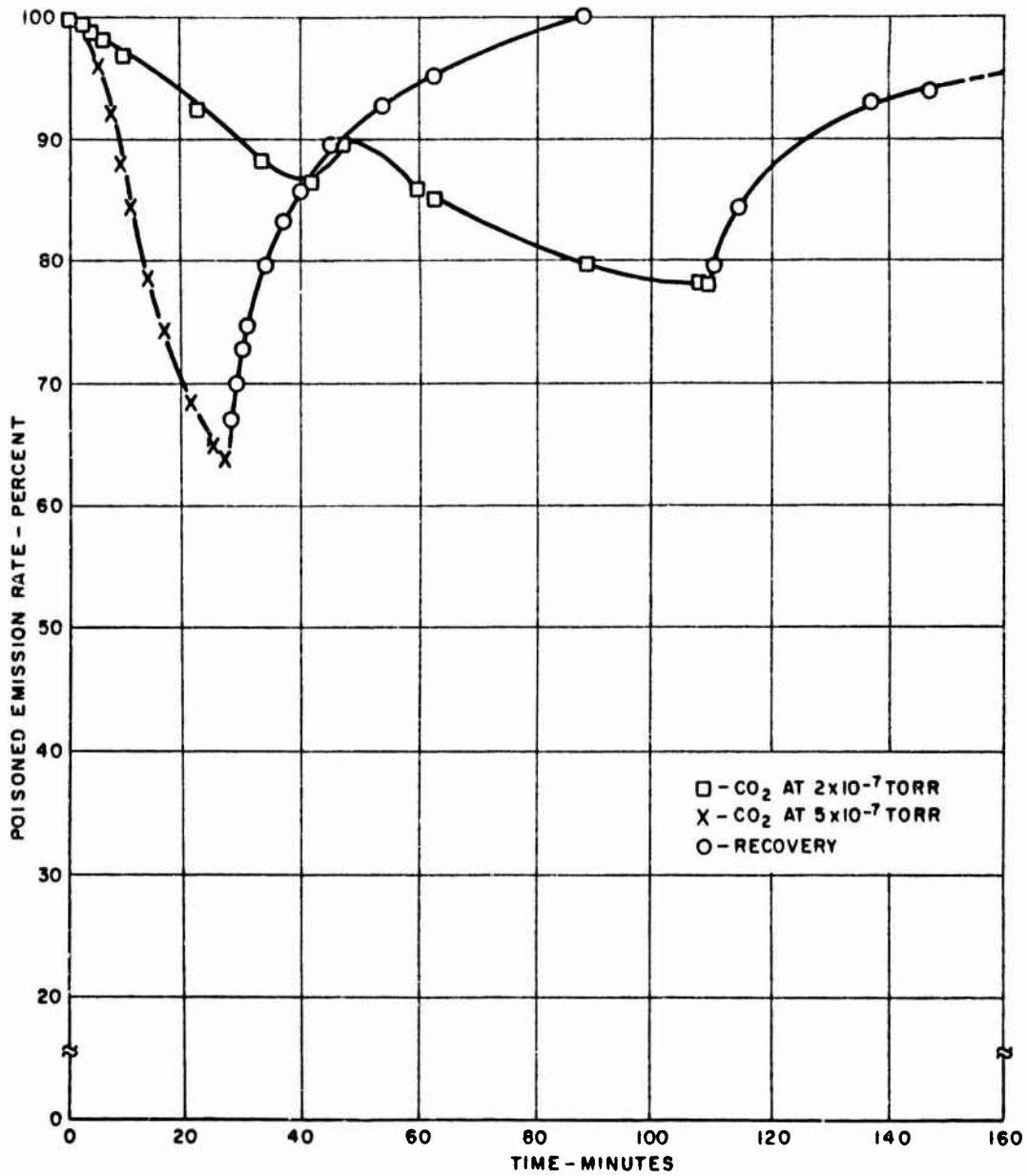


Figure 72 - Emission Poisoning by Carbon Dioxide over Longer Period of Time

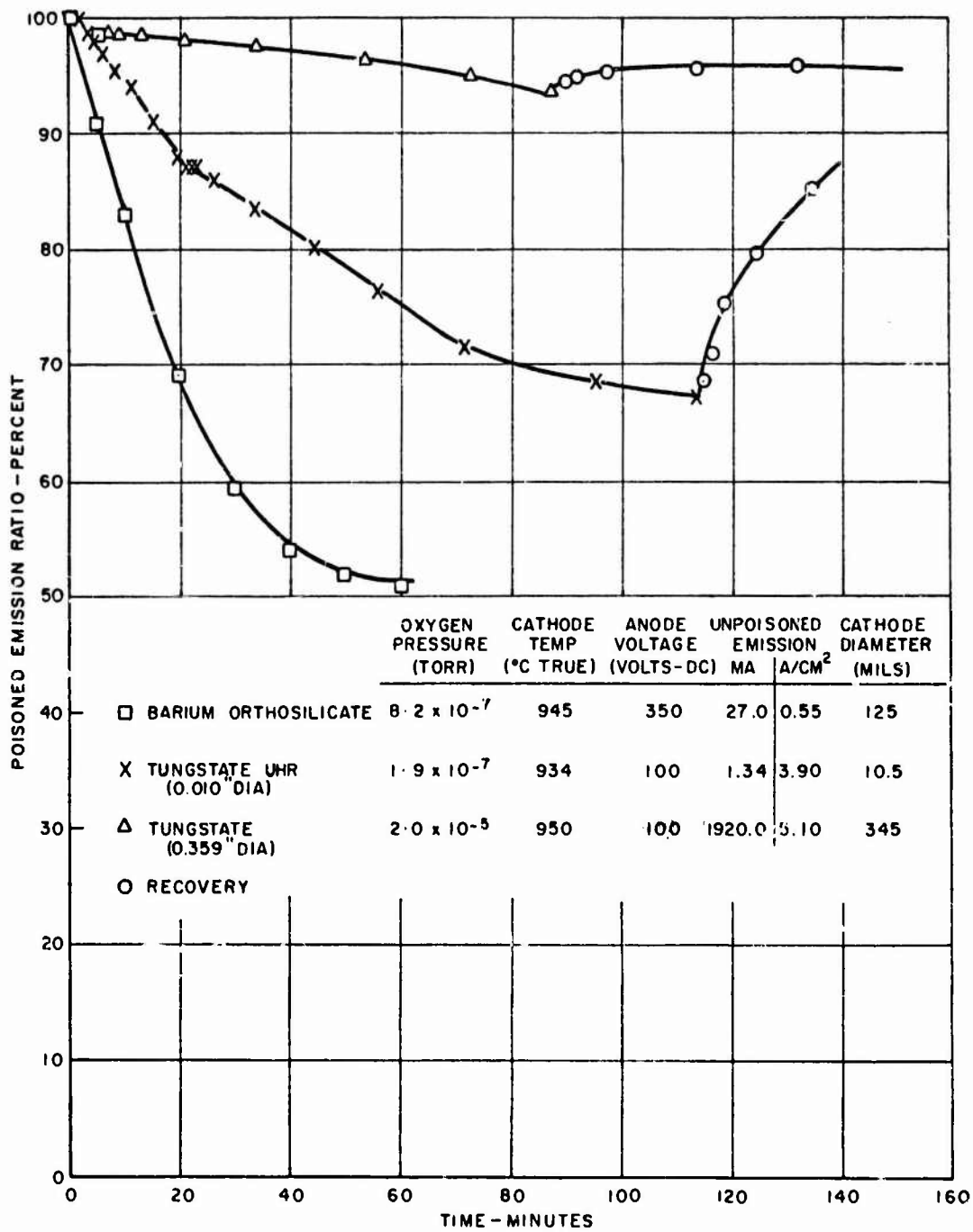


Figure 73 - Comparison of Emission Poisoning by Oxygen of a UHR-CRT Cathode with a Conventional-Size Tungstate Cathode and a Barium Orthosilicate Cathode

Cathode Temperature	934 <sup>o</sup> C <sub>True</sub>
Anode Voltage	100 VDC
Anode-Cathode Spacing	0.005 Inch
Cathode Emission	2.3 A/cm <sup>2</sup>

Hydrogen was admitted to the system by means of a palladium valve, with all other gases being admitted from glass flasks. Specific pressures, as read on an ion pump, were maintained by balancing the gas input against system pumping speed.

Hydrogen and methane both produced emission enhancement (Figure 67). These two gases have also been reported in other work<sup>18</sup> to enhance the emission in various cathode systems, but on larger diameter tungstate cathodes (0.359-inch diameter); no change in emission was detected at pressures up to  $2 \times 10^{-5}$  torr.

The poisoning effects of O<sub>2</sub>, CO, and CO<sub>2</sub> (the oxygen containing gases) at pressures as low as  $1 \times 10^{-7}$  torr are clearly evident from the curves of Figures 68, 69, and 70. It is also noted that the smaller volume emitters are more susceptible to poisoning than cathodes of larger volume, as is shown in Figure 73. Variations in the degree of poisoning from a given gas pressure result from several factors: (1) the degree of poisoning varies inversely with temperature for a given gas pressure, (2) when the anode-cathode spacing is increased, the poisoning susceptibility also increases, and (3) anode voltage applied during gas exposure constitutes a variable. In cathode systems poisoned by methane, an emission slump is found only if anode voltage is present. With oxygen, poisoning occurs whether emission is present or not. Thus, a cathode can be irreversibly poisoned before it is ever tested for emission capability.

A literature survey of cathode poisoning for various cathode systems is given in Table III. The poisoning of barium calcium aluminate cathodes by hydrogen was explained<sup>19</sup> in terms of the barium-producing reaction in a barium-aluminate cathode, in which the reaction product BaWO<sub>4</sub> is believed to be detrimental to emission. It was proposed that the BaWO<sub>4</sub>, normally not present in a well-activated aluminate cathode, could appear during life, and in the presence of hydrogen, result in the formation of oxygen or water vapor, with subsequent decrease in emission.

Table III - Literature Survey of Cathode Poisoning Results

Cathode Type	Gas Type and Effect			Critical Pressure (Torr)	Temperature (°C)	Reference
	Neutral	Activating	Poisoning			
Barium calcium aluminate	N <sub>2</sub>		O <sub>2</sub>	1 x 10 <sup>-7</sup>	1100	44
	Ar		H <sub>2</sub> O	3 x 10 <sup>-7</sup>	1100	
	H <sub>2</sub>		CO <sub>2</sub>	1 x 10 <sup>-6</sup>	1100	
	CO		Air	5 x 10 <sup>-6</sup>	1100	
			C <sub>6</sub> H <sub>6</sub>	1 x 10 <sup>-5</sup>	1100	
Barium calcium aluminate	N <sub>2</sub>		O <sub>2</sub>	2 x 10 <sup>-8</sup>	1100	45
			CO <sub>2</sub>	1 x 10 <sup>-7</sup>	1100	
			CO	2 x 10 <sup>-7</sup>	1100	
Barium calcium tungstate			O <sub>2</sub>	2 x 10 <sup>-7</sup>	1160	46
			CO <sub>2</sub>	5 x 10 <sup>-7</sup>	1100	
		CO	CO	1 x 10 <sup>-4</sup>	1145	
L-cathode			O <sub>2</sub>	1 x 10 <sup>-7</sup>	1160	47
Barium aluminate			O <sub>2</sub>	<1 x 10 <sup>-6</sup>	1000	20
			CO <sub>2</sub>	<1 x 10 <sup>-6</sup>	1000	
			N <sub>2</sub>	<1 x 10 <sup>-6</sup>	1000	
			H <sub>2</sub>	<1 x 10 <sup>-6</sup>	1000	
		CO	CO	>1 x 10 <sup>-5</sup>	1000	
Barium nickel matrix cathode - activated by TiH <sub>2</sub>	CO		H <sub>2</sub> O	2 x 10 <sup>-8</sup>	900	21
	N <sub>2</sub>		CO <sub>2</sub>	8 x 10 <sup>-8</sup>	900	
	H <sub>2</sub>		O <sub>2</sub>	3 x 10 <sup>-7</sup>	900	
Oxide cathode	N <sub>2</sub>	H <sub>2</sub> O	O <sub>2</sub>		-	
		H <sub>2</sub>	CO <sub>2</sub>		-	
		CH <sub>4</sub>	CO		-	
		CO			-	

The same mechanism could also account for the enhancement of a cathode by methane, if it is true that emission is improved with the removal of BaWO<sub>4</sub> and its associated oxygen poisoning agent. Methane could react with oxygen to form the less harmful CO and H<sub>2</sub>.

Impregnated tungsten cathodes display the behavior of both the oxide cathode and also that of barium on a tungsten surface, with cathodes of high porosity being predominately the former.<sup>20</sup> Thus, poisoning behavior similar to that of oxide cathodes might be found in matrix cathodes if patches of BaO are present in the pores or on the tungsten surface.

Both methane and hydrogen have been used to activate oxide cathodes.<sup>21</sup> The enhancement of tungstate cathode emission by these gases could be simply the activation of BaO in the pores of the matrix. Methane activation leaves free carbon on the surface of the cathode through the dissociation of CH<sub>4</sub>. In the presence of oxygen-containing gases, carbon removal takes place as CO, thus producing emission enhancement as long as CO pressure

does not exceed certain equilibrium values. This CO equilibrium value is determined by the methane pressure and the cathode temperature. Above certain pressures, methane will poison the cathode.

In an attempt to evaluate the effects of water vapor, a section of pyrex glass in the vacuum system was heated to 300°C. Approximately half of the gas evolved, at a pressure of  $6 \times 10^{-8}$  torr, consisted of water vapor. No poisoning was noted at this pressure level.

The vacuum system was opened to air at a relative humidity of 70 percent for a period of 15 minutes. After system bakeout, a pressure of  $2 \times 10^{-9}$  torr was attained. The highest emission level reached after exposure to air was 83 percent of that existing at the start of the test.

In summary, the poisoning level of the common gases for barium-activated strontium tungstate cathodes was established. No unique poisoning characteristics were noted, other than the susceptibility to deterioration by water vapor. In unactivated cathodes, the reaction with water vapor can be observed by a swelling and cracking of the matrix. On activated cathodes, the deterioration in emission by air exposure is more rapid. In one series of tests, the emission capability dropped approximately 50 percent after each 4-hour exposure to air, at a relative humidity of 55 percent.

#### Cathode Poisoning by Metal Vapor

The detrimental effects of residual gas in electron tubes is a well-recognized phenomenon. The cathode poisoning resulting from metal coatings accumulating on emissive surfaces is often overlooked, however. The most prevalent sources of metal contaminants are: (a) evaporated films arising from heated portions of the tube structure; (b) metal films transported by sputtering; (c) films resulting from dissociation of metal halides or carbonyls; (d) residual metal films deposited on tube parts that have been processed in contaminated hydrogen or vacuum furnaces; (e) residual metal films acquired through immersion plating of parts processed in contaminated acids or other cleaning baths; (f) alkali-metal residues arising from the difficult-to-remove metal soaps often found in cutting oils and deep-drawing compounds; and (g) accumulations of airborne metal particles, dusts, etc.

The effects of metal coatings on tungstate cathodes was studied by evaporating the particular metal under consideration by electron bombardment in an Alloyd Model 61-F-1 evaporation chamber. The cathode was suspended facing the evaporation source. A glass microscope slide, held at an equal distance from the source, was used as a means of monitoring

the thickness of the evaporated metal. Evaporation was stopped when semi-opaque coatings were reached on the glass, an indication of film thicknesses in the 2000 to 5000 angstrom range.

After being coated by evaporation, the cathodes were assembled in diodes and aged at temperatures ranging from 800°C to 1050°C, depending upon the volatility of the coating element. After 15 hours of aging emission data were taken. These data are labelled (A) in Table IV which summarizes the results. The cathodes were then subjected to normal flashing at 1200°C for 10 minutes, aged to equilibrium conditions, and retested for emission capability. These data are labelled (B) in Table IV.

Elements having the least effect on cathodes were copper, nickel, cobalt, iridium, and iron. Other metals clearly detrimental to emission, in ascending order, are molybdenum, aluminum, boron, platinum, silicon, beryllium, cerium and tantalum. Many other elements often detected or present in electron tubes, i.e., gold, silver, zinc, cadmium, tin, carbon, silicon, manganese, palladium, zirconium, titanium, sulfur, etc., were not examined due to termination of this particular line of research.

Two cathodes, heavily coated with nickel, were placed on life test at 1000°C and 1050°C, respectively. The lower temperature cathode exhibited falling emission after 2000 hours, while at the 1050°C cathode temperature, emission fell after 1200 hours.

Published information<sup>22,23</sup> pertaining to the deactivation of impregnated-type cathodes by metal vapors indicates that nickel is a potent poisoning agent, reducing emission to less than 25 percent of its initial value in a 10-minute period.

In summary, all metal coatings evaluated were detrimental to emission in a widely varying degree. The tungstate cathode was far more resistant to nickel than the commercial impregnated matrix cathodes.

Table IV - Zero-Field Emission and Effective Work Function  
for Various Metal Coatings on Tungstate Cathodes

<u>Evaporant</u>		<u>Cathode Temp. (°C)</u>	<u>I<sub>0</sub> (A/cm<sup>2</sup>)</u>	<u>φ<sub>eff</sub> (EV)</u>
Copper	A	900	2.37	1.819
	B	900	1.87	1.843
Copper*	A	900	1.30	1.881
	B	(Data not taken due to cooling water failure)		
Molybdenum	A	950	1.25	1.974
	B	950	1.25	1.974
Platinum	A	950	0.58	2.055
	B	950	0.71	2.034
Nickel (Test No. 1)	A	850	2.78	1.718
	B	(Heater opened)		
Nickel (Test No. 2)	A	900	3.20	1.790
	B	900	3.11	1.794
Beryllium	A	950	0.086	2.256
	B	950	0.485	2.074
Cobalt (Test No. 1)	A	900	2.05	1.835
	B	900	2.05	1.835
Cobalt (Test No. 2)	A	900	1.45	1.870
	B	(Arbitrarily omitted)		
Iridium	A	900	1.75	1.851
	B	900	1.75	1.851
Cerium	A	1050	0.185	2.371
	B	1050	0.185	2.371
Boron	A	950	0.43	2.086
	B	950	2.00	1.925
Silicon	A	950	0.52	2.066
	B	950	0.20	2.167
Magnesium**	A	900	1.41	1.873
	B	900	0.69	1.945
Tantalum	A	(Arbitrarily omitted since tantalum is not volatile)		
	B	900	0.093	2.379
Iron	A	950	2.80	1.889
	B	900	1.33	1.877
Aluminum	A	900	0.34	2.018
	B	900	1.50	1.867

A Before "flashing"

B After "flashing"

\* In cathode mix, 0.068 weight percent

\*\* Impregnated, 0.77 weight percent

## SUBLIMATION FROM BARIUM-STRONTIUM-TUNGSTATE CATHODES

In addition to being directly dependent upon the life of the cathode, long-life electron tubes are indirectly affected by the evaporation rates of materials sublimed from the cathode, because these evaporated metals may induce grid emission, electrical leakage, secondary emission, RF losses or alter other tube characteristics.

A dozen or more techniques have been employed to measure evaporation from cathodes.<sup>24</sup> Nearly all of these have some particular disadvantage or shortcoming, and a compromise must be made for each procedure relative to the sensitivity of the measurement, the accuracy and reproducibility, the degree of complexity in equipment and procedure, and the identification of the evaporated species.

In most instances, a knowledge of the total amount or rate of evaporation is all that is necessary, since the composition of the cathode gives an insight into the identity of the elements being sublimed. One method of determining cathode evaporation employs a vacuum microbalance.<sup>25</sup> The weight of a heated cathode, attached to one arm of the balance, is recorded as a function of time and temperature.

A modern and perhaps more simple means of obtaining cathode evaporation employs the Deposit Thickness Monitor.\* The operation of this instrument is based on the property that the fundamental resonant frequency of a quartz crystal is a linear function of its mass. Any material collecting on the face of the quartz crystal lowers its resonant frequency. By measuring the change of frequency, the sublimation rates and amounts from any source can be calculated.<sup>26</sup>

The evaporation rates of various cathode systems as compiled from published data<sup>27, 28, 29</sup> are shown in Figure 74, while sublimation results obtained from the Deposit Thickness Monitor are plotted in Figure 75. Other cathode systems and the technique from which the results were obtained are shown as a basis of comparison. These rates are all plotted as a function of temperature. It will be noted that fair agreement exists between the various techniques.

---

\*Sloan Instruments Corporation, Santa Barbara, California

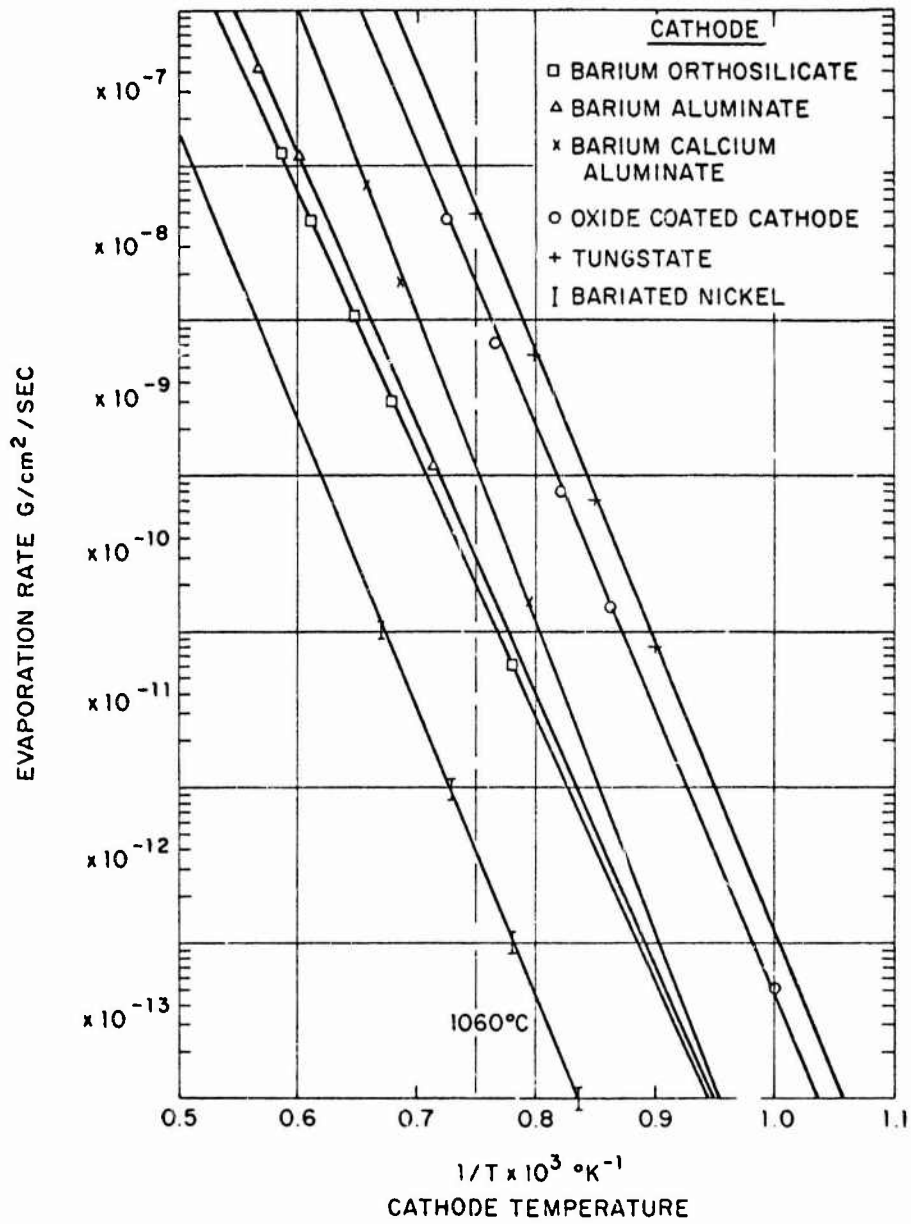


Figure 74 - Survey of Sublimation Rates of Various Cathode Systems

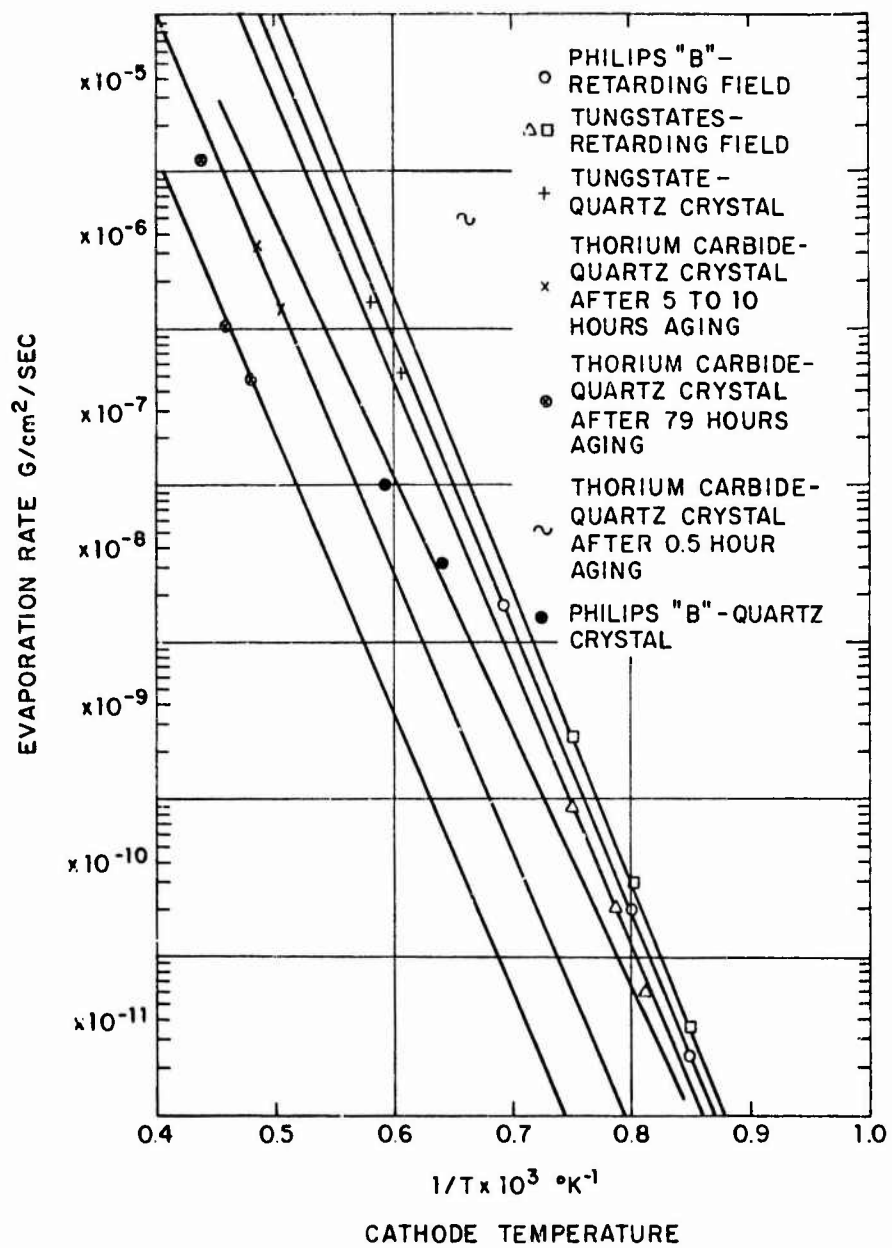


Figure 75 - Sublimation Rates of Various Cathode Systems Measured by Deposit Thickness Monitor

Not given is the previous history of the cathode prior to sublimation measurements. Initial evaporation rates may have been high, tapering off with time. Thus, differing amounts may be stated by various investigators, depending upon how long at what temperature the cathode was operated before sublimation was measured.

Giving the evaporation rate as a function of temperature can be misleading, unless the corresponding emission capability for the particular cathode system at the comparison temperature is known. In Figure 76, the sublimation rate as a function of current density is shown.<sup>30-38</sup> This plot illustrates the outstanding characteristics of the tungstate cathode, i.e., the total evaporation in the continuous current ranges of 1 to 30 A/cm<sup>2</sup> is approaching that of barium oxide on nickel for pulsed emission. From these data, it appears that the sublimation from tungstate cathodes is approximately two orders of magnitude lower than that of commercially available impregnated cathodes at equivalent emission densities.

### CATHODE NOISE

As specified in the technical guidelines for this contract, the determination of noise generated by the tungstate cathode became another of the object of this study. To obtain comparison performance, the noise properties of a Philip's B cathode and an ordinary barium-oxide-on-nickel type were measured in identical diode structures on the same equipment. The associated procedures and analyses are discussed in the paragraphs which follow.

Cathode noise, usually designated as shot noise, is the fluctuation of the current drawn by a thermionic diode. It is well known<sup>39</sup> that the fluctuating components of the current have a uniform frequency spectrum and are independent of the external impedance through which they flow. Figure 77 depicts a circuit diagram of a diode and its RF circuitry, without the associated circuitry for applying heater power and anode voltage. The noise power delivered to resistor R will have the same frequency spectrum as the real part of the impedance between the cathode and anode. The integrated power will be:

$$P = i^2 R \quad (1)$$

where  $i$  is the RMS noise current which is independent of  $R$  and the resonant frequency ( $f_0$ ) but directly proportional to the equivalent bandwidth<sup>40</sup> ( $B$ ).  $B$  is approximately equal to the half-power bandwidth for typical resonance

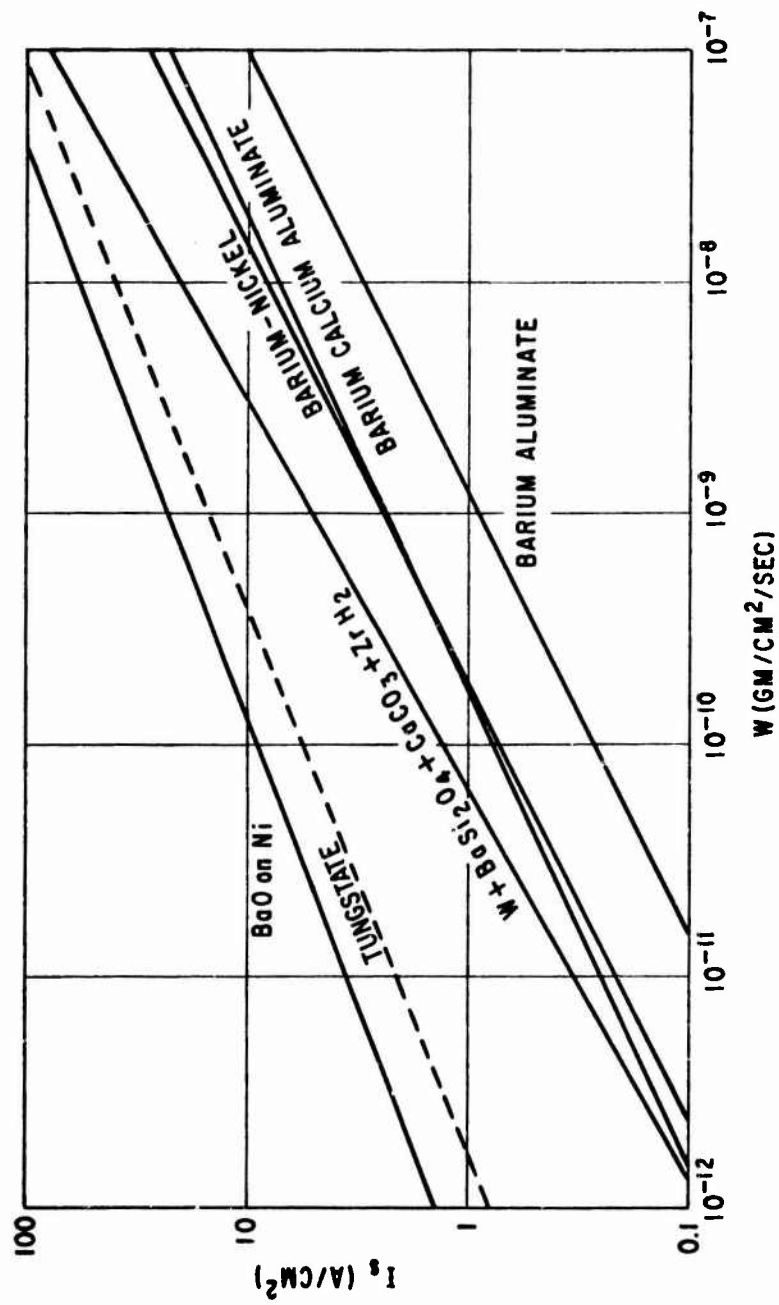


Figure 76 - Current Density versus Evaporation Rate

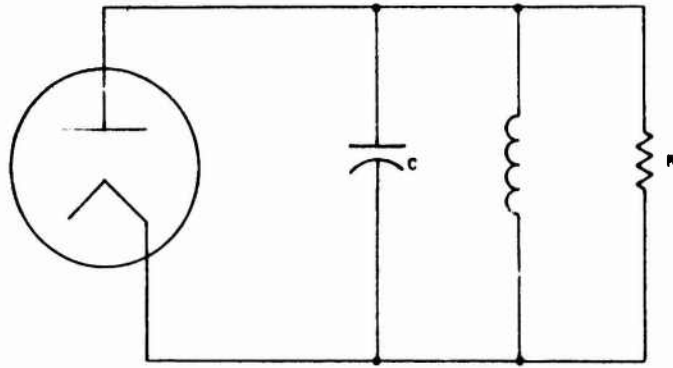


Figure 77 - Simplified Circuit Diagram of Diode and RF Circuitry Used in Noise Measurement

curves. If the noise power for a particular  $f_0$ ,  $R$ , and  $B$  is measured, then the noise current ( $i$ ) for any other  $f_0$ ,  $R$ , and  $B$  can be calculated. Such an experimental procedure has been followed in evaluating the noise properties of some of the cathodes studied under this program.

The test equipment used is diagrammed in Figure 78. The tuned circuit of which the tube is a part has a resonant frequency ( $f_0$ ) of 30 megahertz. The total shunt capacitance ( $C$ ), measured across the diode terminals, is  $47 \times 10^{-12}$  farads. With the diode turned off so that the resonator is loaded only by the external 200-ohm resistance, the measured  $Q$  is 14.5. Thus, the resistance  $R$  into which the total noise power is developed is given by:

$$\frac{1}{R} = \frac{1}{1637 \text{ ohms}} + \frac{dI}{dV} \quad (2)$$

where  $dI/dV$  is the rate of change of diode current with diode voltage. The combination of the amplifiers, attenuators, and noise figure meter forms a sensitive power meter. In the manual position, the noise figure meter is simply a narrowband amplifier and square law detector. With the attenuators adjusted to zero, full scale deflection was obtained with an input power of  $9.72 \times 10^{-14}$  watts from a sine-wave signal generator tuned to 30 megahertz. Varying the frequency of the signal generator revealed a half-power bandwidth for the detector ( $B_d = 1.29$  megahertz). The half-power bandwidth of the resonator is:

$$B_r = \frac{1}{2\pi CR} \quad (3)$$

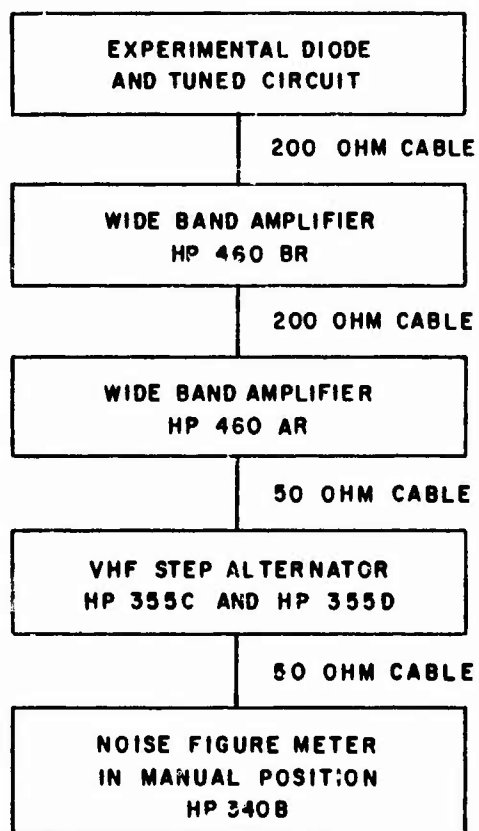


Figure 78 - Block Diagram of Noise Measuring Equipment

and the bandwidth of the two combined is

$$B = \sqrt{\sqrt{\left[\frac{1}{2}(B_d^2 + B_r^2)\right]^2 + (B_d B_r)^2} - \frac{1}{2}(B_d^2 + B_r^2)} \quad (4)$$

A convenient normalization for the measured noise power is the theoretical noise power of a temperature-limited diode, which is expressed as:

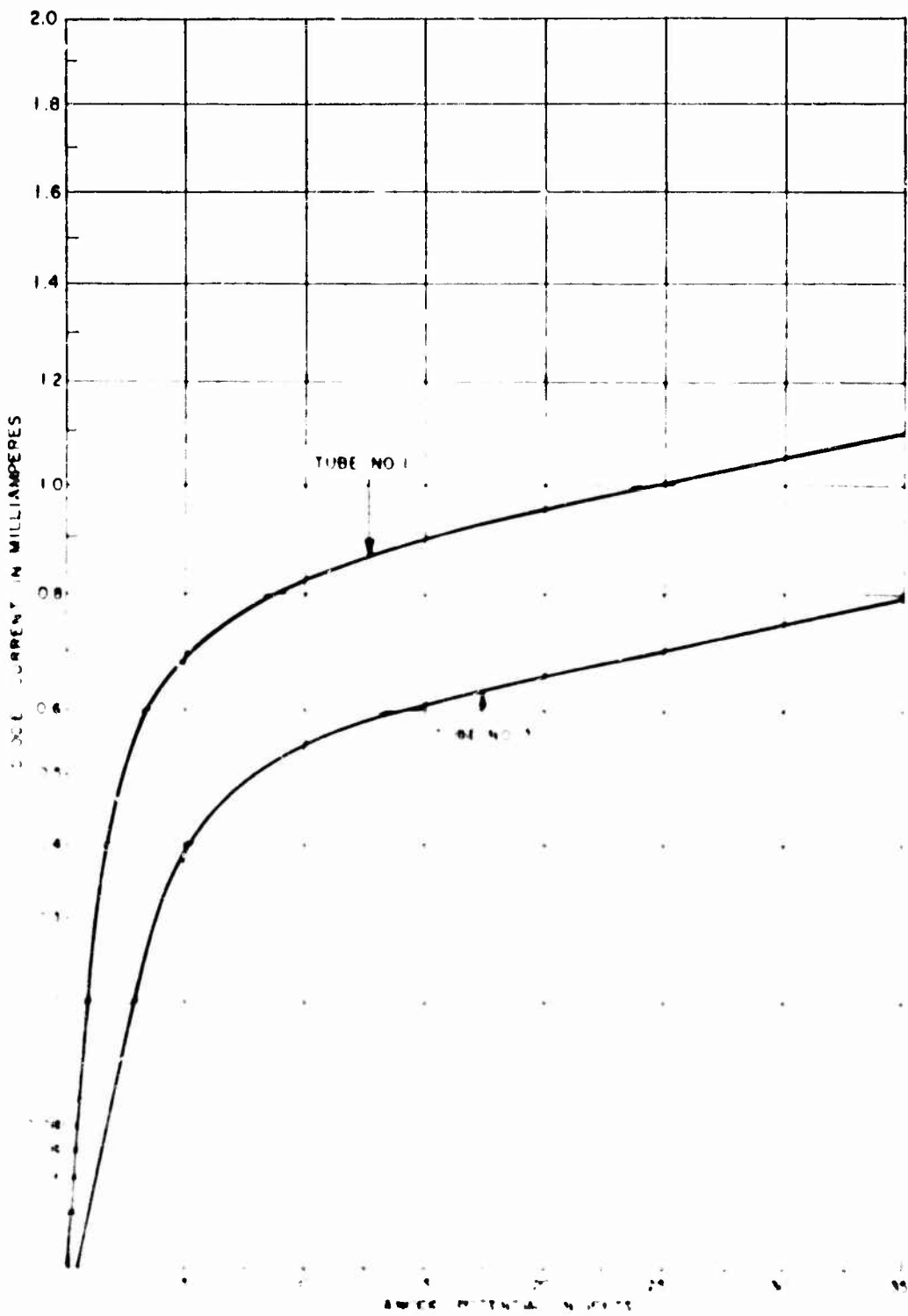
$$P_o = 2eIBR \quad (5)$$

where  $e$  is the electronic charge ( $1.6021 \times 10^{-19}$ ) in coulombs and  $I$  is the DC diode current in amperes. In these terms, one expects to obtain results similar to those shown in Figures 79, 80 and 81. These data are taken from the published results of F. C. Williams,<sup>41</sup> who measured the noise of cylindrical diodes having oxide-coated cathodes. Figure 79 shows the diode characteristic. Figure 80 shows the ratio ( $P/P_o$ ) of the measured noise power to the temperature-limited noise power as it varies with anode potential for the same cathode temperature as the data of Figure 79. When the emission is space-charge limited the noise is reduced by a factor which is approximated by the expression:<sup>42</sup>

$$\frac{P}{P_o} \approx \Gamma^2 = \frac{1.932 kT}{V} \quad (6)$$

where  $k$  is Boltzmann's constant ( $0.8617 \times 10^{-4}$  electron-volts/degree) and  $T$  is the absolute cathode temperature. In that region, the ratio of the noise power to the temperature-limited noise power decreases with increasing voltage, as shown in Figure 80. In the vicinity of the knee of the diode characteristic, the noise tends to approach  $P_o$ , but it does not reach it until well into what is normally considered the temperature-limited region. That it finally does reach  $P_o$  is demonstrated by the portion of Williams' data shown in Figure 81, which was obtained by extrapolating the diode characteristic (Williams plots noise versus diode current, rather than voltage).

Similar results have been obtained for the test diodes used in this program. Figure 82 shows  $P/P_o$  for an oxide-coated cathode (No. 112) at various temperatures. Figure 83 shows the same data plotted in terms of the ratio ( $P/\Gamma^2 P_o$ ) of measured noise power to the theoretical noise power of a space-charge limited diode. Note that the noise approaches the theoretical values only at the extremes.



Graph showing the relationship between tube current (in milliamperes) and tube potential (in kilovolts) for two different tubes, labeled 'TUBE NO. 1' and 'TUBE NO. 2'.

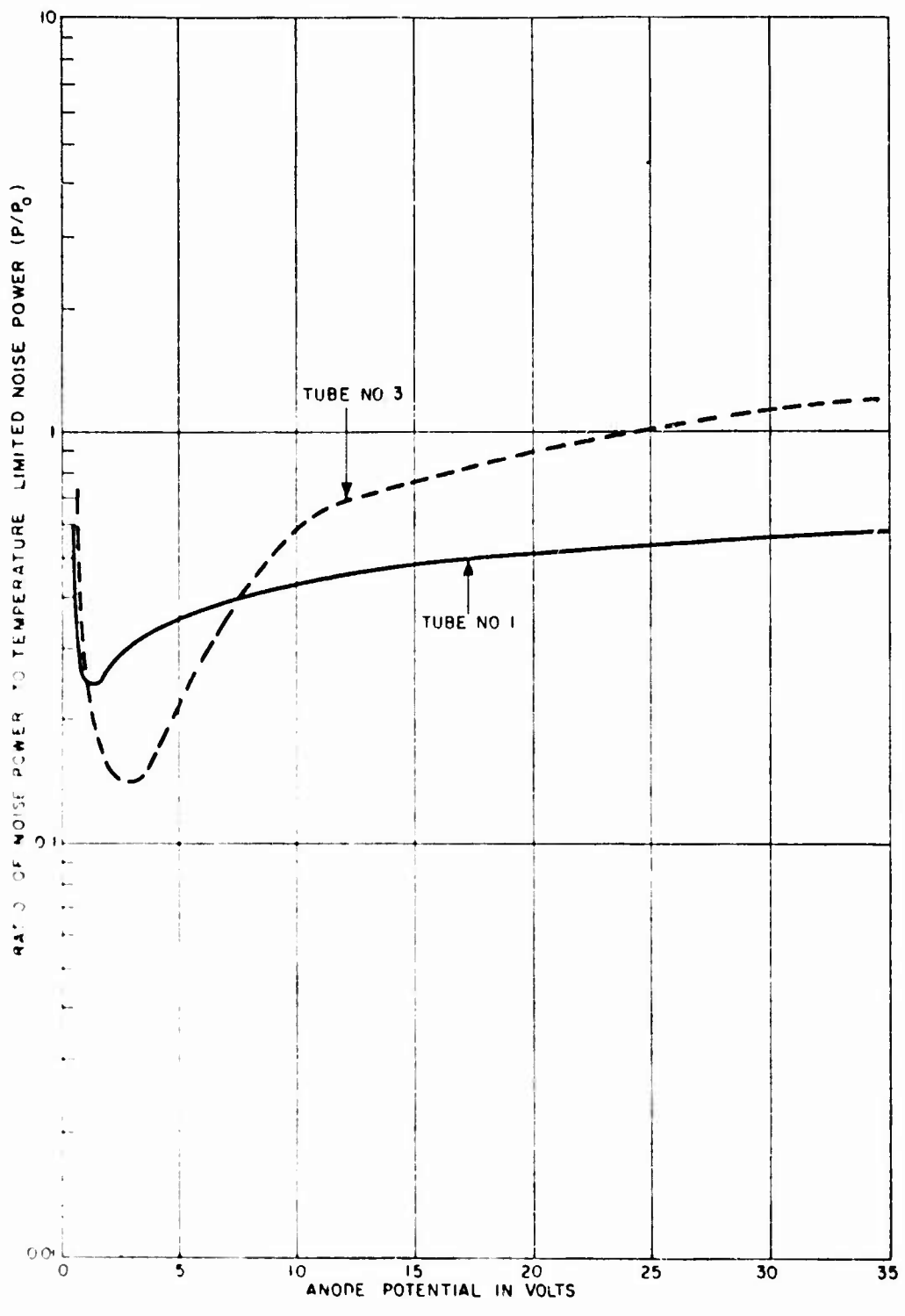


Figure 80 - Noise Measured by Williams

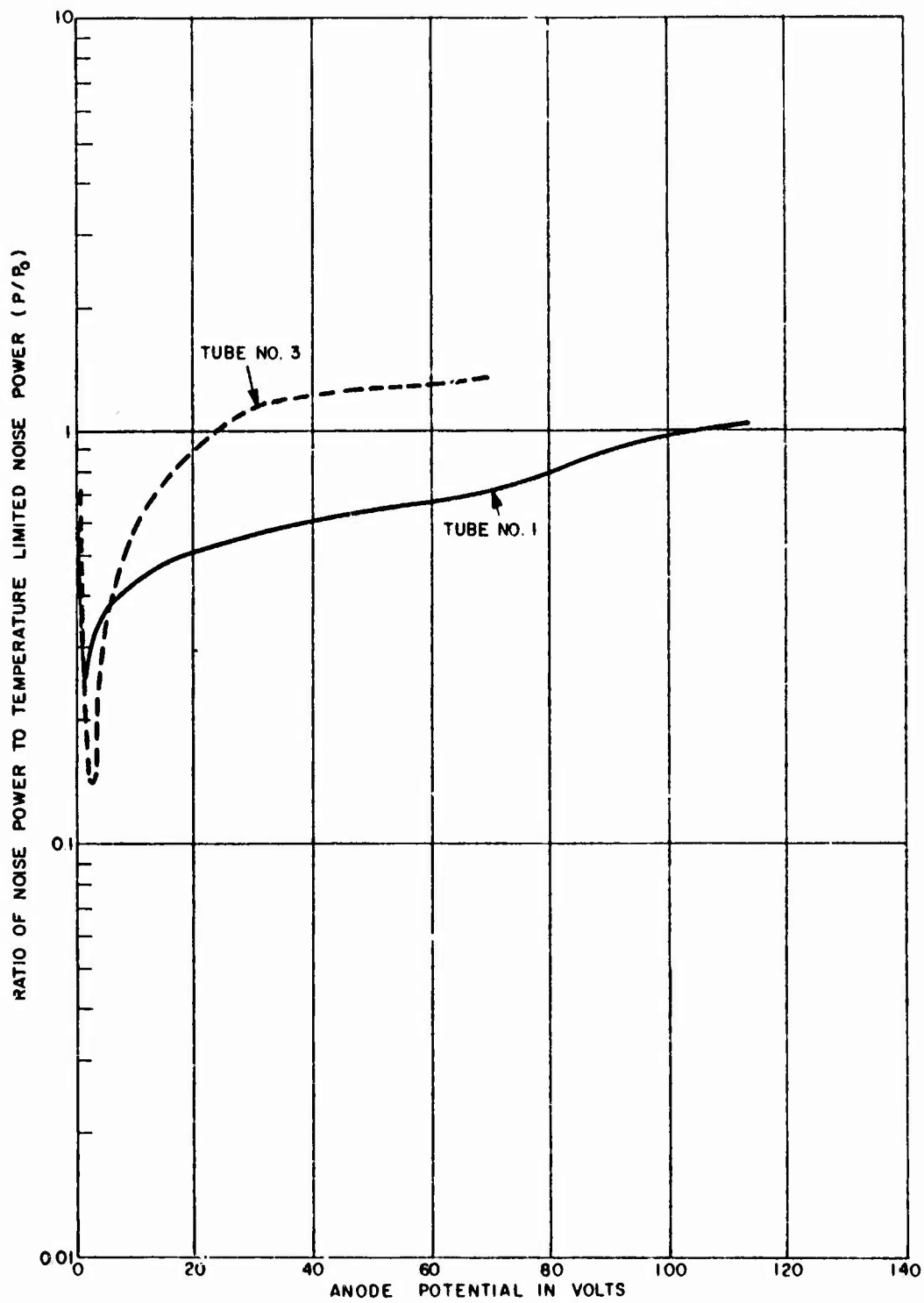


Figure 81 - Noise for High Anode Potentials Measured by Williams

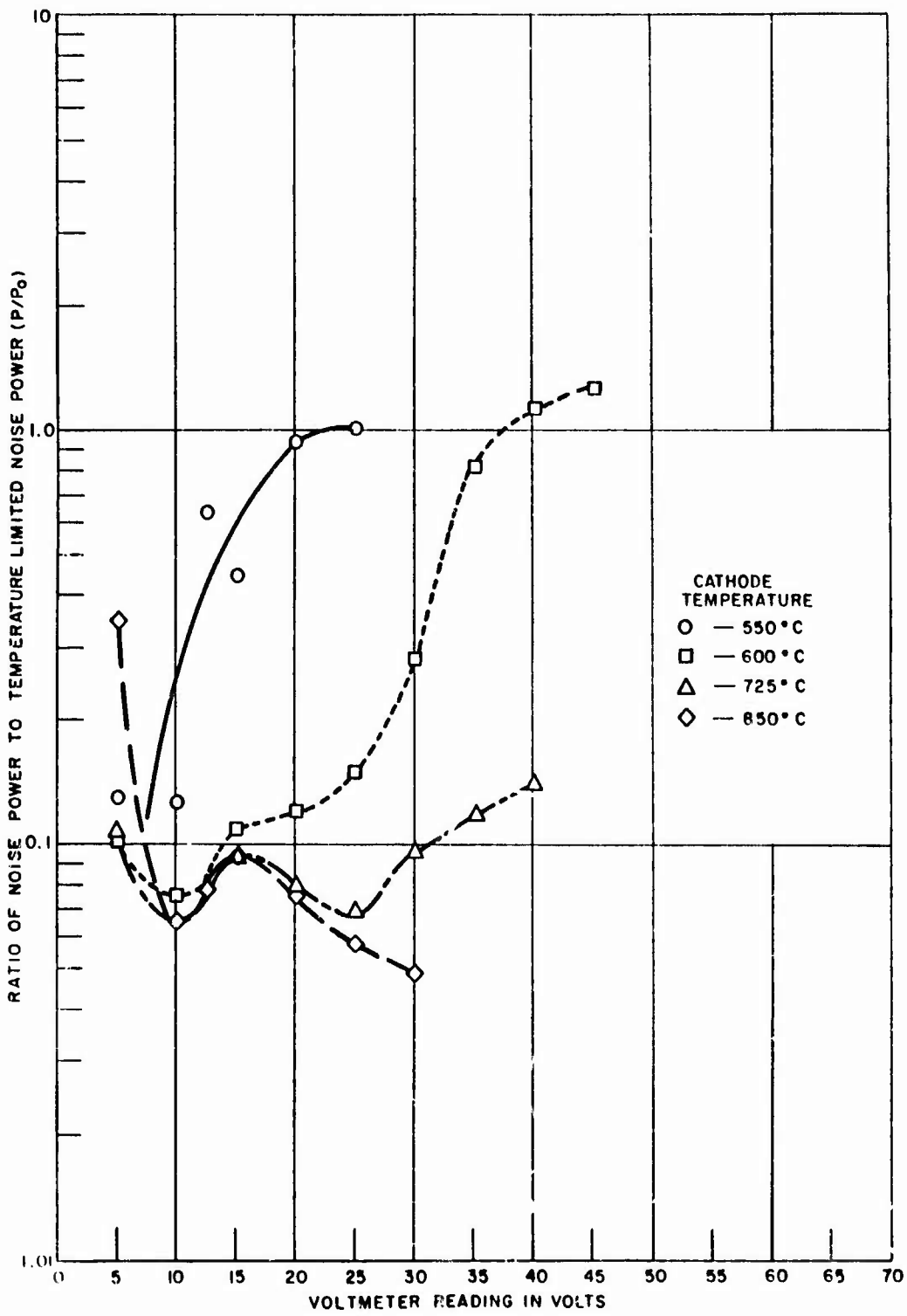


Figure 82 - Noise Normalized to Temperature-Limited Value  
(Tube No. 112)

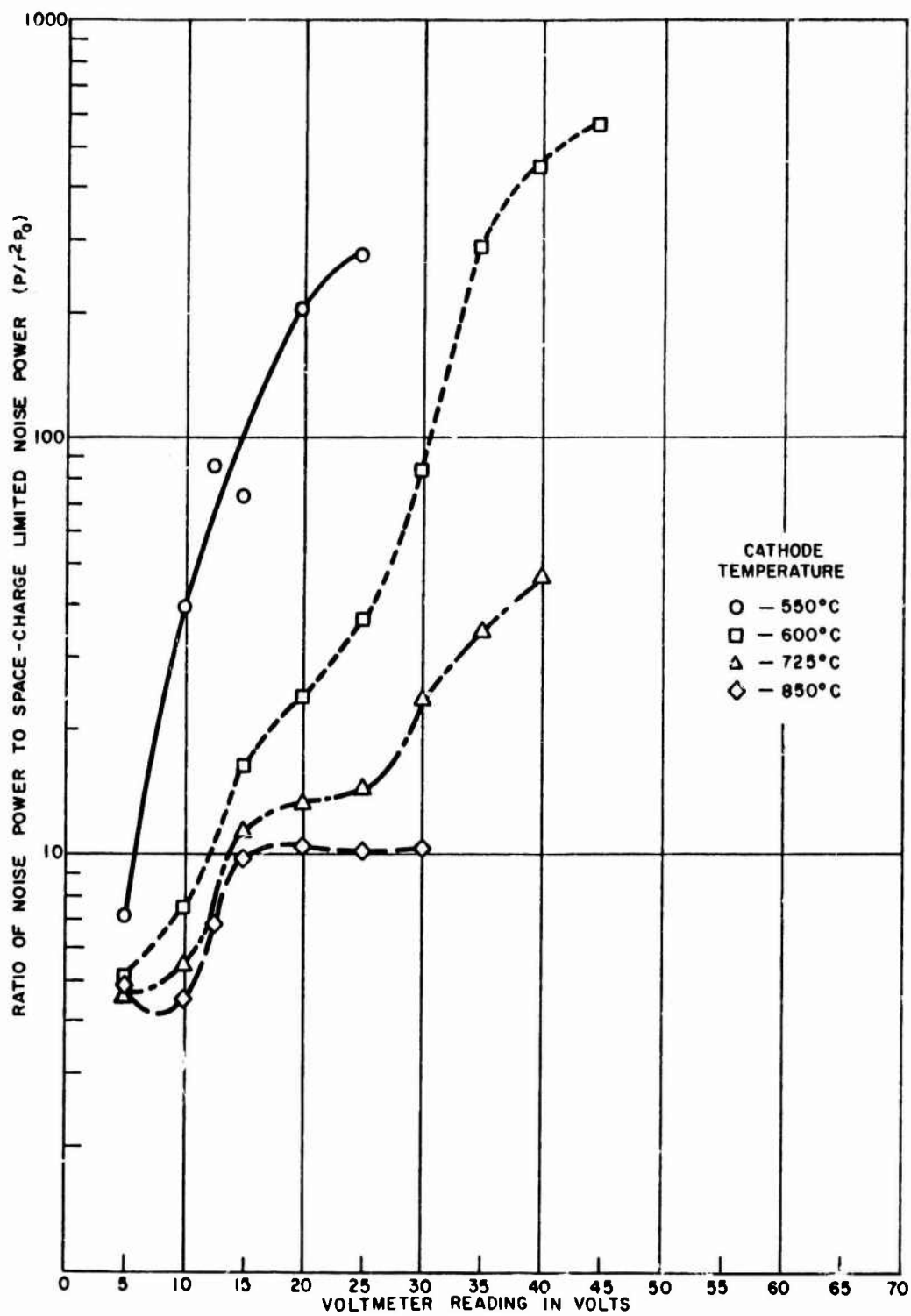


Figure 83 - Noise Normalized to Space-Charge Limited Value  
(Tube No. 112)

Departures from theory in the region intermediate between the space-charge and temperature-limited conditions can be described by a simple model which assumes that the current is made up of a portion ( $I_T$ ) which is temperature limited and gives rise to noise power  $2eI_TBR$ , and a portion ( $I_s$ ) which is space-charge limited and gives rise to noise power  $2e\Gamma^2I_sBR$ . With this assumption it is possible to calculate:

$$I_s = \frac{1 - \frac{P}{P_o}}{1 - \Gamma^2} I \quad (7)$$

and 
$$I_T = I - I_s \quad (8)$$

Figures 84 through 87 show the result of this calculation. While as a valid interpretation this may be oversimplified, it does give a graphic description of the noise performance. Noise power in excess of the theoretical value results in a small  $I_T$  component, even when the total current closely approximates a 3/2 power law. Agreement between the measured and theoretical noise in the temperature-limited case is marked by a vanishing  $I_s$ . The abscissa in these plots is the reading of a voltmeter connected across the diode terminals. This is not the true potential difference between anode and cathode due to the contact potential difference, as indicated by the fact that the current extrapolates to zero for a slightly negative voltmeter reading.

Figures 88 through 95 show data taken on a tungstate cathode tube No. HCD-67 over a wide range of parameters. As in the case of the oxide cathode, the noise approaches the theoretical value asymptotically in the space-charge limited case. Agreement with the theoretical temperature-limited value within 20 percent over a wide range is taken as a verification of the calibration of the noise measuring apparatus.

Test results taken on a tube (No. HCD-9) in which the cathode and anode are known to be non-parallel demonstrate the effect of this factor. The data shown in Figures 96 through 99 illustrate a broadening of the knee of the current-voltage curve and the corresponding intermediate noise performance. The sensitivity of using  $I_T$  and  $I_s$  to describe the noise performance is illustrated by the wide undulations in these parameters due to the relatively small, secondary variations in the measured noise, which are presumably due to experimental error.

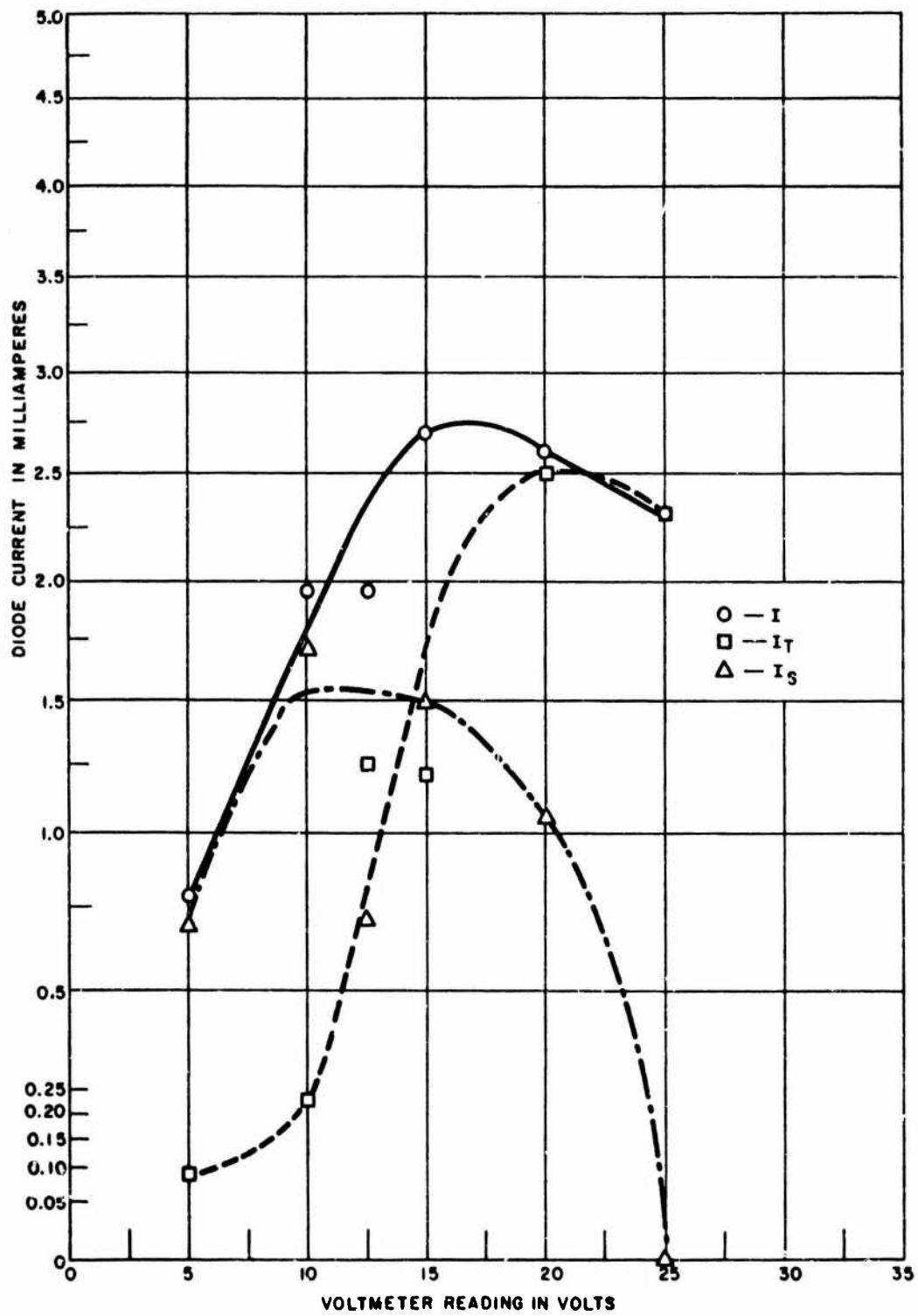


Figure 84 - Current Analysis for Tube No. 112 at 550°C

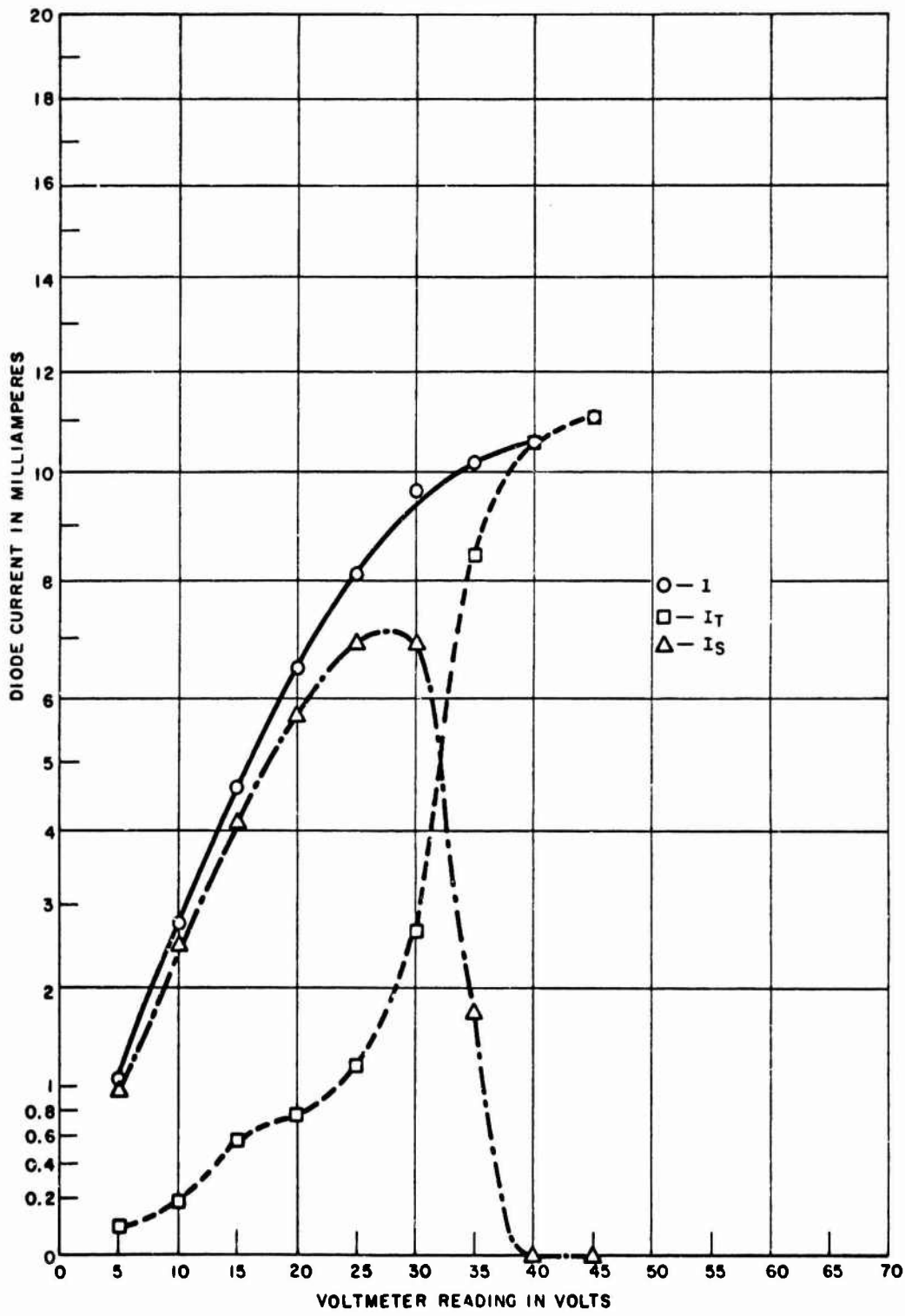


Figure 35 - Current Analysis for Tube No. 112 at 600°C

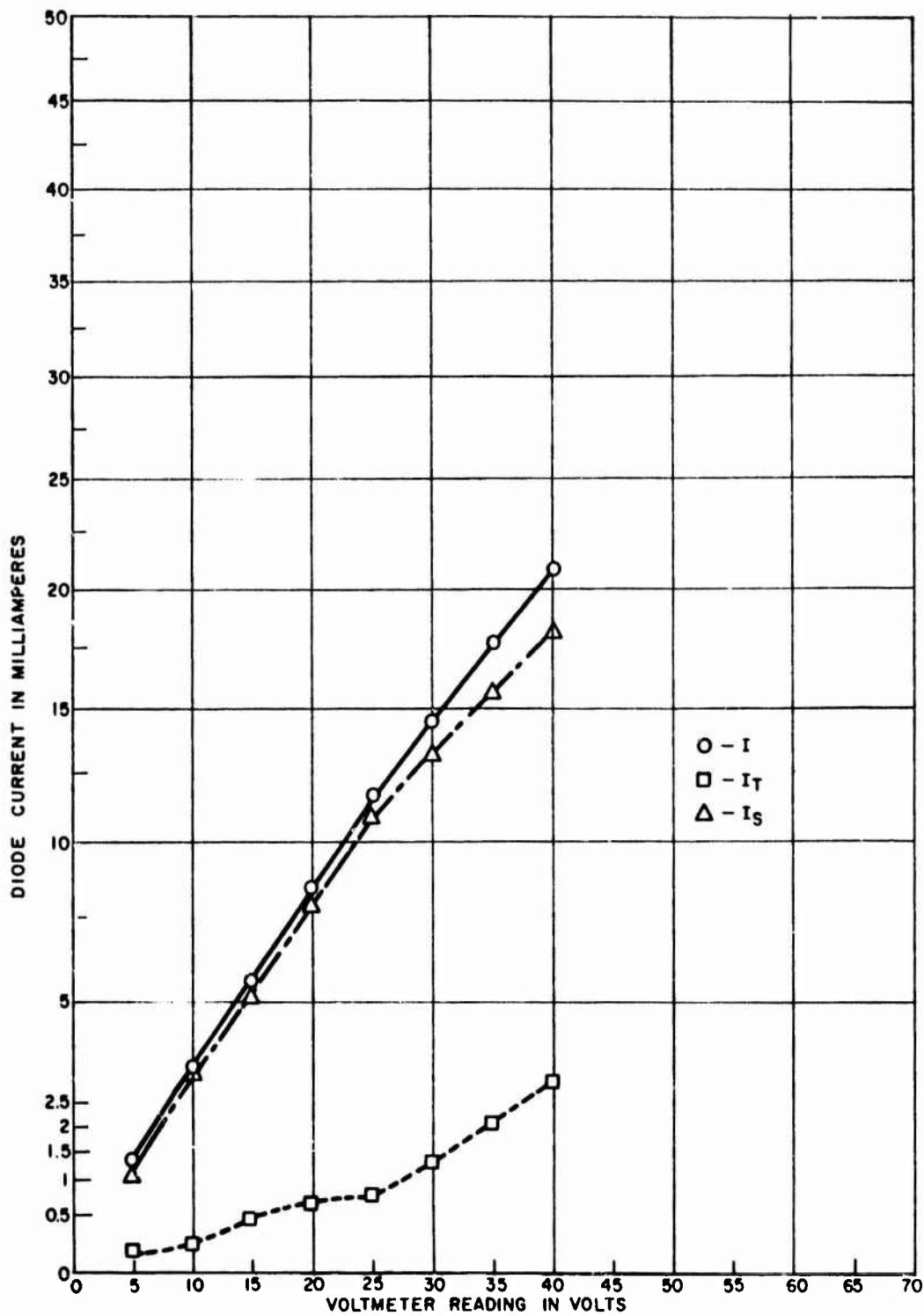


Figure 86 - Current Analysis for Tube No. 112 at 725°C

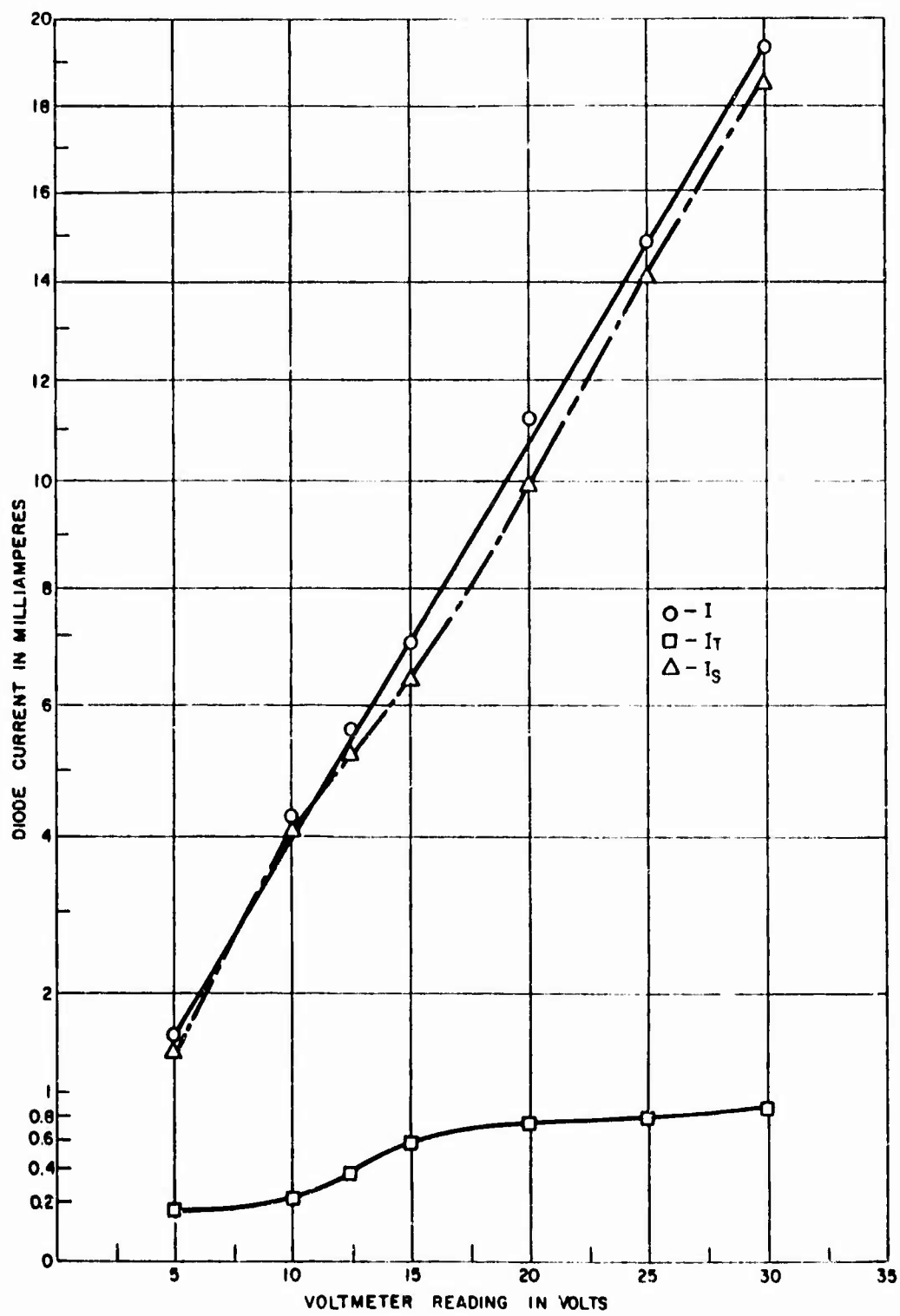


Figure 87 - Current Analysis for Tube No. 112 at 850°C

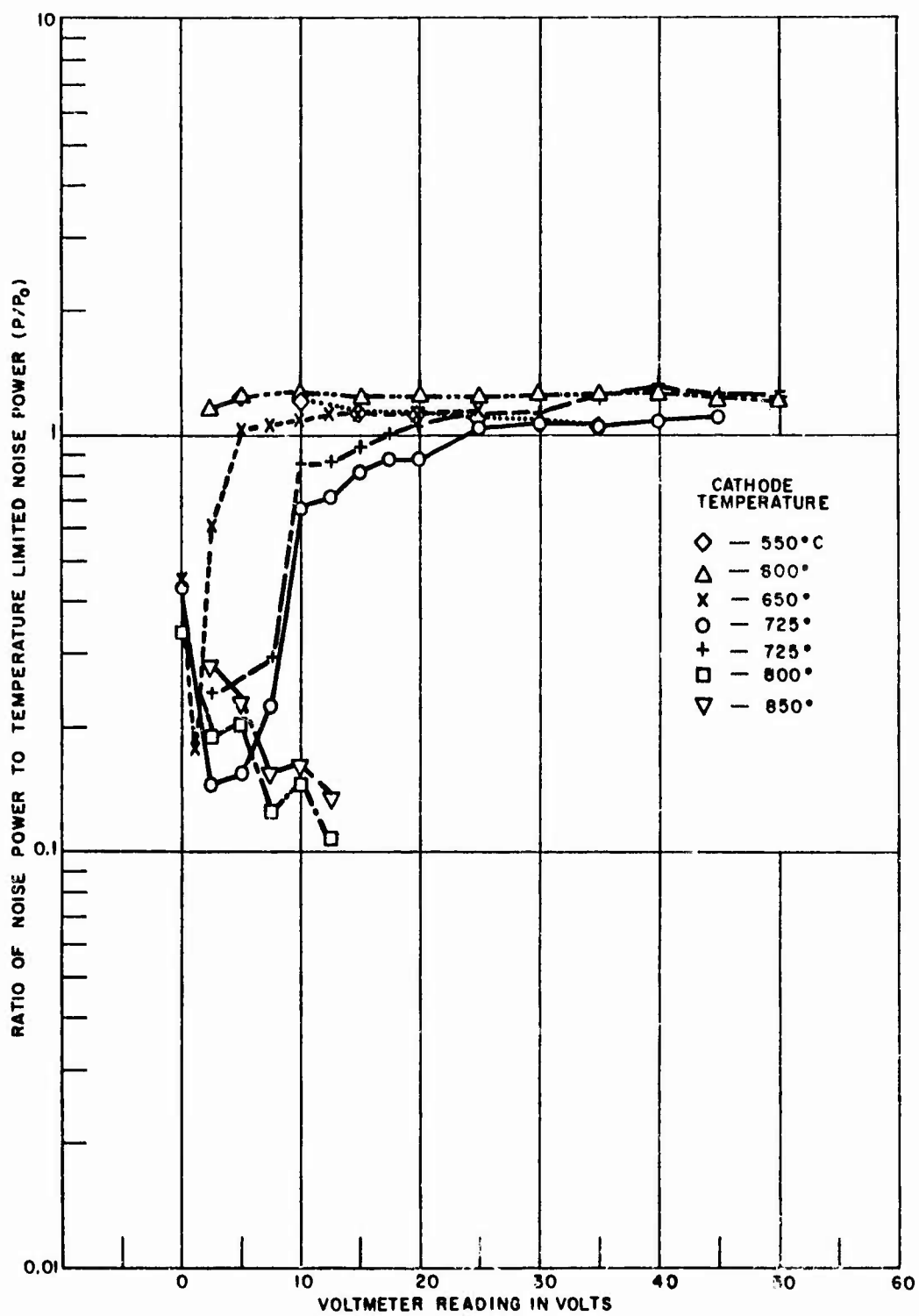


Figure 88 - Measured Noise Normalized to the Temperature-Limited Value for Tube No. HCD-67

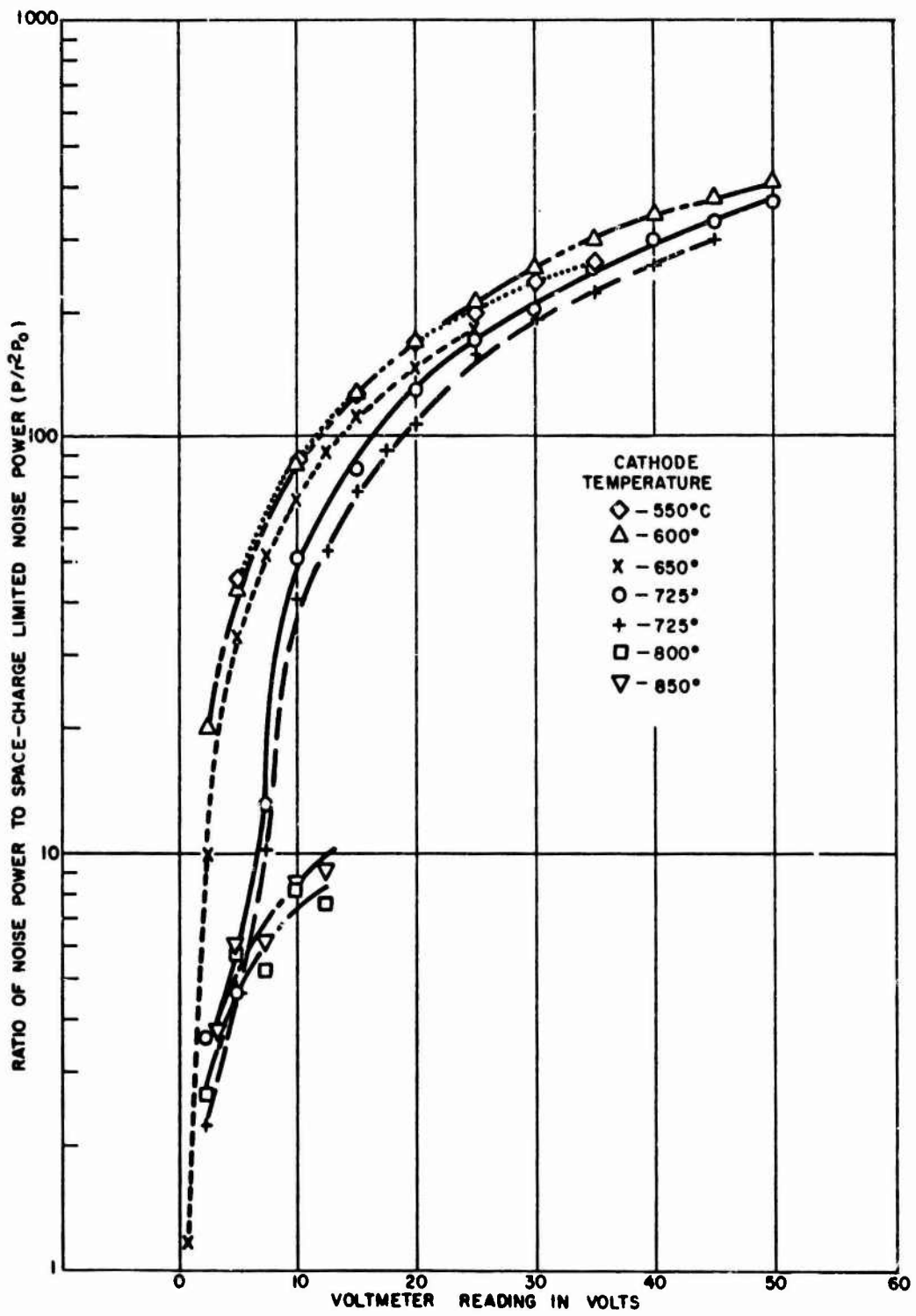


Figure 89 - Measured Noise Normalized to the Space-Charge Limited Value for Tube No. HCD-67

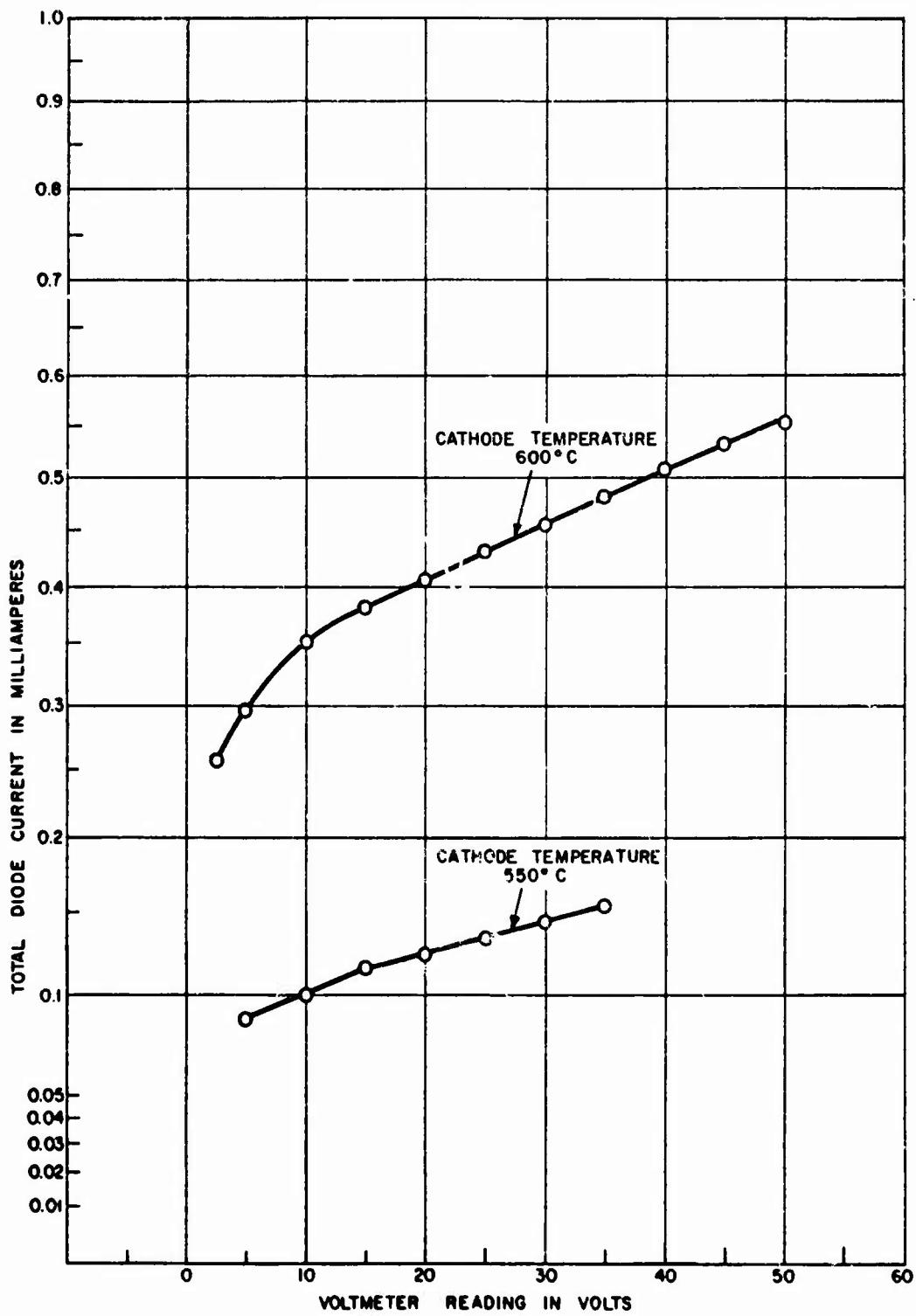


Figure 90 - Current Analysis for Tube No. HCD-67 at 550 and 600°C

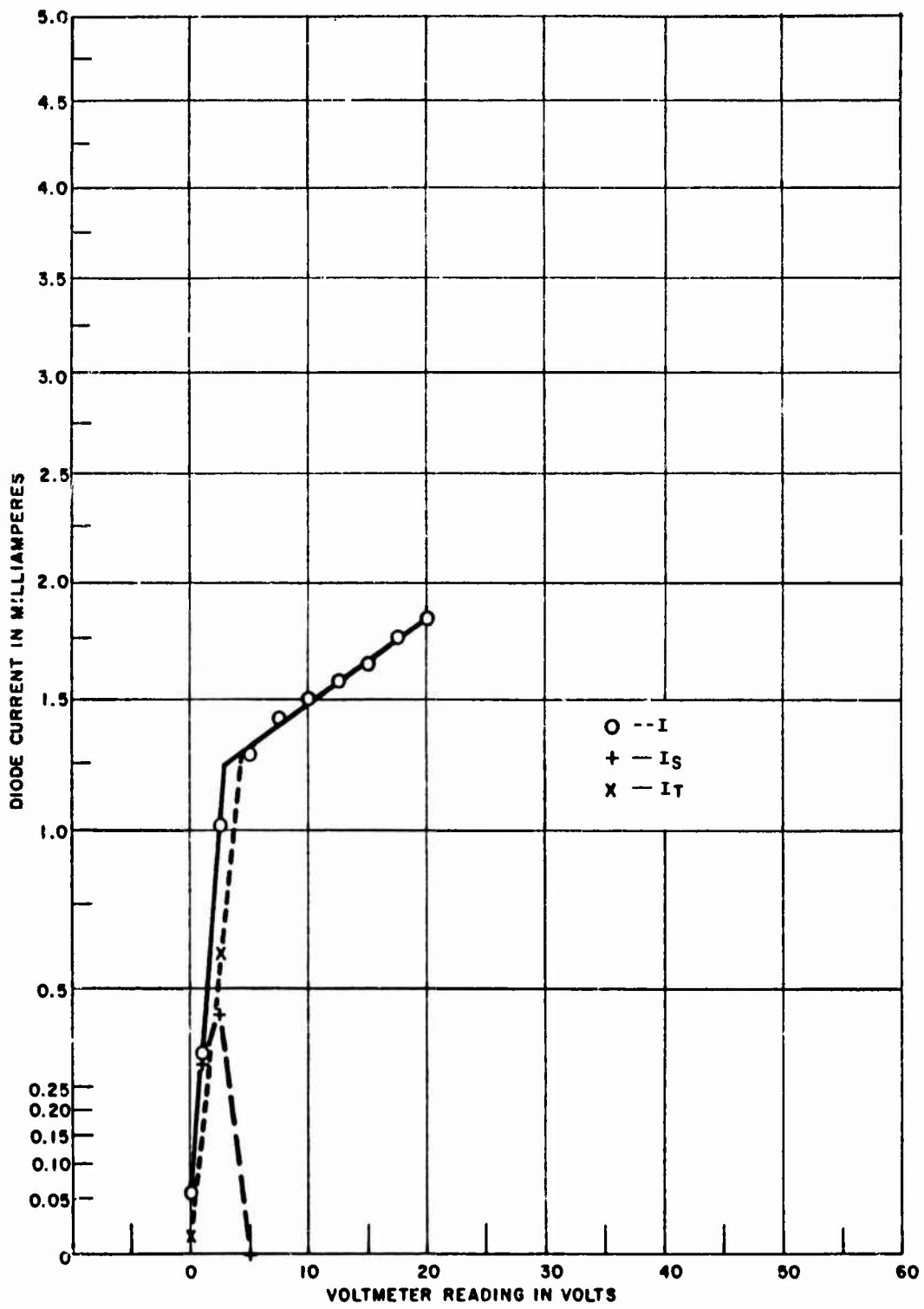


Figure 91 - Current Analysis for Tube No. HCD-67 at 650°C

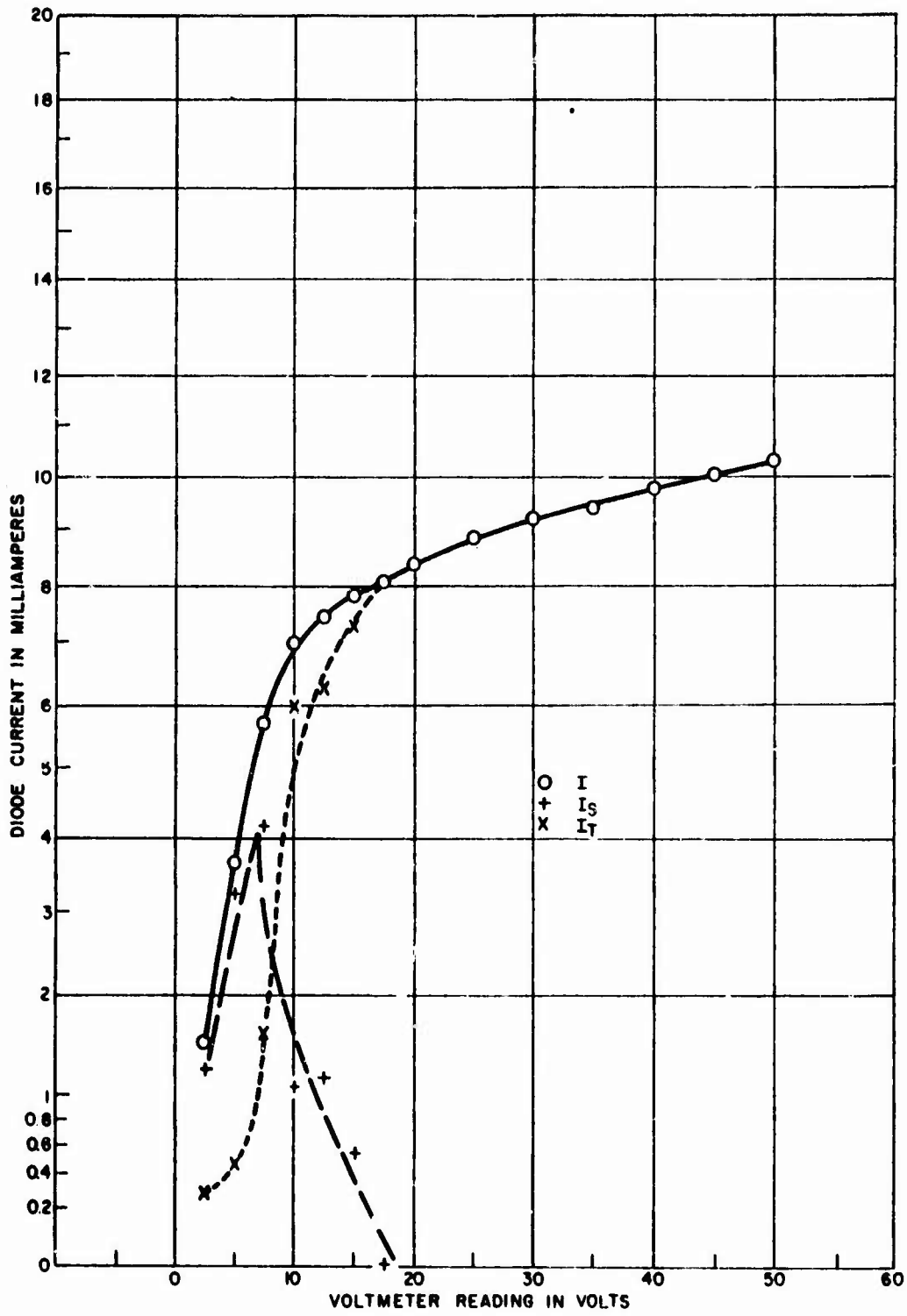


Figure 92 - Current Analysis for Tube No. HCD-67 at 725°C (first run)

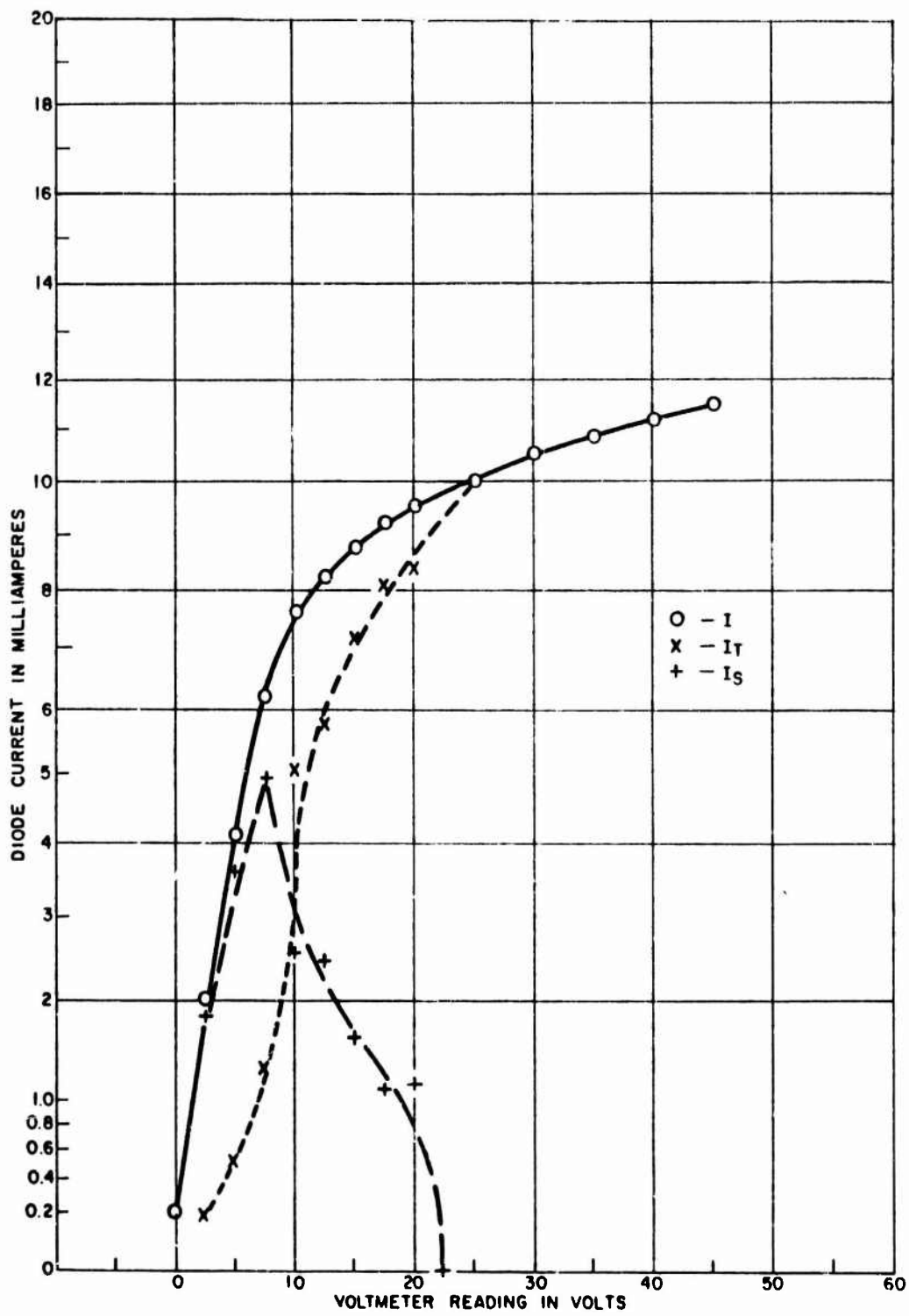


Figure 93 - Current Analysis for Tube No. HCD-67 at 725°C  
(second run)

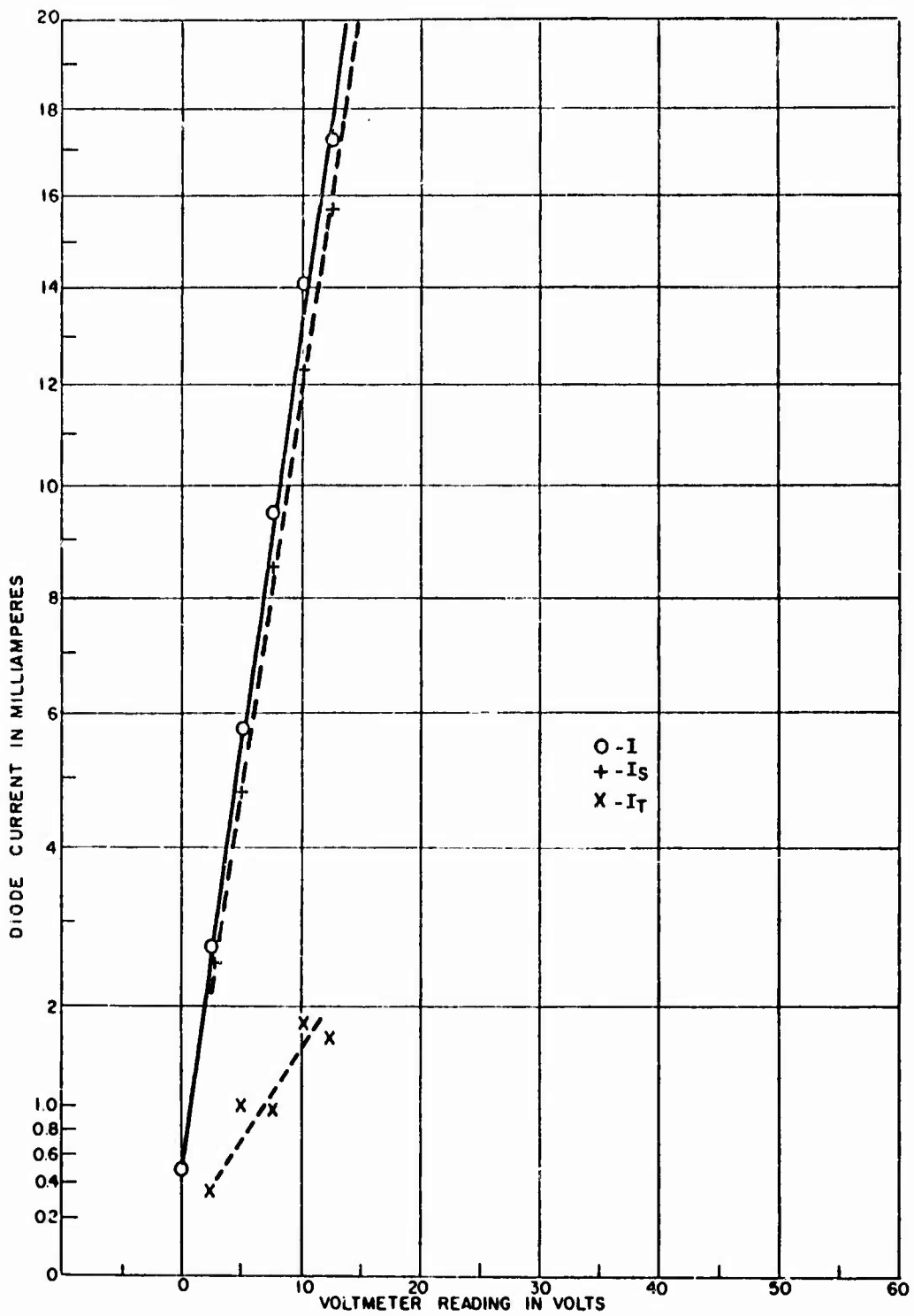


Figure 94 - Current Analysis for Tube No. HCD-67 at 800°C

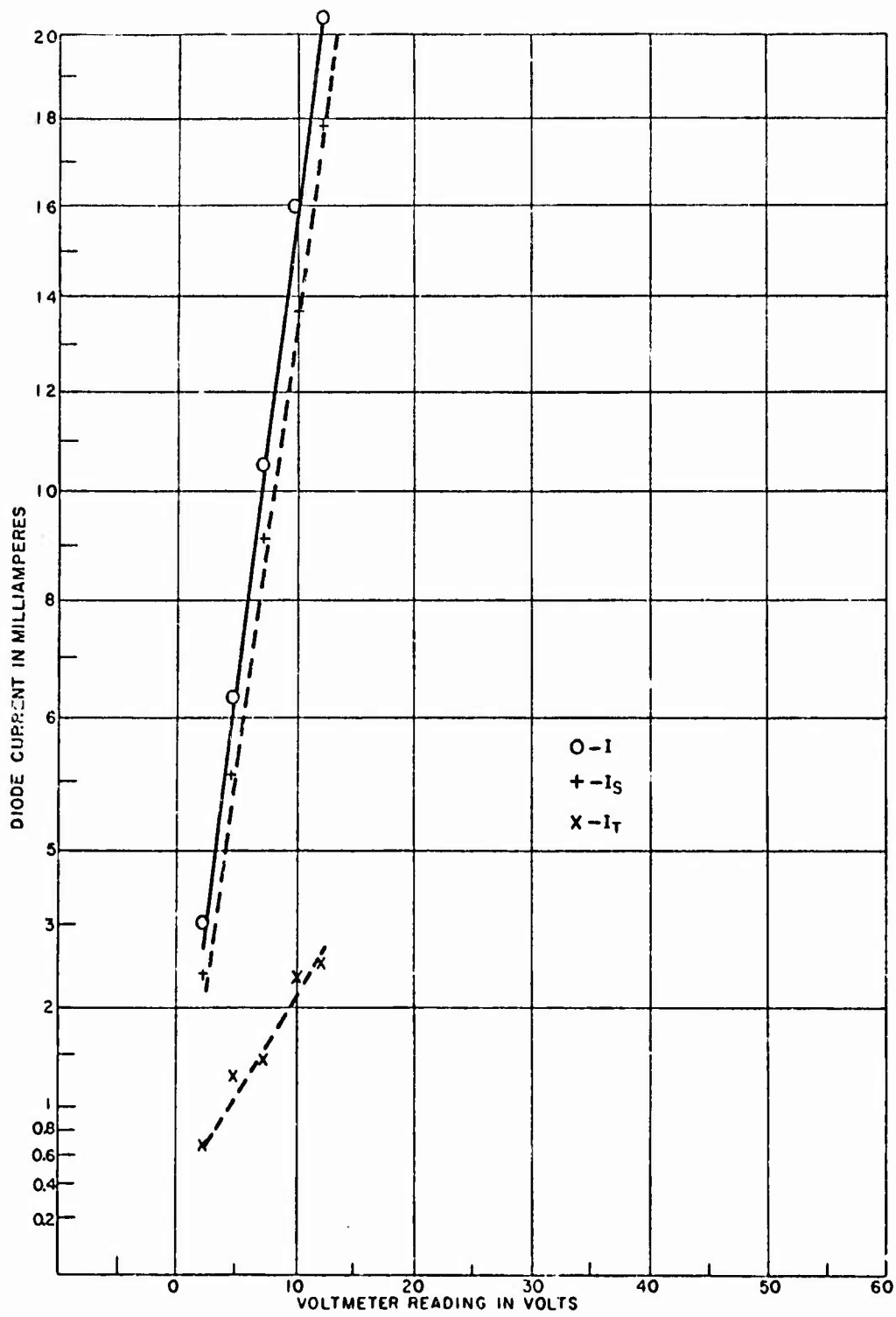


Figure 95 - Current Analysis for Tube No. HCD-67 at 850°C

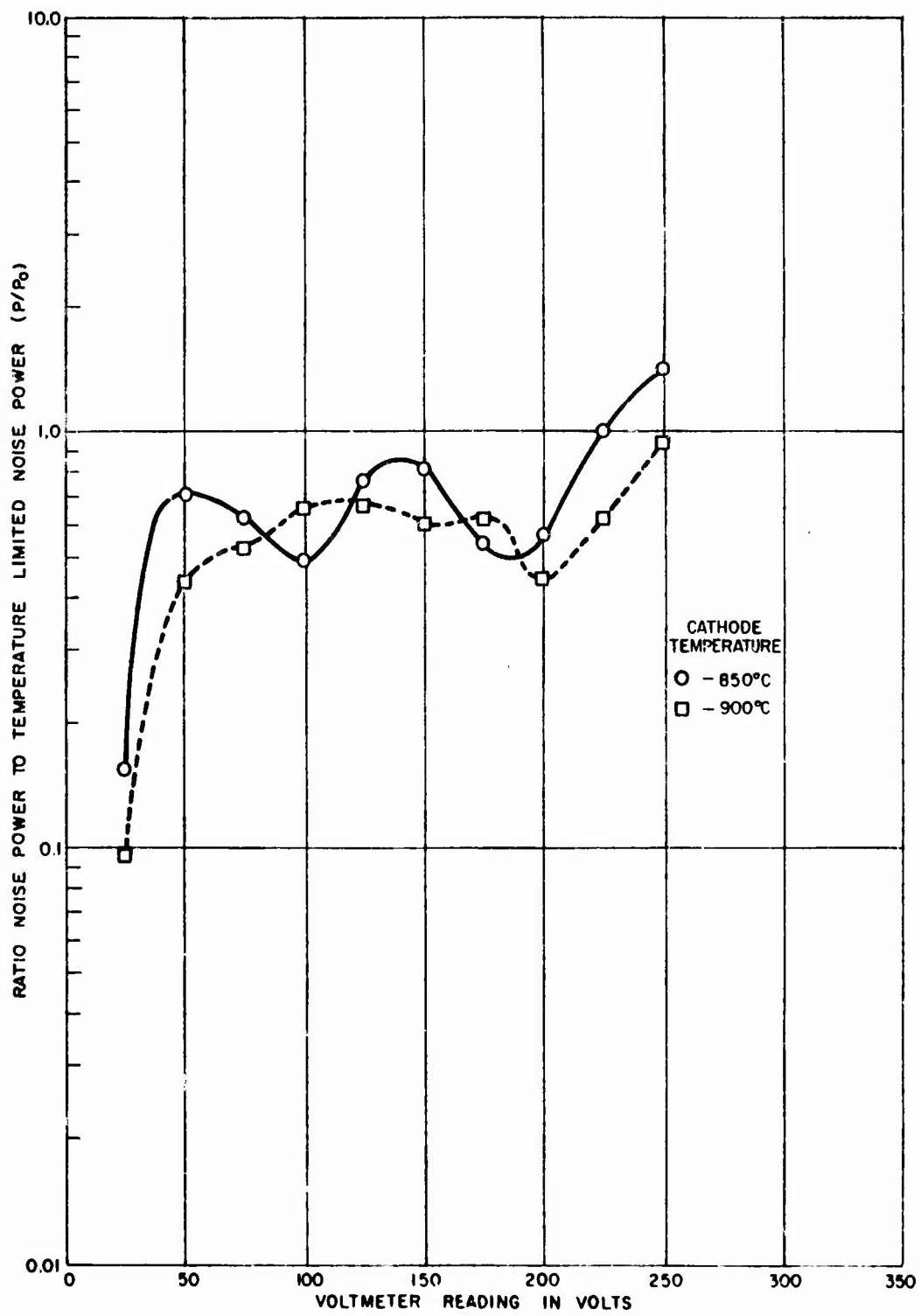


Figure 96 - Measured Noise Normalized to Temperature-Limited Value for Tube No. HCD-9

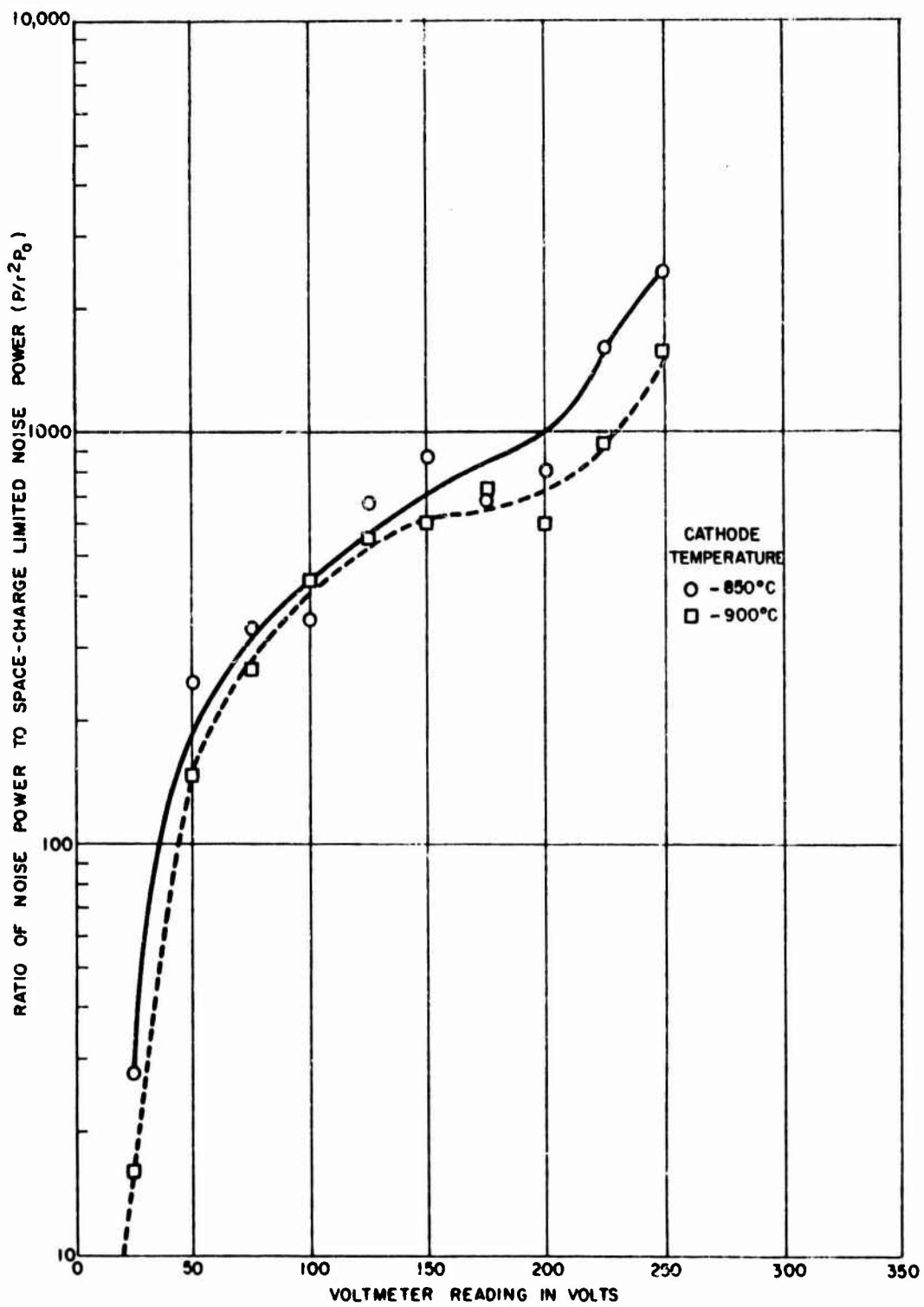


Figure 97 - Measured Noise Normalized to Space-Charge Limited Value for Tube No. HCD-9

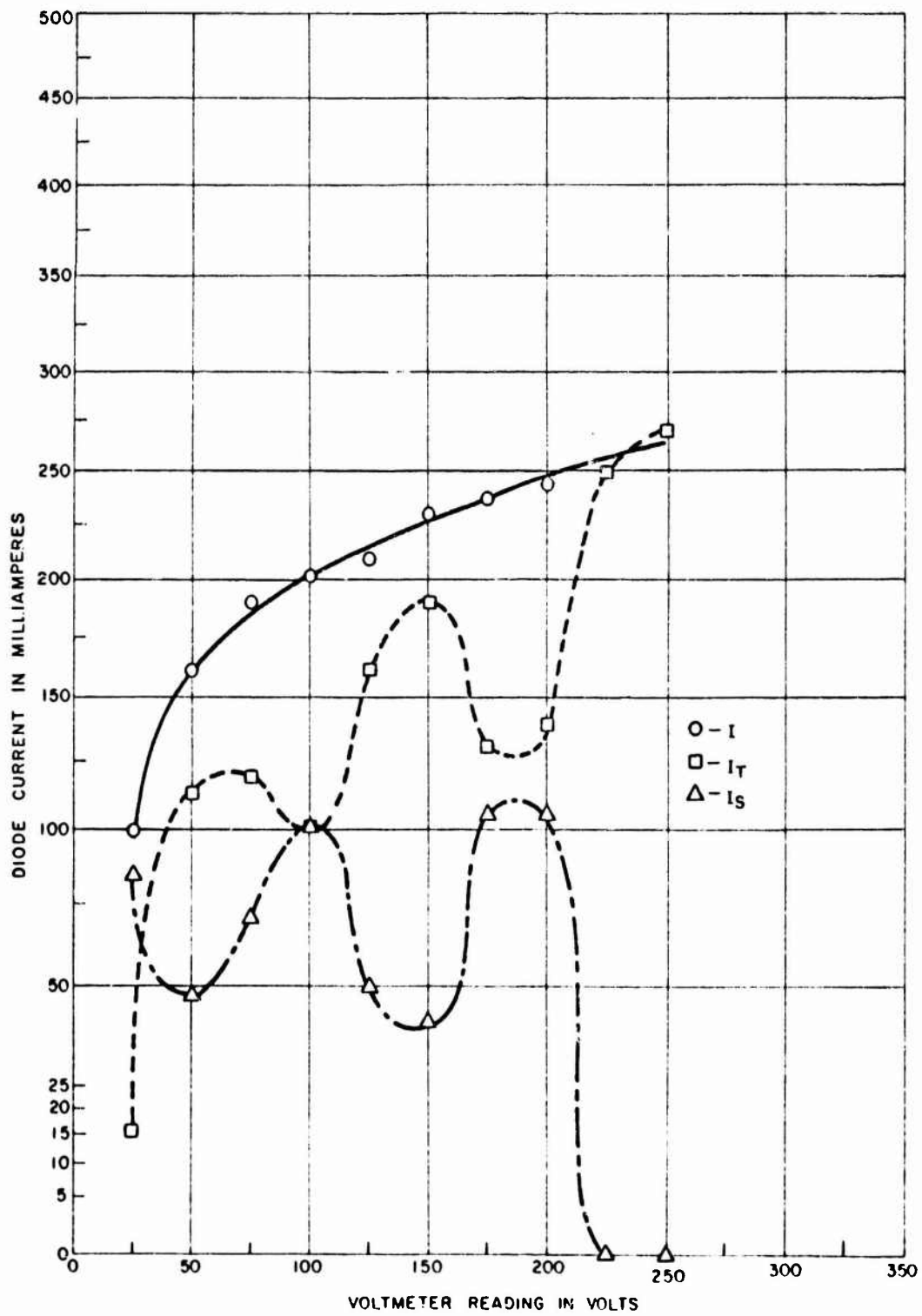


Figure 98 - Current Analysis for Tube No. HCD-9 at 850°C

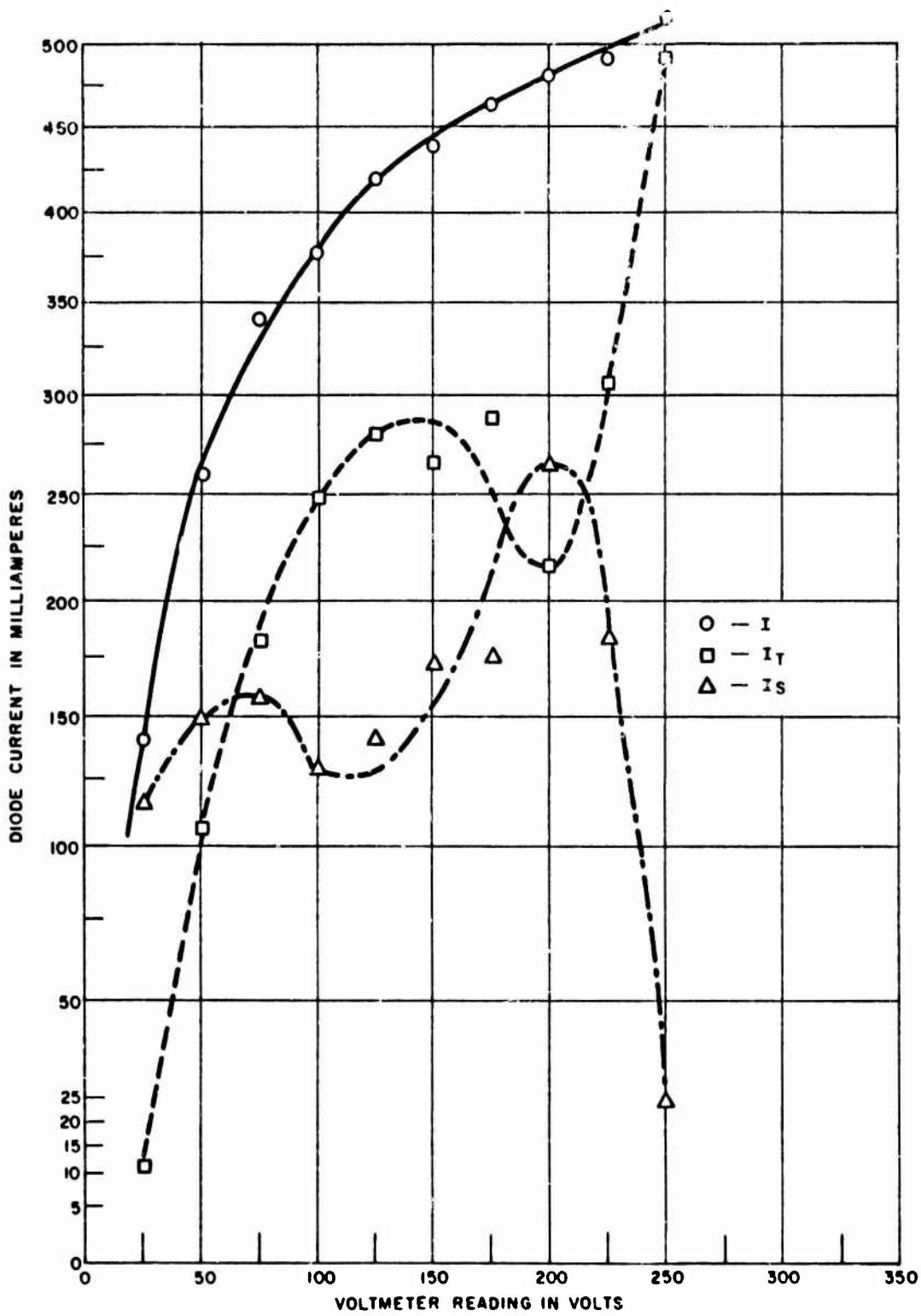


Figure 99 - Current Analysis for Tube No. HCD-9 at 900°C

The noise properties of a Philip's cathode were measured for comparison. The results for tube No. 116 are shown in Figures 100 through 103. The distinctive feature of these data is that the noise output remains substantially below the theoretical value for voltages much greater than that corresponding to the knee of the curve. This seems to indicate that about half the available current comes from small centers of very high emission density. The data shown in Figures 104 through 108 confirm this result for a second Philip's cathode (tube No. HCD-44).

One way to compare the noise performance of different cathodes for a low noise application is to arbitrarily choose an operating point as that at which the noise power reaches some multiple of the theoretical value for the space-charge limited condition. A factor of 10 seems to give a reasonable compromise between noise performance and emission density. The result of applying this definition to the data given in this report is shown in Figure 109.

In summary, the noise properties of the tungstate cathode appear to be comparable with those of other cathodes. One may expect the noise to be reduced by space charge by a factor of:

$$\frac{P}{P_o} = \frac{19.32 kT}{V} \quad (9)$$

at a typical operating point (e. g.,  $2 \text{ A/cm}^2$  at  $900^\circ\text{C}$ ). Cathode surfaces of the types studied appear to be a composite of areas of widely different emission density.

It appears that significant improvements could be made in emission density and in low noise performance if one could reduce the areas of relatively low emission. It is possible to develop a method of measuring the uniformity of emission of cathode surfaces, based on the measurements described here. If diodes were built with a uniform, measurable anode-to-cathode spacing,  $x$ , and allowing for greater anode dissipation so that space-charge limited current could be drawn at voltages that were large compared to the thermal energies, then:

$$I_s = 2.335 \times 10^{-4} \frac{A_s}{x} V^{3/2} \quad (10)$$

where  $A_s$  is the area from which the space-charge limited portion ( $I_s$ ) of the current is obtained. By using this relationship, the distribution of emission could be determined within the limitations of the assumed model.

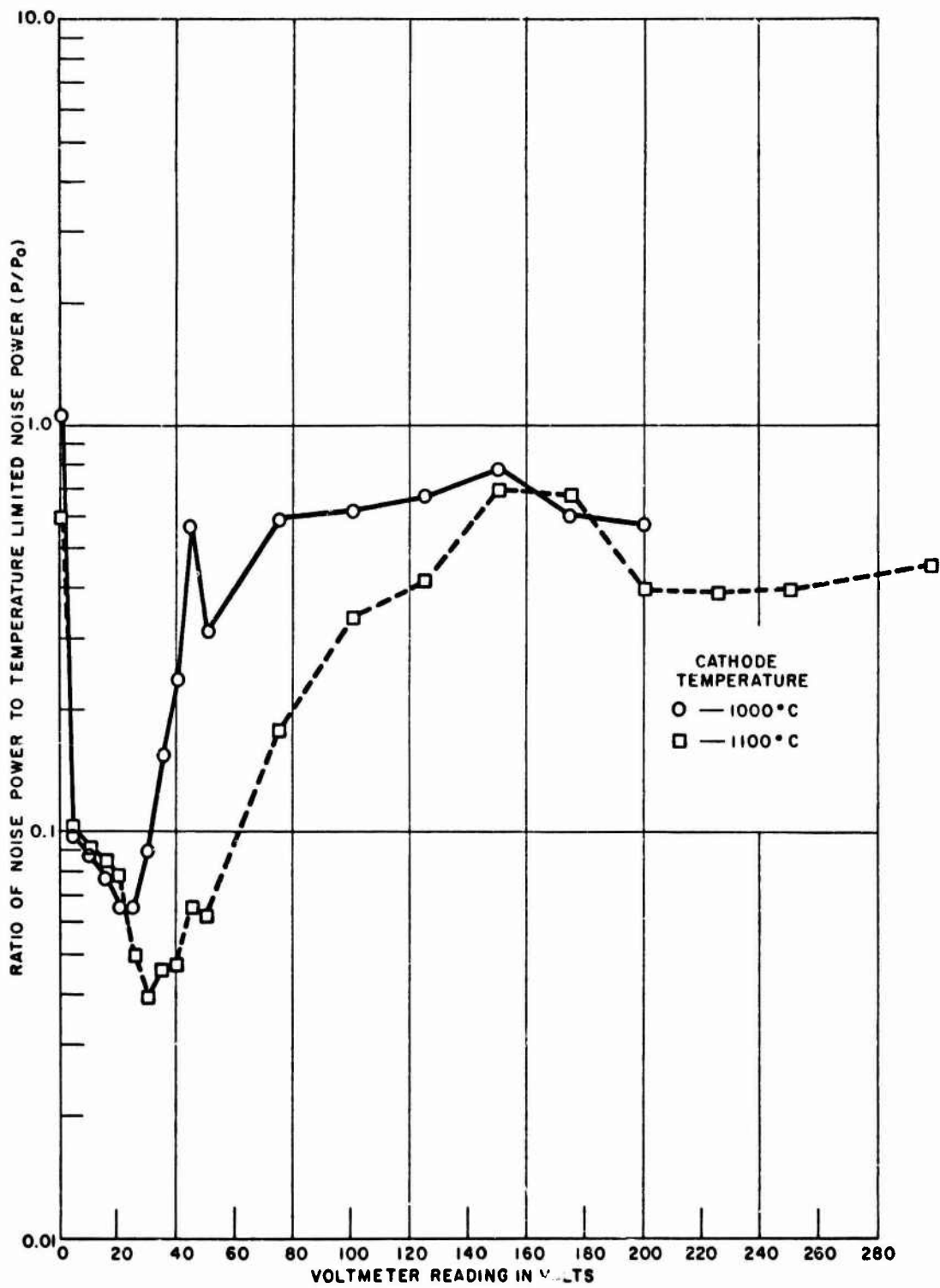


Figure 100 - Measured Noise Normalized to Temperature-Limited Value for Tube No. 116

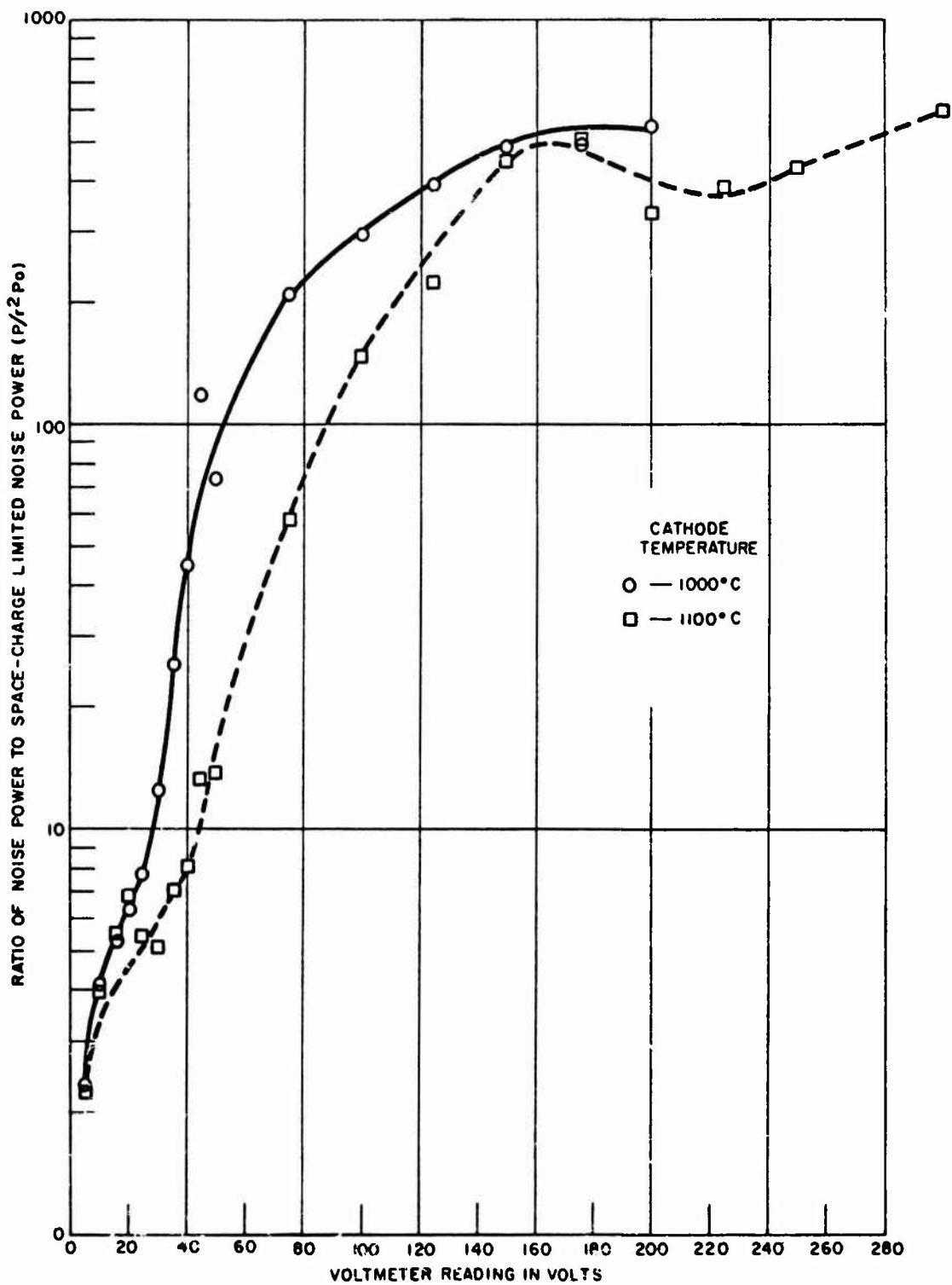


Figure 101 - Measured Noise Normalized to Space-Charge Limited Value for Tube No. 116

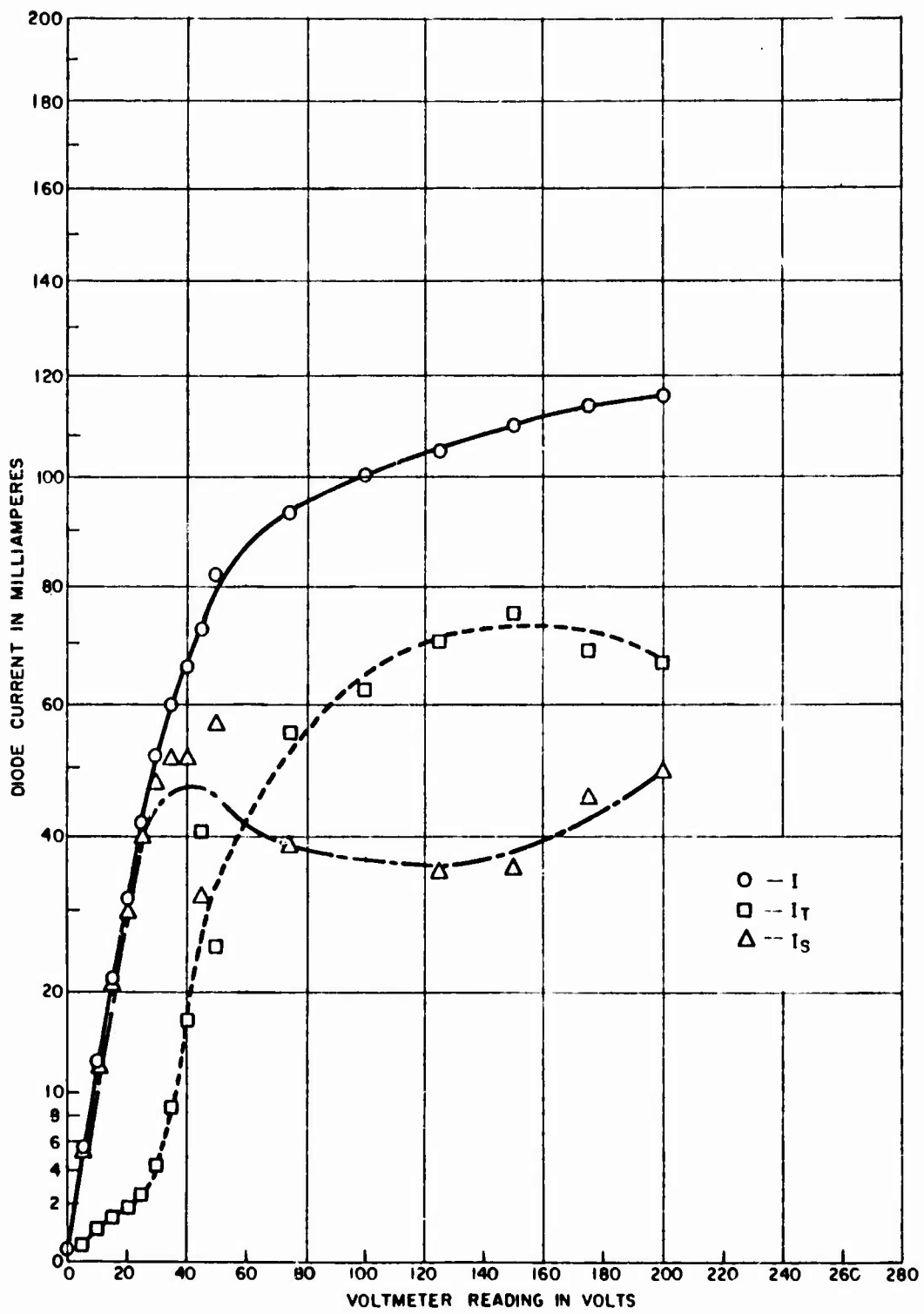


Figure 102 - Current Analysis for Tube No. 116 at 1000°C

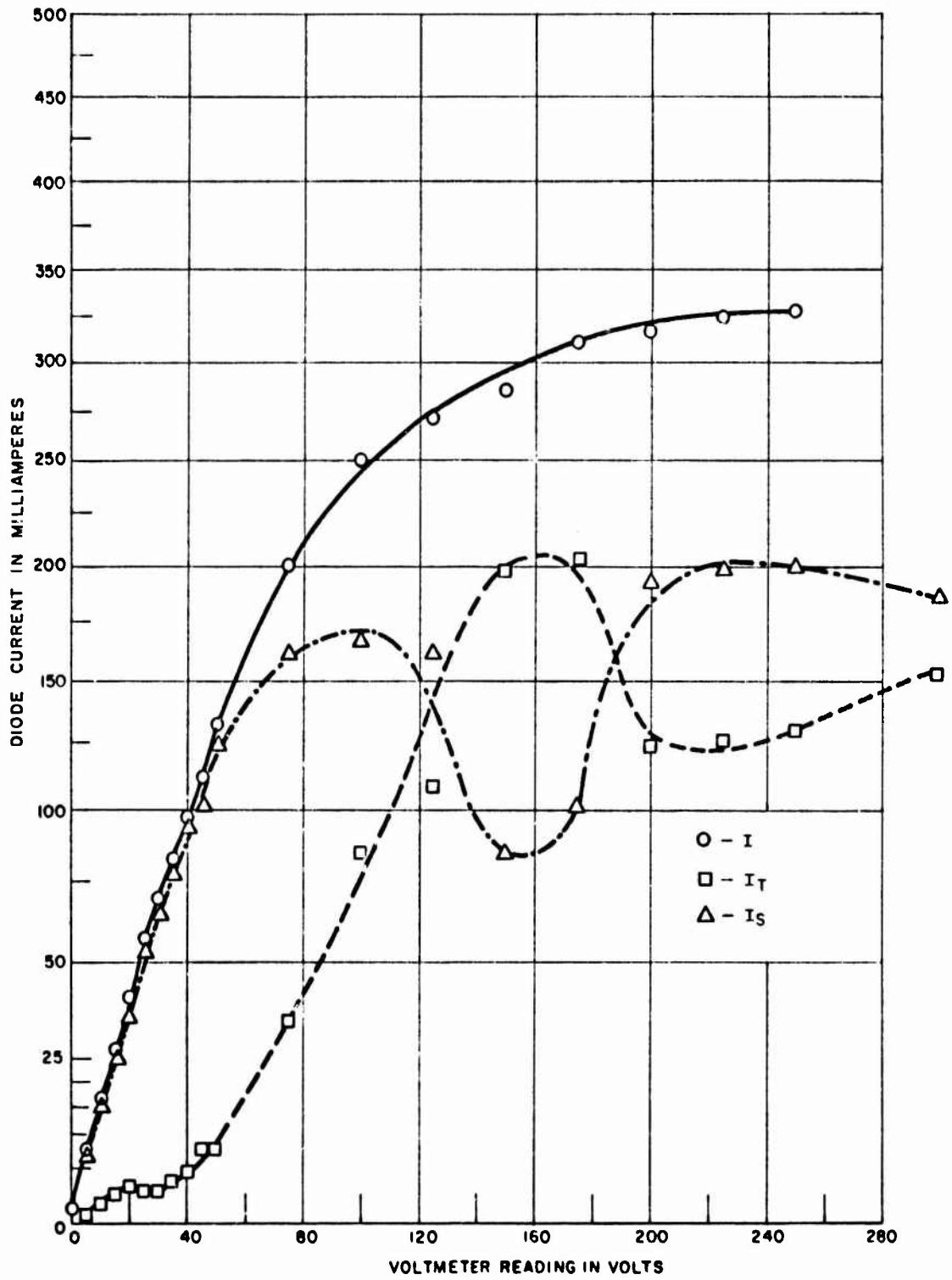


Figure 103 - Current Analysis for Tube No. 116 at 1100°C

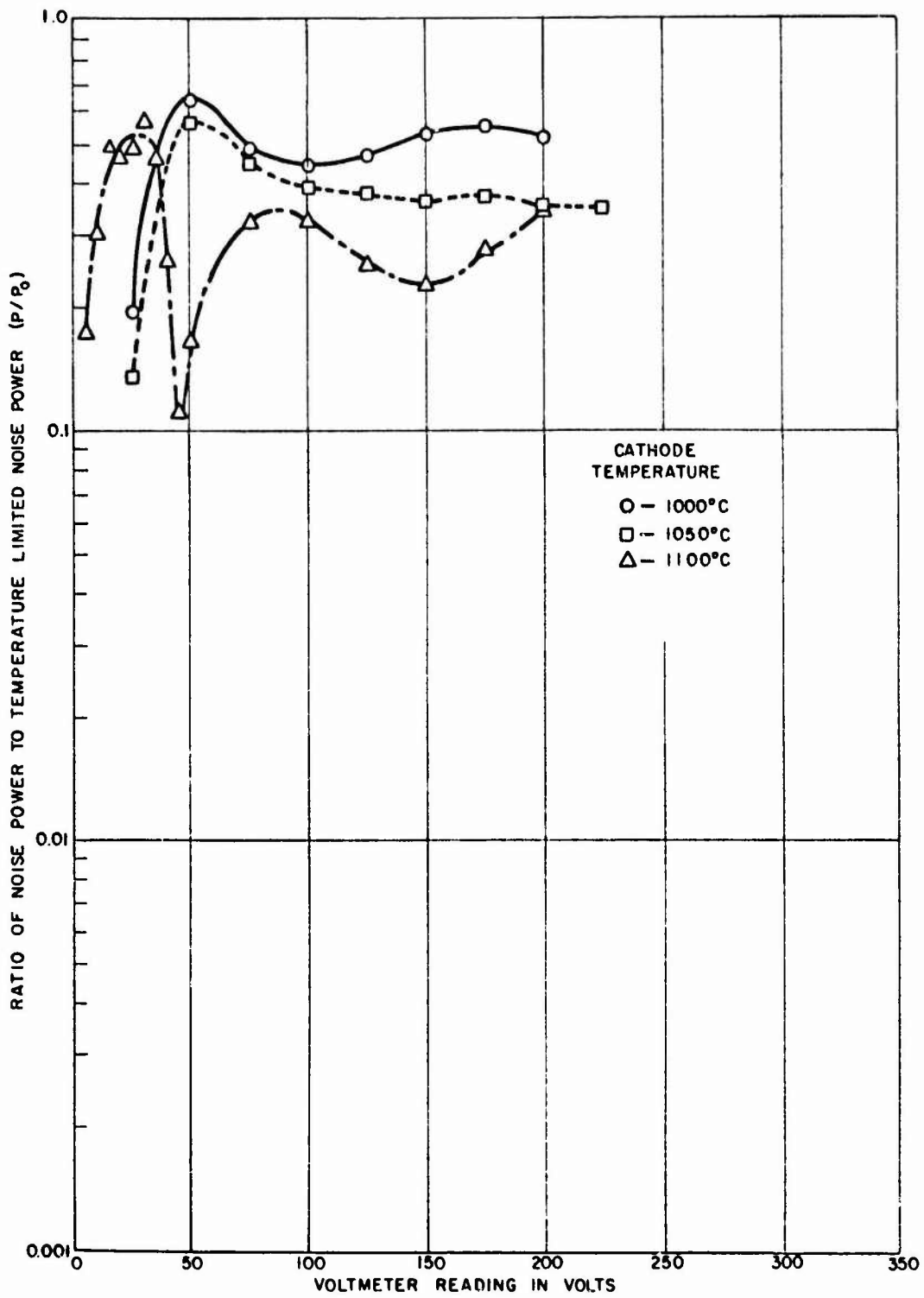


Figure 104 - Measured Noise Normalized to Temperature-Limited Value for Tube No. HCD-44

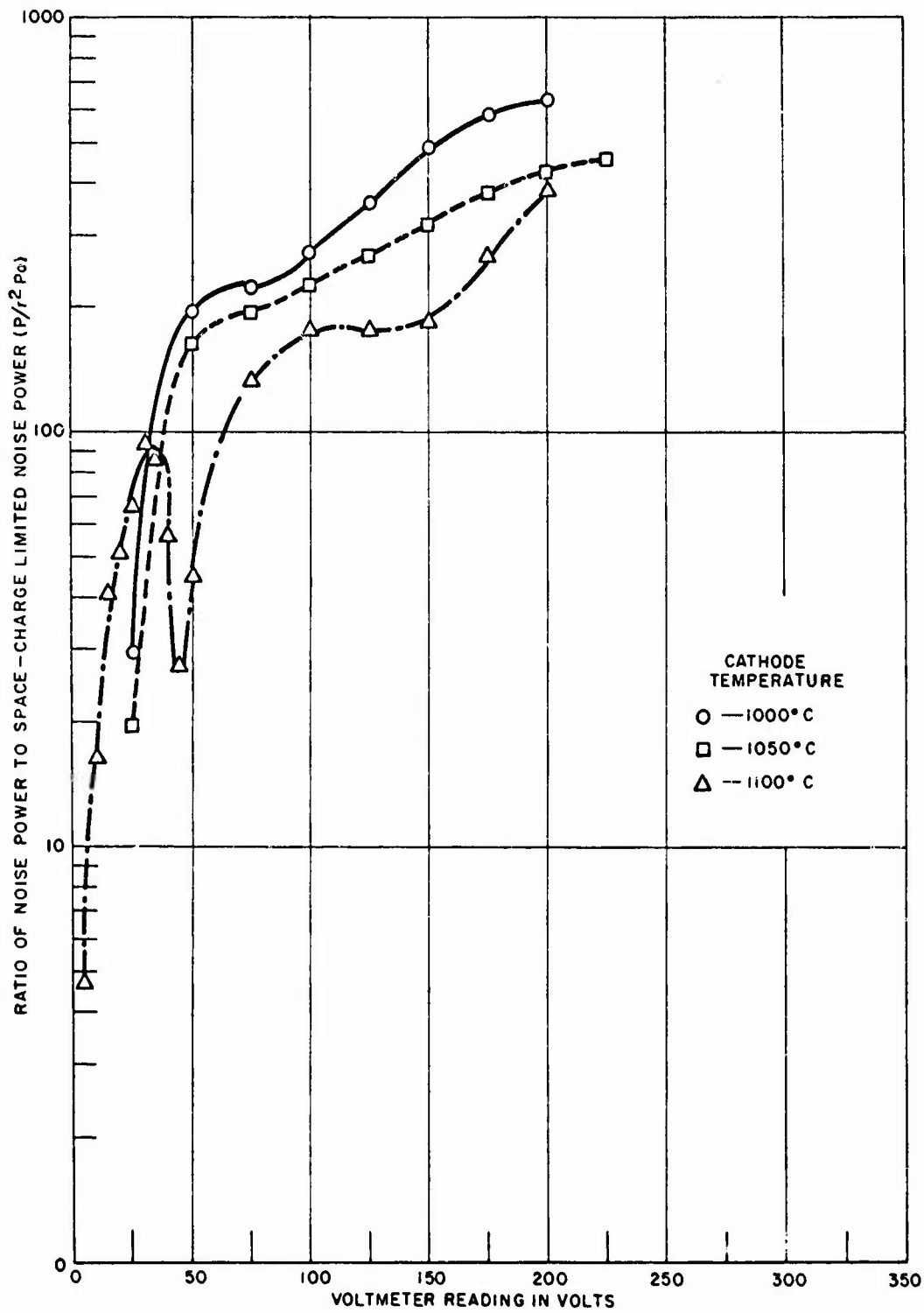


Figure 105 - Measured Noise Normalized to Space-Charge Limited Value for Tube No. HCD-44

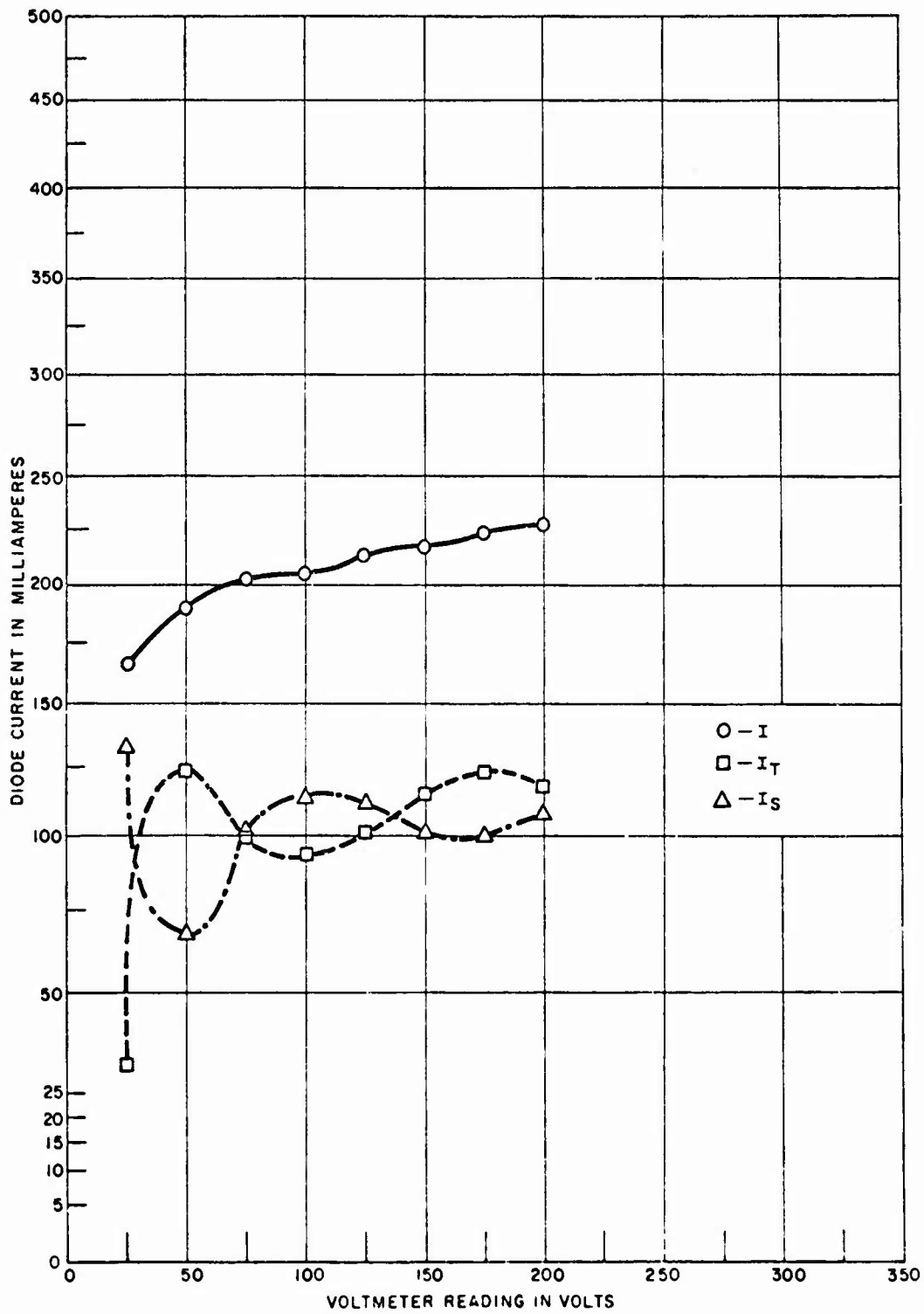


Figure 106 - Current Analysis for Tube No. HCD-44 at 1000°C

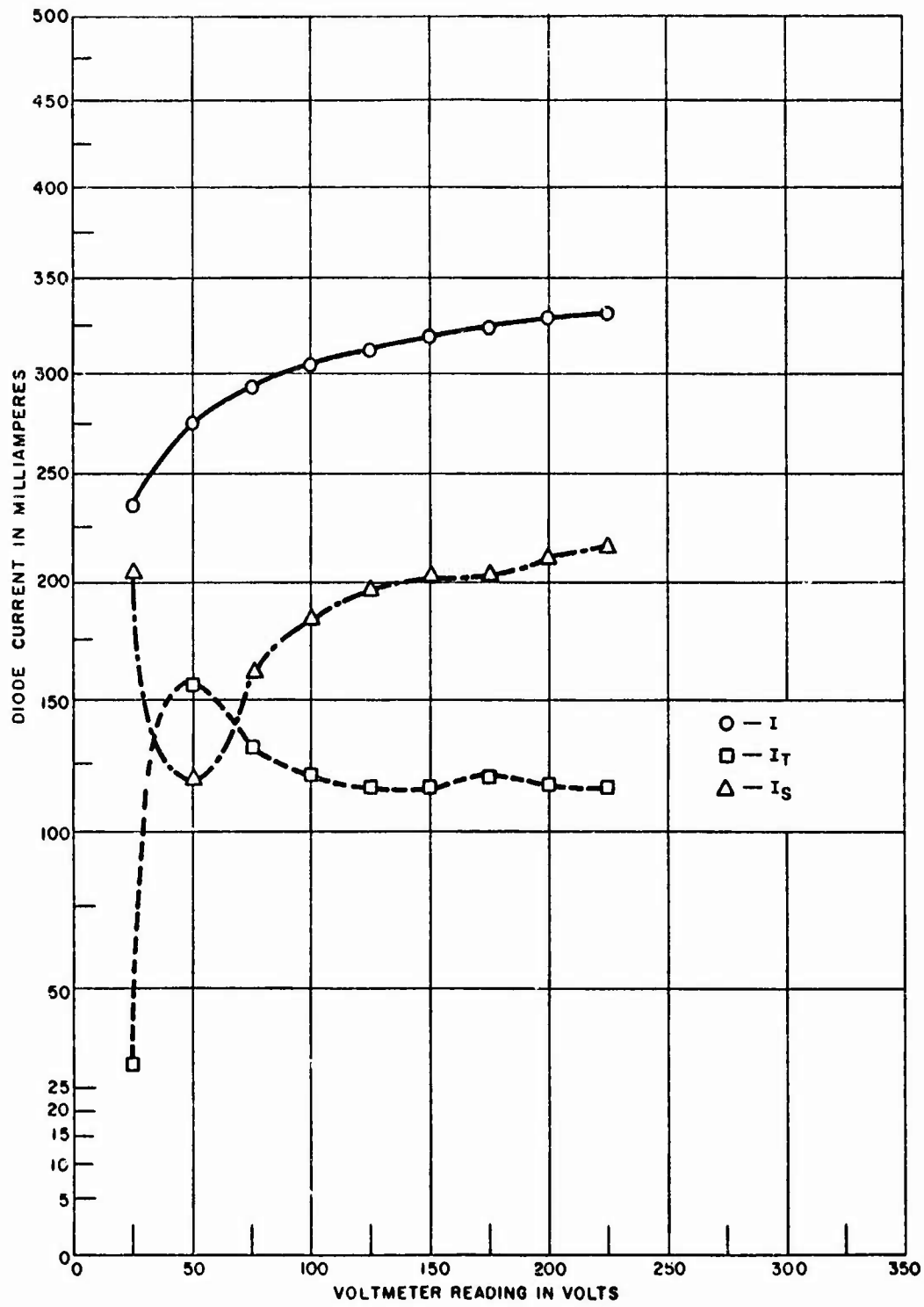


Figure 107 - Current Analysis for Tube No. HCD-44 at 1050°C

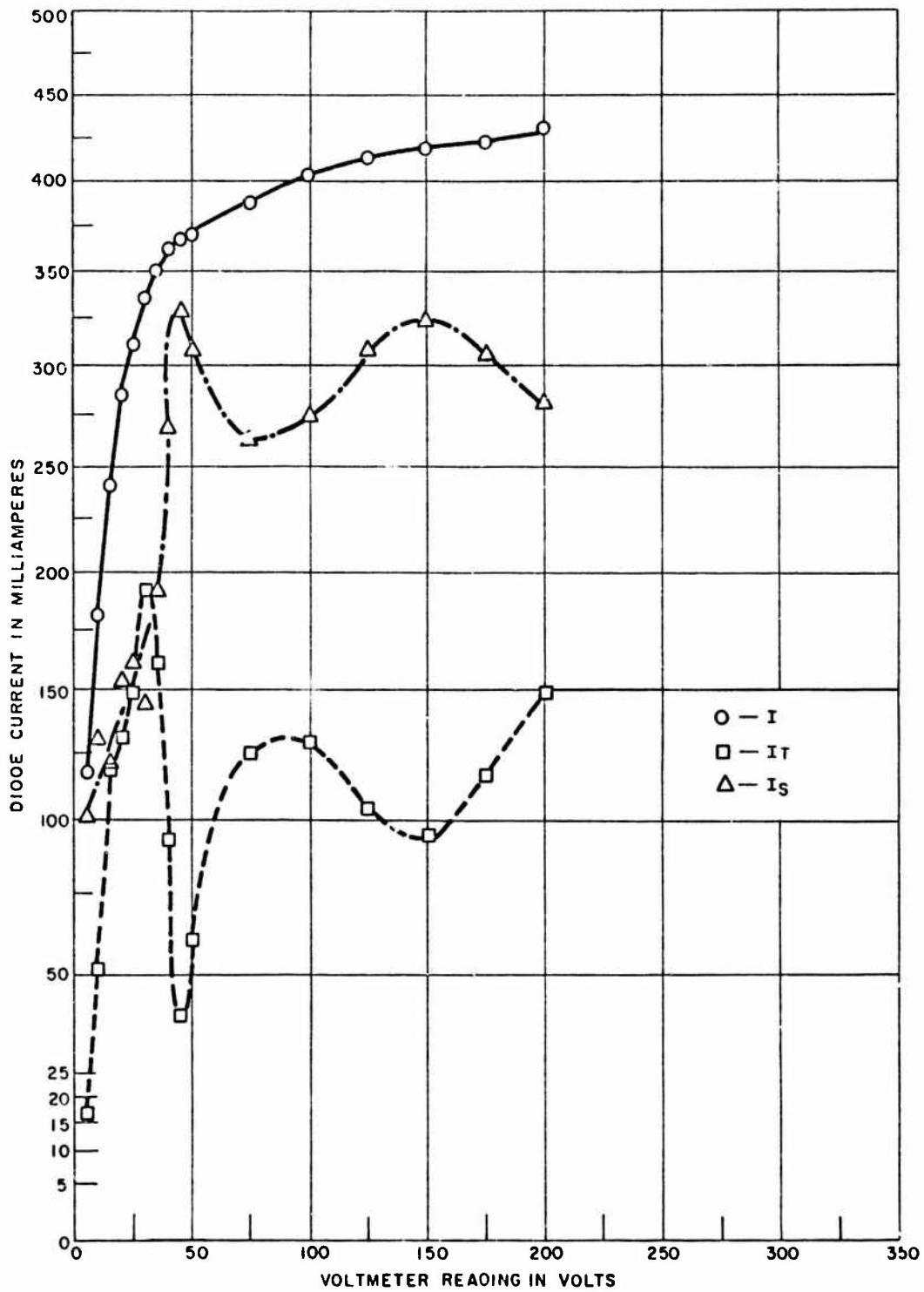


Figure 108 - Current Analysis for Tube No. HCD-44 at 1100°C

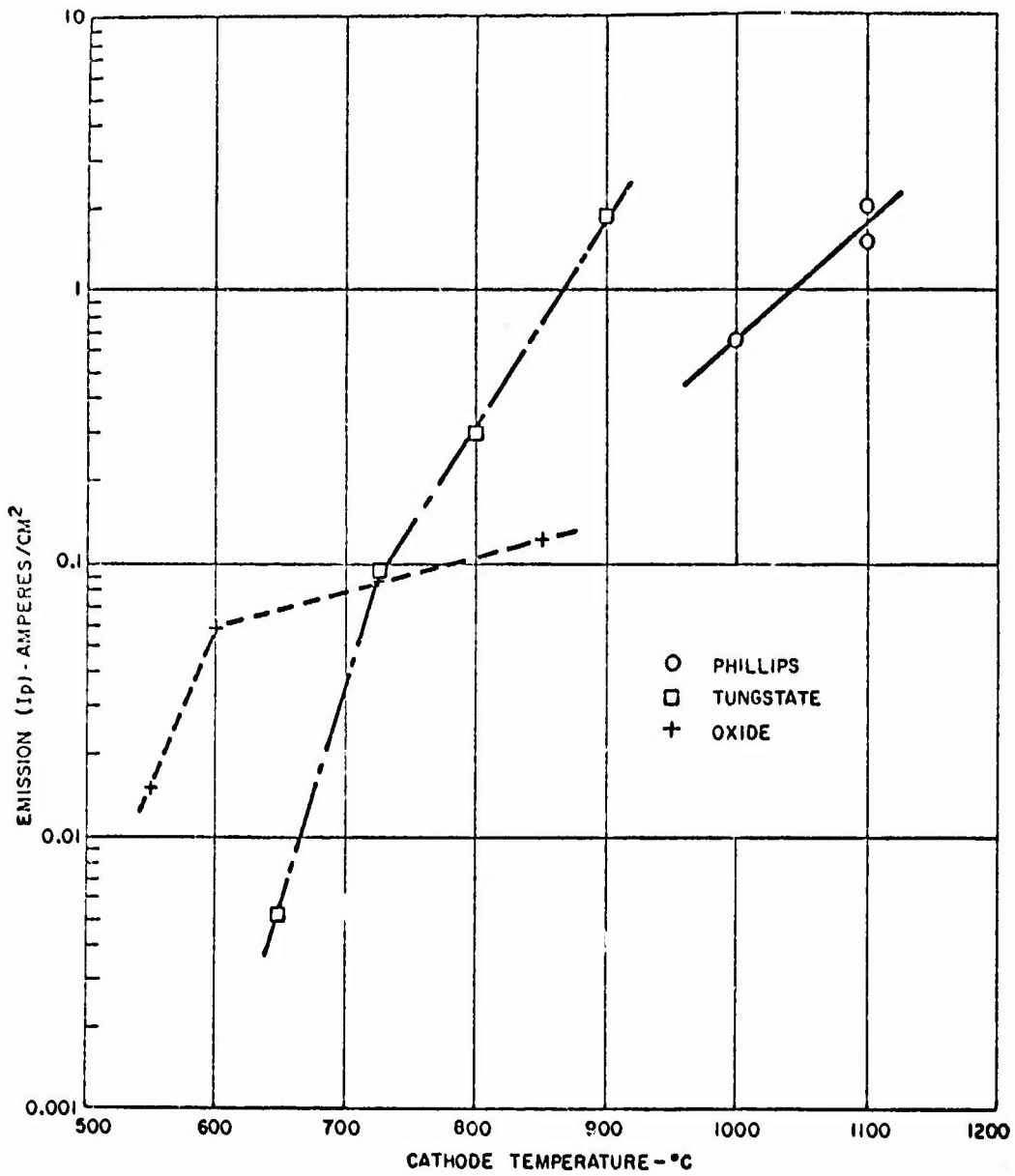


Figure 109 - Emission Properties of Various Cathodes Measured for a Constant Noise Performance

## EMISSION MICROSCOPE STUDIES

The emission microscope is another tool for examining the emissive properties of a cathode. In this instrument, an image of the distribution of current leaving the cathode is projected on a fluorescent screen. Different current densities result in variations in brightness of the phosphor on the screen, producing an optical picture corresponding to the emission variations of the cathode.

Figure 110 is a sketch of the electron gun used in this emission microscope study, and Figure 111 is a photograph of the actual assembly. The gun was designed to give a magnification of 300. The emission microscope equipment is depicted in Figure 112.

Originally, the intention was to actually measure the variations in emission by monitoring the current that passes through a hole in the plate upon which the phosphor is deposited. By sweeping the cathode image across the hole, a visual as well as a current correlation of the emission distribution could be made. To implement this, a 0.010-inch hole was made in a phosphor-coated plate, and a Faraday Cage was positioned behind the hole to collect the beam current passing through. Anticipations were that, using full magnification, a 0.010-inch diameter portion of the cathode would provide an image 3 inches in diameter on the viewing screen. Assuming a beam current of 0.003 ampere, the actual current through the hole would be the ratio of the squares of the diameters, i.e.,  $(3)^2/(0.010)^2$  or 1/90,000 of the beam current, or  $10^{-7}$  amperes, a value that can be easily read by an electrometer.

In actual practice, however, it was impossible to obtain an emission image with beam currents in the milliamperage range. Referring to the sketch of Figure 110, the cloud of negative space charge accumulating between the cathode and  $G_1$ , completely obliterated the image, and gave a uniformly bright display on the screen. The only conditions that could be found to produce sharp contrasting emission patterns were established by making  $G_1$  positive, with respect to the cathode, and then reducing the cathode temperature to the point where it was severely emission limited. Figure 113 is a photograph of emission patterns under these conditions, at three different temperatures. However, the total current to the screen was only a few microamperes. Thus, the current through the aperture became so small that stray charges and leakage currents completely obliterated any variation of currents in the  $10^{-10}$  ampere intensity beam that penetrated the screen.

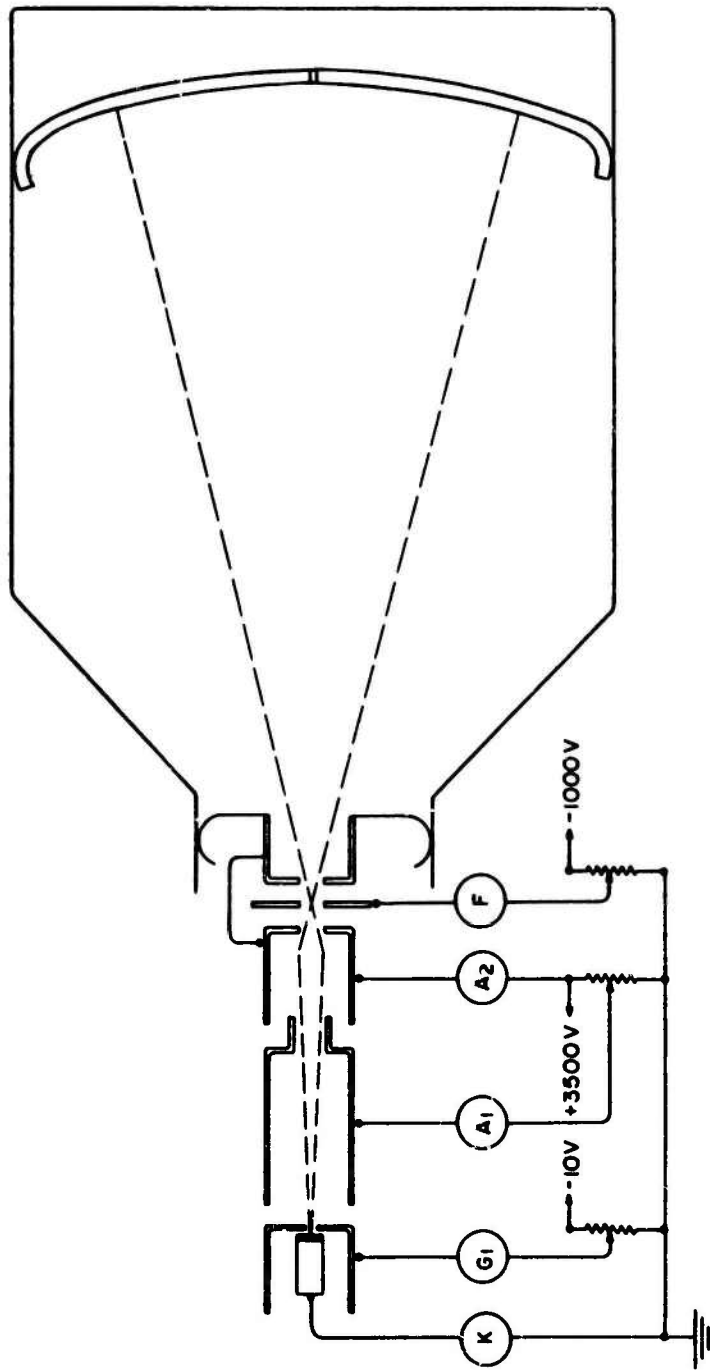


Figure 110 - Electron Gun Schematic

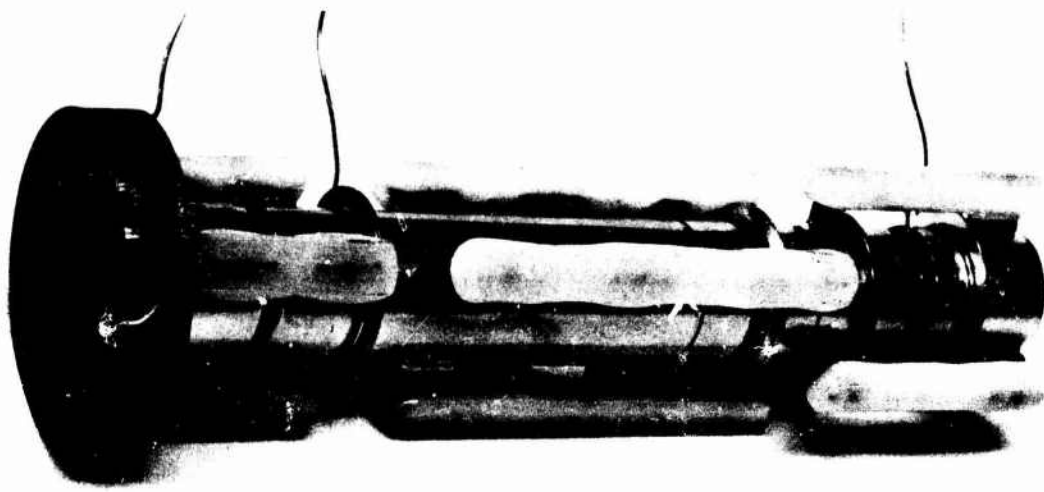


Figure 111 - Electron Gun Used in Emission Microscope Study

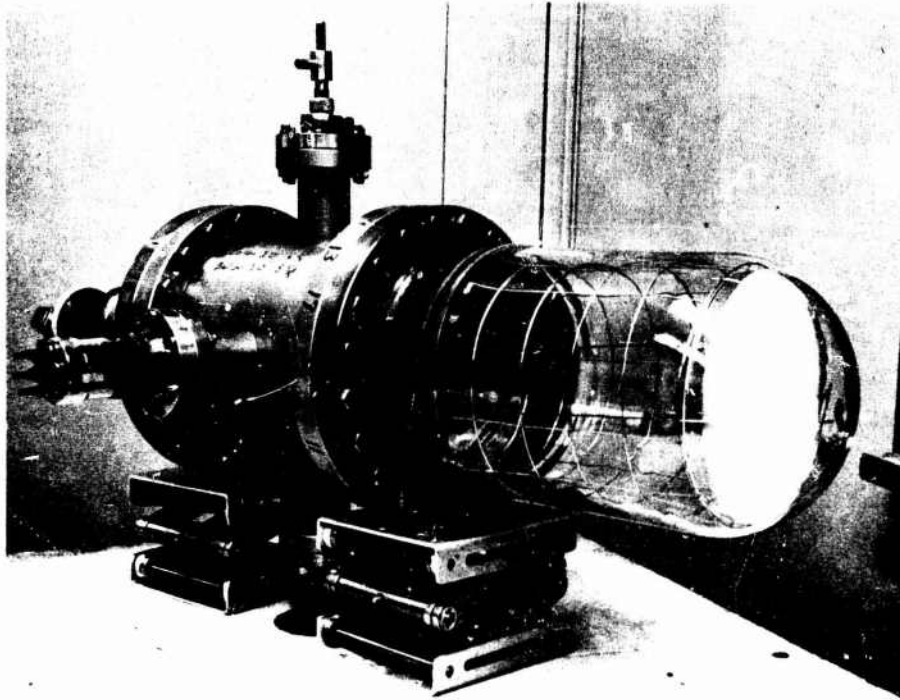


Figure 112 - Emission Microscope Assembly

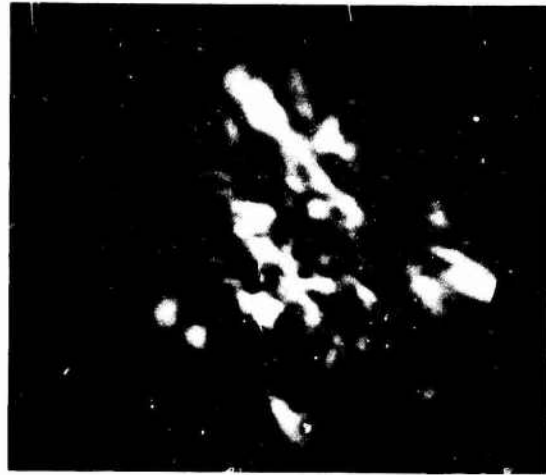


Figure 113 - Representative Emission Patterns

If the analyzing aperture in the screen were made large enough to pass measurable currents the resolution of the image would be ruined. Also, running the cathode cool and current limited will not provide the emission pattern encountered under actual operating conditions.

Figure 114 is a photomicrograph (500X) of the surface of a tungstate cathode, clearly showing the granular surface and the cleaving of the individual grains after machining. It was hoped that a correlation between the optical appearance of the emitter and the actual emission pattern, as seen on the emission microscope, could be established. The only similarity is that the emission comes from localized patches, but these patches appear to come from much larger areas than the intergranular patches shown by the optical microscope.

To overcome the limitations encountered in the emission microscope, a close-spaced diode was constructed to allow direct measurements of the emissive surface of the cathode. A 0.002-inch diameter hole was drilled in the anode, and a collector placed behind the aperture (see Figure 115). Micrometer screw adjustments permitted smooth lateral movement of the cathode parallel to, and at a controlled distance from, the anode. Typical variation in emission across a cathode diameter of 0.110-inch is shown in Figure 116.

The data for Figure 116 were transposed directly from a recorder plot of collector current versus cathode position. Test conditions were as follows:

Cathode Temperature	890 °C <sub>BRT</sub>
Main Anode Voltage	70 Volts
Main Anode Current	42 Milliamperes
Collector Voltage	80 Volts
Collector Current	5 to 11 Microamperes
Anode-Cathode Spacing	~0.005 Inch

The absence of a screen around the collector permitted some secondary electrons, released from the anode, to contribute to the collector current. This effect was small, however, at the specified collector voltage. In determining the variation in cathode work function, secondary electron effects were essentially eliminated, as work function variations were based on the difference between peaks and valleys in the emission-position plot.

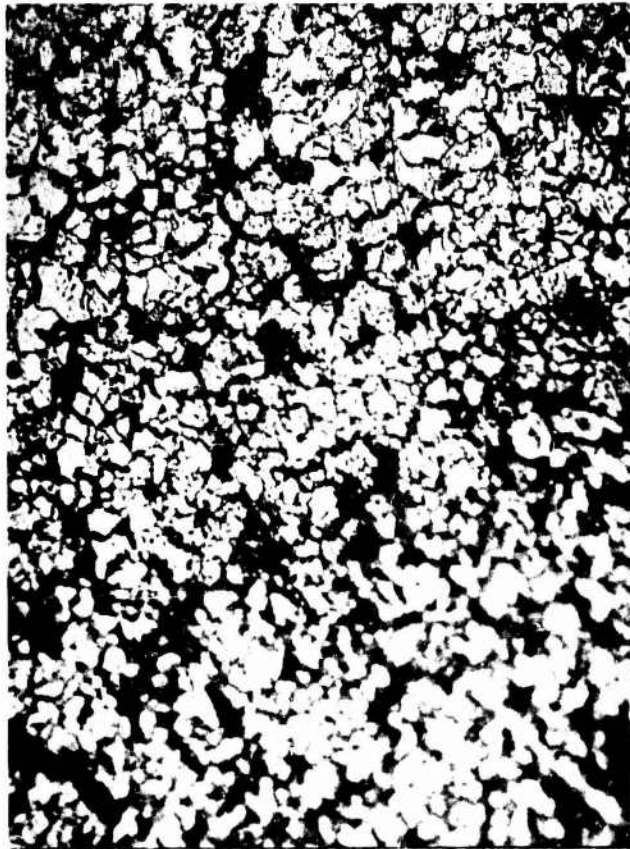


Figure 114 - Photomicrograph of Machined Tungstate Cathode

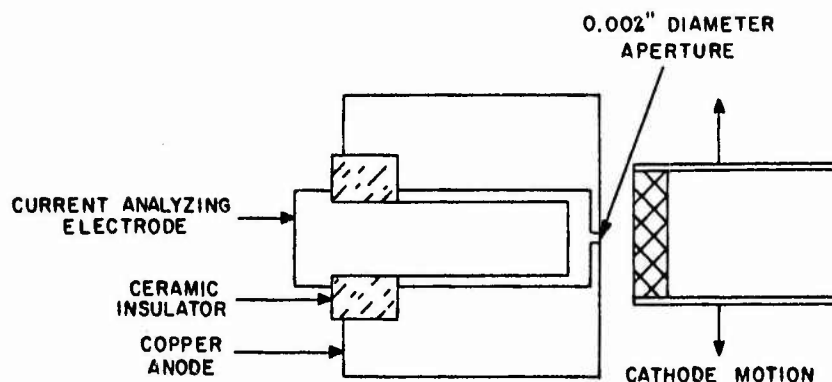


Figure 115 - Details of Diode Used for Analyzing Emissive Surface

The work functions were calculated by: (1) estimating the area of the cathode patch focused by the anode hole to be  $\sim 1/2X$  the hole area; (2) assuming no contribution to the collector current by secondary electrons; (3) assuming an effective work function for each patch, given by the Richardson equation:

$$j_s = A_o T^2 e^{-\frac{e \phi_{eff}}{kT}} \quad (11)$$

with  $\phi_{eff}$  determined from work function tables.<sup>43</sup> These calculations show a maximum change in work function of 0.07 eV across the cathode, with the minimum value of 1.95 eV found near the center of the cathode. By comparison, the effective work function calculated from the  $6.8 \times 10^{-1} \text{ A/cm}^2$  total cathode current density was 1.99 eV. The 0.07 eV variation in work function represents a doubling of emission at  $890^\circ \text{C}_{\text{BRT}}$ .

Wide variance in resolution was obtained in the three methods for examining cathode surfaces. A comparison of the optical microscope, and anode-hole emission patterns shows an apparent decline in resolving power in the techniques. The optical photomicrograph, Figure 114, clearly resolves the five-micron diameter tungsten particles known to exist in these cathodes. The emission microscope pattern in Figure 113 shows straight elongated "grains" which have widths corresponding to those expected for a

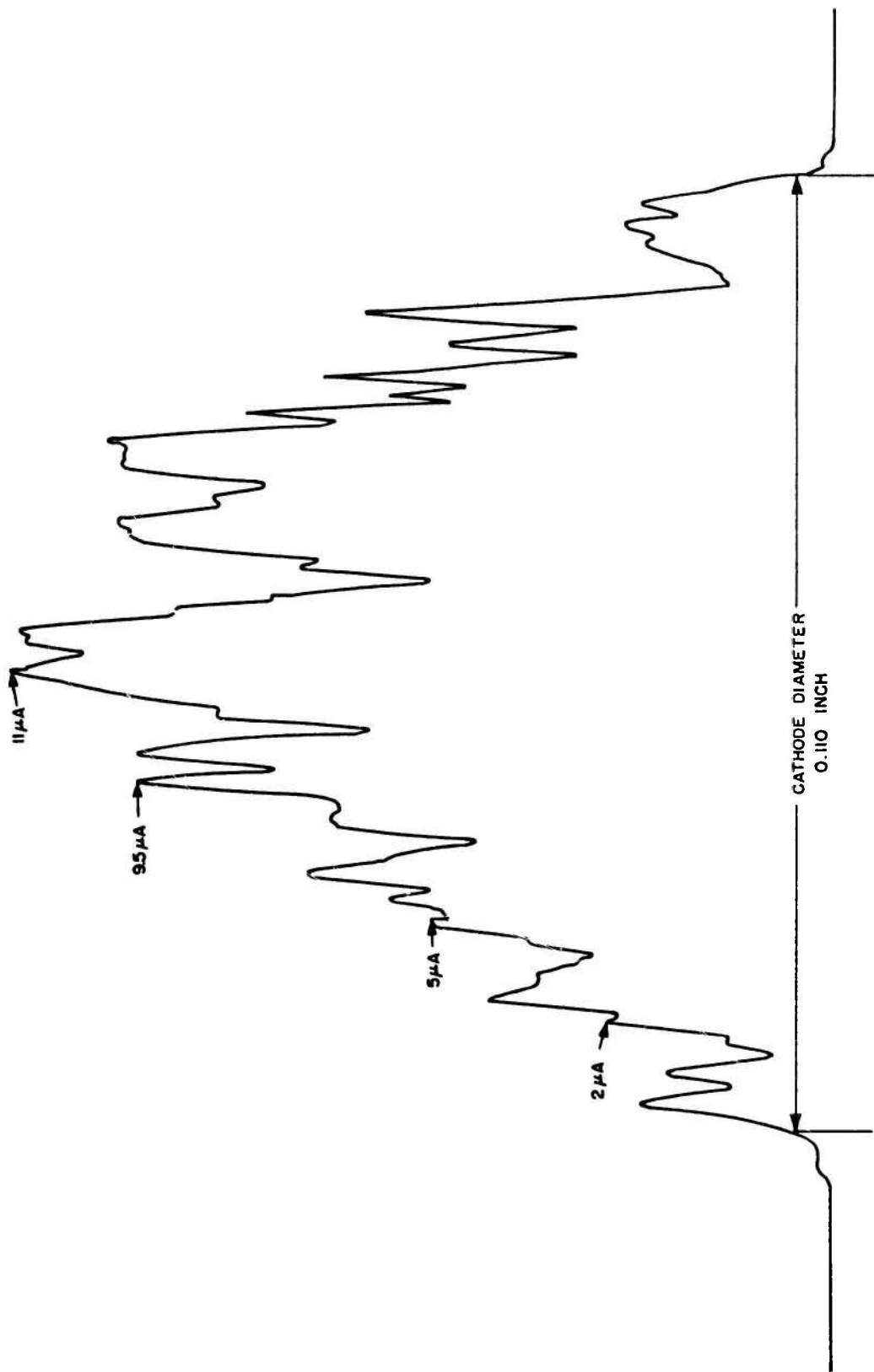


Figure 116 - Emission Profile Across a 0.110-Inch Diameter Tungstate Cathode

300X five-micron particle. The grain length, however, appears several times longer than expected. This may represent (1) lack of resolution of the emission microscope or (2) a true representation of the machining effect on the cathode emission. Several grains along a machined line would give an elongated emission spot, with the expected curvature masked by slight distortion in the emission pattern.

The resolution in the anode-hole scan is limited to approximately 75 microns. The major factor contributing to the poor resolution was the large size of the anode hole. An order of magnitude improvement in resolution should be possible with a hole diameter of approximately 0.0005 inch. Special techniques are required to provide holes as small as this, however. With increased resolution, the anode-hole scan technique provides a simple method for accurately mapping a cathode surface.

Further exploration with these techniques is definitely warranted in determining the operating mechanism of tungstate and other cathodes toward continued improvement in cathode performance.

UNRECORDED COPY - NOT FILMED

## CONCLUSIONS AND RECOMMENDATIONS

The objective of this two-year program was an experimental study of high-current density thermionic cathodes possessing long life and exhibiting reliable operation in electron tubes. The main emphasis, as outlined in Technical guidelines TT29A, and dated 19 November 1965, called for (a) the development of cathodes operating at a current density of  $50 \text{ MA/cm}^2$  for "tens of thousands" of hours at the lowest possible temperature, but with an ultimate temperature objective of  $500^\circ\text{C}$ ; (b) cathodes lasting thousands of hours at emission levels in the  $3$  to  $10 \text{ A/cm}^2$  range, and (c) cathodes lasting hundreds of hours at current densities of  $30 \text{ A/cm}^2$  and possessing reasonable sublimation rates. Another objective was a study of the critical factors and mechanisms involved in achieving reproducible high emission density cathodes.

This study has disclosed that the objectives can be achieved with a pressed tungsten matrix cathode containing barium-strontium tungstate and zirconium as the active ingredients. Objective (a) proved to be the most difficult, and it was only during the latter part of this program that sustained emission at low temperatures was reliably attained. Eight cathodes are now operating stably on life test at low temperature. Although the  $500^\circ\text{C}$  target was not attained, the  $600^\circ\text{C}$  objective has been demonstrated in life test diode HCD-51. The remaining seven cathodes are on life test at  $650^\circ\text{C}$ . Several of these -- namely, HCD-47, HCD-57, HCD-61 and HCD-66 -- all have a  $0.050 \text{ A/cm}^2$  emission capability at  $600^\circ\text{C}$ , although they are on test at  $650^\circ\text{C}$  and at higher current densities. Two cathodes, HCD-40 and HCD-47, are well beyond 10,000 hours on life test with no indication of emission deterioration. Cathodes HCD-51 and HCD-55 are beyond the 5,000 hour mark with similar stable characteristics.

From extrapolation of the data taken on life test diodes operating at higher temperatures and higher current densities, and assuming that no other failure mode is introduced or occurs, the projected failure time curve for low-temperature conditions extends beyond ten-million hours, or over 1000 years. While it is unrealistic to extrapolate cathode life with such long leverage beyond existing data, the life versus temperature curves do, nevertheless, fall within a well-behaved exponential pattern. It will take many additional years of life testing to verify the validity of the extrapolated curve. For the present, it appears to be a reasonable assumption that the tungstate cathode in its present state of development will operate for many tens of thousands of hours at a temperature of  $650^\circ\text{C}$  or lower, at current densities of  $0.050 \text{ A/cm}^2$ .

It is concluded that the addition of extra zirconium to the composition increased the initial activity of the tungstate cathodes, and made the operation at temperatures of 650°C and lower practical. However, this more active cathode composition exhibited declining emission with life when operated at high-temperature, a condition not encountered in the original cathode composition. Cathodes HCD-48 and HCD-59 are the two notable exceptions to this general observation. Additional studies and verification by life test are needed to optimize a composition for a particular operating condition.

The final eighteen cathodes, processed in sequence and placed on life test, all exhibit uniform characteristics. From this rather limited production run, it can be concluded that tungstate cathodes can be manufactured in large quantities with good reliability and reproducibility.

During the course of this two-year investigation, the importance of the surface finish has been repeatedly demonstrated. During the final days of this contract, it was discovered that certain cathodes that were difficult to machine to achieve a defect-free finish, could be machined rapidly and with excellent finish if the matrix were heated to about 200°C. The effect of this technique on emission capability and life is unknown. This phase of the development should be pursued, as it may be the key process in large-quantity production of the tungstate cathode.

While the majority of the cathodes fall within fairly close emission/temperature relationships, an occasional cathode, such as number HCD-48, exhibits superior emission capabilities. Further studies may disclose the reason for this superior performance, and allow the upgrading of the emission density capabilities by another 100 percent.

All of the cathodes studied under this program were of planar geometry. It is recommended that investigations also be undertaken to fabricate and, more specifically, to develop means of mounting and supporting tungstate cathodes having cylindrical configurations.

Emission variations across the emitting surface of the barium-strontium-tungstate matrix cathode, as disclosed by the emission microscope and by current dissecting anode techniques, verify the existence of patches of low-work-function, high emission density areas dispersed on a high-work-function background.

These areas of high emission tend to be accentuated in a path parallel to the direction of machining, thus lending additional emphasis to the interdependence of high emission and proper finishing procedures. Additional

studies appear warranted in an attempt to discover means to increase the size and number of the high emission sites, with the objective of producing cathodes having current densities still higher than those demonstrated with the present tungstate compositions.

It was a general observation that good vacuum practice was essential in producing uniformly high emission cathodes. During cathode outgassing on the vacuum system, it was desirable to maintain pressures at  $10^{-7}$  torr or better. However, once the cathode had been activated and aged, tests indicate that the tungstate cathode is no more susceptible to poisoning from residual gases than other barium type emitters.

Actual operation of tungstate cathodes in high power electron tubes has been rather limited in scope. Major applications include the General Electric ZM-6601 multiple-beam klystron. A ZM-6601 tube containing ten developmental cathodes has been operating for several years with each cathode supplying a DC current of  $1.6 \text{ A/cm}^2$ . Other tungstate cathodes have been successfully used in developmental traveling-wave klystrons<sup>48</sup> at emission levels of  $5 \text{ A/cm}^2$ . The tungstate cathodes have demonstrated their high-current capabilities in numerous sealed off beam tubes developed on Contract DA 28-043 AMC-01719(E).

## REFERENCES

1. Contract AF 33(615)-1726, "Investigation of High Emission Density Cathode"
2. Contract DA 28-043 AMC-00021(E), "High-Current-Density Cathode-Ray Tube Electron Source"
3. Fomenko, V. S., Handbook of Thermionic Properties, Plenum Press Data Division, New York, 1966
4. Koller, L. R., Phys. Rev. 25, 671, 1925
5. Becker, J. A., Phys. Rev. 34, 1323, 1929
6. Sproull, R. L., Phys. Rev. 67, 166, 1945
7. Eisenstein, A. S., Adv. in Electronics, Vol. I, 1, 1948, Academic Press, New York
8. Nergaard, L. S., RCA Rev. 13, 464, 1952
9. Rittner, E. S., Philips Res. Repts. 8, 184, 1953
10. Plumlee, R. H., RCA Rev. 17, 231, 1956
11. Okumura, K. and Hensley, E. B., J. Appl. Phys. 34, 519, 1963
12. Loosjes, R. and Vink, H. J., Philips Res. Repts, 4, 449, 1949
13. Hughes, R. C. and Coppola, P. P., Phys. Rev. 88, 364, 1952
14. Houston, J. M. and Webster, H. F., Adv. Electronics and Electron Phys., Vol. 17, 125, 1962
15. Schmidt, L. D., J. Chem. Phys. 46, 3830, 1967
16. Zalm, P. Dr., Philips Research Laboratories, paper at Conference on Tube Techniques, sponsored by the IEEE Group on Electron Devices, Sept. 17, 1968

17. Dushman, S., "Scientific Foundations of Vacuum Technique", Second Edition, Wiley & Sons
18. Contract AF 19(628)-279, "Investigation of Various Activator Refractory Substrate Combinations", Final Report AF CRL-63-49, p. 91, March 5, 1963
19. Contract AF 30(602)-2947, "Investigation of Various Activator Refractory Substrate Combinations", Final Report, RADC-TDR-64-20, December 1963
20. Jenkins, R. O. and Trodden, W. G., J. Electronics and Control, 10, 2, pp. 81-96, 1961
21. Wagoner, S., Proc. Phys. Soc. London, 67B, 369-86, 1954
22. Vaughn, J., Dudley, K. and Lesensky, L., "The Deactivation of Impregnated Type Cathodes Due to Metal Vapors", Vacuum, Vol. II, No. 2, 1961
23. Champion, J. A., Brit. J. Appl. Phys., 395, 1956
24. ASTM Standards, Part 8, Nov. 1966; F53-65T, "Tentative Recommended Practices for Measurement of Sublimations"
25. Rouse, Glenn F. Dr., National Bureau of Standards, Contract AFCRC58-31.2-268, ASTIA Document No. 211448
26. Boyd, W. T., paper, "Measurement of Cathode Sublimation with Commercial Quartz-Crystal Oscillators", presented at the 1968 IEEE Conference on Tube Techniques, New York City, Sept. 17, 1968
27. Affleck, J. H., "The Properties Required for High Current Density Cathodes" Sixth National Conference on Electron Tubes Techniques, Pergamon Press, 1963
28. Slivka, M. J., Technical Report AFML-TR-65-196, Contract AF 33(615)-1726, June 1965
29. Beck, A. H. W., "High-Current Density Thermionic Emitters: A Survey", Institution of Electrical Engineers, paper No. 2750R, November 1958

30. Beck, A. H. W., "High-Current-Density Thermionic Emitters: A Survey", Proc. Inst. of Elect. Eng., B106, 372, 1959
31. Rittner, E. S., "On the Mechanism of Operation of the Barium-Aluminate Impregnated Cathode", J. Appl. Phys., 28, 1468, 1957
32. Sparks, I. L., and Phillip, H. R., "A Retarding Potential Method for Measuring Conductivity of Oxide-Coated Cathodes", J. Appl. Phys. 24, 453-461, 1953
33. Levi, R., "Improved Impregnated Cathode", J. Appl. Phys. 2b, 639, 1955
34. Affleck, J. H., "Properties of Several Barium Dispenser Cathodes", Paper presented at the Twenty-Second Annual Conference on Physical Electronics, MIT, 1962
35. Affleck, J. H., "Investigation of Various Activator-Refractory Substrate Combinations", Air Force Contract AF 19(604)-4093, Scientific Report Nos. 14 and 15 (AFCRL-1114 and AFCRL-62-110)
36. Gibbons, M. D. and Stout, V. L., "Evaporation Rate of Oxide Cathodes by X-Ray Emission Spectrometry", Bull. Amer. Phys. Soc. No. 4, 1958
37. Fane, R. W., "A Sintered Nickel Matrix Cathode", Brit. J. Appl. Phys. 9, No. 4, 149, 1958
38. Jenkins, R. O. and Trodden, W. G., "Evaporation of Barium from Cathodes Impregnated with Barium-Calcium Aluminate", J. of Elec. and Control, 6, 149, 1959
39. Spangenberg, K. R., Vacuum Tubes, McGraw-Hill Book Co., New York, pp. 306-309, 1948
40. Spangenberg, K. R., Op. Cit., pp 304-305
41. Williams, F. C., "The Fluctuations of Space-Charge-Limited Currents in Diodes", Jr. of the Inst. of Elec. Eng., Vol. 88, Part III, No. 4, pp. 219-237, 1941
42. Spangenberg, K. R., Op. Cit., pp. 308-309
43. Read, P. L., Tables of Effective Work Function, General Electric Research Laboratories Report 64-RL-3605E, March 1964

44. Jenkins, R. O., and Trodden, W. G., J. Electronics and Control, 7, 5, 393-415, 1959
45. Vaughn, J., Dudley, K., and Lesensky, L., MIT Physical Electronics Conference, 1960
46. Popov, B. N., and Gugin, A. H., Radioteknika i elektronika, 3, 18, 66-78, 1958
47. Brous, J., et al, WADD Tech. Report 60-324, Contract AF 33(616)-6563, 1960
48. Contract DA 36-039 AMC-00007(E) "High-Power Traveling-Wave Multiple-Beam Klystron" Final Report ECOM-00007-F, October 1967

## Appendix A

### PREPARATION OF BARIUM-STRONTIUM-TUNGSTATE CATHODES

#### STARTING MATERIALS

##### Activator Compound $[\text{Ba}_5\text{Sr}(\text{WO}_6)_2]$

The stoichiometric quantities of  $\text{BaCO}_3$ ,  $\text{SrCO}_3$  and  $\text{WO}_3$  (all Reagent Grade) required to form 30 grams of the activator compound are ball milled, together with 75 cc of methanol, in an all-molybdenum mill\* for 4 hours. The resulting slurry is then filtered, using a fine Buechner funnel.

The filter cake is fired in a platinum crucible, in air, at 1400-1450°C for 2 hours. After cooling to room temperature, the product is ground in an Alundum mortar and refired as before. The refired product is then ground in an Alundum mortar and screened through a 325-mesh sieve.

##### Cathode Mix

The following materials in the given weight ratios are dry ball-milled in an all-molybdenum ball mill (see above) for 15 hours:

(1) $\text{Ba}_5\text{Sr}(\text{WO}_6)_2$ 325 mesh	2.813 g	(9.19 wt. %)
(2) $\text{ZrH}_2$ Grade C - 325 mesh	0.188 g	(0.61 wt. %)
(3) Tungsten Type UB - 5.3 Purity - 99.9% min. Avg. Particle Dia. - 5 microns	27.6 g	(90.2 wt. %)

---

\*1. Mill - molybdenum cup, 2-3/4 inch dia. x 2-3/4 inch deep with molybdenum cover plate

2. Grinding Media - 50 molybdenum pieces, 1/4 inch dia. x 1/4 inch long

## COMPACTION

95 tons per square inch

## SINTERING

1500°C<sub>B</sub> for 5 minutes in pure dry hydrogen, followed by 1840°C<sub>B</sub> for 5 minutes.

## FINISHING

Machine (face) emitting surface, using tungsten carbide cutting tool.

## STORAGE

Short-time storage (several days) in desiccator. Long-time storage in evacuated glass containers.

## BAKE-OUT

The exhaust tubing is attached to the vacuum manifold by means of a Compression Port, (Varian No. 954-5052, or equivalent) and the tube is baked at a temperature of 400 to 450°C for 2 hours, with an ultimate vacuum of  $2 \times 10^{-8}$  torr or better. The cathode is heated to 1200°C for 10 minutes, and the tube is pinched-off from the system. The rate of increase of cathode temperature is determined by gas pressure, which is limited to a maximum of  $2 \times 10^{-7}$  torr.

## ACTIVATION AFTER BAKE-OUT

1. Cathode temperature is adjusted to 1050°C, and sufficient anode potential is applied to yield 1 to 2 A/cm<sup>2</sup> emission from the cathode for a period of 16 hours.

2. After 16 hours of aging, the emission capability is determined by maintaining cathode temperature constant at 950°C, and increasing  $E_p$  in steps, recording  $E_p$  and  $I_p$  at each step, and continuing until saturation is indicated from a plot of the data on a 2/3 power emission graph paper. This is termed the "Initial Emission Characteristic". The tubes are then ready for life test.



**ERNEST F. FULLAM**  
**INCORPORATED**  
*Scientific Consultants*  
P.O. BOX 444 • SCHENECTADY, N. Y. 12301

Appendix B

**SURFACE CHARACTERIZATION  
OF TUNGSTEN CATHODES**

for

**General Electric Company**  
**Schenectady, New York**

**June 20, 1968**



ERNEST F. FULLAM  
INCORPORATED  
*Scientific Consultants*  
P. O. BOX 444 • SCHENECTADY, N. Y. 12301

For: General Electric Company  
Schenectady, New York  
June 20, 1968  
Page One

SURFACE CHARACTERIZATION  
OF TUNGSTEN CATHODES

The surfaces of two tungsten cathodes, BTA-104 and BTA-45 HCD-25 have been characterized as part of a program to define those features that enhance thermo emission. The characterization included both electron microscopy and scanning electron microscopy to observe the surface features. Electron diffraction analysis to identify materials on the surface and electron microprobe analysis to identify the elements and distribution of the elements at the surface. Cathode BTA-104 had not been activated but had been machined while the second cathode, BTA-45 had been run on a life test for 8,500 hours at 950°C.

The purpose of this analysis was to determine the differences between the two cathode surfaces. In addition, comparisons would be made between these cathodes and the ones described in our previous report of January 29, 1968. In this manner surfaces of cathodes representing three different levels of activation (none, activated, and after life test) will be discussed.



General Electric Company  
Schenectady, New York  
June 20, 1968  
Page Two

The test samples were encapsulated in evacuated glass tubes and remained in these tubes until analyzed. Each cathode was removed from the glass tube and as soon as practical examined by reflection electron diffraction. The purpose for this was to minimize the exposure to the atmosphere so that if there were any crazing it would be kept to a minimum. These particular samples did not show any evidence of crazing as was noted in the previous work. Subsequent to the electron diffraction analysis each sample was examined with the electron microprobe and then replicated for electron microscopy. They were also examined in the scanning electron microscope.

The scanning electron micrographs on sample BTA-104 are shown in Figures 1 and 2. These show typical machined surfaces at 3 different magnifications. Figures 3 and 4 are scanning electron micrographs of sample BTA-45 which show recrystallization and voids. The scanning images show an overall view of the surfaces of each of the cathodes.

Electron micrographs of replicas from BTA-104 are shown in Figures 5 through 8. These micrographs show relatively clean surfaces. The dark ragged material is the replicating material pulled from the crevices, and are shown more clearly in



General Electric Company  
Schenectady, New York  
June 20, 1968  
Page Three

stereomicrographs. (Figure 13). In the previous report surfaces of the activated samples had a film or a dispersion of small particles spread over the surfaces; whereas the unactivated cathode surface is clean and almost free of particulate material suggesting the film forms after activation of the cathode.

Electron micrographs of replicas from sample BTA-45 are shown in Figures 9 through 12. These micrographs show grains and dark particles on the surface of the tungsten. The surfaces also show the recrystallization growth of tungsten particles. The black particles are material which have been lifted from the surface of the cathode by the replicating plastic. The small round bubbly structure is a replica of the same material. The dark ragged material is the plastic which has gone into the crevices and has been pulled out. This can be seen more clearly in the stereomicrographs shown in Figure 14. A group of particles from a grain boundary of this specimen are shown in Figure 15. This material has been identified as  $ZrO_2$  by selected area diffraction.

Electron diffraction analysis was used to identify the crystalline material on the surfaces of the samples. Two methods of electron diffraction analysis were used; reflection diffraction whereby the actual samples are examined with a beam about one millimeter in



General Electric Company  
Schenectady, New York  
June 20, 1968  
Page Four

diameter (the beam being much larger than the structural features) and selected area diffraction whereby the replica of the sample is examined by a beam several microns in diameter; the beam being in the same size range as the microstructural features. Reflection diffraction is sensitive to only the material within the first few hundred angstroms of the surface.

X-ray diffraction which penetrates further than electron diffraction was employed to identify the subsurface material.

The reflection electron diffraction pattern from sample BTA-104 indicated strong tungsten lines with additional weak lines whose best fit was for  $\text{SrWO}_4$ ;  $\text{Ba}_5\text{Sr}(\text{WO}_6)_2$ ;  $\text{SrZrO}_3$  etc. type of material. X-ray diffraction, with its greater depth of penetration, produced patterns from a similar sample which also showed strong tungsten as well as additional weak lines fitting  $\text{SrWO}_4$ ;  $\text{Ba}_5\text{Sr}(\text{WO}_6)_2$  and  $\text{ZrW}_2\text{O}_8$  structure. Several other possible combinations were studied. Since the lines in the electron diffraction pattern differ from the weak lines in the X-ray pattern there may very well be two different end products that are being observed at different levels from the surface. In order to pin this down an additional sample was



General Electric Company  
Schenectady, New York  
June 20, 1968  
Page Five

obtained from Mr. Bondley, one pink powder  $Ba_5Sr(WO_6)_2$  as well as a black powder  $Ba_5Sr(WO_6)_2$  mixed with tungsten. The pattern from sample BTA-104 by both X-ray and electron diffraction had weak lines and although these lines could be identified as  $Ba_5Sr(WO_6)_2$  they could also be matched with other compounds therefore the conclusions are that some change has occurred in the initial firing or compacting of the cathodes.

Sample BTA-45 showed barium zirconate  $BaZrO_3$  by electron diffraction. This was also found on the previous samples which had been activated, therefore it appears that once the sample is activated,  $BaZrO_3$  is formed on the surface.

Electron microprobe analysis, is a technique used to determine the elements present on the surface and the distribution of these elements. Traverses of the surface were made for the elements barium, strontium and zirconium. The charts representing the distribution of these elements for sample BTA-104 are shown in Figure 16. There one can observe strong evidence of barium and zirconium. Small amounts of strontium are also distributed across the surface. The peaks probably represent the crevices or boundaries where the material is originally located



General Electric Company  
Schenectady, New York  
June 20, 1968  
Page Six

during the sintering process. The charts in Figure 17 represent traverses for the barium, strontium and zirconium across sample BTA-45. It will be noted that the barium content tends to be less than that in BTA-104 and the strontium scan shows essentially only background radiation. There is still a considerable amount of zirconium present in BTA-45 as compared to BTA-104. There is a change in scale factor which must be taken into consideration on sample BTA-104; the full scale value is a hundred counts per second whereas on BTA-45 the full scale value is two hundred counts per second. This shows the barium and strontium are greatly reduced after the sample has undergone a life test. The zirconium content tends to be unchanged in comparing the two concentrations under study. No quantitative work has been done in this phase of the study.

In summary, the cathode BTA-104 surfaces appeared to be relatively clean as well as being a typical machine surface as displayed by the scanning electron micrographs. A change in the structure is indicated by the diffraction studies of the original material, although precisely to what extent is not clearly defined. Further study would require additional work authorization. The electron microprobe



ERNEST F. FULLAM  
INCORPORATED  
*Scientific Consultants*  
P. O. BOX 444 • SCHENECTADY, N. Y. 12301

General Electric Company  
Schenectady, New York  
June 20, 1968  
Page Seven

showed the presence of barium, strontium and zirconium on the surface primarily located at the grain boundaries in the sintering operation. The characterization of the previous cathodes as described in our report January 29, 1968 showed a particulate material on the surface almost as a film. There was also a strong indication of  $\text{BaZrO}_3$  and no evidence of strontium. These cathodes had been just activated, that is with low emission time.

Cathode BTA-45 has small round particles spread over the surface of the cathode. Reflection electron diffraction showed evidence of  $\text{BaZrO}_3$ , the same as the previous cathodes. In addition, the particles from grain boundaries consisted of  $\text{ZrO}_2$  and this is consistent with the data shown by the electron probe in that there is a depletion of barium, and an absence of strontium, and little change in the zirconium content, in the comparison of the machine surface and a surface that has undergone life test.

ERNEST F. FULLAM, INC.

  
Selby E. Summers

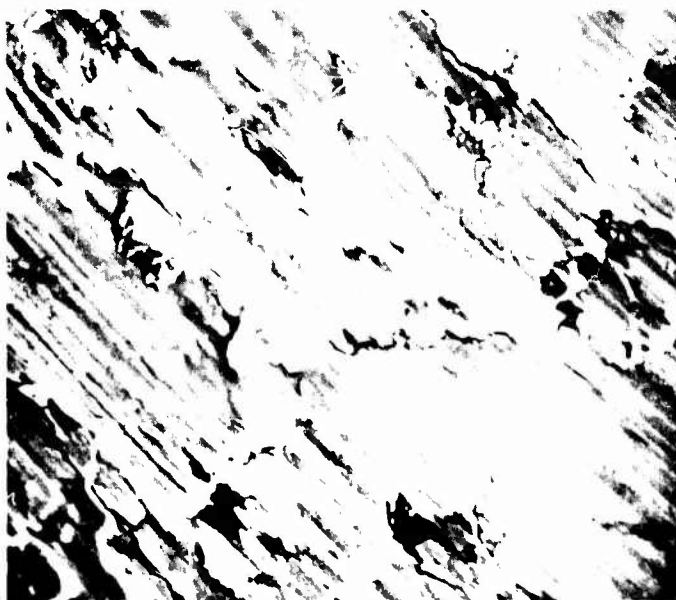
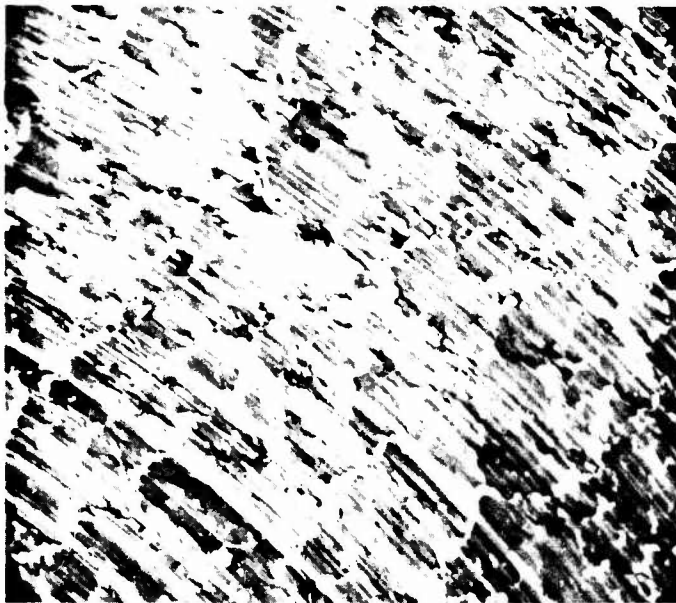


Figure 1. Scanning electron micrographs of the surface of sample BFA-104.

Top - Plate 41768-4

200X.

Bottom - Plate 41768-3

650X.





Figure 2. Scanning electron micrographs of the surface of sample BTA-104

Plate 41768-2

2,000X.



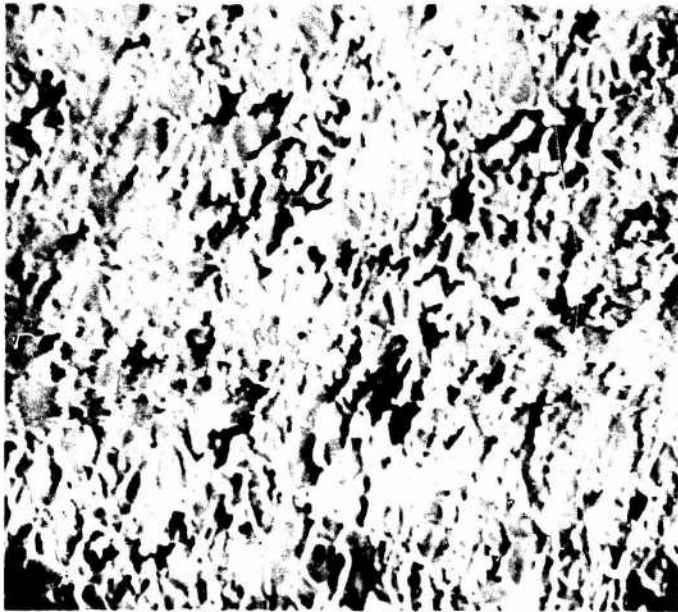


Figure 3. Scanning electron micrographs of the surface of sample BTA-45 HCD-25.

Top - Plate 41768-8

200X.

Bottom - Plate 41768-7

650X.

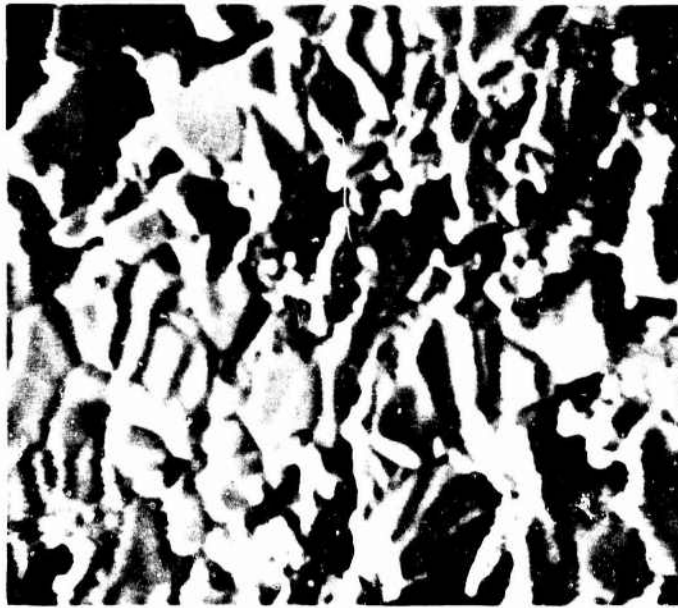


Figure 4. Scanning electron micrographs of the surface of sample BTA-45 HCD-25.

Plate 41768-6

2,000X.



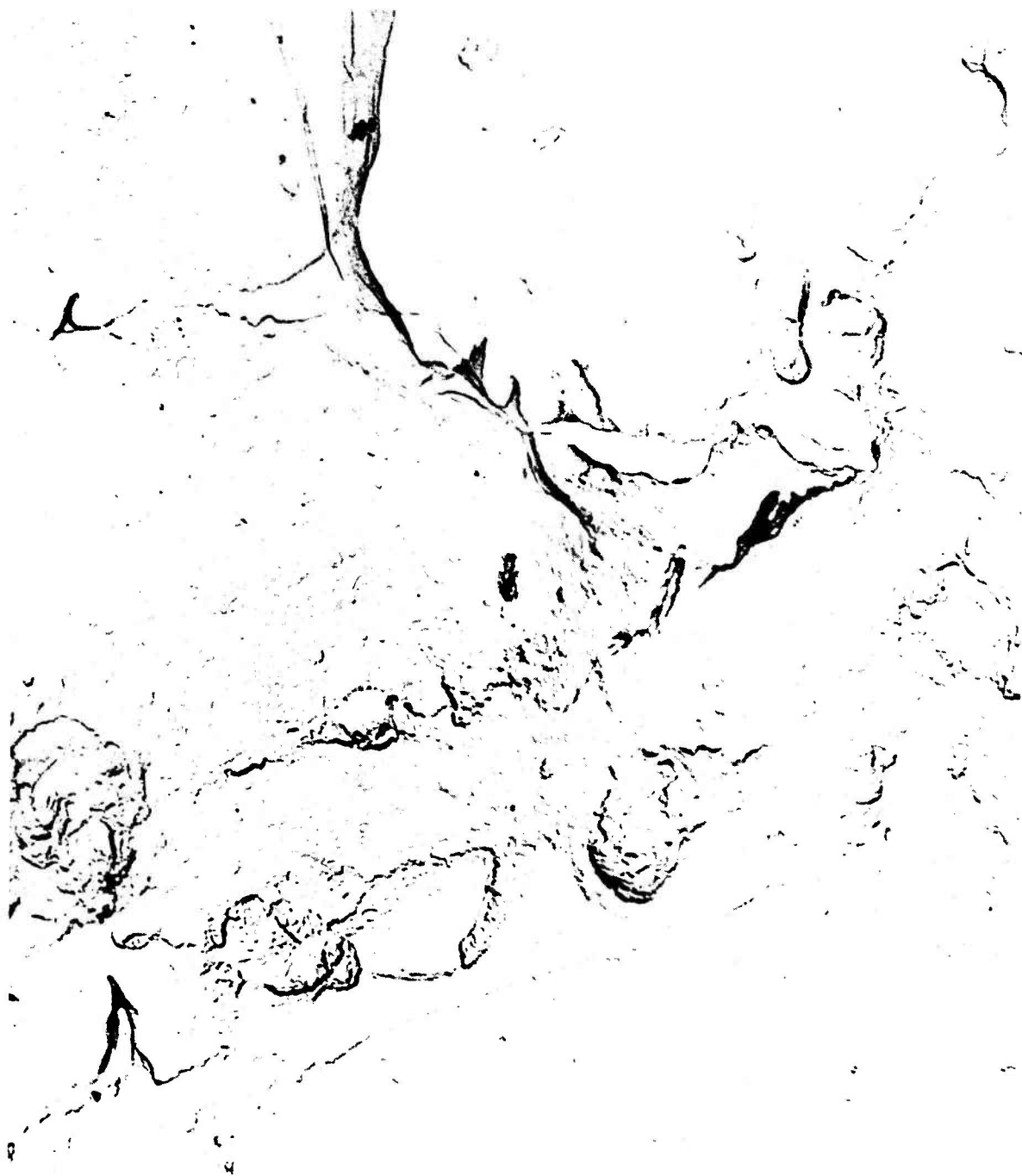


Plate # 5543-3

10,000X.

Figure 5. Electron micrograph of replicated surface of sample BTA-104.



Plate # 5542-3

10,000X.

Figure 6. Electron micrograph of replicated surface of sample BTA-104.



Plate # 0649-1

10,000X.

Figure 7. Electron micrograph of replicated surface of sample BTA-104.



Plate # 0649-3

10,000X.

Figure 8. Electron micrograph of replicated surface of sample BTA-104.



Plate # 5546-1

10,000X.

Figure 9. Electron micrograph of replicated surface of sample BTA-15 HCD-25.



Plate # 5546-3

10,000X.

Figure 10. Electron micrograph of replicated surface of sample BTA-45 HCD-25.

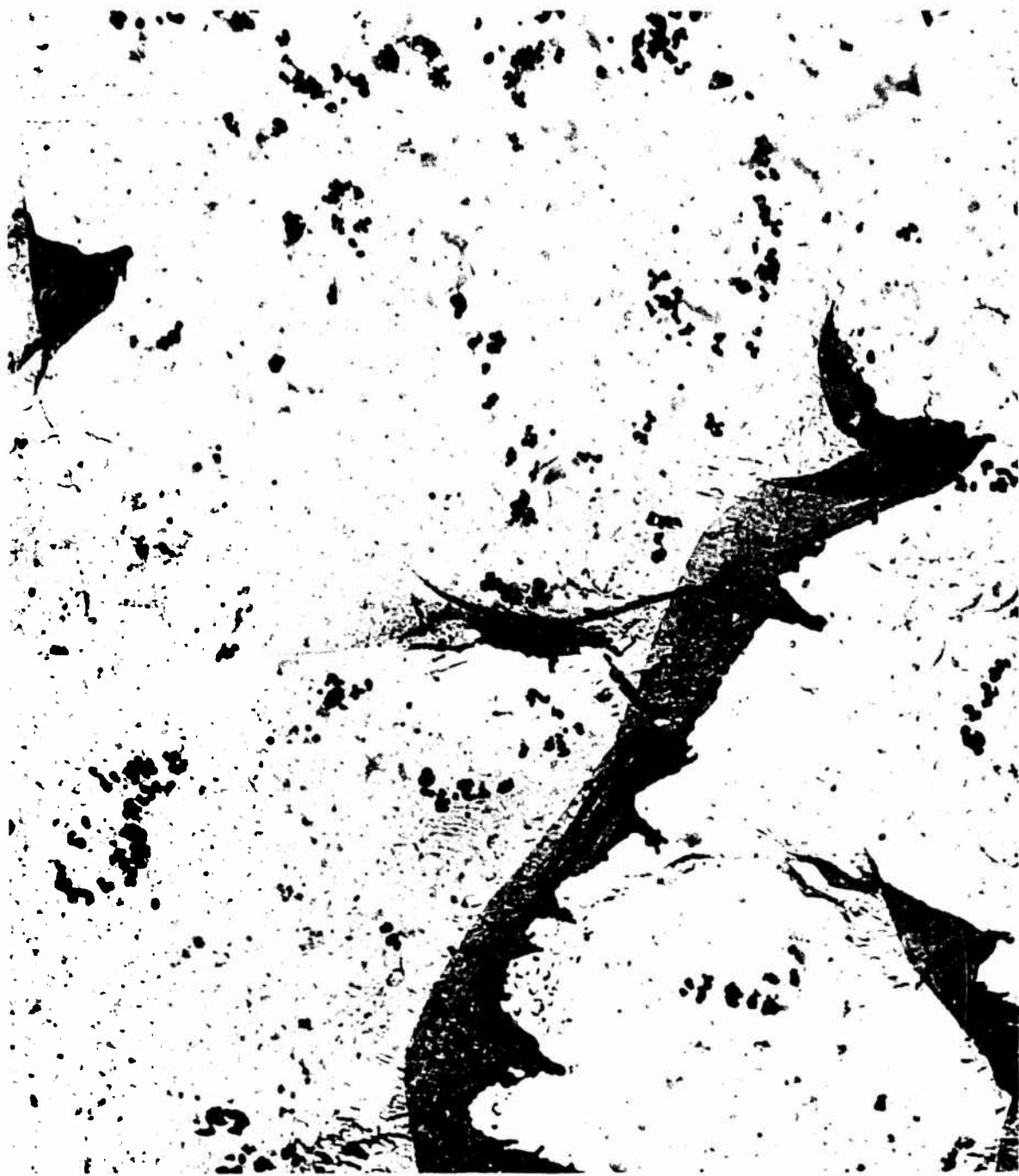


Plate # 5545-1

10,000X.

Figure 11. Electron micrograph of replicated surface  
of sample BTA-45 HCD-25.



Plate # 5544-2

10,000X.

Figure 12. Electron micrograph of replicated surface  
of sample BTA-15 HCD-25.

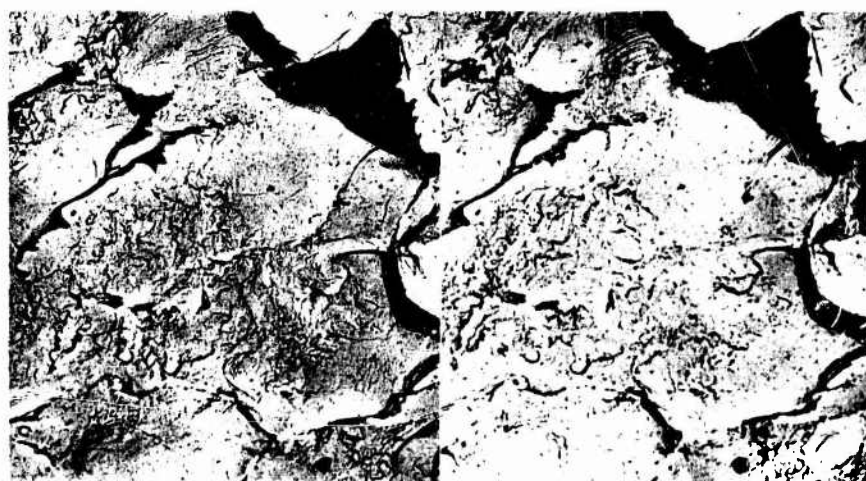
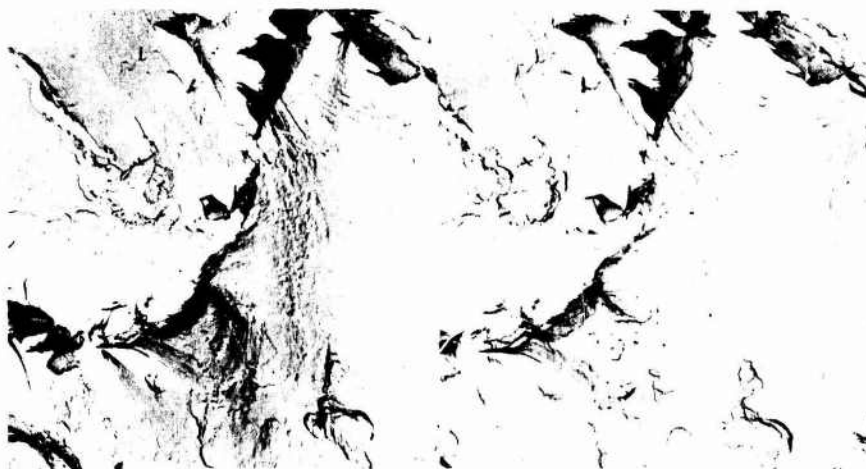


Figure 13. Stereographic electron micrographs of replicated surfaces of sample BTA-104.

Top - Plate 5543 1&2                      3,600X.  
Bottom - Plate 5542 4&5                    3,600X.



Figure 14. Stereographic electron micrographs of replicated surfaces of sample BTA-45 HCD-25.

Top - Plate 5545 3&4 3,600X.

Bottom - Plate 5544 3&4 3,600X.

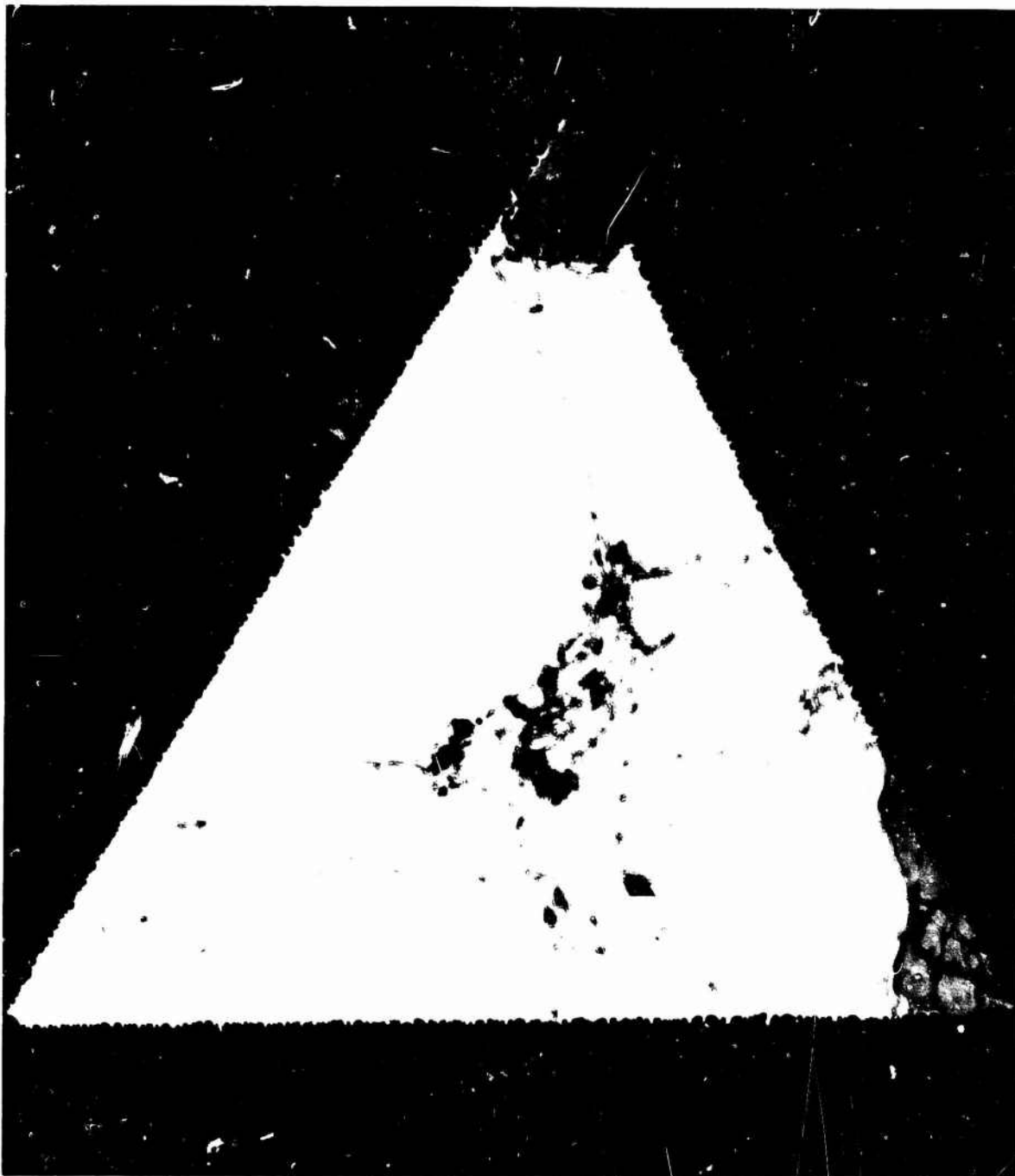


Figure 15. Electron micrograph of an area with particles on sample BTA-45 HCD-25 analyzed by selected area diffraction.

Plate 0652

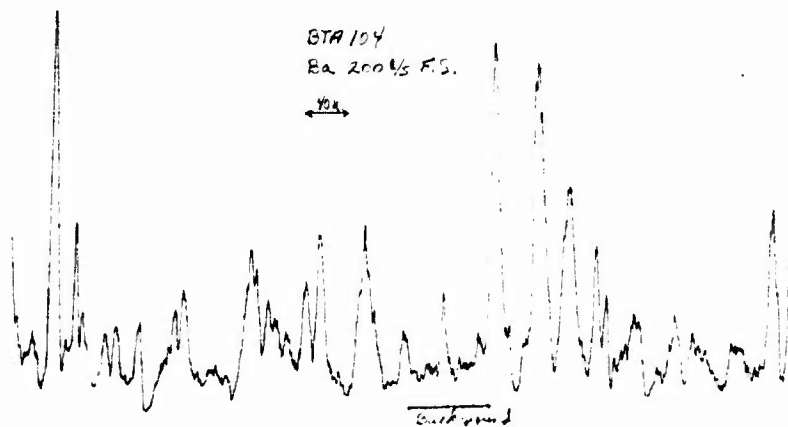
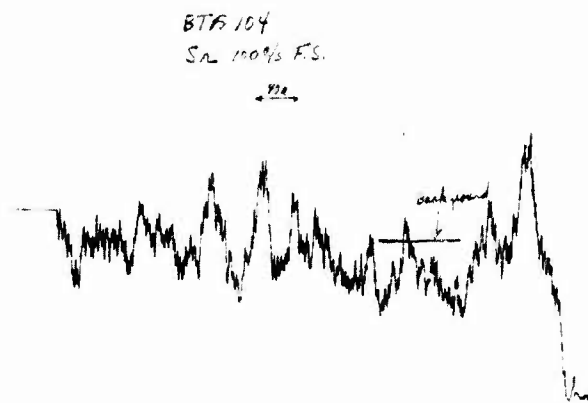
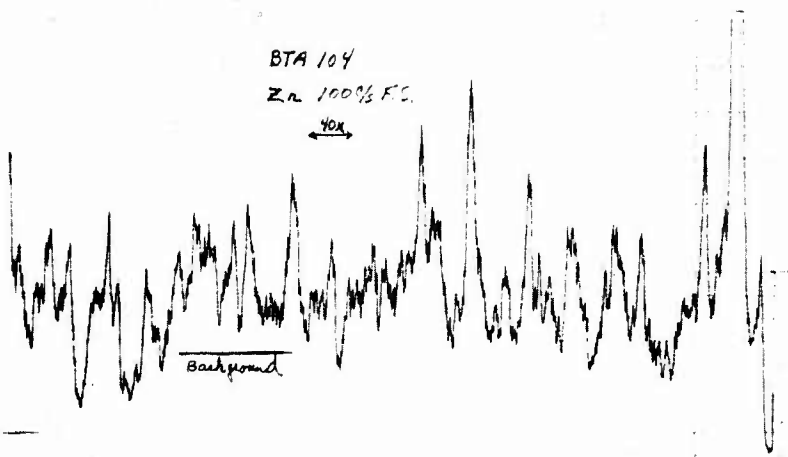
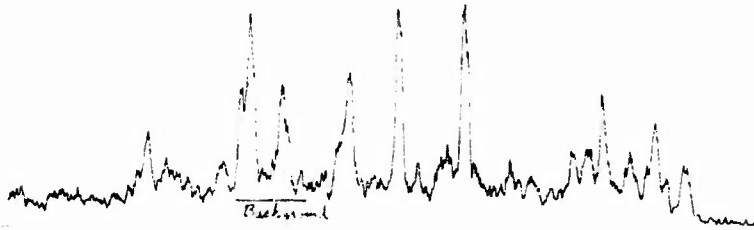


Figure 16. Electron microprobe traverses on sample BTA-104.

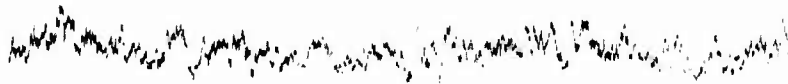


BTA-45  
HCD-25  
R<sub>2</sub> 2000 FS.

← 404 →



BTA-45  
HCD-25  
R<sub>2</sub> 2000 FS.



BTA-45  
HCD-25  
R<sub>2</sub> 2000 FS.

← 404 →

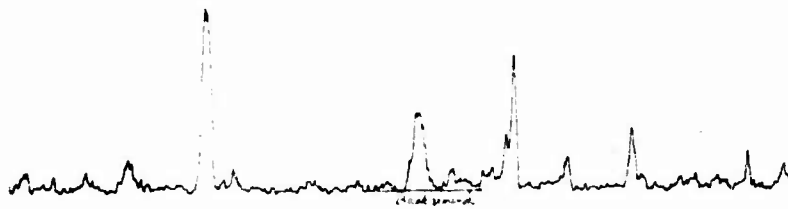


Figure 17. Electron microprobe traverses on sample BTA-45 HCD-25.



## Appendix C

### PREPARATION AND PROCESSING OF BARIUM-STRONTIUM TUNGSTATE CATHODES CONTAINING EXTRA AMOUNTS OF ZIRCONIUM HYDRIDE

#### STARTING MATERIALS

Activator Compound  $[\text{Ba}_5\text{Sr}(\text{WO}_6)_2]$

The stoichiometric quantities of  $\text{BaCO}_3$ ,  $\text{SrCO}_3$  and  $\text{WO}_3$  (all Reagent Grade) required to form 30 grams of the activator compound are ball milled, together with 75 cc of methanol, in an all-molybdenum mill\* for 4 hours. The resulting slurry is then filtered, using a fine Buechner funnel.

The filter cake is fired in a platinum crucible, in air, at  $1400-1450^\circ\text{C}$  for 2 hours. After cooling to room temperature, the product is ground in an Alundum mortar and refired as before. The refired product is then ground in an Alundum mortar and screened through a 325-mesh sieve.

#### Cathode Mix

The following materials in the given weight ratios are dry ball-milled in an all-molybdenum ball mill (see above) for 15 hours:

(1) $\text{Ba}_5\text{Sr}(\text{WO}_6)_2$ 325 mesh	2.813 g	(9.14 wt. %)
(2) $\text{ZrH}_2$ Grade C - 325 mesh	0.376 g	(1.22 wt. %)
(3) Tungsten Type UB - 5.3 Purity - 99.9% min. Avg. Particle Dia. - 5 microns	27.6 g	(89.64 wt. %)

---

\*1. Mill - molybdenum cup, 2-3/4 inch dia. x 2-3/4 inch deep with molybdenum cover plate

2. Grinding Media - 50 molybdenum pieces, 1/4 inch dia. x 1/4 inch long

## COMPACTION

78 tons per square inch.

## SINTERING

Temperature is raised at rate of  $300^{\circ}\text{C}_B$  per minute in pure dry hydrogen until  $1500^{\circ}\text{C}_B$  is reached. At  $1500^{\circ}\text{C}_B$ , temperature is held for 5 minutes, then increased rapidly to  $1840^{\circ}\text{C}_B$  and held for 2.5 minutes. Power is cut and the cathode allowed to cool for 30 minutes before it is removed from hydrogen atmosphere.

## FINISHING

Emitting surface is machined (faced) using tungsten-carbide cutting tool. Cutting feed of 0.0003 inches per revolution is used.

## STORAGE

Short-time storage (several days) in desiccator. Long-time storage in evacuated glass containers.

## BAKE-OUT

Tube is attached to vacuum manifold, and baked out at  $400^{\circ}\text{C}$  to  $450^{\circ}\text{C}$  until a vacuum of  $2 \times 10^{-8}$  torr is reached. (Time will generally fall between 2 hours and 12 hours, depending on condition and complexity of the tube.) Heater power is applied and the cathode outgassed -- not exceeding  $9 \times 10^{-7}$  torr pressure at any time while heating cathode to  $1050^{\circ}\text{C}_T$ . The temperature is held at  $1050^{\circ}\text{C}$  until cathode is outgassed, then raised to  $1200^{\circ}\text{C}_T$  and held for 10 minutes, following which time the tube is pinched off from system.

## ACTIVATION AFTER BAKE-OUT

Cathode temperature is adjusted to  $1050^{\circ}\text{C}$ , and anode potential applied to yield emission currents to 1 to 2  $\text{A}/\text{cm}^2$ . A minimum of 16 hours aging is usually required to reach full and stable emission.

DOCUMENT CONTROL DATA - R&D		
<i>(Security classification of title, body of abstract and indexing annotation must be entered when the overall report is classified)</i>		
1. ORIGINATING ACTIVITY <i>(Corporate author)</i> General Electric Company Schenectady, New York		2a. REPORT SECURITY CLASSIFICATION UNCLASSIFIED
		2b. GROUP N/A
3. REPORT TITLE  HIGH CURRENT DENSITY CATHODES		
4. DESCRIPTIVE NOTES <i>(Type of report and inclusive dates)</i> Final Report - 1 June 1966 to 31 August 1968		
5. AUTHOR(S) <i>(Last name, first name, initial)</i> Bondley, R.J.; Boyd, W.T.; Lock, R.G.; Nall, T.J.; Slivka, M.J.		
6. REPORT DATE January 1969	7a. TOTAL NO OF PAGES 185	7b. NO OF REFS 48
8a. CONTRACT OR GRANT NO. DA 28-043 AMC-02289(E)	9a. ORIGINATOR'S REPORT NUMBER(S)	
b. PROJECT NO. 1H6-22001-A-055-01		
c. Task: 1H6-22001-A-055-01	9b. OTHER REPORT NO(S) <i>(Any other numbers that may be assigned this report)</i>	
d. Subtask: 1H6-22001-A-055-01-14	ECOM-02289-F	
10. AVAILABILITY/LIMITATION NOTICES Each transmittal of this document outside the Department of Defense must have prior approval of CG, U. S. Army Electronics Command, Fort Monmouth, N. J. 07703 - Attn: AMSEL-KL-TQ		
11. SUPPLEMENTARY NOTES	12. SPONSORING MILITARY ACTIVITY US Army Electronics Command Attn: AMSEL-KL-TQ Fort Monmouth, N. J. 07703	
13. ABSTRACT <p>This is the last of a series of reports describing an experimental study of the critical factors and mechanisms involved in achieving high-emission-density cathodes capable of long life and reliable operation in electron tubes. Detailed results of the work of the last reporting period of this investigation are included herein, along with a review of the more significant developments of the entire two-year program. All of the objectives of the program have essentially been met, and in some cases exceeded, resulting in a tungstate cathode which represents an advance in the state of the art for high current density emitters. Reliability and reproducibility were demonstrated by consecutively fabricating and life testing eighteen cathodes. No rejects or deviations were encountered, and initial characteristics were uniform for the entire group.</p> <p>The tungstate cathode is unique in that it can supply higher continuous emission currents over longer periods of time than any other known cathode system. Such performance was substantiated by extensive life testing in diode tubes during the program. This investigation also has led to the development of generally optimum composition and processing procedures (see Appendix A). The tungstate cathode upon which the bulk of the work was placed is a metal-matrix unit containing porous tungsten as the matrix. Distributed uniformly</p>		

14. KEY WORDS	LINK A		LINK B		LINK C	
	ROLE	WT	ROLE	WT	ROLE	WT
Thermionic Emitters		4				
Tungstate Cathodes		4				
High-Current Density Cathode		4				
Low-Current Density Cathode		4				
Nickel Coated Triple Carbonate		4				

INSTRUCTIONS

1. ORIGINATING ACTIVITY: Enter the name and address of the contractor, subcontractor, grantee, Department of Defense activity or other organization (corporata author) issuing the report.

2a. REPORT SECURITY CLASSIFICATION: Enter the overall security classification of the report. Indicate whether "Restricted Data" is included. Marking is to be in accordance with appropriate security regulations.

2b. GRCUP: Automatic downgrading is specified in DoD Directive 5200.10 and Armed Forces Industrial Manual. Enter the group number. Also, when applicable, show that optional markings have been used for Group 3 and Group 4 as authorized.

3. REPORT TITLE: Enter the complete report title in all capital letters. Titles in all cases should be unclassified. If a meaningful title cannot be selected without classification, show title classification in all capitals in parenthesis immediately following the title.

4. DESCRIPTIVE NOTES: If appropriate, enter the type of report, e.g., interim, progress, summary, annual, or final. Give the inclusive dates when a specific reporting period is covered.

5. AUTHOR(S): Enter the name(s) of author(a) as shown on or in the report. Enter last name, first name, middle initial. If military, show rank and branch of service. The name of the principal author is an absolute minimum requirement.

6. REPORT DATE: Enter the date of the report as day, month, year; or month, year. If more than one date appears on the report, use date of publication.

7a. TOTAL NUMBER OF PAGES: The total page count should follow normal pagination procedures, i.e., enter the number of pages containing information.

7b. NUMBER OF REFERENCES: Enter the total number of references cited in the report.

8a. CONTRACT OR GRANT NUMBER: If appropriate, enter the applicable number of the contract or grant under which the report was written.

8b, 8c, & 8d. PROJECT NUMBER: Enter the appropriate military department identification, such as project number, subproject number, system numbers, task number, etc.

9a. ORIGINATOR'S REPORT NUMBER(S): Enter the official report number by which the document will be identified and controlled by the originating activity. This number must be unique to this report.

9b. OTHER REPORT NUMBER(S): If the report has been assigned any other report numbers (either by the originator or by the sponsor), also enter this number(s).

10. AVAILABILITY/LIMITATION NOTICES: Enter any limitations on further dissemination of the report, other than those imposed by security classification, using standard statements such as:

- (1) "Qualified requesters may obtain copies of this report from DDC."
- (2) "Foreign announcement and dissemination of this report by DDC is not authorized."
- (3) "U. S. Government agencies may obtain copies of this report directly from DDC. Other qualified DDC users shall request through \_\_\_\_\_."
- (4) "U. S. military agencies may obtain copies of this report directly from DDC. Other qualified users shall request through \_\_\_\_\_."
- (5) "All distribution of this report is controlled. Qualified DDC users shall request through \_\_\_\_\_."

If the report has been furnished to the Office of Technical Services, Department of Commerce, for sale to the public, indicate this fact and enter the price, if known.

11. SUPPLEMENTARY NOTES: Use for additional explanatory notes.

12. SPONSORING MILITARY ACTIVITY: Enter the name of the departmental project office or laboratory sponsoring (paying for) the research and development. Include address.

13. ABSTRACT: Enter an abstract giving a brief and factual summary of the document indicative of the report, even though it may also appear elsewhere in the body of the technical report. If additional space is required, a continuation sheet shall be attached.

It is highly desirable that the abstract of classified reports be unclassified. Each paragraph of the abstract shall end with an indication of the military security classification of the information in the paragraph, represented as (TS), (S), (C), or (U).

There is no limitation on the length of the abstract. However the suggested length is from 150 to 225 words.

14. KEY WORDS: Key words are technically meaningful terms or short phrases that characterize a report and may be used as index entries for cataloging the report. Key words must be selected so that no security classification is required. Identifiers, such as equipment model designation, trade name, military project code name, geographic location, may be used as key words but will be followed by an indication of technical context. The assignment of links, rules, and weights is optional.

throughout the matrix in specific proportions are a barium-strontium-tungstate compound corresponding to the formula  $Ba_5Sr(WO_6)_2$ , and zirconium. After processing, a surface film of barium zirconate was identified.

In addition to life testing of the standard-composition cathode, as defined in Appendix A, studies were made of other compositions including those containing greater zirconium content. During the last reporting period, eighteen new cathodes, all containing extra zirconium, were started on life test under widely differing emission densities and temperatures. The increased zirconium appears to have stabilized the very low temperature operation, and six cathodes are now beyond the 2,000-hour point with no downward deviations in emission levels.

An analysis of two tungstate cathodes, one of which had completed life test, and the other a new and unactivated cathode, was made of electron diffraction, electron microprobe, electron microscopy, and x-ray diffraction to gain an insight into the emission mechanisms of the barium-strontium-tungstate cathodes. Structural and chemical changes that occur with life were identified.

A review of the resistance to poisoning by various gases and metal vapor deposits on tungstate cathodes was completed.

Sublimation rates for tungstate cathodes were reviewed and compared to the rates of other cathode systems.

Noise properties of the tungstate cathode were determined. The noise properties of a standard barium oxide-on-nickel emitter, and a commercially available barium-aluminate cathode, were evaluated on the same equipment for purposes of comparison.

The emitting characteristics of tungstate cathodes were studied with an emission microscope. The existence of local areas of high emission density dispersed through other areas of low activity was verified at typical operating levels in a diode containing a dissecting anode aperture and an auxiliary current probe.